KAUNAS UNIVERSITY OF TECHNOLOGY

SUMAN KUMAR ADHIKARY

INVESTIGATIONS ON STRUCTURE AND PROPERTIES OF LIGHTWEIGHT SELF-COMPACTING CEMENT COMPOSITE INCORPORATING SILICA AEROGEL AND EXPANDED GLASS AGGREGATES

Doctoral dissertation
Technological Sciences, Civil Engineering (T 002)

Kaunas, 2023

This doctoral dissertation was prepared at Kaunas University of Technology, Faculty of Civil Engineering and Architecture, Department of Civil Engineering and Architecture Competence Centre during the period of 2018–2022.

Scientific Supervisor
Prof. Dr. Žymantas RUDŽIONIS (Kaunas University of Technology, Technological Sciences, Civil Engineering, T 002)

Edited by: English language editor Dr. Armandas Rumšas (Publishing House *Technologija*), Lithuanian language editor Rozita Znamenskaitė (Publishing House *Technologija*)

The official defense of the dissertation will be held at 10 a.m. on 14 April 2023 at the public meeting of Dissertation Defense Board of Civil Engineering Science Field in M7 Hall at Kaunas University of Technology.

Address: Studentų 48–M7, Kaunas, LT-51367, Lithuania.
Phone: +370 608 28 527; email doktorantura@ktu.lt

Doctoral dissertation was sent out on 14 March 2023.
The doctoral dissertation is available on the internet at http://ktu.edu and at the library of Kaunas University of Technology (Donelaičio 20, Kaunas, LT-44239, Lithuania).

KAUNO TECHNOLOGIJOS UNIVERSITETAS

SUMAN KUMAR ADHIKARY

LENGVOJO SUSITANKINANČIO CEMENTINIO KOMPOZITO SU SILICIO AEROGELIO IR PUTSTIKLIO UŽPILDAIS STRUKTŪROS IR SAVYBIŲ TYRIMAI

Daktaro disertacija
Technologijos mokslai, statybos inžinerija (T 002)

Kaunas, 2023

Disertacija rengta 2018–2022 metais Kauno technologijos universiteto Statybos ir architektūros fakultete, Statybos ir architektūros kompetencijų centre.

Mokslinis vadovas
Prof. dr. Žymantas RUDŽIONIS (Kauno technologijos universitetas, technologijos mokslai, statybos inžinerija, T 002)

Redagavo: anglų kalbos redaktorius dr. Armandas Rumšas (leidykla „Technologija“), lietuvių kalbos redaktorė Rozita Znamenskaitė (leidykla „Technologija“)

Statybos inžinerijos mokslo krypties disertacijos gynimo taryba:
prof. dr. Kęstutis BALTAKYS (Kauno technologijos universitetas, technologijos mokslai, chemijos inžinerija – T 005), – **pirmininkas**;
prof. dr. Ruben Paul BORG (Maltos universitetas, Malta, technologijos mokslai, statybos inžinerija – T 002);
prof. dr. Mindaugas DAUKŠYS (Kauno technologijos universitetas, technologijos mokslai, statybos inžinerija – T 002);
prof. dr. Ina PUNDIENĖ (Vilniaus Gedimino technikos universitetas, technologijos mokslai, medžiagų inžinerija – T 008);
prof. dr. Lina ŠEDUIKYTĖ (Kauno technologijos universitetas, technologijos mokslai, statybos inžinerija – T 002).

Disertacija bus ginama viešame statybos inžinerijos mokslo krypties disertacijos gynimo tarybos posėdyje 2023 m. balandžio 14 d. 10 val. Kauno technologijos universiteto Studentų miestelio bibliotekoje, salėje M7.

Adresas: Studentų g. 48–M7, Kaunas, LT-51367, Lietuva.
Tel. (+370) 608 28 527; el. paštas doktorantura@ktu.lt

Disertacija išsiųsta 2023 m. kovo 14 d.
Su disertacija galima susipažinti interneto svetainėje http://ktu.edu ir Kauno technologijos universiteto bibliotekoje (K. Donelaičio g. 20, Kaunas, LT-44239, Lietuva).

TABLE OF CONTENTS

LIST OF ABBREVIATIONS AND TERMS

Materials:

EGA – expanded glass aggregate
GGBS – ground granulated blast-furnace slag
FGA – foam glass aggregate
LECA – lightweight expanded clay aggregate
SF – silica fume
SP – superplasticiser
VMA – viscosity modifying agent
POC – palm oil clinker
OPC – ordinary Portland cement
CNT – carbon nanotube
GNP – graphene nano platelet
SBR – styrene-butadiene rubber
TEOS – tetraethoxysilane
EPS – expanded polystyrene
COK – crushed olive kernel

Parameters:

f_c – compressive strength
f_{fl} – flexural strength
w/b – water/binder ratio

Experimental methods:

SEM – scanning electronic microscopy
XRD – X-ray diffraction analysis
EDS – energy-dispersive X-ray spectroscopy

Other terms:

LWA – lightweight aggregates
CA – coarse aggregate
FA – fine aggregate
NA – natural aggregate
ITZ – interfacial transition zone
EGAC – expanded glass aggregate concrete
LWC – lightweight concrete
LWAC – lightweight aggregate concrete
SCC – self-compacting concrete
SCCC – self-compacting cement composite
SCM – self-compacting mortar
LWSCC – lightweight self-compacting concrete
LWSCCC – lightweight aggregate self-compacting cement composite
EFNARC – European Federation of National Associations Representing for Concrete

-COOH – carboxylic
-OH – hydroxyl
C-S-H – calcium-silicate-hydrate
RH – relative humidity
ASR – alkali silica reaction

Key terms:

SCC: Self-compacting concrete is an optimized product of conventional concrete that is denoted by better workability, flowability, and pumpability, and does not require any internal or external vibrations for compaction. There are certain criteria for the passing ability, filling ability, and segregation resistance set by several organizations that concrete needs to satisfy to be termed as SCC.

LWSCC: Lightweight self-compacting concrete is an optimized product of lightweight concrete, and it demonstrates similar fresh characteristics as SCC. Besides, it has to meet all of the same requirements as the regular SCC. According to the EN 206-1 Standard, the density of lightweight concrete is 800–2000 kg/m^3, whereas the density of LWSCC is also similar to lightweight concrete.

LWSCCC: Concrete is a composite material as it contains combinations of versatile building materials. Concrete is mainly prepared by combinations of coarse and fine aggregates, while cementitious composites can be prepared with fine or combinations of fine and coarse aggregates. In this study, LWSCCC was prepared with both fine aggregates and combinations of coarse and/or fine aggregates; it termed as a cementitious composite other than concrete.

EFNARC: EFNARC is a European federation dedicated to specialist concrete systems and construction chemicals. EFNARC also provides guidelines for SCC, and most European countries follow their specified guidelines.

1. INTRODUCTION

Self-compacting concrete (SCC) was developed in 1986 by Ozawa and his colleagues and represented a significant leap forward in the concrete construction technology (Adebayo Mujedu et al., 2020). Not only did the invention of SCC lead to a higher-quality concrete, but it also increased productivity and provided a better working atmosphere. Despite the fact that lightweight self-compacting concrete (LWSCC) components are nearly identical to those of lightweight aggregate concrete (LWAC), their compositions and workability are vastly different (Yu et al., 2013). Higher volumes of binders and admixtures are needed to keep the desired fluidity at a constant level (Yu et al., 2013). LWAC has been used for a long time, and today LWSCC is regarded as an improved version of SCC and LWAC (Yu et al., 2019). Today, LWSCC uses a variety of natural and synthetic lightweight aggregates. However, the majority of LWSCCs were made with synthetic aggregates. POC, EPS, rubber, coconut shale, and plastic waste are all denoted by significant potential. The physical and mechanical properties of LWA may vary depending on the type, which could have an impact on the characteristics of LWSCC (Ting et al., 2019).

LWA offers a lower mechanical strength than the normal, natural aggregates (Altalabani et al., 2020; Nguyen et al., 2018; Zhu et al., 2016); thus, using more LWA in concrete could result in a lower compressive strength (Kurt et al., 2016a; Wan et al., 2018). It is possible that using LWA in concrete will cause segregation issues because of LWA's tendency to float (Adhikary and Rudzionis, 2020; Juradin et al., 2012). Segregation and inadequate self-compaction in the form of uneven distribution of LWA could compromise the structural performance and durability of concrete (Kwasny et al., 2012). A large volume of LWA is needed to prepare SCC below the density of 1400 kg/m^3, which could increase the risk of water absorption (Kurt et al., 2016b; Kwasny et al., 2012; Wan et al., 2018). Low-density concrete could be used to insulate against noise and heat (Ting et al., 2019). Due to the differences in the surface structure and adhesion quality of lightweight aggregates, the quality of ITZ of LWSCC made with various types of LWAs may also vary. Literature studies suggest that LECA, expanded glass, perlite, and scoria show good adhesion with cementitious materials leading to a better ITZ (Adhikary et al., 2022a). Meanwhile, EPS, polymeric waste, and aerogel offer weaker adhesion with cementitious materials, which leads to weaker adhesion and poorer ITZ (Angelin et al., 2020; Cheboub et al., 2020; Da Silva et al., 2020; Ranjbar and Mousavi, 2015). Furthermore, in recent years, mostly, LWSCC developed by using LWA was above 1400 kg/m^3 density. Somehow, a few researchers have managed to achieve a self-compacting cementitious composite below the density of 1400 kg/m^3, but the compressive strength was less than 10–12 MPa.

In the past few decades, numerous studies have been carried out on LWSCCC incorporating several types of lightweight aggregates. Aerogel is a promising material featuring a very low density; it can be used in the production of very lightweight cementitious composites. While EGA is also a lightweight aggregate, it has a lower density. Yet, despite the lower density, aerogel is fragile in nature.

Moreover, hydrophobic aerogel might exhibit weaker adhesion with cementitious materials, which would lead to a weaker strength of cementitious composites. The development of a lightweight self-compacting cementitious composite incorporating a combination of EGA and aerogel can be a promising material for building applications. A lightweight cementitious composite incorporating such low-density aggregate would be denoted by a lower density. Moreover, the use of such materials in a cementitious composite might lead to a decrease in the mechanical performance, and would increase the risk of water absorptions. A hydrophobic aerogel may also suffer from weaker adhesion problems, and further studies are required to extensively investigate the characteristics of cementitious composites incorporating aerogel and EGA in terms of their fresh, mechanical performances, microstructure, and water absorption capacity. Furthermore, problems related to aerogel and EGA aggregate-based cementitious composite should be eliminated. Moreover, most developed LWSCCs below the density of 1400 kg/m^3 feature a lower compressive strength than the recommended value of ACI-213R-03 2003, ACI-213R-2014 and CEB/RILEM so that they could be used as structural applications. In this context, the current investigation is performed. To achieve the aim of the study, several cementitious composites have been developed by using the mixing and trial methods. Firstly, lightweight cement composites were prepared by using EGA and aerogel in order to identify their impact and probable problems regarding the lightweight cementitious composites. By the mixing and trail method, the mixing composition was optimized, and the self-compatibility factor was achieved. Such problems as higher water absorption, inferior mechanical performance, and weaker adhesion levels of aerogel with cementitious materials have been mitigated by using polymer coatings on LWA. Furthermore, mechanical performances and water absorption and ITZ between the aerogel and cementitious materials have been improved by using carbon nanotubes and graphene platelets.

The main goal of the current work is to investigate the physical, mechanical and microstructural properties of lightweight self-compacting cementitious composites developed with aerogel and expanded glass aggregates with a density of less than 1400 kg/m^3.

Tasks of the work to achieve the desired aim

1. To research the impact of binding materials, the concentration of fine particles and lightweight aggregates on the physical, mechanical, and microstructural properties of a lightweight self-compacting cementitious composite (<1400 kg/m^3).
2. To improve the water absorption and compressive strength and microstructure of lightweight self-compacting cementitious composites using polymer coatings on lightweight aggregates.
3. To enhance the compressive strength, microstructure, and water absorption characteristics of lightweight cementitious composites using carbon nanotubes and graphene platelets.

Scientific novelty of the study

In this study, a new type of lightweight self-compacting cementitious composite has been developed below the density of 1400 kg/m^3. The developed lightweight self-compacting cementitious composite has satisfied the required strength of ACI-213R-03 (versions of 2003 and 2014) to be used as a structural application even below the density of 1400 kg/m^3. Manual mixing of the fresh cementitious composite enables the lower crushing of aerogel particles. Moreover, this experimental study shows that aerogel offers weaker adhesion with cementitious materials, and a separation gap was observed in the ITZ between the aerogel and the cementitious materials. Moreover, the aerogel-based cementitious composite suffers from a lower mechanical strength and porous microstructure, and, on top of that, it incurs the risk of higher water absorption levels. In this study, the separation gaps between the aerogel and the cementitious materials have been improved by using nanomaterials and polymer coatings. Furthermore, water absorption, mechanical properties, and microstructure have also been improved.

Methods of research

The initial materials for the development of lightweight cement composites were selected from the data sourced from the available literature. SEM and XRD analyses were conducted to understand the microstructure of pozzolanic additives and lightweight aggregates. Mostly, the mixing and trial method is widely adopted, and, in the current experimental studies, the mixing and trial method is also widespread. The fresh properties of the cement composite were investigated according to the guidelines of EFNARC 2005. Cement hydration of the cement paste was monitored by employing the semi-adiabatic calorimetry method using the Pico Technology which conforms to the EN 196-9:2010 Standard. The mechanical strength of the cement composite was tested in accordance with the EN 196-1:2016 Standard. The porosity and thermal conductivity of the cementitious composite was calculated in accordance with GOST 12730.4-2020 Standard and EN 1745:2012 Standard, respectively. The water absorption, density, porosity, and SEM of the cement composite were determined so that to analyze the obtained results and to determine a relationship between them. After developing the LWSCCC by the mixing and trialing methods, such properties of the composite as the mechanical performance, microstructure, and water absorption characteristics have been targeted in terms of improvement by adopting several measures.

Practical significance of the dissertation

The manual mixing of lightweight cementitious composites by hand lowers the crushing of aerogel and keeps the integrity of aerogel in the cementitious system. The developed lightweight cementitious composites also satisfied the ENFRAC 2005 requirements to be used as self-compacting cementitious materials. The developed cementitious composites can be used as thermal insulating materials, and their self-compacting ability will help to reach the congested areas without using any external vibration equipment. The self-compactibility characteristics allow for easy handling, placing, and compactness. The thermal conductivity of the developed

material obtained in the study was much lower than the corresponding values of the conventional concrete and it is denoted by high potential of use in the construction sector. However, in this study, the thermal conductivity of the cementitious composites was calculated by using EN 1745:2012 Standard which can be different from the real-time-tested thermal conductivity in a laboratory. Moreover, the optimized lightweight cementitious composites presented in the study can also be used as structural applications as they satisfy the required strength of ACI-213R-03 (versions of 2003 and 2014) recommendations. The obtained strength and thermal conductivity below the density of 1400 kg/m^3 is a novelty, and this may lead to potential use in the construction sector.

Statements to be defended in the dissertation

1. The lightweight cement composites with optimized mixing composition are able to achieve self-compactibility even below the 1400 kg/m^3 density with the slump flow class of SF2 and SF3.
2. Due to the hydrophobic characteristics of the aerogel, it may entrap air bubbles during the mixing of the fresh cementitious composite and show lower adhesion levels and weaker ITZ.
3. The separation gaps between the aerogel and cementitious materials have been significantly improved by using nanomaterials and polymer coatings. The incorporation of CNT and GNP into the lightweight cement composite leads to an improvement of the compressive strength at 41.5% and 43.8% levels, and to an improvement at 30.5% and 29% levels in terms of water absorption, respectively.

Structure and scope of the work

This doctoral dissertation has been prepared as a body of work comprising three chapters. It consists of an introduction, results and discussion, and conclusions. In addition, a list of references, a brief summary of the dissertation in the Lithuanian language, a resume of the doctoral student's work, and a list of publications related to the doctoral dissertation, and additional publications other than the dissertation topic are provided along with the author's acknowledgments. The full volume of the doctoral dissertation includes 52 Figures, 10 Tables, and 50 references.

Approval of the results of the study

The findings of the investigations that have been carried out have been compiled and presented in a total of five research articles in scientific journals. The journals feature in the *Clarivate Analytics Web of Science* database (with the citation index) and fall within the Q1, and Q2 quartiles.

List of scientific publications on the topic of the dissertation

In this PhD thesis, the scientific novelty and achieved results have been covered in a set of five articles. The research results are summarized in three stages.

In the first stage, the preliminary investigation was conducted in terms of defining the self-compacting criteria of concrete. The first stage of the study is

covered in two articles. The first article was published in the *Journal of Building Engineering*, 2020, 101399 (Adhikary et al., 2020). The aim of this stage of the study was fulfilled in two stages. At first, the impact of binders and lightweight aggregates was investigated while preparing flowable lightweight cement composite. Afterwards, the mixing composition described in the first article was optimized based on the obtained results so that to satisfy the self-compacting criteria. The results of this step were published in *Case Studies in Construction*, 2022, e00879 (Adhikary et al., 2022b).

In the second stage of the research, the identified problems associated with EGA and aerogel-based cement composites in the previous stage were attempted to be improved. Such problems as higher water absorption and weaker adhesion between the aerogel and the cementitious materials were sought to be improved by employing polymer coatings. The results of this study were published in *Materials Today Communications*, 2022, 103496 (Adhikary, 2022).

In the third stage of the research, the identified problems of the lightweight cement composite prepared with EGA and aerogel were sought to be rectified alternatively with nanomaterials. Such problems as weaker mechanical performance, weaker ITZ between the aerogel and the cementitious materials, and a higher risk of water absorption were targeted by using such new-generation nanomaterials as CNTs and graphene platelets. At first, carbon nanotubes were used on the flowable lightweight concrete; the results of the study were published in *Scientific reports*, 2021, 2104 (S.K. Adhikary et al., 2021). Afterwards, the mechanical performance, water absorption, and ITZ between the lightweight aggregates and the cementitious materials of lightweight cementitious composites were improved by incorporating graphene platelets (GNP). The results of the study were published in *Journal of Building Engineering*, 2022, 104870 (Adhikary et al., 2022c).

1. **Suman Kumar Adhikary**, Žymantas Rudžionis, Danutė Vaičiukynienė; Development of flowable ultra-lightweight concrete using expanded glass aggregate, silica aerogel, and prefabricated plastic bubbles; Journal of Building Engineering, ISSN 2352-7102. 2020, vol. 31, art. No. 101399, p. 1-10; https://doi.org/10.1016/j.jobe.2020.101399

2. **Suman Kumar Adhikary**, Žymantas Rudžionis, Simona Tučkutė; Characterization of novel lightweight self-compacting cement composites with incorporated expanded glass, aerogel, zeolite and fly ash; Case Studies in Construction, ISSN 2214-5095. 2022, vol. 16, art. No. e00879, p.1-19.; https://doi.org/10.1016/j.cscm.2022.e00879

3. **Suman KumarAdhikary**; The influence of pre-coated EGA and aerogel on the properties of lightweight self-compacting cementitious composites; Materials Today Communications, ISSN 2352-4928. 2022, vol. 31, art. No. 103496, p. 1-8; https://doi.org/10.1016/j.mtcomm.2022.103496

4. **Suman Kumar Adhikary**, Žymantas Rudžionis, Simona Tučkutė, Deepankar Kumar Ashish; Effects of carbon nanotubes on expanded glass

and silica aerogel based lightweight concrete; Scientific reports, ISSN 2045-2322. 2021, vol. 11, iss. 1, art. No. 2104, p. 1-11; https://doi.org/10.1038/s41598-021-81665-y

5. **Suman Kumar Adhikary**, Žymantas Rudžionis, Simona Tučkutė; Characterization of aerogel and EGA-based lightweight cementitious composites incorporating different thickness of graphene platelets; Journal of Building Engineering, ISSN 2352-7102. 2022, vol. 57, art. No 104870, p. 1-14; https://doi.org/10.1016/j.jobe.2022.104870

Author's contribution

The selection of the materials and the research plan was carried out by Suman Kumar Adhikary and Žymantas Rudžionis. The materials were provided by Kaunas University of Technology and Žymantas Rudžionis. This thesis is covered in five articles, and the contributions of each author to each article are listed below.

The first article published in the *Journal of Building Engineering*, art. No. 101399, was prepared with the effort of three authors. The experiments were performed, the data was collected, and the manuscript was written by doctoral student Suman Kumar Adhikary under the supervision of Žymantas Rudžionis. Danutė Vaičiukynienė helped through the investigation of the SEM and XRD results, and Žymantas Rudžionis helped to finalize the manuscript during the publication of the article.

The second article was published in the Journal *Case Studies in Construction Materials*, art. No. e00879. The experiments were performed, the data was collected, and the manuscript was written by doctoral student Suman Kumar Adhikary under the supervision of Žymantas Rudžionis. Simona Tučkutė helped through the implementation of the SEM and XRD tests. Žymantas Rudžionis helped to finalize the manuscript in preparing for the publication of the article.

The third article was published in the journal *Materials Today Communications*, art. No. 103496. The experiments were performed, the data was collected, and the manuscript was written by doctoral student Suman Kumar Adhikary. Simona Tučkutė helped through the implementation of the SEM and XRD tests. Žymantas Rudžionis helped to finalize the manuscript in preparing for the publication of the article.

The fourth article was published in the journal *Scientific Reports*, art. No. 2104. The The experiments were performed, the data was collected, and the manuscript was written by doctoral student Suman Kumar Adhikary. Simona Tučkutė helped through the implementation of the SEM and XRD tests. Žymantas Rudžionis and Deepankar Kumar Ashish helped to finalize the manuscript in preparing for the publication of the article.

The fifth article was published in *Journal of Building Engineering*, art. No. 104870. The experiments were performed, the data was collected, and the manuscript was written by doctoral student Suman Kumar Adhikary. Žymantas Rudžionis and Deepankar Kumar Ashish helped to finalize the manuscript in

preparing for the publication of the article. Simona Tučkutė helped through the implementation of the SEM and XRD tests.

2. RESULTS AND DISCUSSION

This chapter covers mixture compositions and a detailed analysis of the obtained results of the prepared cement composites. The obtained results were divided into several categories according to the stages of the research.

The aim of this study is to develop lightweight self-compacting cement composites with 10 to 17 MPa compressive strength. From the rigorous study of the relevant academic literature, several lightweight self-compacting cementitious composites were prepared by using the mixing and trial methods. EGA and aerogel were used as a prime lightweight aggregate to develop LWSCCC. At first, LWSCCC was developed, and the problems related to aerogel-based LWSCCC were eliminated by using polymer coatings and nanomaterials. The steps of the investigations of this study are presented in Fig. 2.1.

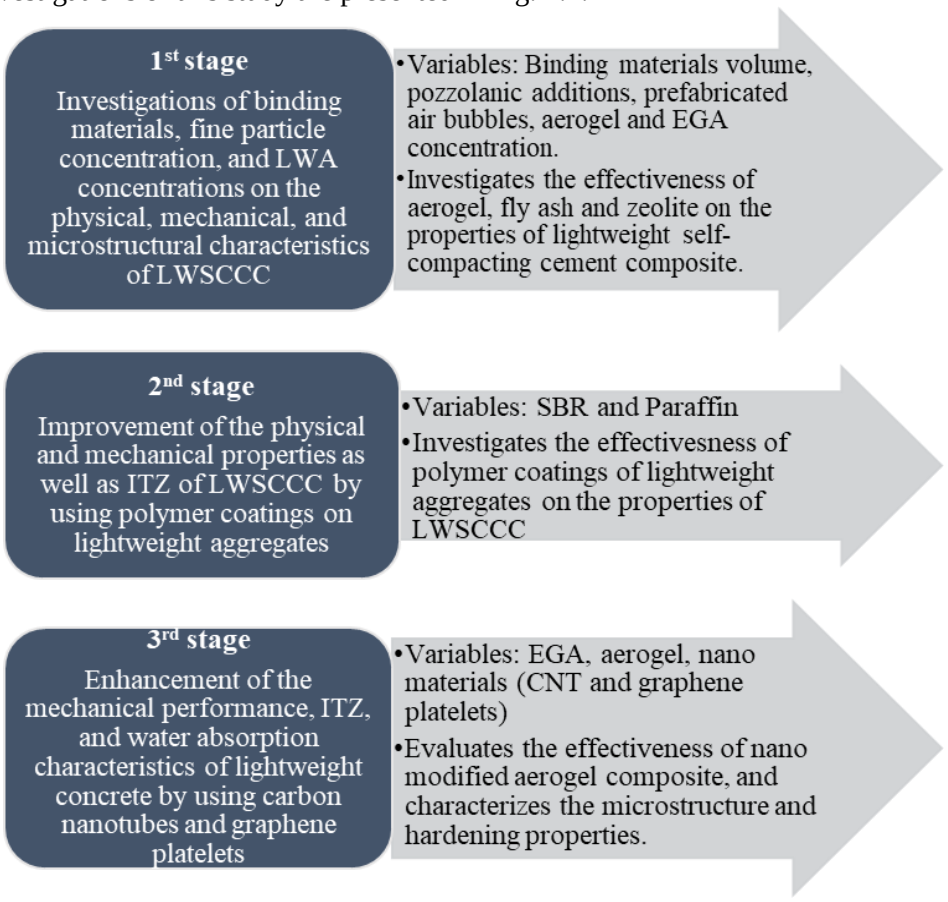

Fig. 2. 1 A schematic view of the stages of the investigation of the dissertation

Stage 1: Investigations of binding materials, fine particle concentration, and LWA concentrations on the physical, mechanical, and microstructural characteristics of LWSCCC

This study is the first experimental stage of the dissertation. To understand the impact of the binder's concentration and lightweight aggregates on the lightweight concrete, several cementitious composites were prepared. The experimental study was carried out by using the mixing and trial method. From the literature studies and a previous scholarly study (Adhikary and Rudzionis, 2020), the proper fractions of LWA were used to develop flowable lightweight cementitious composites. Besides the microstructure, cement hydration and strength characteristics of the lightweight cement composites were primarily studied. This study helps to get basic information about the microstructure of LWA, LWAC, and the mechanical strength of lightweight concrete. Moreover, it gives an idea about the further required modification for the improvement of the mechanical performance and workability.

After the preliminary investigation, the mixing composition was optimized to achieve self-compactibility. The optimized mixing composition with self-compactibility aimed to achieve the compressive strength above 10 to 15 MPa featuring a density below 1400 kg/m^3.

In this stage of the study, a combination of EGA and aerogel was used as lightweight aggregates to achieve a lightweight self-compacting cement composite. The novelty of the dissertation and the further required improvement of the obtained lightweight cement composite were identified in this stage.

Stage 2: Improvement of the physical and mechanical properties as well as ITZ of LWSCCC by using polymer coatings on lightweight aggregates

At this stage of the research, the identified problems associated with EGA and aerogel-based cement composites in the previous stage were attempted to improve. Such problems as higher water absorption levels and weaker adhesion between the aerogel and the cementitious materials were attempted to be improved with polymer coatings. Two different types of polymer coatings, such as SBR and paraffin, were used in this stage of the study to coat the lightweight aggregates. From the previous stage of the study, the best mixing composition was selected and further modified in this study. The target compressive strength of the self-compacting cement composite was kept above 10 MPa, while achieving a density below 1200 kg/m^3.

Stage 3: Enhancement of the mechanical performance, ITZ, and water absorption characteristics of lightweight concrete by using carbon nanotubes and graphene platelets

At this stage of the research, the identified problems of the lightweight cement composite prepared with EGA and aerogel were tried to improve alternatively with nanomaterials. Two different types of nanomaterials, such as carbon nanotubes and graphene nanoplatelets, were used. The cement hydration, water absorption, strength, and mineralogical characteristics of lightweight cement composites were evaluated.

2.1. Investigation of binding materials, fine particle concentration, and LWA concentration on the physical, mechanical, and microstructural characteristics of LWSCCC

2.1.1. Preliminary investigation of the impact of pozzolanic additions and lightweight aggregates on the characteristics of flowable lightweight cement composites

This chapter is based on the paper published in *Journal of Building Engineering*, 2020, 101399 (Adhikary et al., 2020). This chapter investigates the impact of the binders and lightweight aggregates on the properties of lightweight cementitious composites. The experiments were performed, the data was collected, and the manuscript was written by doctoral student Suman Kumar Adhikary under the supervision of Žymantas Rudžionis. Danutė Vaičiukynienė helped through the investigation of the SEM and XRD results, and Žymantas Rudžionis helped to finalize the manuscript for the publication of the final version of the article.

Two groups of flowable lightweight cementitious composites were prepared by using aerogel and expanded glass aggregates. The first series of the composite was aimed to study the impact of fly ash as partial replacement of cement. Up to 30% of the cement mass was replaced with fly ash in the first series. From the results obtained with the composite, the best mix in terms of workability, strength, and visual segregation was considered for the next composite series. In the second series, 1 to 2 mm EGA was replaced with 1 to 2 mm-sized silica aerogel. The replacement volume was aerogel with 25%, 50%, 75%, and 100% of 1–2 mm-sized EGA. The mixing composition of the composites is presented in Table. 2.1.

Table 2. 1 Mixing composition of cement composite, kg/m^3

Series	Cement	Aerogel	Aggregate (1/2+1/0.5+ 0.5/0.25+0. 01/0.3)	Fly ash	Super plasticiser, 1.8%	Stabiliser, 0.3%	Water, (w/b=0.65)
C100FA0	500	-	138+54+34+40	-	9	1.5	325
C90FA10	454.5	-	138+54+34+40	45.45	8.18	1.37	325
C80FA20	416.7	-	138+54+34+40	83.34	7.50	1.25	325
C70FA30	385	-	138+54+34+40	115.5	6.93	1.16	325
C90FA10AG25	454.5	10.5	103.5+54+34+40	45.45	8.18	1.37	325
C90FA10AG50	4545	21	69+54+34+40	45.45	8.18	1.37	325
C90FA10AG75	454.5	31.5	34.5+54+34+40	45.45	8.18	1.37	325
C90FA10AG100	454.5	42	0+54+34+40	45.45	8.18	1.37	325

In this study, the fresh properties of the cement and the composites were tested by a flow table. The flow table spread of the cement composite is presented in Table. 2.2. The study results clearly indicate that the workability of the cement composites decreased with an increase in aerogel concentrations. Meanwhile, the workability of the cement composite was improved by incorporating fly ash as a replacement of

cement. The flow table spread of sample C100FA0 was measured at 21 cm which subsequently increased to 23.4 cm by incorporating 30% fly ash as a substitute of cement. The improved workability may be associated with the ball-bearing effect of fly ash. The flow table spread of sample C90FA10AG25 containing 25% replacement volume of 1–2 mm size EGA by aerogel was measured at 21 cm which decreased to 18.4 cm for composite C90FA10AG100 containing 100% replacement volume of 1–2 mm EGA. The reduction in the flowability of aerogel added cement composites may be attributed to the air entrapped by the silica aerogel. However, the workability of the composite can be modified by adjusting the doses of water and superplasticizer.

Table 2. 2. Workability of lightweight cement composites (stage – I-A).

Series	Flow table test, cm	Series	Flow table test, cm
C100FA0	21	C90FA10AG25	21
C90FA10	21	C90FA10AG50	20
C80FA20	23	C90FA10AG75	18.9
C70FA30	23.4	C90FA10AG100	18.4

Semi-adiabatic calorimetry analysis was performed with the objective to analyze the impact of fly ash and aerogel additions on the hydration of cement. Semi-adiabatic calorimetry analysis yielded information about two important characteristic points, such as the initial and the final setting time.

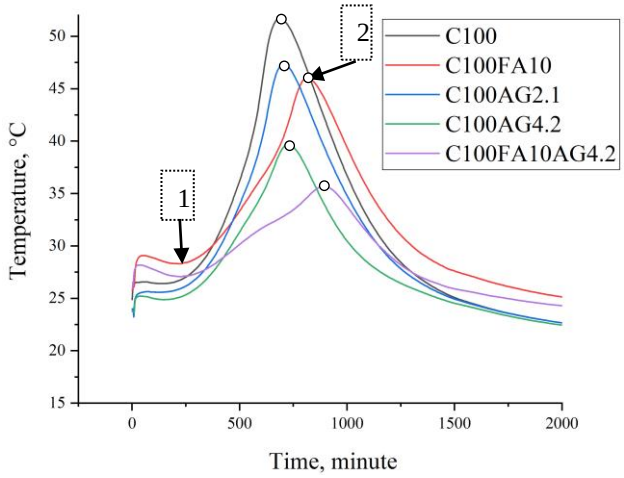

Fig. 2. 2 Hydration of cement paste containing fly ash and aerogel

The initial setting time is at the lowest point of the peak of the curve, while the final setting time is at the highest point of the curve. The initial and final setting times are marked ‘1’ and ‘2’ in Fig. 2.2. Sample C100 serves as the reference sample where only cement is used, whereas the initial setting time starts at 196 min and finishes at 788 min. It was observed that, by incorporating 10% fly ash with

cement in sample C100FA10, the initial setting time was retarded, and the initial setting time started at 222 min and finished at 818 min. This phenomenon may be attributed to the pozzolanic activity of fly ash. Figure 2.2 also shows that the incorporation of aerogel into the cement paste significantly impacted the setting times. When incorporating 2.1% aerogel with cement paste, the initial setting time was shortened to 134 minutes, and the process finished at 709 minutes. When the aerogel content was increased to 4.2%, the initial setting time started at 148 min and finished at 726 min. It can also be observed that the inclusion of silica aerogel also resulted in a lower amount of the produced exothermic heat. It was also discovered that when fly ash and aerogel were added to the paste, the initial setting time was extended to 222 min, and the process finished at 888 min. Moreover, the inclusion of fly ash and aerogel in combination yields much lower exothermic heat than the other samples. This phenomenon suggests that silica aerogel is slightly reactive with cement.

In this stage of the study, f_c and f_{fl} of the composites were measured on the 7th and 28th days of the hydration process. The f_c and f_{fl} values of the composites on the 7th and 28th days of hydration are presented in Table. 2.3.

Table 2. 3 Mechanical strength of lightweight cement composites at 28 days (stage – I-A)

Series	7th day strength test, MPa		28th day strength test, MPa		Dry density, kg/m^3	Thermal conductivity [W/(m·K)]
	f_c	f_{fl}	f_c	f_{fl}		
C100FA0	9.32	2.5	12.2	2.68	862.4	0.356
C90FA10	8.2	2.3	11.4	2.56	848.0	0.348
C80FA20	6.92	2.2	10	2.1	834.5	0.345
C70FA30	5.2	1.9	8	2.04	826.4	0.342
C90FA10AG25	5.72	1.7	6.52	2.38	816	0.337
C90FA10AG50	5.88	1.84	6.40	2.01	793	0.328
C90FA10AG75	3.32	1.11	4.8	1.61	774.5	0.322
C90FA10AG100	3.2	1.097	4.48	1.45	749.5	0.314

The study results indicate that, with an increase in the fly ash content, the f_c value of the cement composite declines. It was also observed that an increase in the aerogel concentration declines for both f_c and f_{fl}. By replacing 100% 1–2 mm EGA with aerogel, concrete lost about 60.7% f_c on the 28th day. The lower strength gains of the composites may be attributed to the addition of fly ash and aerogel which presumably delays the hydration of cement. Semi-adiabatic calorimetry analysis made it evident that there is an extension in the hydration of cement achieved by the addition of aerogel and fly ash. Besides, aerogel is a fragile material having a very low strength, and, perhaps, due to this reason, with an increase of the aerogel content in the composites, the compressive and flexural strength was reduced.

The oven dry density of the samples was measured after 28 days of the curing process, and, thereafter, the thermal conductivity of the composites was calculated; it was found to satisfy EN1745:2012 Standard. Table 2.4 shows that, with an increase in aerogel concentration, the density of the composite was reduced. The oven dry density of the composite C90FA10AG25 was measured as 816 kg/m^3, which decreased to 749.5 kg/m^3 for composite C90FA10AG100 containing 100% replacement of 1–2 mm EGA with aerogels. Due to the reduction in density of the composites, the thermal conductivity is also reduced. The thermal conductivity of C90FA10AG25 and C90FA10AG100 was calculated and determined about 0.337 and 0.322 W/(m·K), respectively. Aerogel is very lightweight material, and the incorporation of aerogel with EGA lowers the density, which leads to an improvement in the thermal conductivity of the composites. On a special note, this calculation of thermal conductivity may differ from the actual thermal conductivity of lightweight cementitious composites. Aerogel is a highly thermally insulating material, and a real-time test of its thermal conductivity may yield much lower values than the calculated one.

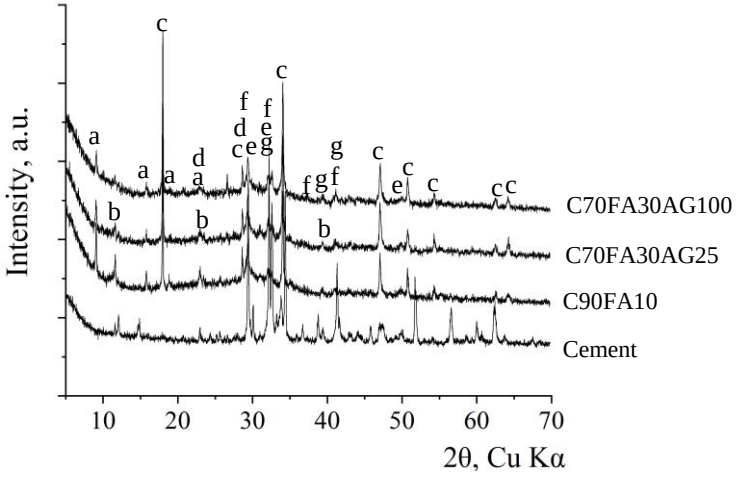

Fig. 2. 3 X-ray diffraction analysis of cementitious composites

Note: a – ettringite $Ca_6Al_2(SO_4)_3(OH)_{12}\cdot 26H_2O$ (41–1451), b – hydrotalcite $Mg_4Al_2CO_9\cdot(OH)_{12}CO_3(H_2O)_3)_{0.5}$ (70–2151), c – portlandite $Ca(OH)_2$ (1–837), d – calcite $Ca(CO)_3$ (24–27), e – calcium silicate hydrate $Ca_{1.5}SiO_{3.5}\cdot x\ H_2O$ (33–306), f – alite $Ca_{54}MgAl_2Si_{16}O_{90}$ (13–272), g – belite Ca_2SiO_4 (33–302)

The XRD analysis of the composite was performed after 28 days of the hydration of cementitious composites. From the obtained results, it can be observed that portlandite, calcium silicate hydrate, ettringite, and hydrotalcite are the main hydration products of the cement composites. The X-ray diffraction analysis of the composites is presented in Fig. 2.3. It was observed that the intensity of ettringite near 8° and the peak of hydrotalcite near 12° decreased with an enhancement in aerogel concentrations. This reduction phenomenon of hydrotalcite and ettringite with an increase in aerogel concentrations suggests partial dissolving and implies reactions of silica aerogel with cementitious materials. Silica aerogel is amorphous

in nature, and it is expected to dissolve and react in the alkaline environment provided by cement hydration.

In the DSC–TGA analysis, the DSC and TGA curves are presented in Fig. 2.4 and Fig. 2.5. The first endothermic peaks at 98.6 ℃ to 102.1 ℃ for composite specimens C90FA10, C90FA10AG25, C90FA10AG50, C90FA10AG75, and C90FA10AG100 suggest the driving-out of the physically bound water. The endothermic peaks near 140.6 °C to 139.2 °C for composites C90FA10, C90FA10AG25, C90FA10AG50, C90FA10AG75, and C90FA10AG100 report the formation of calcium silicate hydrate by the loss of water. The dehydration of portlandite for samples C90FA10, C90FA10AG25, C90FA10AG50, C90FA10AG75, and C90FA10AG100 was observed in between 446.6 ℃ to 452.8 °C. The dehydration of calcium carbonate of the composites was observed between the endothermic peaks of 620.3℃ to 688.7 °C. The presence of C-S-H due to the addition of aerogel was observed at 830 °C.

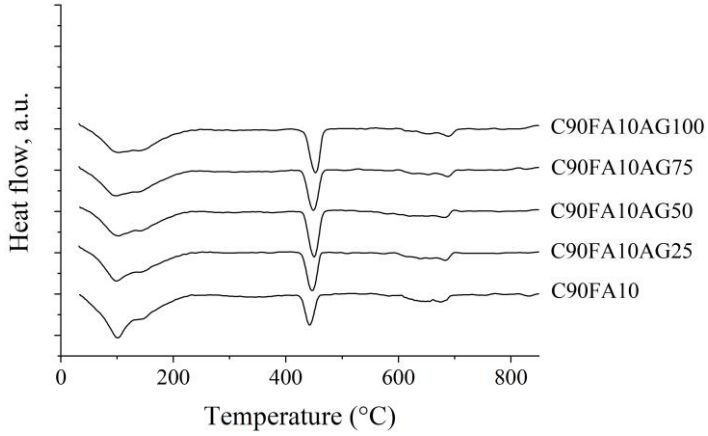

Fig. 2. 4 Differential scanning calorimetry curves of lightweight cement composites

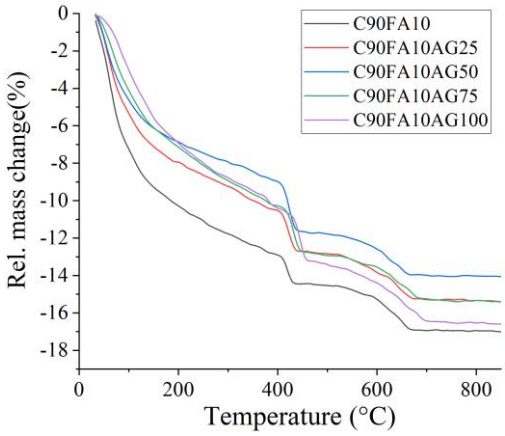

Fig. 2. 5 Derivative thermogravimetric curves of lightweight cement composites

The weight loss due to the dehydration of calcium hydroxide for samples C90FA10, C90FA10AG25, C90FA10AG50, C90FA10AG75, and C90FA10AG100 was measured to equal 1.71%, 2.15%, 2.63%, 2.36%, and 2.80%, respectively. The presence of portlandite for sample C90FA10 C90FA10AG25, C90FA10AG50, C90FA10AG75, and C90FA10AG100 was about 7.03, 8.84%, 10.81%, 9.70% and 11.51%, respectively. It can be evidently observed that, with an increase in the aerogel concentration in the lightweight cementitious system, the amount of portlandite increased.

Aerogel is an extremely brittle material in nature; an SEM image of aerogel is presented in Fig. 2.6. It can be observed that the surface of aerogel consists of several microscopic level cracks which are likely to lead to the weakening of the strength properties. The SEM image presented in Fig. 2.7 also shows the distribution of irregular-shaped silica aerogel in the cement composite.

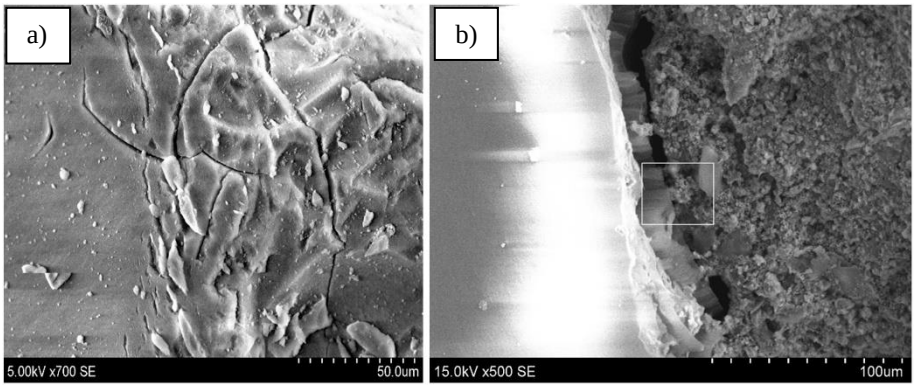

Fig. 2. 6 SEM image showing a) cracks in aerogel particles on the microscale level; b) a separation gap between an aerogel particle and cementitious material

The smooth and clean surface of silica aerogel suggests that no degradation occurred during the cement hydration. During the cement hydration, aerogel particles remained fairly stable. Similar phenomena were observed by (Gao et al., 2014). (Zhu et al., 2019) reported that aerogel particles partially dissolve in the alkaline environment provided by cement hydration, and aerogel particles may react with the pore solution, which leads to the formation of C-S-H at a low Ca/Si ratio. The SEM images presented in Fig. 2.6 show separation gaps between the hydrophobic silica aerogel and cementitious composites. This phenomenon indicates a weaker adhesion level of silica aerogel with cementitious composites. Through these gaps, air or water can easily transport harmful ions and impact the durability characteristics of the composite, and especially the composite exposed to aggressive environments. The SEM image presented in Fig. 2.8 also shows the presence of C-S-H gels and a needle of ettringite. The presence of the honeycomb structure of C-S-H gels was at a higher amount for the composite containing higher concentrations of aerogels in the composites. C-S-H gel is responsible for the strength gain of

concrete. The SEM image also shows that expanded glass aggregates and prefabricated air bubbles exhibit greater adhesion with cementitious materials.

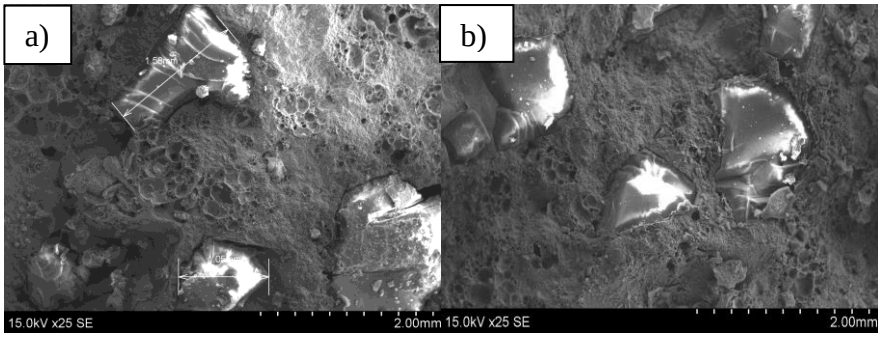

Fig. 2. 7 SEM image showing a) and b) distribution of aerogel particles in lightweight concrete samples

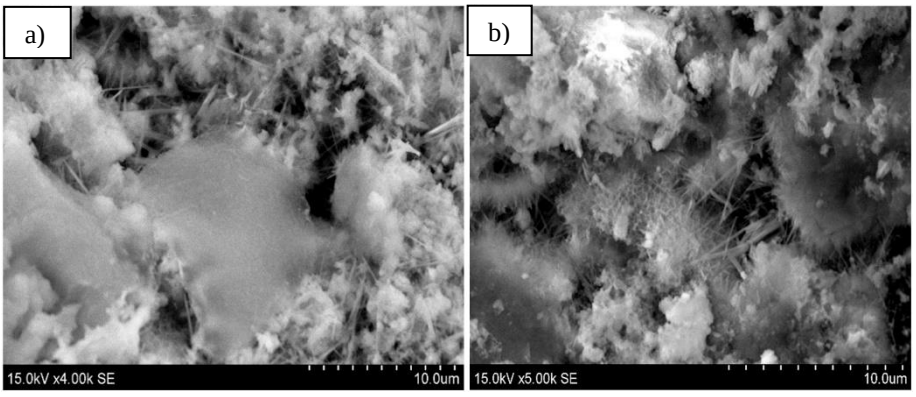

Fig. 2. 8 Scanning electron microscopy image of LWC samples (a) C90FA10AG50 and (b) C90FA10AG100 showing the presence of the honeycomb structure of calcium-silicate-hydrate gels

2.1.2. Investigation of the impact of pozzolanic additions and lightweight aggregates on the characteristics of self-compacting lightweight cement composites

This chapter is based on the paper published in *Case Studies in Construction Materials*, 2022, e00879 (Adhikary et al., 2022b). In this study, the self-compacting criteria of the lightweight cementitious composite were satisfied in accordance with the EFNARC guidelines. The experiments were performed, the data was collected, and the manuscript was written by doctoral student Suman Kumar Adhikary under the supervision of Žymantas Rudžionis. Simona Tučkutė helped to perform the SEM and XRD tests. Žymantas Rudžionis helped to finalize the manuscript in the process of the publication of the article.

From the obtained results of the first step, the mixing composition was optimized by using the mixing and trail methods to achieve self-compactibility. The

self-compacting criteria, such as the passing ability and the filling ability were fulfilled in accordance with the EFNARC recommendations. Several samples were prepared by using varied EGA and aerogel concentrations. In this study, comparatively higher binders and fine grains of EGA were used to eliminate the floating of lightweight aggregates and to maintain uniform aggregate distributions. We also aimed to develop several lightweight self-compacting cementitious composites within the 1400 kg/m^3 density range featuring 10–20 MPa compressive strength. The impact of pozzolanic additives, such as fly ash, zeolite, and aerogel, on the physical and mechanical properties of LWSCCC were also investigated. The impact of aerogel on the physical, mechanical, and microstructural properties was systematically investigated. In addition, the porosity of the cementitious composite was calculated, and the relationships with the mechanical strength were also established. This study agreed with the outcome of the first step of the study, and separation gaps between aerogel and cementitious materials were also observed. Moreover, entrapped air bubbles surrounding aerogel particles were presumed to potentially increase the porosity, which leads to a decline in the mechanical performance.

Expanded glass and aerogel were employed as LWA in the production of LWSCCC with the addition of OPC (CEM I 42.5 R) and zeolite powder (50m) used as mineral admixtures. The first series of cement composites was prepared to study the influence of the EGA content and pozzolanic additives on the characteristics of LWSCCC. Composition mixture C100S100 was formed by combining natural sand with EGA of various sizes (0.1–0.3 mm, 0.25–0.50 mm, 0.5–1 mm, and 1–2 mm) in various proportions. In sample C100S50, half of the volume of sand was replaced with a very fine fraction of 0.1–0.3 mm EGA, which resulted in a lower density of the investigated material. An increase in the fine content marginally increases the amount of the required water and superplasticizer so that to keep the desired flowability of the composite at its intended level. As pozzolanic additives for the concrete mixes, C90ZL10, C90FA10 and C90ZL5FA5, a total of 10% of the total mass of the total binders was used. The fresh properties of LWSCCC, such as the slump flow, J-ring, V-funnel, and T-50 flow time, were measured. The obtained fresh properties of the composite were validated with EFNARC recommendations. EFNARC is a European federation dedicated to specialist concrete systems and construction chemicals, and it also provides guidelines for SCC. Most European countries follow their specified guidelines.

Afterwards, a few more LWSCCCs were developed, thereby optimizing the finest sample from C100S100 to C90ZL5FA5. Sample C90ZL10 was considered to be optimized, and this sample was used as a control sample for the upcoming LWSCCC samples. Four more LWSCCC samples were prepared with different amounts of the aerogel content. 0.5–1- and 1–2-mm size EGA were replaced with aerogel (75 kg/m^3 bulk density) in amounts of 25%, 50%, 75%, and 100%. Throughout all the composite samples, the water-to-binder ratio was sustained at 0.55. In the following Table 2.4, the mixing composition of all LWSCCCs is presented. During the process of mixing, EGA, zeolite powder, and cement were all

carefully mixed together in the dry state. Following that, 70% of the total water content was mixed, which was then manually mixed for another three minutes. The superplasticizer and stabilizer were then combined with 30% water solution and gently mixed for 2 minutes before being added to the composite mixture. In the final stage, aerogel was added to the composite mixture in an attempt to reduce the crushing of the aerogel particles, and the mixture was then mixed for the next two minutes.

Table 2. 4 Mixing composition of lightweight self-compacting cement composite, kg/m^3 (stage – I-B)

Mix	Cement	Sand	Aggregate (1/2+1/0.5+0.5/ 0.25+0.01/0.3)	Aerogel	Zeolite	Fly ash	VMA	SP	Water	
									kg/m^3	w/b
C100S100	550	380	45+56+44+56	-	-	-	0.38	5.5	247	0.45
C100S50	530	183	43.4+54+42.4+ 43.6	-	-	-	0.38	6.9	309	0.58
C90ZL10	525	-	47.7+59.4+46.6 +59.4+95.8	-	58.3		0.36	8.7	321	0.55
C90FA10	525	-	47.7+59.4+46.6 +59.4+95.8	-	-	58	0.36	8.7	321	0.55
C90ZL5F A5	525	-	47.7+59.4+46.6 +59.4+95.8	-	29.2	29.2	0.36	8.7	321	0.55
C90ZL10 AG25	525	-	35.8+44.5+46.6 +59.4+95.8	8	58.3	-	0.36	8.7	321	0.55
C90ZL10 AG50	525	-	23.9+29.7+46.6 +59.4+95.8	16	58.3	-	0.36	8.7	321	0.55
C90ZL10 AG75	525	-	11.9+14.9+46.6 +59.4+95.8	24	58.3	-	0.36	8.7	321	0.55
C90ZL10 AG100	525	-	0+0+46.6+59.4 +95.8	32	58.3	-	0.36	8.7	321	0.55

The workability of the LWSCCC samples is shown in Table 2.5. According to the findings of the study, a composite mixture with fly ash is denoted by the largest flow diameter. The mini-slump flow and the mini-V-funnel time of samples C100S100, C100S50, C90ZL10, C90FA10, and C90ZL5FA5 were 247 to 258 mm and 7.2 to 9 seconds, respectively. The use of irregularly shaped sand, a lower w/b ratio, and reduced superplasticizer doses all contributed to the smallest slump flow diameter of sample C100S100. An increase in fine EGA concentration in cement composite mixture C100S50 increases the water needs and superplasticizer doses to keep the workability of LWSCC at a desired satisfactory level. Additionally, EGA has a greater water absorption capacity than the natural aggregates, which may result in a rise in the demand for water/superplasticizer doses. Meanwhile, on the other hand, the workability of composite samples C90ZL10, C90FA10, and C90ZL5FA5 was significantly improved, which could be attributed to the addition of fine pozzolans and the increased superplasticizer doses. As shown in Fig 2.9, no visual segregation of the lightweight cement composites was observed. The addition of fly

ash may have a dilution effect on the cement particles as the amount of flocculation that occurs between them was reduced. Apart from that, spherical-shaped fly ash particles offer the additional benefit of facilitating the movement of the neighboring particles, which results in ball-bearing effects. The fresh properties of LWSCCC were slightly diminished by adding aerogel.

Table 2. 5 Workability of LWSCCC (stage – I-B)

Composite Mix	Flow table diameter, mm	V-funnel time, seconds (according to EFNARC guideline V-funnel dimensions for mortar)	Slump cone diameter, mm		V-funnel time, seconds (EFNARC guideline V-funnel dimensions for concrete)	
C100S100	247	9	720	SF2	6	VF1
C100S50	248	8	725	SF2	5	VF1
C90ZL10	256	7.2	800	SF3	4	VF1
C90FA10	258	8	820	SF3	5	VF1
C90ZL5FA5	257	8.1	807	SF3	5	VF1
C90ZL10AG25	256	8	795	SF3	5	VF1
C90ZL10AG50	251	8.5	750	SF2	5.5	VF1
C90ZL10AG75	247	9.2	717	SF2	6.1	VF1
C90ZL10AG100	245	9.5	700	SF2	6.3	VF1

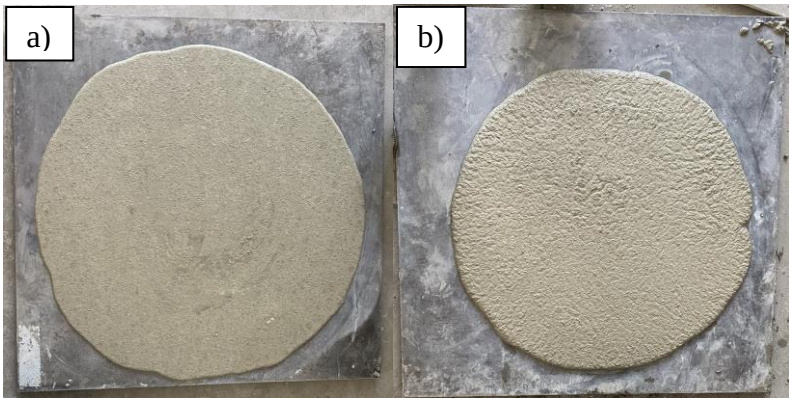

Fig. 2. 9 Slump flow of cement composites a) without aerogel and b) with aerogel showing no visual segregation

The slump flow diameter slightly declines as the aerogel replacement concentration increases, while the V-funnel time increases as the concentration of the aerogel replacement increases. The mini-slump flow diameter is reduced by nearly 4.3% by replacing 100% of the volume of aerogel with EGA in sizes of 2/1 and 1/0.5 mm. Aerogel's surface chemicals, carboxylic (–COOH) and hydroxyl (–OH), have the ability to absorb some water, which results in a reduction in the workability of the material (Suman Kumar Adhikary et al., 2021a). In this study, a slight decrease in the workability of LWSCCC was observed, which may have been caused by a similar factor. However, all the samples satisfied the requirements of EFNARC to be called SCC. Aerogel-based cement composite C90ZL10AG25

satisfied the SF3 slump class, while C90ZL10AG50, C90ZL10AG75, and C90ZL10AG100 satisfied the SF2 slump class.

Table 2.6 shows the f_c and f_{fl} of all the LWSCCC samples. The LWSCCC samples from F through J feature f_c and f_{fl} ranging from 21.3 to 12.4 MPa and 5.5 to 2.56 MPa, respectively. Sample C100S100 of LWSCCC was prepared by using a mix of sand and EGA, which exhibits the greatest growth in f_c and f_{fl}.

Table. 2. 6 Physical and mechanical characteristics of lightweight cementitious composites

Samples	f_c, MPa	f_{fl}, MPa	Density, kg/m^3	Total porosity, %	Thermal conductivity, [W/(m·K)]
C100S100	21.3	5.5	1343	50	0.62
C100S50	19.8	4.8	1178	56.5	0.5
C90ZL10	15.1	2.6	1126	56.9	0.475
C90FA10	12.8	3.5	1154	55.1	0.495
C90ZL5FA5	14.8	3	1146	55.7	0.485
C90ZL10AG25	13.6	2.3	1126	58.7	0.47
C90ZL10AG50	11	2.3	1076	60.2	0.45
C90ZL10AG75	9.1	2.0	1044	62.1	0.427
C90ZL10AG100	7.9	1.7	1019	64.2	0.418

Compressive strength is reduced as the EGA content is increased in the composite. An explanation for this phenomenon is that sand and EGA work better together, which leads to the development of greater strength. The mechanical strength of porous-structured EGA is lower, and a large amount of EGA in concrete reduces its strength. Owing to slower hydration, fly ash could contribute to a weaker strength at an early age. Despite this, composite samples C90ZL10 and C90ZL5FA5 with zeolite are denoted by higher compressive strengths than sample C90FA10. This shows that the addition of zeolite to LWSCCC will improve its compressive strength more effectively. Composite specimens C90ZL10, C90FA10, and C90ZL5FA5 show a higher water/binder ratio, which may have contributed to their decreased strength. According to the findings, f_c and f_{fl} decreased as the aerogel concentration increased. The deterioration of f_c was more significant than f_{fl} degradation. When 100% aerogel replaced 1/0.5 and 2/1 mm EGA, f_c and f_{fl} decreased by 49.2% and 34.6%, respectively. The f_c of the control sample, C90ZL10AG25, C90ZL10AG50, C90ZL10AG75, and C90ZL10AG100 was measured and determined as 15.12, 13.59, 11.01, 9.08, and 7.69 MPa, respectively. Meanwhile, the f_{fl} of samples C90ZL10AG25, C90ZL10AG50, C90ZL10AG75, and C90ZL10AG100 ranged between 2.56 and 1.67 MPa. The brittleness of the aerogel is responsible for the decrease in strength. The use of a combination of aerogel and expanded glass reduces strength, especially at higher aerogel concentrations. The addition of aerogel to a cement composite will unquestionably diminish the composite's strength, but it can also reduce its density while improving the material's thermal insulation (Suman Kumar Adhikary et al., 2021a).

The porosity of cementitious composite may have a notable impact on its strength and durability. The porosity of the LWSCCC samples is represented graphically in Table 2.6. The porosity of C100S50, C90ZL10, C90FA10, and C90ZL5FA5 increases with an increasing water/binder ratio and EGA concentration. Adding large amounts of EGA to LWSCCC may increase its overall porosity. The drying of free water by evaporation in cementitious composites results in the formation of pores increasing the porosity of concrete.

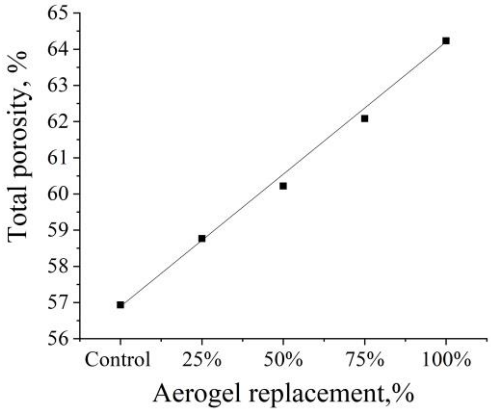

Fig. 2. 10 Relationship between the total porosity and aerogel replacement concentration in lightweight self-compacting cementitious composites

The use of EGA and a greater water/binder ratio resulted in an increased porosity. There was no significant difference in the porosity observed for the samples of pozzolan ingredients. Porosity was increased in all the LWSCCC samples by increasing the aerogel content. The total porosity of the control samples C90ZL10AG25, C90ZL10AG50, C90ZL10AG75, and C90ZL10AG100 was determined to equal 56.93%, 58.77%, 60.22%, and 62.08%, respectively. Fig. 2.10 shows that the presence of aerogel in LWSCCC enhances porosity. During the mixing process, hydrophobic aerogel entrapped some air bubbles, thereby increasing porosity and leading to a decreasing strength. EGA is a porous structural material that may also substantially enhance the porosity of concrete. Probably, the use of aerogel and EGA in combination may lead to reaching such high porosity levels.

Table 2.6 depicts the dry density of all LWSCCC samples which ranges from 1343 to 1126 kg/m^3 for the first series. According to the findings, the density of LWSCCC decreased significantly as natural sand concentrations decreased and EGA concentrations rose. A high concentration of EGA in a cement composite could lead to a decrease in its density because EGA is a much lighter material than a natural aggregate. With the addition of a pozzolan, the density slightly changes. Zeolite is lighter than fly ash; adding it to cement composites could help to reduce the density even further.

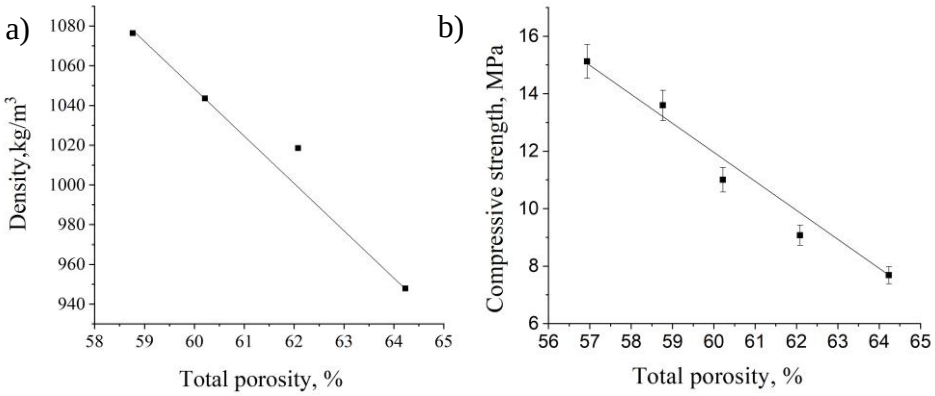

Fig. 2. 11 a) Relationship between porosity and density, and b) relationships between porosity and compressive strength of lightweight cement composites

The study results also suggest that an increase in the aerogel concentration results in a significant decline of the LWSCCC density. The density of LWSCCC was reduced by 15.8% when 1/0.5 and 2/1 EGA were completely replaced with aerogel. The oven dry density of C90ZL10AG25, C90ZL10AG50, C90ZL10AG75, and C90ZL10AG100 was measured at about 1126, 1076, 1044, 1019, and 948 kg/m^3, respectively. In light of the findings, it is obvious that the concentration of the aerogel, its density, strength, and porosity are all linked together. The porosity of LWSCCC increases along with the aerogel concentration, which results in a decrease of the density and strength. Fig. 2.11 depicts the relationship between porosity and density as well as the relationship between the porosity and compressive strength of cementitious composites. Aerogel is a much more lightweight material than EGA, and the inclusion of aerogel as a replacement of EGA significantly lowers the density of the cement composite. Moreover, the porosity of the cement composite was increased by incorporating aerogel, which may also be another reason for the decrease in density.

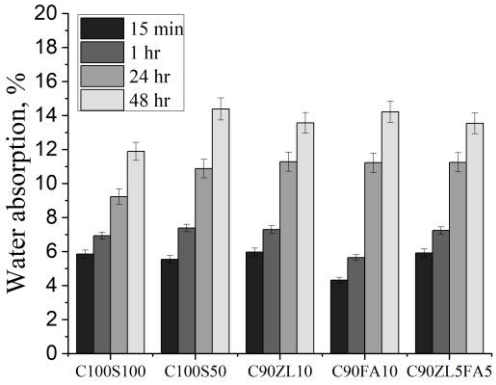

Fig. 2. 12 Water absorption of lightweight cement composite samples without aerogel content

Besides, EGA is a very light aggregate, and the combined use of EGA and aerogel results in low-density cement composites.

Fig. 2.12 and Fig. 2.13 depict water absorption for all LWSCCCSs. After 48 hours of the water absorption test, the W_A capacity of LWSCCC samples C100S100 to C90ZL5FA5 ranges from 11.9 to 14.3%. A composite specimen made with a lower water/binder ratio and EGA/natural sand mixtures exhibits lower water absorption levels than the other composite specimens.

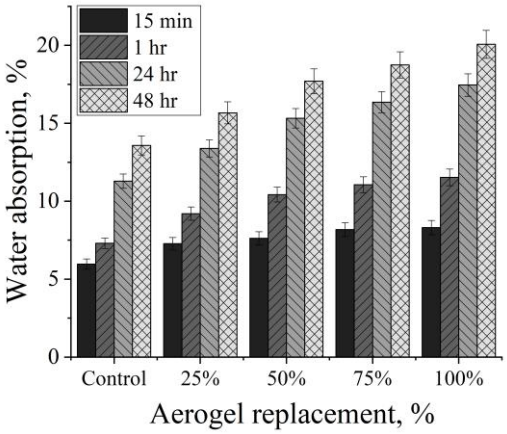

Fig. 2. 13 Water absorption of lightweight cement composite samples with aerogel content

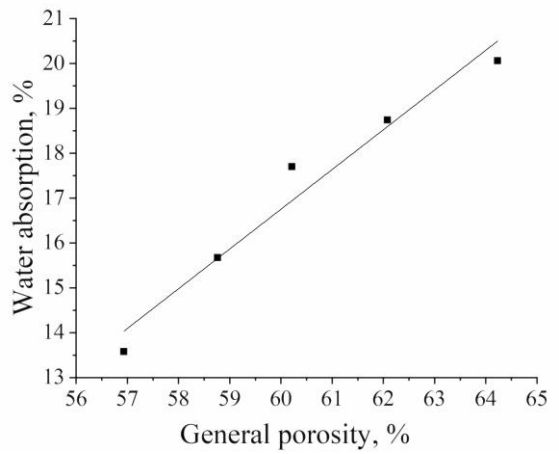

Fig. 2. 14 Relationship between water absorption and general porosity of aerogel added LWSCCC (stage – I-B)

However, the inclusion of pozzolanic materials shows no discernible effects in this study. Following a 48-hour period, the maximum water absorption of the control sample, C90ZL10AG25, C90ZL10AG50, C90ZL10AG75, and C90ZL10AG100

was measured at 13.57%, 15.67%, and 17.70%, 18.74%, and 20.06%. The rise in the content of aerogel leads to a rise in the general porosity and the open porosity of LWSCCC, which enhances water absorption. The increased porosity and water absorption capacity may be caused by trapped air bubbles in hydrophobic aerogels. Fig. 2.14 presents the relationship between porosity and the water absorption of LWSCCC incorporating aerogel.

The SEM image of LWSCCC evidently shows that a separation gap exists between the ITZ of aerogel and the cementitious materials attributed to the hydrophobic nature of aerogel.

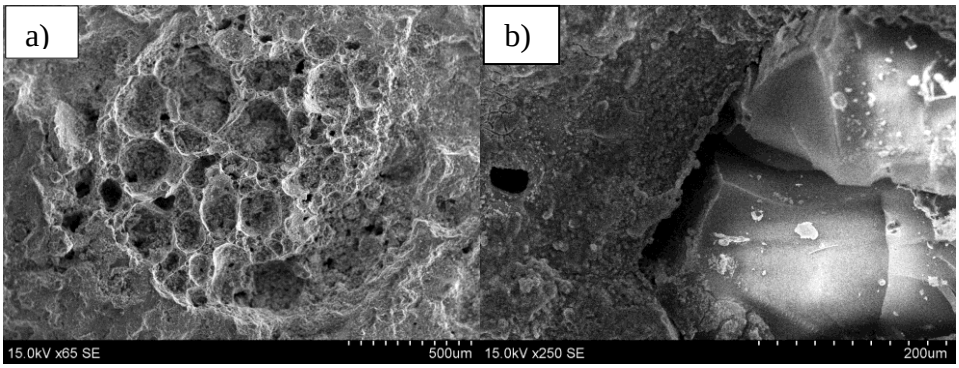

Fig. 2. 15 Scanning electron microscope image of lightweight cement composites showing a) the interfacial transition zone between the expanded glass aggregate and cementitious composites; and b) interfacial transition zone between aerogel and cementitious materials

Meanwhile, the ITZ between EGA and cement paste does not reveal any cracks or gaps. Fig. 2.15 depicts the ITZ of aerogel and EGA. This phenomenon suggests that EGA offers better adhesion with cementitious materials than aerogel. Fig. 2.16 shows several pores around aerogel particles in LWSCCC, which makes it evident that aerogel may entrap air bubbles during the mixing of fresh cementitious composites. The ITZ of EGA, as well as the presence of crystals of ettringite in the pores of EGA, is shown in Fig. 2.17. (Bumanis et al., 2013) also found ettringite in foamed glass pores and in ITZ. Fig. 2.18 shows the presence of hydration products in cementitious composites. The needle-shaped hydration products (ettringite) were observed in the cementitious system. Fig. 2.15 (b) also shows the smooth and clean surface of aerogel in the composite specimen, which suggests that no degradation of aerogel due to the hydration of cementitious materials was observed. This phenomenon suggests that aerogel particles remained rather stable during the hydration process of cement. Study results suggest that the weaker adhesion of aerogel and the presence of pores entrapped by aerogel will lead to the loss of strength and will lead to a rise in porosity.

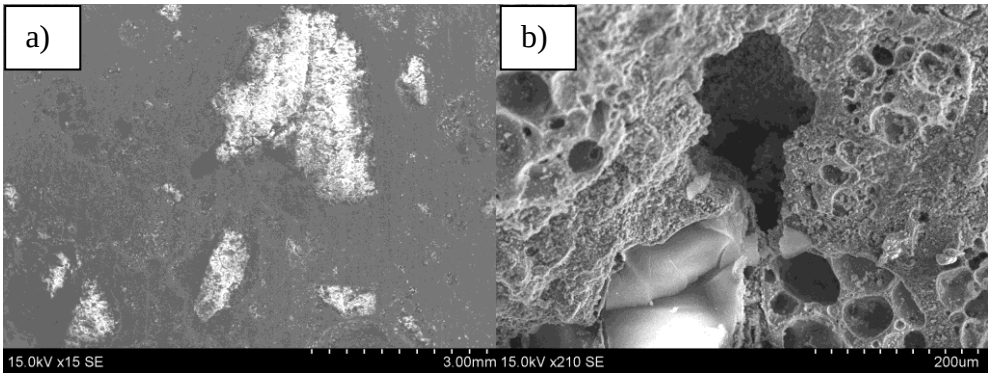

Fig. 2. 16 Scanning electron microscopy image of lightweight concrete a) and b) entrapped voids surrounding aerogel particles

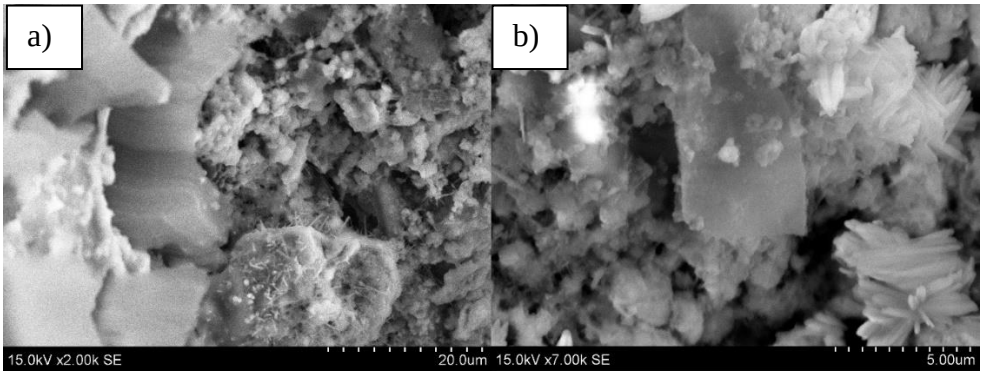

Fig. 2. 17 Scanning electron microscopy image of a) and b) aerogel added cement composite (28 days) showing the growth of hydration products

2.2. Improvement of physical, mechanical, and ITZ of LWSCCC when using polymer coatings on lightweight aggregates

This chapter is based on the paper published in *Materials Today Communications*, 2022, 103496 (Adhikary, 2022). In this study, the mechanical and water absorption of lightweight cementitious composites was improved by using polymer coatings on lightweight aggregates. The experiments were performed, the data was collected, and the manuscript was written by doctoral student Suman Kumar Adhikary under the supervision of Žymantas Rudžionis. Simona Tučkutė helped to conduct the SEM and XRD tests. Žymantas Rudžionis helped to finalize the manuscript for the publication of the article.

This study aimed to improve the physical and mechanical properties of lightweight self-compacting cementitious composites (LWSCCC) and ITZ between aerogel and cementitious materials using polymer coatings. Previously conducted studies suggested that aerogel and EGA-based lightweight cementitious composites

may increase the risk of higher water absorption. Aerogel particles also feature weaker adhesion levels with cementitious materials, which leads to weaker ITZ. In this context, polymer coatings were employed on lightweight aggregates with the objective to improve the characteristics of aerogel and EGA-based lightweight self-compacted cementitious composites. Aerogel particles were coated (a single layer) with styrene-butadiene rubber (SBR), while EGA particles were coated with single and double layer coatings of SBR and paraffin. The study results suggest that the use of polymer coating effectively improves the workability, water absorption, and ITZ between lightweight aggregates and cementitious materials. When using polymer coating, almost 6.9% and 26% improvement in the slump flow and water absorption was detected, respectively. The use of polymer coating also had a positive impact on improving the compressive strength of LWSCCC, and an almost 16% increase in compressive strength was determined.

In this experimental study, several grades of EGA were used as LWA. To coat the LWA, at first, liquid polymers were poured into a container, and lightweight aggregates were immersed for a short period of time. After about 20 seconds, the lightweight aggregates were taken out and spread on flat surfaces for the drying process. The process of creating a second layer of a similar coating was repeated. The used grades of EGA for the preparation of the first sample EGAC were 0.1–0.3 mm, 0.25–0.5 mm, 0.5–1 mm, 1–2 mm, 2–4 mm, and 2–4 mm. The second sample of the study was named A50, where 50% volume of the 2–1 mm and 1–0.5mm EGA was replaced with 2–0.5 mm aerogel particles. The first two samples, EGAC and A50, were prepared without any pre-coatings. Later on, following a similar mixing composition of A50 several samples were prepared by using different polymer coatings. Sample SBR1 was prepared with coatings of a single layer of SBR polymers on the surface of 1–0.5 mm, 2–1 mm, 4–2 mm, and 8–4 mm EGA. Similarly, PAR1 was prepared with single layer paraffin coatings on the surface of 1–0.5mm, 2–1 mm, 4–2 mm, and 8–4 mm EGA. For the composite sample SBR2, double layers of SBR coatings were employed on the surface of EGA. Subsequently, the SBR-PAR sample was coated with the first layer of SBR polymer and the second layer of paraffin coatings. In addition, aerogel particles were coated with SBR and used in the samples SBR1, PAR1, SBR2, and SBR-PAR. The water/binder ratio was kept at 0.48. Table 2.7 shows the mixing composition of the LWSCCC samples.

The initial step of mixing involves manually mixing cement, zeolite, and EGA for two minutes. The mixture was then manually mixed for three minutes with 50% water. Then, SP and stabilizer were combined with the remaining water and added to the composite. Aerogel was added last to the composite mixture so that to avoid the crushing of aerogel particles. The final LWSCCC mixture was mixed for two minutes, and the research afterwards proceeded to the workability test.

The workability of LWSCCC is presented in Table 2.8. The findings of the study show that the addition of aerogel to the composite greatly reduces the slump flow of the composite. Aerogel was used to partially replace EGA in LWSCCC, which resulted in a reduction of the slump flow from 81 cm to 73.2 cm. The surface chemicals of aerogel may absorb water, which leads to a decline in the workability

of the cementitious system (Suman Kumar Adhikary et al., 2021a; Venkateswara Rao et al., 2003).

Table 2. 7. Mixing composition of polymer modified LWSCCC, kg/m^3 (stage – II)

Mix	Cement	Aggregate (4/8+2/4+1/2+1/ 0.5+0.5/0.25+0.0 1/0.3)	Aerogel	Zeolite	SP	Water	
						Kg/m^3	w/b
EGAC	568.4	12.8+14.3+36.2+49.62+50.5+168.1	-	63.2	9.42	302.4	0.48
A50	568.4	12.8+14.3+18.1+24.8+50.5+168.1	11.8	63.2	9.42	302.4	0.48
SBR1	568.4	12.8+14.3+18.1+24.8+50.5+168.1	11.8	63.2	9.42	302.4	0.48
PAR1	568.4	12.8+14.3+18.1+24.8+50.5+168.1	11.8	63.2	9.42	302.4	0.48
SBR2	568.4	12.8+14.3+18.1+24.8+50.5+168.1	11.8	63.2	9.42	302.4	0.48
SBR-PAR	568.4	12.8+14.3+18.1+24.8+50.5+168.1	11.8	63.2	9.42	302.4	0.48

Table 2. 8. Workability of polymer modified LWSCCC, (stage – II)

Mix	Slump flow, cm		T_{50}, sec		V-funnel time, sec		J-ring height, cm
EGAC	81	SF3	5	VS2	6	VF2	9.4
A50	73.2	SF2	5.5	VS2	6.5	VF2	9
SBR1	74.5	SF2	5	VS2	5.4	VF2	9
PAR1	78.2	SF3	4.5	VS2	5	VF2	9.6
SBR2	75	SF2	5	VS2	6	VF2	8.5
SBR-PAR	76	SF3	5	VS2	6	VF2	9.5

The inclusion of aerogel in a cementitious system may trap air bubbles, which leads to a decline in workability. However, a single layer of SBR and paraffin-coated EGA shows modest improvement in workability. The study also produces evidence that a single-layer paraffin-coated EGA is more workable than an SBR-coated EGA. The slump flow of PAR1 and SBR1 shows 6.9% and 1.8% improved workability over sample A50. T_{50} flow time, as shown in Table 2.8, is in the range between 4.5 to 5.5 seconds. T_{50} flow time of EGAC was observed to equal 5 seconds, which increased to 5.5 seconds when aerogel was used as a replacement in A50. T_{50} flow time was slightly shortened in a single-layer SBR and paraffin-coated EGA-based cementitious system. The composite samples had J-ring heights ranging from 8.5 cm to 9.6 cm. The composite samples showed no signs of blockage. Probably due to the polymer coatings, the absorption by EGA in the fresh mixture of the cementitious system was reduced, and the frictional forces between particles (Yashar and Behzad, 2021) were also reduced, which led to an improvement in workability. However, all the LWSCCC samples still satisfied the requirements of EFNARC to be termed as SCC. The slump classes of polymer-modified LWSCCC were classified as SF2 and SF3, while the V-funnel of LWSCCC was categorized as VF2.

Fig. 2.18 depicts the f_c of polymer-modified cementitious composite samples. Study results showed that the samples showed f_c values ranging from 25.9 MPa to 17.03 MPa.

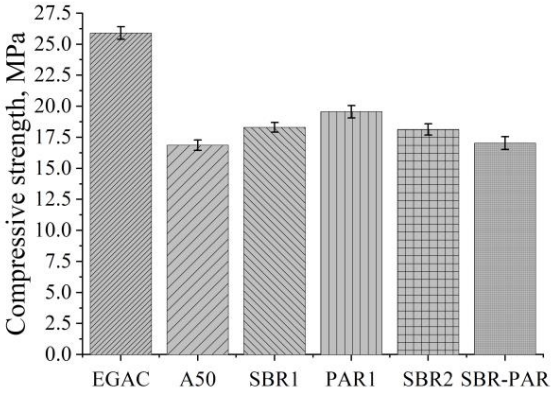

Fig. 2. 18 Compressive strength of polymer modified lightweight self-compacted cementitious composites (stage – II)

The incorporation of aerogel as partial replacement of EGA in LWSCCC reduced the f_c value by 38.9%. Aerogel is hydrophobic by nature, which leads to weaker adhesion with cementitious materials and results in an increase in porosity and a weaker mechanical strength (Adhikary et al., 2022b; Suman Kumar Adhikary et al., 2021b; Lu et al., 2020). In this study, a slight improvement in the compressive strength can be observed by pre-treating LWA with polymers. The compressive strength of the composite was improved by 8.4 and 15.9% when EGA was coated with a single layer of SBR or paraffin. The experimental study revealed that paraffin-coated EGA concrete gains a slightly higher rate of increased strength than SBR-coated concrete. Possibly due to the improvement in ITZ, polymer-coated composite samples showed an increase in strength. However, when a double layer of polymer coatings was used on EGA, the effectiveness in improving compressive strength declined. Probably, air bubbles were trapped in the composite mixture during the mixing process when double-layer coated LWA was being used, which led to an increase in porosity and a decrease in strength.

Porosity exerts key influence on the strength and long-term durability of any cementitious system. The porosity of cementitious composite samples is presented in Fig. 2.19. The porosity of composite samples ranges between 54.7 and 61.37%. The open porosity of cementitious composites ranged from 44.36% to 50.4%, and their closed porosity ranged from 10.06% to 12.57%. By replacing the partial amount of EGA in sample A50 with aerogel, the total porosity and the closed porosity both increased by 5.87% and 4.87%, respectively. Previous studies (Adhikary et al., 2022b; Suman Kumar Adhikary et al., 2021a) suggested that the combined use of aerogel and EGA in a cementitious system make it porous. Aerogel is hydrophobic, and, due to its hydrophobic nature, it may trap some air bubbles

during the mixing of a fresh cementitious composite, thereby making this material more porous (Gao et al., 2014).

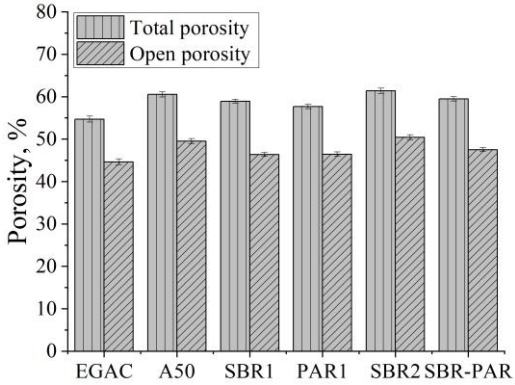

Fig. 2. 19 Porosity of polymer modified lightweight self-compacted cementitious composites (stage – II)

The porosity of LWSCCC sample A50 is likely to be enhanced by the addition of aerogel over EGAC. In contrast, single-layer coatings of SBR and paraffin on EGA showed a marginal improvement in porosity. SBR1 and PAR1 showed a decrease in the total porosity at 1.63% and 2.9% levels, respectively, as well as a drop in the closed porosity of 3.1% compared to A50. When it comes to porosity reduction, it was observed that the second layer of polymer coating on EGA did not have a great impact. Interestingly, a slight increase in porosity was observed for double-layer coated LWA. Probably some air bubbles were trapped due to the increase in hydrophobicity because of the double layer coating, which led to a rise in the porosity of composite samples.

Fig. 2.20 shows the oven-dried density of polymer-modified lightweight self-compacting cementitious composite samples. The oven-dried density of polymer-modified LWSCCC ranges between 1164 and 1065 kg/m^3. A 9.3% reduction in density was measured when aerogel was used as partial replacement of EGA. Aerogel is a much more lightweight material in comparison to other lightweight aggregates, and, probably, due to this fact, the use of aerogel as a replacement of EGA reduces the density (Adhikary et al., 2022b; Zhu et al., 2020). In addition, the air entrapped by aerogel in a cementitious system also leads to an increase in porosity, which results in a decrease in density. Polymer coatings on aerogel and EGA somewhat enhance the density of composite samples SBR1, PAR1, SBR2, and SBR-PAR. For the composite samples, a modest increase in density can be achieved by using polymer coatings on lightweight aggregates (Yashar and Behzad, 2021).

Fig. 2.21 shows the water absorption of cementitious systems. Composites feature water absorption ranging from 8.25% to 13.16% after 48 hours of immersion in water. Using aerogel as a partial replacement for EGA leads to a 59.5% increase in the water absorption capacity. However, polymer-coated lightweight aggregates were able to improve the water absorption capacity of cementitious composites. The

water absorption of lightweight cementitious composites was shown to improve more by single-layer polymer coatings applied to EGA than by double-layer coatings.

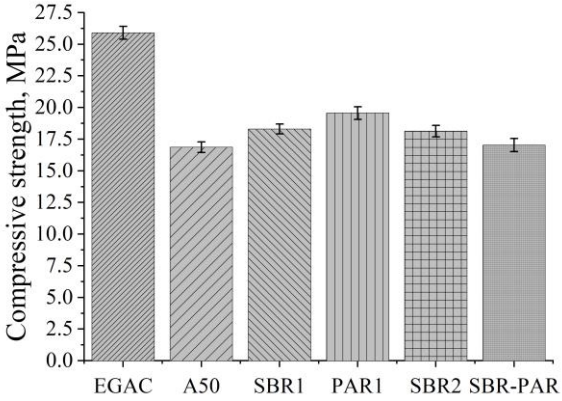

Fig. 2. 20 Density of polymer modified lightweight self-compacted cementitious samples (stage – II)

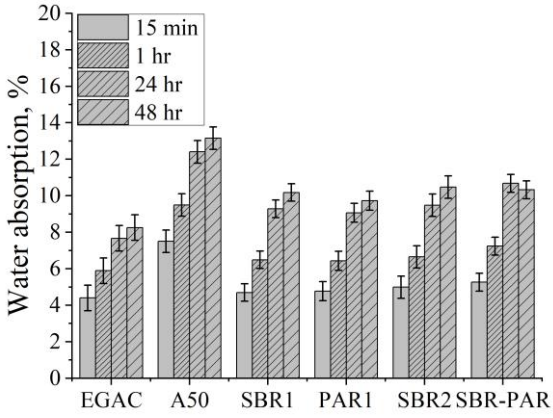

Fig. 2. 21 Water absorption of polymer modified lightweight self-compacted cementitious samples (stage – II)

LWSCCC prepared with paraffin-coated EGA exhibits a lower water absorption capacity than SBR-coated EGA. Cementitious composite SBR1 coated with a single layer of SBR and PAR1 coated with a single layer of paraffin show 22.6% and 26% lower water absorption over A50 after 48 hours of water immersion. However, LWSCCC prepared with a double polymer layer coated EGA does not appear to be significantly superior. Double-layer coated EGA shows a slight increase in water absorption when compared to single-layer coated EGA. A rise in porosity may be responsible for this outcome. Adding a second layer of coating to

LWA may trap some air bubbles and increase the porosity thereby raising the water absorption capacity.

SEM images of EGA and SBR polymers coated with EGA are shown in Fig. 2.22**.** The SEM image shows that the surface of EGA seems to be rough, and some broken shell pores may be seen. A single-layer SBR coated EGA, and a single layer paraffin coated EGA are shown in Fig. 2.22 b) and Fig. 2.23 a)**.**

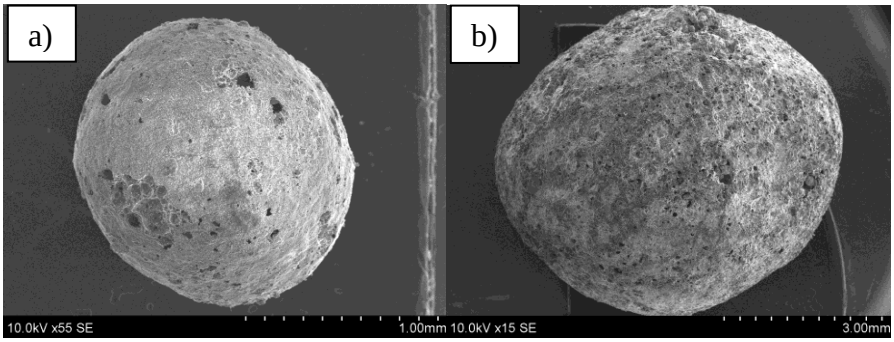

Fig. 2. 22 SEM image of a) non-coated EGA; b) single layer SBR coated EGA

The SEM image presented in Fig. 2.23 b) makes it evident that the polymer layer is well-bound on the surface of EGA, and the pores are mostly filled with polymers. Fig. 2.24 a) shows the brittleness of aerogel; many cracks are clearly visible on the surface of aerogel. Previous investigations (Adhikary et al., 2022b; 2020) also reported similar surface fractures. Fig. 2.25 a) indicates a moderate improvement in the ITZ of aerogel and cementitious materials. It seems from Fig. 2.25 that the aerogel particles were not damaged by cementitious materials. Fig. 2.25 b) shows ITZ polymer coated EGA nicely bonded with cementitious materials. Fig. 2.25 a) also reveals that the ITZ between cementitious materials and polymer-coated EGA features an extraordinarily homogeneous and dense microstructure of polymer-coated EGA. The separation gaps and the weaker adhesion between the aerogel and cementitious materials seem to have improved with polymer coatings.

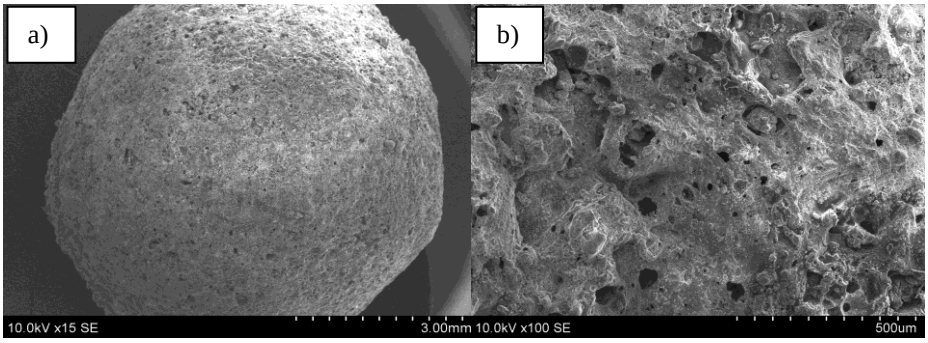

Fig. 2. 23 SEM image of a) single layer paraffin coated EGA; b) microscopic surface texture of paraffin coated EGA.

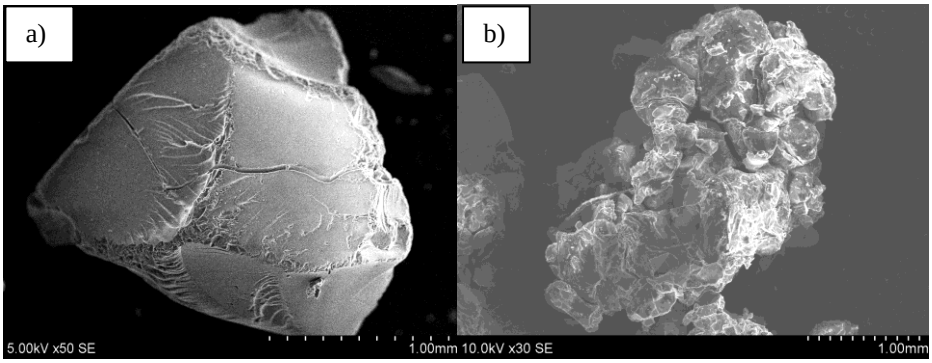

Fig. 2. 24 SEM image of a) non-coated aerogel; b) SBR coated aerogel

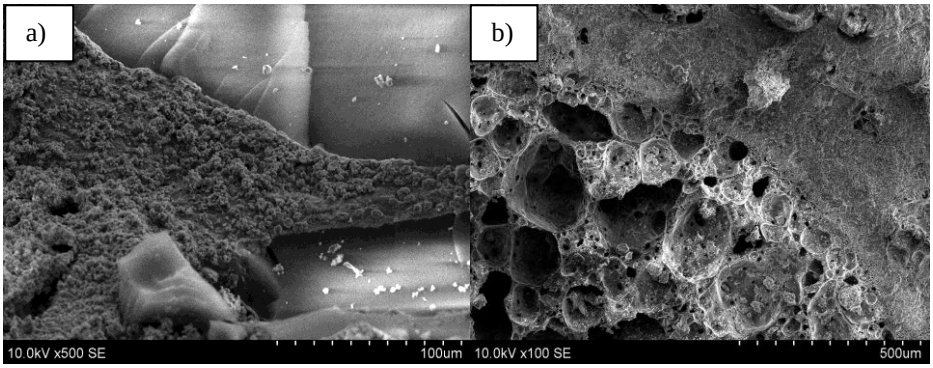

Fig. 2. 25 a) Interfacial transition zone between cementitious materials and polymer coated aerogel, b) interfacial transition zone between cementitious materials and polymer coated expanded glass

2.3. Enhancement of mechanical performance, ITZ, and water absorption characteristics of lightweight concrete by using carbon nanotubes and graphene platelets

2.3.1. Enhancement of mechanical performance, ITZ, and water absorption characteristics of lightweight cement composites by using carbon nanotubes

This chapter is based on the paper published in *Scientific reports*, 2021, 2104 (S.K. Adhikary et al., 2021). In this study, the mechanical and water absorption of lightweight cementitious composites was improved by using carbon nanotubes. The experiments were performed, the data was collected, and the manuscript was written by doctoral student Suman Kumar Adhikary under the supervision of Žymantas Rudžionis. Simona Tučkutė helped to perform the SEM and XRD tests. Žymantas Rudžionis and Deepankar Kumar Ashish helped to finalize the manuscript for the publication of the article.

This study aimed to improve the mechanical performance and water absorption of lightweight cementitious composites incorporating carbon nanotubes (CNT). The results of previous studies suggested that cementitious composites prepared with EGA and aerogel may encounter a higher risk of water absorption and lower mechanical performance attributed to the porous structure of EGA and brittleness of aerogel, respectively. In this context, CNT was incorporated into lightweight cementitious composites. Carbon nanotubes were treated with an aquacise solution of superplasticizer and water while using ultrasonic energy for 3 min. The study results suggest that the use of 0.6% CNT improves the compressive strength and water absorption of the investigated lightweight cement composite by 41% and 30%, respectively. The study results also make it evident that the separation gaps between aerogel and cementitious materials were also improved when using CNT. The presence of CNT and hydration products was observed in ITZ between aerogel and cementitious materials. The higher growth of C-S-H and pore filling effects of CNT were also confirmed in this study.

Table 2. 9 Mixing composition of carbon nanotube modified lightweight cement composite, kg/m^3 (stage – III-A)

Series	Cement	Aerogel	CNT %		Aggregate (1/2+1/0.5+0.5/0.25+0.01/0.3)	Zeolite	SP	VMA	Water w/b=0.65	Sonication time, min
			%	kg/m^3						
LWC	454.5	31.5	0	-	34.5+54+34+40	45.45	8.181	1.3635	325	-
LWCC NT0.04	454.5	31.5	0.04	0.1818	34.5+54+34+40	45.45	8.181	1.3635	325	3
LWCC NT0.1	454.5	31.5	0.1	0.4544	34.5+54+34+40	45.45	8.181	1.3635	325	3
LWCC NT0.15	454.5	31.5	0.15	0.6816	34.5+54+34+40	45.45	8.181	1.3635	325	3
LWCC NT0.30	454.5	31.5	0.30	1.3632	34.5+54+34+40	45.45	8.181	1.3635	325	3
LWCC NT0.45	454.5	31.5	0.45	2.0453	34.5+54+34+40	45.45	8.181	1.3635	325	3
LWCC NT0.60	454.5	31.5	0.60	2.7264	34.5+54+34+40	45.45	8.181	1.3635	325	3

In this stage, aerogel-based cement composites were reinforced with carbon nanotubes containing up to 0.6% of cement mass. At first, cement zeolite and expanded glass aggregates were mixed in dry conditions for 2 minutes. Afterwards, carbon nanotubes were dispersed with ultrasonic energy. A polycarboxylate-based superplasticizer was added with 40% of the total water. Subsequently, nanotubes were added to the solution and dispersed with ultrasonic energy for 3 minutes. The remaining constituent (60% water) was poured into the dry mixture and mixed by hand for 2 minutes. The solution of sonicated CNT was added to the lightweight cement composite mixture and mixed for 3 minutes. As the last stage of the study,

aerogel particles were added and mixed for another 2 minutes. The mixing composition of CNT reinforced cement composites is presented in Table 2.9.

The research of the flowability of CNT-modified lightweight cement composites was performed by using a flow table. From the study, it was observed that the workability of CNT-modified cement composites decreased with an increase in CNT concentration. By incorporating 0.6% CNT in cement composites, almost 17% reduction in the flow diameter was observed. The flow diameter of cement composites is presented in Fig. 2.26.

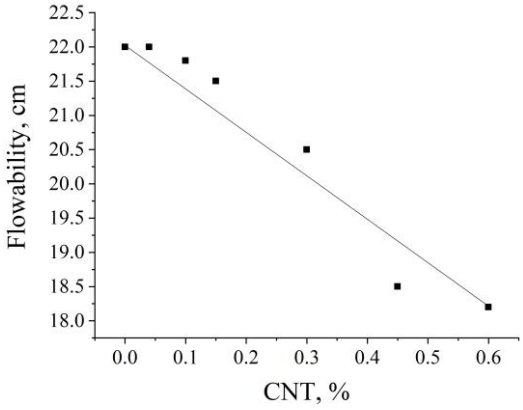

Fig. 2. 26 Flowability of sonicated CNT-LWAC specimens

The reduction in the flowability of cement composites by incorporating CNT may be attributed to the surface area and the elongated shape of nanoparticles. At higher CNT doses, the high specific gravity of CNTs also enhances the demand for superplasticizers to overcome the intermolecular forces. Moreover, the incorporation of nanoparticles in concrete increases the packing density by filling up the mesopores and micropores, which may significantly impact the demand for superplasticizers (Farooq et al., 2020).

The semi-adiabatic temperature was also investigated so that to study the impact of aerogel and carbon nanotubes on cement hydration. The semi-adiabatic temperature rise of the composite samples is presented in Fig. 2.27. From the study results, it is completely evident that the inclusion of silica aerogel with cement achieves lower exothermic heat compared to plain cement mortar. The study results also suggest that the initial setting time of plain cement paste was determined at 27 min, and the process finished at 388 min. When aerogel was added to cement paste sample C100AG31.5, the initial setting time was retarded to 67 min, while the final setting time was observed at 385 min. However, by adding CNT, the initial setting was shortened, and the final setting time was slightly retarded compared to the aerogel added cement paste. The initial setting time of 0.04% and 0.15% CNT added cement paste samples, C100AG31.5CNT0.04 and C100AG31.5CNT0.15, was observed at 52 min and 28 min, respectively. Meanwhile, the final setting time of

C100AG31.5CNT0.04 and C100AG31.5CNT0.15 was observed at 401 min and 414 min, respectively.

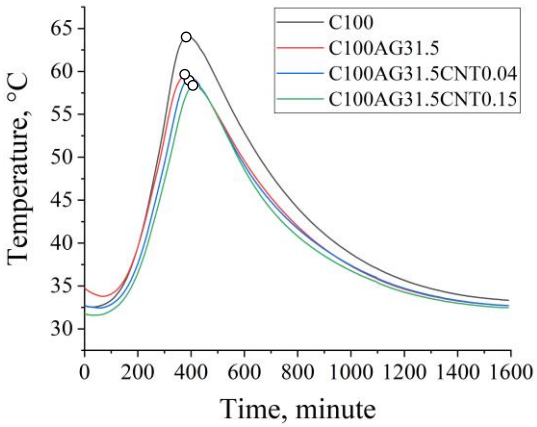

Fig. 2. 27 Hydration of cement mortar containing aerogel and sonicated CNTs

The f_c values of CNT modified cement composite specimens are shown in Fig. 2.28. The control sample had an average compressive strength of 5.4 MPa. Study results suggest that the incorporation of CNT to lightweight cement has a substantial impact on the mechanical properties. The f_c value of the cement composite was continuously increased as the proportion of CNTs was increased as well.

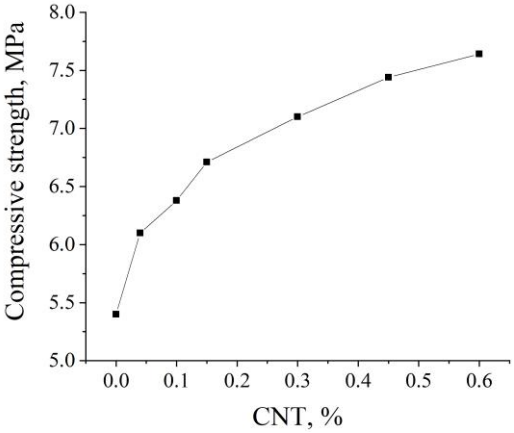

Fig. 2. 28 Compressive strengthsof CNT-LWAC specimens

Cement composite with 0.60 wt.% CNT improved the f_c of LWC by 41.48%. Fig. 2.29 depicts the proportionate rise in f_c of CNT modified LWC. A considerable improvement in f_c was observed when CNTs were added to aerogel-based lightweight cement composites. Probably, the improved microstructure and nucleating effects of

CNT led to an increase in the compressive strength. The presence of the C-S-H structure around the CNTs was observed, and the nucleating effects of CNT were made evident. The presence of hydration products and CNTs in the microcracks/gaps was also observed which may provide additional support and contribute to the improvement in compressive strength. The literature also suggests that the addition of nanoparticles in a controlled manner enhances the microstructure and results in a denser concrete structure (Farooq et al., 2020).

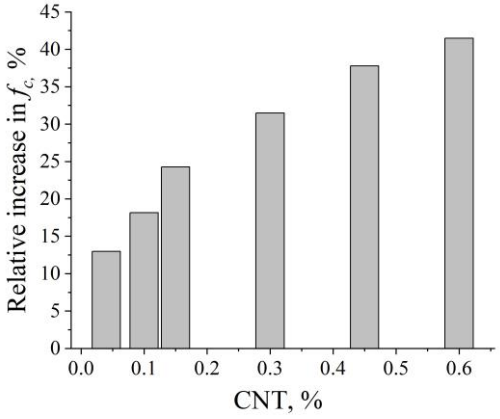

Fig. 2. 29 Relationship between the relative increase in doses of carbon nanotubes and compressive strength of lightweight cement composites

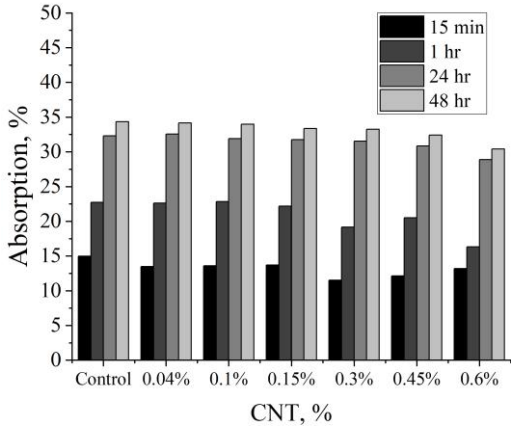

Fig. 2. 30 Water absorption of CNT-LWAC specimen

Water absorption kinetics of the CNT-LWAC specimen with up to 0.60 wt.% CNTs is shown in Fig. 2.30. The water absorption of the control sample after 24 hr and 48 hr of water immersion was measured at 32.33% and 34.33%, which was reduced to 28.86% and 30.42% at 0.6% CNT reinforcements. Nano reinforcement improves the water absorption by 12% over the control sample. (T.Ch et al., 2012)

and (Leonavičius et al., 2018) observed that the addition of CNTs reduced the total pore volume by filling gaps, which, in turn, reduced water absorption in the test samples. The study results made it evident that, as the concentration of CNTs increased in the cementitious system, the effectiveness in the improvement of water absorption was also increased. The reduced water absorption is conditioned by the addition of CNTs to lightweight concrete, which reduces micropores and results in a denser concrete structure.

As seen in Fig. 2.31, hydrophobic silica aerogel appears to be a brittle material with surface cracks. As a result, the mechanical properties of the researched lightweight cement composite were reduced.

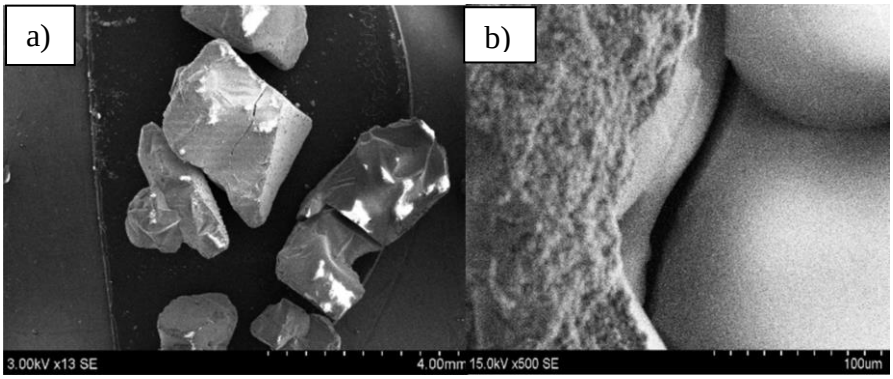

Fig. 2. 31 Scanning electron microscopy image a) showing cracks on the surface of native silica aerogel, b) cracked aerogel in the hydrated concrete specimen

Fig. 2.31 also shows cracked aerogel particles in the lightweight cement composite which may be attributed to the weaker mechanical strength of aerogel. During the mixing of fresh, lightweight cement composite, aerogel particles may easily break into pieces. Literature evidently states that aerogel is brittle, and the incorporation of aerogel reduces the mechanical performance (Liu et al., 2016; Westgate et al., 2018).

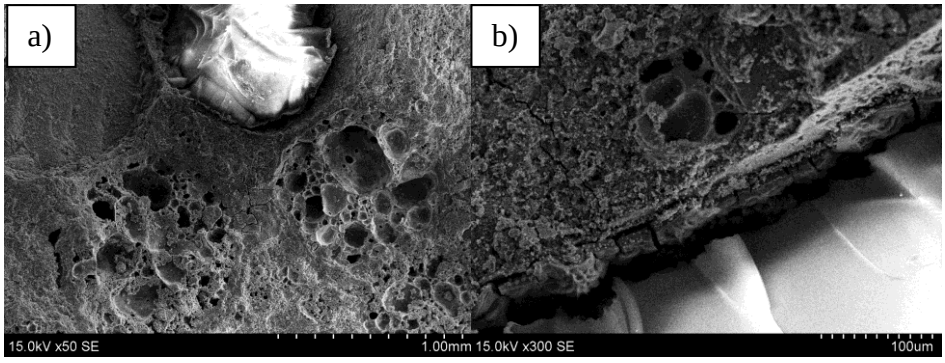

Fig. 2. 32 SEM image a) and b) showing the interfacial transition zone of aerogel evidencing the separation gaps between aerogel and cementitious materials

Hydrophobic silica aerogel has no chemical bonds with hydrophilic cement. Probably due to this fact, a separation gap in ITZ between the aerogel and cementitious materials was observed, as shown in Fig. 2.32. Several researchers also observed a similar phenomenon of lower adhesion of aerogel and the presence of separation gaps in ITZ between aerogel and cementitious materials (Gao et al., 2014). Air and water can easily move through the gaps in the separation, thereby weakening the concrete in the process. The study results also make it evident that the use of carbon nanotubes in a small content helped to reduce the separation gaps (Fig. 2.33). Hydration products and CNTs bridged the gap between the hydrophobic silica aerogel and cement-based materials. Fig. 2.34 also evidently shows that carbon nanotubes were well dispersed within cementitious composites. A network-like distribution within the composite structure was observed at high CNT concentrations.

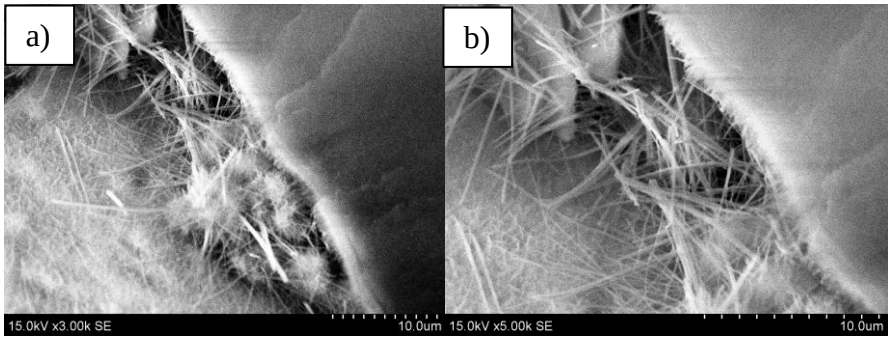

Fig. 2. 33 SEM image a) and b) showing the agglomeration of CNTs and the presence of ettringite and the honeycomb structure of C-S-H gel in the transition zone of aerogel and cementitious material

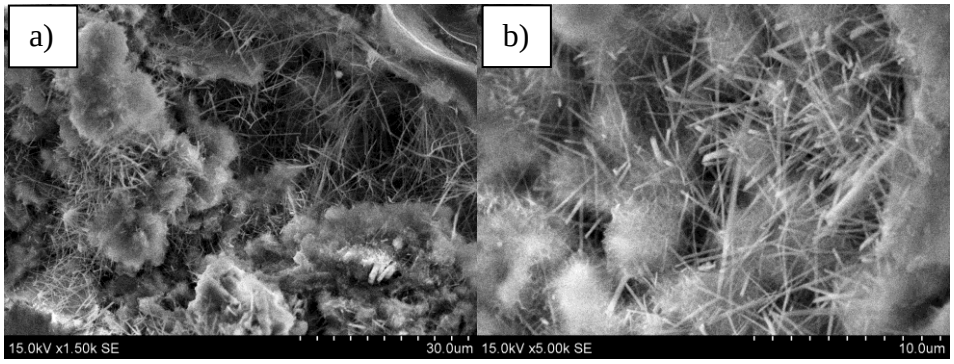

Fig. 2. 34 SEM image showing a) well-dispersed concrete sample under high concentration of CNT at different magnifications; b) presence of C-S-H gel surrounding CNTs

X-ray diffraction analysis of LWAC specimens is shown in Fig. 2.35. The X-ray diffraction pattern of a CNT-modified lightweight cement composite shows that the concentration of CNT enhances the intensity of portlandite at 34° and 47°.

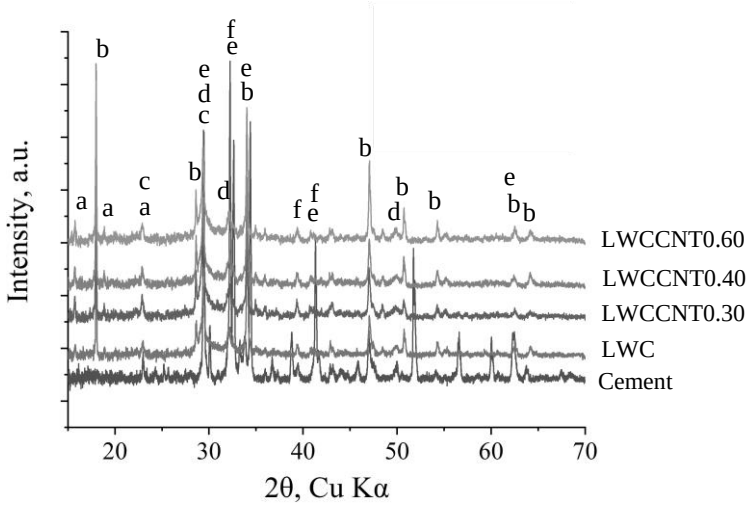

Fig. 2. 35 X-ray diffraction pattern of sonicated CNT-LWAC specimens (stage – III-A)

Note: a – ettringite $Ca_6Al_2(SO_4)_3(OH)_{12}\cdot 26H_2O$ (41–1451), b – portlandite $Ca(OH)_2$ (1–837), c – calcite $Ca(CO)_3$ (24–27), d – calcium silicate hydrate $Ca_{1.5}SiO_{3.5}\cdot x\ H_2O$ (33–306), e – alite $Ca_{54}MgAl_2Si_{16}O_{90}$ (13–272), f – belite Ca_2SiO_4 (33–302).

The nucleation effects of CNT were explained by the increasing peak of calcium silicate hydrate at 29°, 32°, and 50°. CNT-modified cement composites exhibit higher concentrations of calcite and ettringite over the control sample. When the amount of CNTs in the cement composite increases, the growth of hydration products is also increased. According to (El-Gamal et al., 2017), introducing CNT into the cementitious composite increases the hydration peak in a similar way.

2.3.2. Enhancement of mechanical performance, ITZ, and water absorption characteristics of self-compacting lightweight cement composites by using graphene platelets

This chapter is based on the paper published in *Journal of Building Engineering*, 2022, 104870 (Adhikary et al., 2022c). In this study, the mechanical and water absorption of lightweight cementitious composites was improved by using graphene platelets. The experiments were performed, the data was collected, and the manuscript was written by doctoral student Suman Kumar Adhikary under the supervision of Žymantas Rudžionis. Simona Tučkutė helped with the implementation of the SEM and XRD tests. Žymantas Rudžionis and Deepankar Kumar Ashish helped to finalize the manuscript for the publication of the article.

This study aimed to improve the mechanical performance, water absorption, and ITZ between lightweight aggregates and cementitious materials of lightweight

cementitious composites incorporating graphene platelets (GNP). The results of previous studies suggested that self-compacting cementitious composites prepared with EGA and aerogel may encounter a higher risk of water absorption and suffer from inferior mechanical performance attributed to the porous structure of EGA and the brittleness of aerogel, respectively. In this context, graphene platelets were incorporated into lightweight cementitious composites. Similarly to the previous studies, graphene platelets were also treated with ultrasonic energy in the aquacise solution of superplasticizer and water for 3 min. The study results suggest that the use of 0.25% graphene platelets improves the compressive strength of lightweight cement composite by 43.8%. The water absorption of the lightweight cementitious composite was also improved by 29% by incorporating graphene platelets. Moreover, the separation gaps between aerogel and cementitious materials were also improved by using GNP. The higher growth of C-S-H and the pore filling effects of GNP were also confirmed in this study.

Three different thicknesses of GNP of dosed range of 0.025% to 0.50% by cement mass were employed in the lightweight cementitious composite. The optimized mixing composition of this experimental study was also obtained by the mixing and trail methods. The concentration of the lightweight aggregate was kept constant, whereas the doses of GNP were increased from 0.025% to 0.5%. A combination of EGA of the grade of 0.1–0.3 mm, 0.25–0.5 mm, 0.5–1 mm, 1–2 mm, 2–4 mm, 4–8 mm was used. Meanwhile, 0.5 to 2 mm aerogel particles were also used as lightweight aggregates. The water/binder ratio was kept constant at 0.48. The used thickness of GNP was 2 nm, 6–8 nm, and 11–15 nm. The mixing composition of the cement composite is presented in Table. 2.11. In the first stage, GNP was dispersed with the total amount of water and superplasticizer by ultrasonication energy for 3 minutes. Afterward, zeolite powder, cement, and EGA were mixed manually by hand for 2 minutes. Subsequently, the ultrasonically dispersed GNP solution was added to the mixture and manually gently mixed for a further 2 minutes. At the last stage of mixing, the aerogel particle was employed and mixed for another 1 minute. Aerogel particles were mixed in the last stage of the study to avoid maximum crushing of aerogel particles. After determining the fresh properties of the cement, the composite was molded into 16.0×4.0×4.0 cm prims and kept at room temperature for one day for the hardening process to take place. The hardened cement composite was kept immersed in water in a climatic room for 28 days while maintaining ≥ 95 RH and 20±1°C temperature.

In order to study the semi-adiabatic calorimetry, several cement pastes were prepared incorporating similar doses of GNP, while maintaining a 0.40 water-cement ratio. The GNP was ultrasonically disposed of in the solution of water and superplasticizer for 3 minutes. The temperature rises of the semi-adiabatic calorimetry are presented in Fig 2.36, Fig. 2.37 and Fig 2.38. The initial setting time of the control sample only with cement paste was observed at 578 min and finished at 1153 min. Meanwhile, with the incorporation of 0.025% GNP of 2 nm thickness, the initial setting time was slightly shortened to 545 min, whereas the final setting time was extended to 1161 min. The initial setting time of cement paste containing

0.05% GNP shows a shortened initial setting time over the other samples containing 2 nm thickness of GNP. The initial setting time of cement paste containing 0.050%, 0.10% and 0.5% GNP of 2 nm thickness was observed at 515, 572 and 548 min, while the final setting time was detected at 1159, 1184 and 1195 min, respectively. A slightly higher exothermic effect of the produced heat over cement paste was observed for the sample containing 0.025% GNP of 2 nm thickness.

Table 2. 10 Mixing composition of graphene platelet modified lightweight cement composite, kg/m^3 (stage – III-B**)**

Mix	Cement	Aggregate (4/8+2/4+1/2+1/0.5+0.5/0.25+0.01/0.3)	Aerogel	Zeolite	Graphene		SP	Water
					%	kg/m^3		
Control	524.7	11.82+13.2+16.70 +22.9+46.6+155.2	10.92	58.3	0	0	8.7	279.2
2nm0.025	524.7	11.82+13.2+16.70 +22.9+46.6+155.2	10.92	58.3	0.025	0.131	8.7	279.2
2nm0.050	524.7	11.82+13.2+16.70 +22.9+46.6+155.2	10.92	58.3	0.05	0.262	8.7	279.2
2nm0.1	524.7	11.82+13.2+16.70 +22.9+46.6+155.2	10.92	58.3	0.1	0.524	8.7	279.2
2nm0.25	524.7	11.82+13.2+16.70 +22.9+46.6+155.2	10.92	58.3	0.25	1.311	8.7	279.2
2nm0.50	524.7	11.82+13.2+16.70 +22.9+46.6+155.2	10.92	58.3	0.5	2.623	8.7	279.2
6-8nm0.025	524.7	11.82+13.2+16.70 +22.9+46.6+155.2	10.92	58.3	0.025	0.131	8.7	279.2
6-8nm0.050	524.7	11.82+13.2+16.70 +22.9+46.6+155.2	10.92	58.3	0.05	0.262	8.7	279.2
6-8nm0.1	524.7	11.82+13.2+16.70 +22.9+46.6+155.2	10.92	58.3	0.1	0.524	8.7	279.2
6-8nm0.25	524.7	11.82+13.2+16.70 +22.9+46.6+155.2	10.92	58.3	0.25	1.311	8.7	279.2
6-8nm0.50	524.7	11.82+13.2+16.70 +22.9+46.6+155.2	10.92	58.3	0.5	2.623	8.7	279.2
11-15nm0.025	524.7	11.82+13.2+16.70 +22.9+46.6+155.2	10.92	58.3	0.025	0.131	8.7	279.2
11-15nm0.050	524.7	11.82+13.2+16.70 +22.9+46.6+155.2	10.92	58.3	0.05	0.262	8.7	279.2
11-15nm0.1	524.7	11.82+13.2+16.70 +22.9+46.6+155.2	10.92	58.3	0.1	0.524	8.7	279.2
11-15nm0.25	524.7	11.82+13.2+16.70 +22.9+46.6+155.2	10.92	58.3	0.25	1.311	8.7	279.2
11-15nm0.50	524.7	11.82+13.2+16.70 +22.9+46.6+155.2	10.92	58.3	0.5	2.623	8.7	279.2

Similarly, for the series of 6–8 nm GNP reinforced cement paste, the initial and the final setting time of the control sample was observed at 552 min and finished at 1254 min. However, it was discovered that 6–8 nm GNP reinforced cement paste behaves differently from 2 nm GNP reinforced cement paste. The

initial and the final setting times of 6–8 nm GNP reinforced cement paste were extended to 0.1% concentration of 6–8 nm GNP. Meanwhile, the initial and the final setting times at 0.5% GNP of 6–8 nm thickness were suddenly shortened. The initial setting times of cement paste containing 6–8 nm GNP at 0.025%, 0.050%, 0.10%, and 0.50% were observed at 569, 580, 612, and 515 min, whereas the final setting times were detected at 1257, 1264, 1316, and 1177 min, respectively.

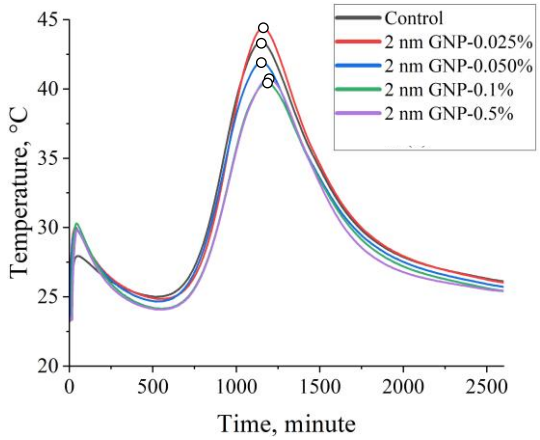

Fig. 2. 36 Hydration of nano reinforced cement paste, 2 nm graphene platelets

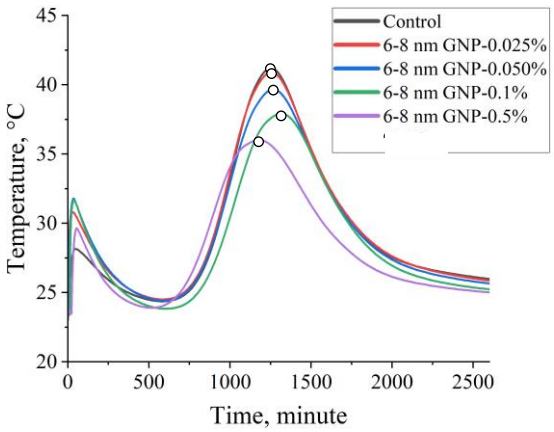

Fig. 2. 37 Hydration of nano reinforced cement paste, 6–8 nm graphene platelets

The obtained results suggest that GNP and its thickness exert notable impact on cement hydration. It was also observed that, with an increase in GNP concentration, the produced exothermic heat was decreased. However, all the cement pastes containing 0.025% GNP of various thicknesses show slightly higher produced exothermic heat over the control sample. The delay in cement hydration after certain doses of GNP may be attributed to the surface anionic charge density of GNP. Literature studies suggest that a higher anionic charge density may also lead to a delay in the formation of C-S-H (Schönlein and Plank, 2018; Zhu et al., 2021).

Study results reported that the initial growth of C-S-H may be held back by the surface area of nanomaterials (Schönlein and Plank, 2018).The hydration of cement paste containing a higher thickness of GNP may be accelerated by the formation of hydration products leading to acceleration in cement hydration.

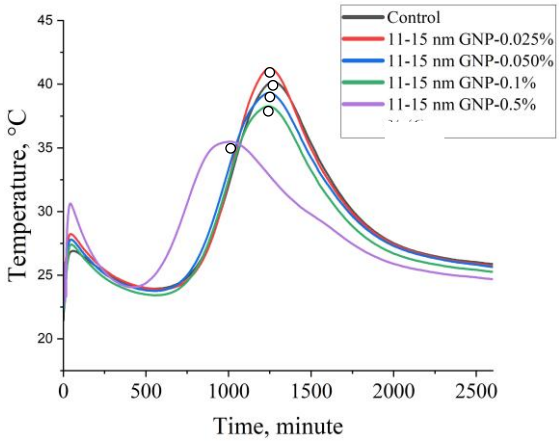

Fig. 2. 38 Hydration of nano reinforced cement paste, 11–15 nm graphene platelets

Fig. 2.39 depicts the workability of cement composite incorporating GNP. It can be clearly observed that the incorporation of GNP significantly impacts the workability of the cement composite. Moreover, the impact of the thickness of GNP was also observed. It was determined that the cement composite incorporating 2 nm GNP shows an adverse effect of up to 0.05% doses, and an almost 22.4% decline in the workability was measured. However, with the incorporation of above 0.05% GNP, an improvement in workability was observed. Meanwhile, the cement composite incorporating 6–8 nm GNP suggests a completely different observation. A slight improvement in workability (3% increase) was measured at 0.05% doses of 6–8 nm GNP; afterwards, a significant decline in workability was initiated. The decline in the workability when incorporating 0.25% and 0.5% GNP of 6–8 nm thickness was measured at about 12.2% and 20.4%, respectively. On the other hand, almost 8.1% improvement in the workability was measured when incorporating 11–15 nm GNP at 0.025%. The workability of the cement composite incorporating 11–15 nm GNP was decreased above 0.025% to 0.25%. According to EFNARC recommendations, the minimum flow table spread of self-compacted mortar is 24 mm. Our study results suggest that most cement composites incorporating GNP satisfy the required at 0.025%. However, the workability of the composite may be enhanced by adding an additional amount of water. The higher specific surface area of GNP may lead to a demand for water and also trigger a decline in the workability of cement composites (Ahmad et al., 2022). Fig. 2.40 suggests that there was no visual segregation observed for GNP-modified lightweight cement composites.

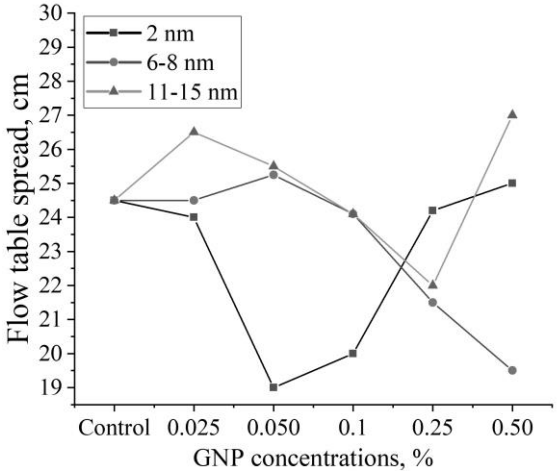

Fig. 2. 39 Workability of GNP reinforced lightweight cementitious composites, (stage – III-B)

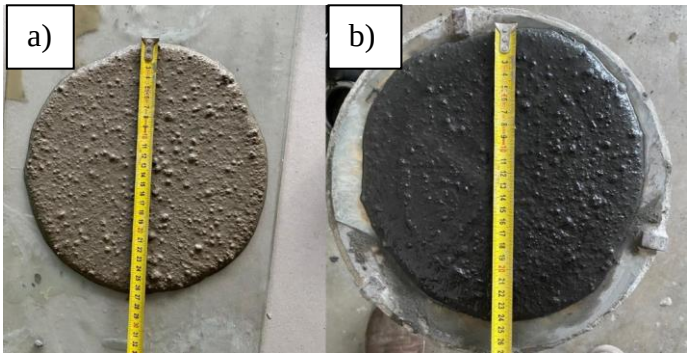

Fig. 2. 40 Flow table of a) cementitious composite without graphene platelets, and b) with graphene platelets showing no visual segregation

The f_c and f_{fl} values of the cement composite incorporating GNP are presented in Fig. 2.41 and Fig. 2.42, respectively. Study results evidently show that the incorporation of GNP and its thickness has a significant effect on the mechanical strength of the grain. The study results show that f_c value of the cementitious composite was improved by an increase in doses of GNP up to 0.25% doses. The f_c value of the control sample was measured as 11.32 MPa, which increased to 15.88 MPa, 15.52 MPa, and 14.92 MPa when incorporating 0.25% GNP of a thickness of 2 nm, 6–8 nm, and 11–15 nm, respectively. The optimum level of improvement in compressive strength was measured at about 43% over the control sample incorporating 11–15 nm GNP. However, a sudden drop in the compressive strength of the cement composite incorporating above 0.25% GNP was observed.

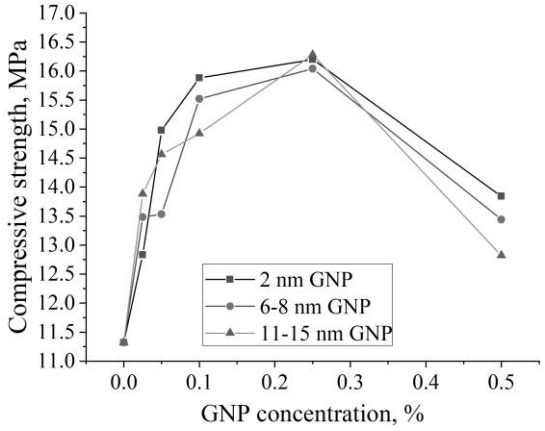

Fig. 2. 41 Compressive strength of GNP-reinforced lightweight cement composites

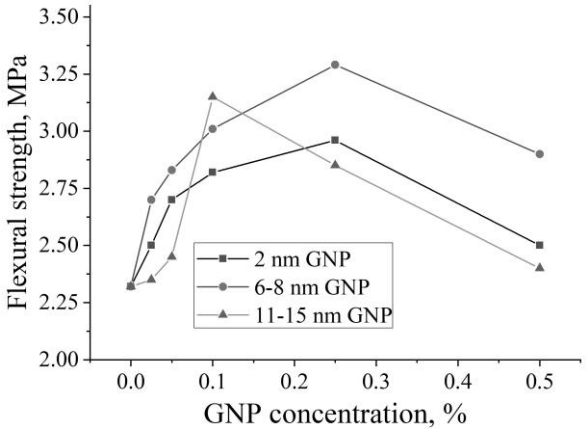

Fig. 2. 42 Flexural strength of GNP-reinforced lightweight cement composites

Similarly, the f_{fl} value of the cement composite was also increased up to a certain dose of GNP; however, it started decreasing afterwards. The optimum improvement in the flexural strength of cement composites incorporating 2 nm and 6–8 nm GNP was measured at 0.25% doses. Meanwhile, 11–15 nm GNP reinforced cementitious composite gains optimum f_{fl} at 0.1%. Almost 41.8% improvement in flexural strength of the cement composite was observed when incorporating 0.25% GNP of a thickness of 6–8 nm. Literature studies also confirm that the use of GNP in the cementitious system may improve mechanical performance (Arslan et al., 2022; Cao et al., 2016). The pore filling and nucleation effect of GNP may lead to an improvement in mechanical performance (Chen et al., 2019; Du and Pang, 2015; Matalkah and Soroushian, 2020). Probably due to these reasons, the mechanical performance of the cement composite incorporating GNP was observed. However, a drop in the mechanical performance of cement composites incorporating certain doses of GNP was also observed in this study; this phenomenon can be attributed to

the hydrophilic behavior of nanomaterials (Arslan et al., 2022). By absorbing water from the cement surface, GNP's hydrophilic behavior may prevent cement hydration (Barnard and Snook, 2008; Nazari and Riahi, 2011). Moreover, at high doses of nanomaterials, the demand for water may rise and disrupt the homogeneous distribution of nanomaterials, which would lead to a decline in mechanical performance (Chen et al., 2019). Probably, due to these facts, the mechanical performance of the cement composite declines above certain doses of GNP.

The water absorption (W_A) of the lightweight cement composite after 24 hours and 48 hours of water immersion is presented in Fig. 2.43 and Fig. 2.44, respectively.

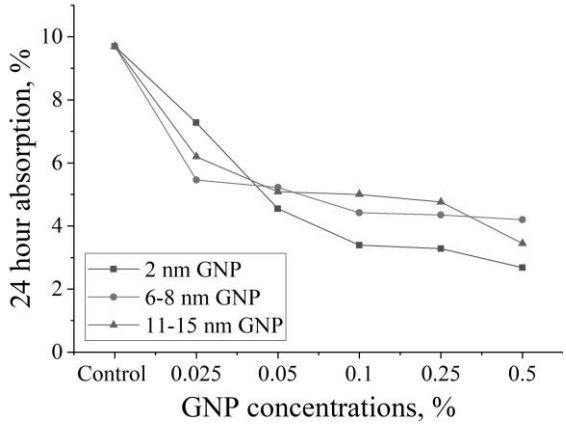

Fig. 2. 43 Relationship between doses of graphene platelets and water absorption of lightweight cement composite after 24 hours of water immersion

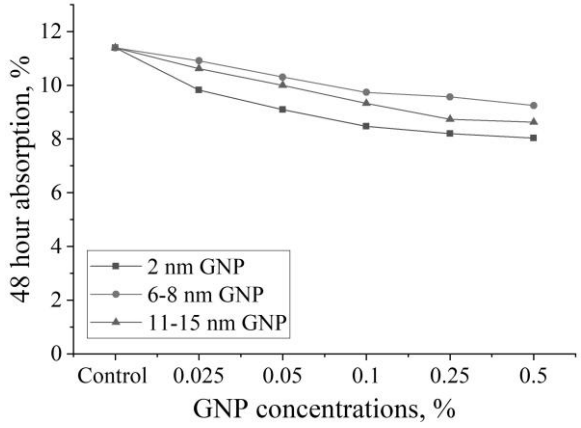

Fig. 2. 44 Relationship between doses of graphene platelets and water absorption of lightweight cement composite after 48 hours of water immersion

The outcomes of the research suggest that an increase in the concentration of GNP reinforcement resulted in a decline of water absorption of lightweight cement

composites. After 48 hours, the cement composite with 2 nm GNP had the lowest amount of water absorption. After 24 hours, the improvement in water absorption of cement composites incorporating 2nm, 6–8 nm, and 11–15 nm GNP was measured at about 72.4%, 56.7%, and 64.4%, respectively. This study also provided evidence that GNP thickness also affects the W_A of the cementitious system. GNP particles fill the pores of the cementitious composite, which leads to an improvement in W_A (Chen et al., 2019; Du and Pang, 2015). This reduction in the water absorption of cementitious composites incorporating GNP suggests that, likely, nanoreinforcements densified the microstructure, which leads to a decrease in water absorption.

The effectiveness of ultrasonication energy to disperse GNP particles is evident in Fig. 2.45. Meanwhile, Fig. 2.46 shows the ITZ of EGA and cementitious materials with nano reinforcements. Fig. 2.46 suggests that EGA offers good adhesion with cementitious materials; there was no significant improvement in ITZ between EGA, and cementitious materials were observed to incorporate GNP. However, the presence of nanomaterials was clearly observed in the ITZ of EGA. Meanwhile, a separation gap in ITZ between aerogel and cementitious materials without nano reinforcement is clearly observed in Fig. 2.47. However, a significant improvement in ITZ was observed between aerogel and cementitious materials with nano reinforcements. The presence of GNP was also clearly visible in the ITZ of aerogel. At higher magnification in Fig. 2.48 evidently shows the presence of hydration products surrounding GNP in the cementitious composite. This phenomenon clearly suggests the nucleation effects of GNP. Fig. 2.49 also highlights that GNP provides pore filling effects, which leads to an improvement in the microstructure of cementitious composites. Probably, due to these phenomena, the mechanical and water absorption characteristics of the cementitious composite were improved.

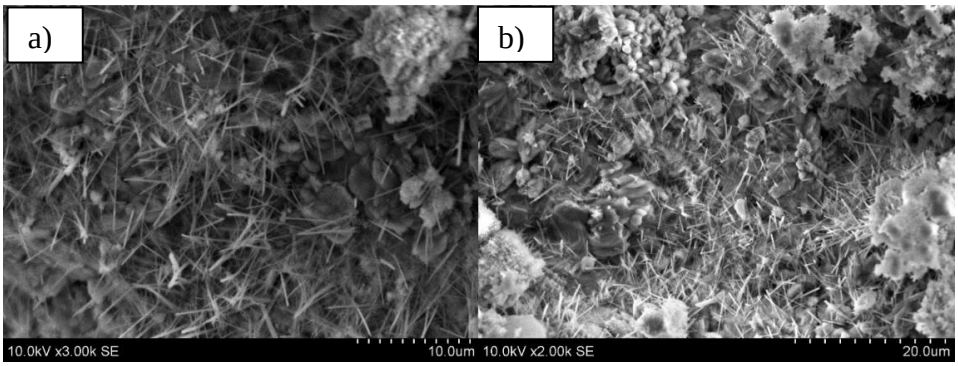

Fig. 2. 45 Scanning electron microscopy image showing a) and b) dispersion of GNP within cementitious composites

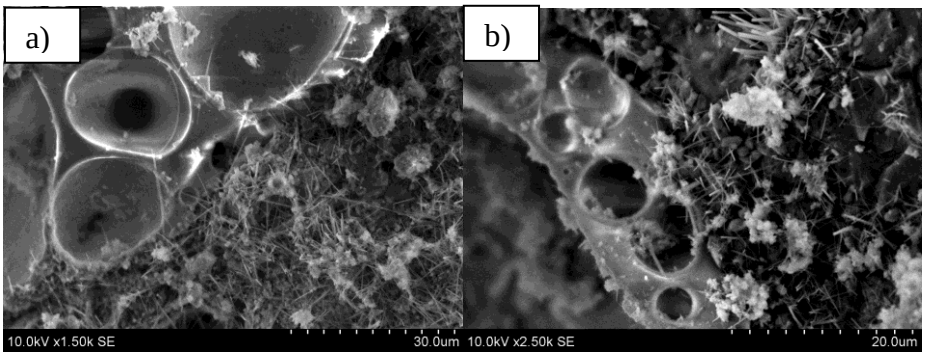

Fig. 2. 46 Scanning electron microscopy showing a) and b) interfacial transition zone of expanded glass with graphene platelet reinforcements

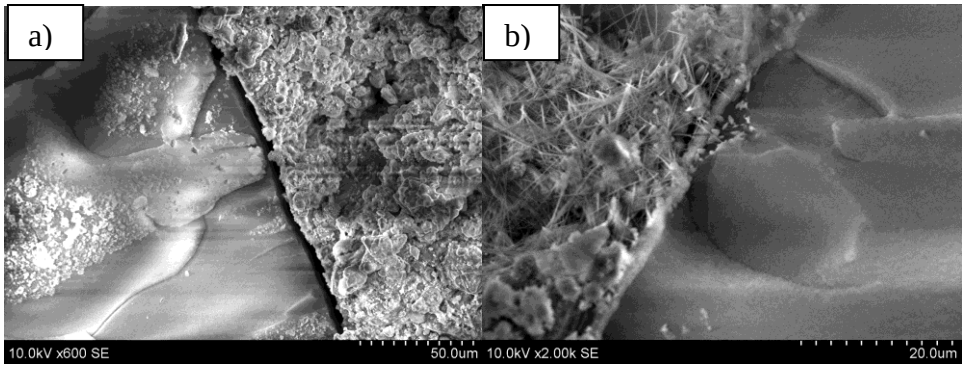

Fig. 2. 47 SEM image showing a) interfacial transition zone of aerogel without GNP reinforcements, and b) interfacial transition zone of aerogel with GNP reinforcements

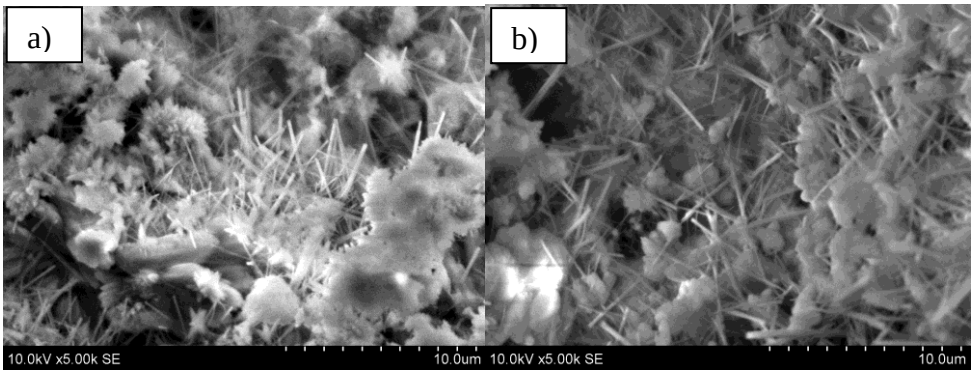

Fig. 2. 48 SEM image showing a) and b) the presence of hydration products surrounding graphene platelets in lightweight cement composite

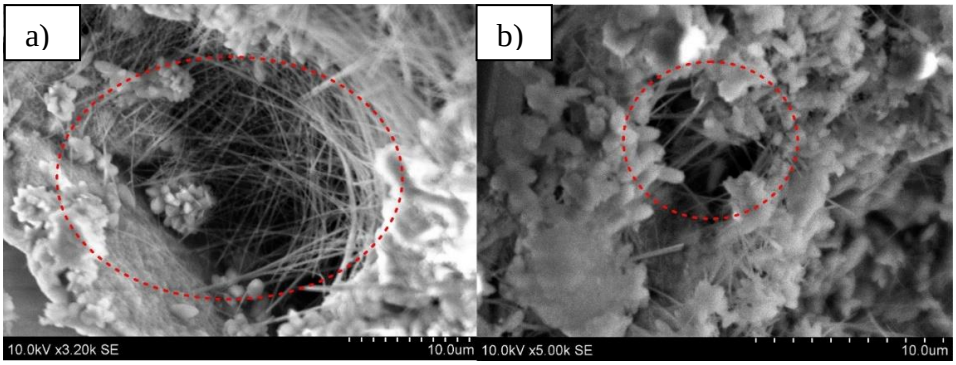

Fig. 2. 49 SEM image showing a) and b) pore filling effects of GNP

The XRD pattern of cementitious composites is presented in Fig. 2.50, Fig. 2.51, and Fig. 2.52. Our study results reveal that the addition of GNP did not significantly impact the XRD pattern of the cementitious composites. There were no additional peaks observed when adding GNP in the cementitious system. The incorporation of GNP only impacted the intensity of the XRD pattern. This phenomenon suggests that almost the same hydration products were grown and that, with the addition of GNP, only the crystallinity of the hydration products was impacted. The primary hydration products of cement composites include calcite, portlandite, and ettringite. These figures also suggest that the growing GNP concentration resulted in an increase in the intensity of ettringite at 8° and 19°. All the cementitious composites had portlandite peaks detected at 18° and 34°. It was observed that the intensity of portlandite varied with the change in the thickness of GNP. 0.5% GNP reinforced cementitious composite exhibited a higher intensity of portlandite at 34°.

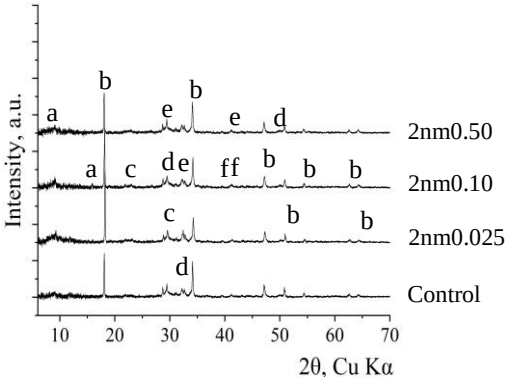

Fig. 2. 50 XRD pattern of 2 nm GNP reinforced lightweight cement composites

Note: a – ettringite $Ca_6Al_2(SO_4)_3(OH)_{12}\cdot 26H_2O$ (41–1451), b – portlandite $Ca(OH)_2$ (1–837), c – calcite $Ca(CO)_3$ (24–27), d – calcium silicate hydrate $Ca_{1.5}SiO_{3.5}\cdot x\ H_2O$ (33–306), e – alite $Ca_{54}MgAl_2Si_{16}O_{90}$ (13–272), f – belite Ca_2SiO_4 (33–302)

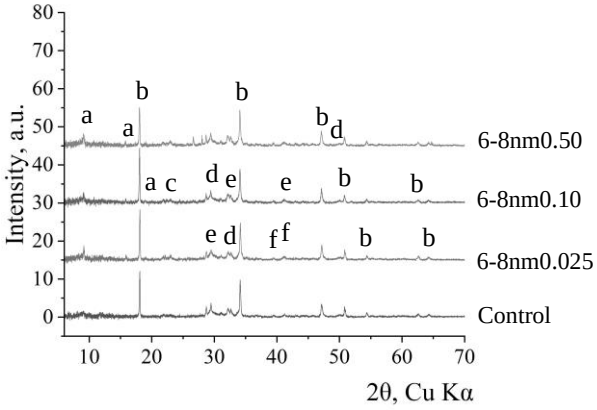

Fig. 2. 51 XRD pattern of 6–8 nm GNP reinforced lightweight cement composites

Note: a – ettringite $Ca_6Al_2(SO_4)_3(OH)_{12}\cdot 26H_2O$ (41–1451), b – portlandite $Ca(OH)_2$ (1–837), c – calcite $Ca(CO)_3$ (24–27), d – calcium silicate hydrate $Ca_{1.5}SiO_{3.5}\cdot x\ H_2O$ (33–306), e – alite $Ca_{54}MgAl_2Si_{16}O_{90}$ (13–272), f – belite Ca_2SiO_4 (33–302)

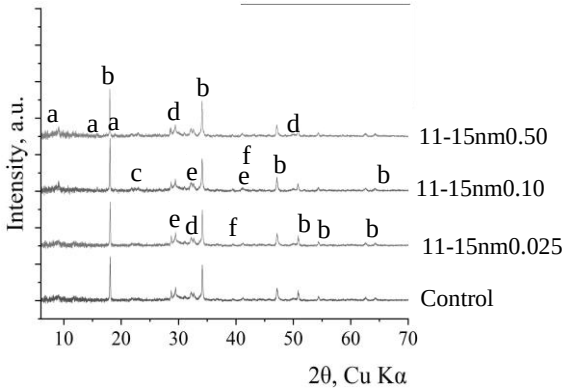

Fig. 2. 52 XRD pattern of 11–15 nm GNP reinforced lightweight cement composites

Note: a – ettringite $Ca_6Al_2(SO_4)_3(OH)_{12}\cdot 26H_2O$ (41–1451), b – portlandite $Ca(OH)_2$ (1–837), c – calcite $Ca(CO)_3$ (24–27), d – calcium silicate hydrate $Ca_{1.5}SiO_{3.5}\cdot x\ H_2O$ (33–306), e – alite $Ca_{54}MgAl_2Si_{16}O_{90}$ (13–272), f – belite Ca_2SiO_4 (33–302)

3. CONCLUSIONS

This study aimed to develop a lightweight cement composite by using EGA and silica aerogel satisfying EFNARC self-compactibility requirements. The novelty of the study is the achievement of the self-compatibility of the lightweight cement composite below the density of 1400 kg/m^3. Moreover, such problems as separation gaps in ITZ between aerogel and cementitious materials, a weaker mechanical performance, and high water absorption of the cementitious composite were improved by using polymer coatings and nano reinforcements.

Stage 1: Investigations of binding materials, fine particle concentration, and LWA concentrations on the physical, mechanical, and microstructural characteristics of LWSCCC

The use of aerogel in the cementitious system significantly lowers the density of the composite. Partial replacement of EGA by aerogel (incorporation of 32.04 kg/m^3) lowers the density of the cement composite by almost 15.8%. Aerogel is lighter than EGA, and the incorporation of aerogel into a cement composite increases the porosity by entrapping air bubbles, which leads to a decline in density. Hydrophobic aerogel has weaker adhesion with cementitious materials, and the use of 32.04 kg/m^3 and 42 kg/m^3 silica aerogel as partial replacements for EGA decreases the compressive strength by 49.15 and 60.70%, respectively.

The use of very lightweight aggregates, such as EGA and aerogel, makes it possible to develop LWSCCC within the density range of 1343 to 948 kg/m^3. The optimized cementitious composite achieves a workability range of 700 to 820 mm slump flow satisfying EFNARC 2005 recommended SF2 and SF3 classes within the density range of 1400 to 1000 kg/m^3. Moreover, the cementitious composite achieves 21.3 to 12.4 MPa compressive strength, which also satisfies the recommended mechanical strength requirements of ACI-213R-03 2003 (≥17 MPa) and ACI-213R-2014 (≥17 MPa) CEB/RILEM (≥15 MPa) guidelines. However, microstructural investigation recommended that aerogel offers weaker adhesion with cementitious materials, and separation gaps were observed in ITZ. Moreover, the use of high volumes of aerogel and EGA in cementitious systems leads to a higher risk of water absorption.

Stage 2: Improvement of physical, mechanical, and ITZ of LWSCCC by using polymer coatings on lightweight aggregates

The addition of coatings of SBR and paraffin to lightweight aggregates was observed to slightly improve the workability of the investigated material. An improvement in workability of almost 6.8% of the pre-coated LWA added cement composite was observed. The obtained slump flow was measured as 810 to 732 mm, which satisfies the acceptance criteria of SF2 and SF3 classes. The use of the polymer coating on LWA also enhances the quality of ITZ and lowers the separation gaps between aerogel and cementitious materials. Moreover, the use of polymer coatings improves the total porosity by 2.9% and ensures about 26% water absorption capacity of lightweight cementitious composites. The mechanical

strength of the self-compacted cementitious composite was measured to equal about 25.9 MPa to 17.03 MPa, thereby satisfying the requirement of CEB/RILEM, ACI-213R-03 2003, and ACI-213R-2014. The use of polymer coatings improves the compressive strength by almost 8.4 and 15.9 % when using single-layer coatings of SBR or paraffin.

Stage 3: Enhancement of mechanical performance, ITZ, and water absorption characteristics of lightweight concrete by using carbon nanotubes and graphene platelets

The addition of 0.6% CNT improved the compressive strength of the lightweight cement composite by nearly 41%. The separation gaps between aerogel and ITZ were effectively improved by incorporating carbon nanotubes attributed to the higher growth of higher hydration products. CNT was also observed to fill the pores of the cement composite, which led to improvement in the mechanical and water absorption characteristics of LWC. Carbon nanotube reinforcement improves the water absorption capacity of the lightweight cement composite by almost 12%.

The optimum doses for the improvement in compressive strength when incorporating GNP were observed at 0.025%. When incorporating GNP, almost 43% improvement in the compressive strength and 72.4% improvement in water absorption (24 hours of immersion) of the cementitious composite was determined. Moreover, GNP improves the separation gaps between the aerogel and cementitious materials attributed to the pore filling and nucleating effects.

Future recommendations

Aerogel is a new generation material, and the use of such materials in lightweight cementitious composites shall improve thermal and noise insulation properties. Moreover, aerogel is a highly fire-resistant material. The use of aerogel in combination with other lightweight materials will lower the density of the cementitious composite. The self-compactibility properties of cementitious composite will allow the product to reach the congested areas of the building easily and to compact by itself without any required external vibration energy. This present study was only aimed at developing self-compacting cementitious composites using aerogel and EGA below the density of 1400 kg/m3. Moreover, such problematic areas as weaker adhesion, a weaker mechanical performance, and water absorption properties were improved. However, more research on aerogel-based lightweight self-compacting cementitious composites is still needed, and future recommendations are listed below.

1. The use of alternate lightweight aggregates with the combination including aerogel to develop LWSCCC also needs to be investigated. The use of more sustainable materials will reduce production costs while also moving us closer to sustainability.
2. The thermal insulation of aerogel and EGA-based lightweight cementitious composites needs to be performed in the laboratory in future work. The developed product is expected to offer better thermal insulation characteristics in the laboratory tests than the theoretically calculated value. Moreover, the

pore dispersion and porosity of lightweight cementitious composites have a great impact on the thermal insulation characteristics, and, in future studies, a detailed study is also required to understand the impact of porosity and pore size distribution on the thermal, mechanical, and durability characteristics of aerogel based LWSCCC.

3. Aerogel and EGA both contain silica, and a detailed study on ASR needs to be performed. Moreover, other durability properties, such as shrinkage, frost resistance, water penetration depth, and long-term durability in aggressive environments, such as chloride, sulfate attack, etc., need to be extensively studied.
4. The use of the developed products in real buildings as practical applications will provide the actual thermal performance numbers. Also, it should be easy to differentiate the performance of aerogel-based products from other thermal insulation materials that are conventionally used.
5. In the present study, polymer coatings and nanomaterials were used to improve ITZ, mechanical, and durability characteristics of aerogel-based LWSCCC. However, in future studies, more sustainable and cost-effective alternative materials must be identified.

Santrumpos

SSB – susitankinantis betonas (angl. *self-compacting concrete*)
LSSB – lengvasis susitankinantis betonas (angl. *light-weight self-compacting concrete*)
SRUKZ – sukietėjusio rišiklio (cementinio akmens) ir užpildo kontaktinė zona (betone) (angl. *Interfacial transition zone*)
LSSK – lengvasis susitankinantis kompozitas (angl. *light-weight self-compacting composite*)
SEM – skenuojamoji elektroninė mikroskopija (angl. *scanning electronic microscopy*)
XRD – rentgenodifrakcinė analizė (angl. *X-ray diffraction analysis*)
LSSCK – lengvasis susitankinantis cementinis kompozitas (angl. *lightweight self-compacting cement composite*)
ANV – anglies nanovamzdeliai (angl. *carbon nanotubes*)
GNP – grafeno nanoplokštelės (angl. *graphene nanoplatelets*)
SBK – stireno ir butadieno kopolimeras (angl. *styrene butadiene rubber*)

SANTRAUKA

Susitankinantį betoną (SSB) 1986 m. sukūrė Ozawa ir jo kolegos, ir tai buvo reikšmingas betono ir gelžbetonio statybos technologijos žingsnis (Adebayo Mujedu et al., 2020). Lengvasis betonas buvo naudojamas ilgą laiką, o šiandien lengvasis susitankinantis betonas (LSSB) laikomas patobulinta SSB ir lengvojo betono atmaina (Yu et al., 2019). Gaminant LSSB šiandien naudojami įvairūs natūralūs ir dirbtiniai lengvi užpildai. Tačiau dauguma LSSB yra gaminami iš dirbtinių užpildų. LSSB gamyboje didelį potencialą turi palmių aliejaus klinkerio, polistireninio putplasčio, gumos, kokoso lukšto ir plastiko atliekos. Lengvųjų užpildų fizinės ir mechaninės savybės gali skirtis pagal jų tipą, o tai gali turėti įtakos LSSB savybėms (Ting et al., 2019). Gali būti, kad lengvųjų užpildų naudojimas betone sukels segregacijos problemų dėl lengvųjų užpildų išplaukimo į paviršių efekto (Adhikary and Rudzionis, 2020; Juradin et al., 2012; Kwasny et al., 2012). Išsisluoksniavimas ir netinkamas savaiminis sutankėjimas dėl netolygaus lengvųjų užpildų pasiskirstymo gali pakenkti betono konstrukcinėms eksploatacinėms savybėms ir ilgaamžiškumui (Kwasny et al., 2012). Norint paruošti mažesnio nei 1400 kg/m^3 tankio SSB, reikalingas didelis lengvųjų užpildų kiekis, o tai gali padidinti vandens absorbcijos riziką (Adhikary and Rudzionis, 2020; Juradin et al., 2012; Kurt et al., 2016c, 2016b; Kwasny et al., 2012; Wan et al., 2018). Mažo tankio betonas gali būti naudojamas garsą ir šilumą izoliuojančioms pastato atitvaroms įrengti (Ting et al., 2019). Dėl lengvųjų užpildų paviršiaus struktūros ir sukibimo kokybės skirtumų iš įvairių lengvųjų užpildų tipų pagamintų LSSB sukietėjusio rišiklio ir užpildo kontaktinės zonos (SRUKZ) kokybė taip pat gali skirtis. Literatūros šaltinių tyrimai rodo, kad keramzitas, putstiklis, perlitas ir vulkaninė pemza gerai sukimba su cementinėmis medžiagomis, todėl pagerėja SRUKZ kokybė (Barnat-Hunek et al., 2018; Duplan et al., 2014; Yashar and Behzad, 2021; Yu et al., 2013). Polistireninis

putplastis, kitos polimerinės atliekos ir aerogelis silpniau sukimba su cementinėmis medžiagomis, todėl blogesnis jų sukibimas ir silpnesnė SRUKZ (Adhikary et al., 2021a; Angelin et al., 2020; Cheboub et al., 2020; Da Silva et al., 2020; Ranjbar and Mousavi, 2015). Be to, pastaraisiais metais LSSB iš lengvųjų užpildų daugiausia buvo kuriamas didesnio tankio nei 1400 kg/m^3.

Aerogelis yra perspektyvi labai mažo tankio medžiaga, kuri gali būti naudojama gaminant labai lengvus cemento kompozitus. Putstiklis taip pat yra mažesnio tankio lengvasis užpildas. Nepaisant mažesnio tankio, aerogelis yra trapus. Be to, hidrofobinis aerogelis gali silpniau sukibti su cementinėmis medžiagomis, todėl cementiniai kompozitai gali būti mažesnio stiprumo. Lengvasis susitankinantis cementinis kompozitas, kuriame yra putstiklio ir aerogelio derinys, galėtų būti perspektyvi medžiaga statyboms. Lengvasis cemento kompozitas, kuriame yra tokio mažo tankio užpildų, sumažins cemento kompozito tankį. Be to, naudojant tokias medžiagas cementiniame kompozite, gali pablogėti mechaninės savybės ir padidėti vandens absorbcijos rizika. Hidrofobinis aerogelis taip pat gali turėti silpnesnę SRUKZ; todėl reikalingi išsamesni tyrimai, kad būtų ištirtos cementinių kompozitų, kuriuose yra naudojami aerogelio ir putstiklio užpildai, savybės, atsižvelgiant į jų šviežio mišinio savybes ir sukietėjusio kompozito mechanines bei kitas savybes, taip pat mikrostruktūrą. Be to, reikėtų pašalinti problemas, susijusias su aerogelio ir putstiklio užpildų pagrindu pagamintu cementiniu kompozitu. Daugumos iki šiol sukurtų LSSB, kurių tankis mažesnis nei 1400 kg/m^3, gniuždymo stipris yra mažesnis už rekomenduojamą ACI-213R-03 (2003), ACI-213R-2014 ir CEB/RILEM vertę, skirtą naudoti konstrukcijoms. Atsižvelgiant į aerogelio ir putstiklio kaip perspektyvių ir mažai ištyrinėtų lengvųjų užpildų tinkamumą pagaminti ypač lengvą ir pakankamai stiprų LSSB, buvo atliekami šio darbo moksliniai tyrimai siekiant geriau ištirti jų panaudojimo galimybes LSSB gamyboje. Tyrimo tikslui pasiekti buvo taikomi įvairūs mišinio paruošimo ir sukietėjusio konglomerato tyrimo metodai. Pirmiausia paruošti mažo tankio cemento kompozitai naudojant putstiklį ir aerogelį, siekiant nustatyti šių užpildų poveikį cemento kompozito savybėms. Taikant įvairius LSSB tyrimo metodus, optimizuota betono mišinio sudėtis ir pasiektas savaiminis sutankinamumo kriterijus. Tokios problemos kaip didesnė vandens absorbcija, mažesnės stiprumo savybės ir blogesnis aerogelio sukibimas su cementinėmis medžiagomis buvo išspręstos naudojant polimerines dangas, kuriomis padengti lengvieji užpildai. Be to, naudojant anglies nanovamzdelius ir grafeno nanoplokšteles pagerintos mechaninės LSSB savybės ir vandens absorbcija bei SRUKZ tarp aerogelio ir sukietėjusio cemento rišiklio.

Pagrindinis šio darbo tikslas – ištirti lengvuosius susitankinančius cementinius kompozitus (LSSCK), kurių tankis mažesnis nei 1400 kg/m^3, naudojant aerogelio bei putstiklio užpildus ir ištirti jų fizikines, mechanines bei mikrostruktūrines savybes.

Darbo uždaviniai norimam tikslui pasiekti

1. Ištirti rišamųjų medžiagų, smulkiųjų dalelių ir lengvųjų užpildų koncentracijos poveikį LSSCK (<1400 kg/m^3) fizikinėms, mechaninėms ir mikrostruktūrinėms savybėms.
2. Atlikti LSSB, paruošto iš lengvųjų užpildų, padengtų polimerinėmis dangomis, tyrimus ir nustatyti jų įtaką LSSB vandens įgėriui, gniuždomajam stipriui, SRUKZ ir mikrostruktūros pokyčiams.
3. Ištirti anglies nanovamzdelių ir grafeno nanoplokštelių įtaką LSSCK fizikinėms bei mechaninėms savybėms ir jo mikrostruktūrai.

Tyrimo mokslinis naujumas

Atlikus šį mokslinį darbą buvo sukurtas naujo tipo lengvasis susitankinantis cementinis kompozitas (LSSCK), kurio tankis mažesnis nei 1400 kg/m^3. Sukurtas LSSCK atitiko ACI-213R-03 (2003 ir 2014 m.) normų keliamus stiprumo reikalavimus, kad būtų galima naudoti jį statyboje kaip konstrukcinę medžiagą net esant mažesniam nei 1400 kg/m^3 tankiui. Rankinis šviežio cementinio kompozito maišymas leidžia mažiau susmulkinti aerogelio daleles. Be to, šie eksperimentiniai tyrimai rodo, kad aerogelio sukibimas su cementinėmis medžiagomis yra silpnesnis, o SRUKZ tarp aerogelio ir cementinių medžiagų buvo pastebėti vientisi atskyrimo tarpai. Aerogelio pagrindu pagamintas cementinis kompozitas įgyja mažesnį mechaninį stiprumą, porėtą mikrostruktūrą ir padidėjusią vandens absorbcijos riziką. Šio tyrimo metu aerogelio ir cementinių medžiagų atskyrimo tarpai buvo pagerinti naudojant nanomedžiagas ir polimerines dangas. Be to, pagerėjo vandens absorbcija, mechaninės savybės ir mikrostruktūra.

Tyrimo metodai

Pradinės medžiagos lengvųjų cementinių kompozitų kūrimui buvo parinktos remiantis literatūros analize. SEM ir XRD analizės buvo atliekamos siekiant suprasti pucolaninių priedų ir lengvųjų užpildų mikrostruktūrą. Dažniausiai moksliniuose tyrimuose taikomas maišymo ir eksperimentinių tyrimų metodas, o atliktame disertaciniame darbe jis taip pat taikomas. Šviežio cementinio kompozito savybės buvo ištirtos pagal EFNARC 2005 rekomendacijas. Cemento hidratacija cemento tešloje buvo stebima pusiau adiabatinės kalorimetrijos metodu taikant Pico technologiją, sukurtą pagal EN 196-9:2010 standartą. Cementinio kompozito mechaninis stipris buvo išbandytas pagal EN 196-1:2016 standartą. Cementinio kompozito poringumas ir šilumos laidumas apskaičiuoti atitinkamai pagal GOST 12730.4-2020 ir EN 1745:2012 standartus. Gautiems rezultatams išanalizuoti ir jų tarpusavio ryšiui nustatyti buvo atlikti cementinio kompozito vandens įgėrio, tankio, poringumo ir SEM tyrimai. Sukūrus lengvojo susitankinančio cementinio kompozito (LSSCK) gamybos metodologiją, pagrįstą tinkamais maišymo ir tyrimų metodais, taikant daugybę priemonių buvo bandoma pagerinti tokias kompozito savybes kaip mechaninės savybės, mikrostruktūra ir vandens įgėrio charakteristikos.

Praktinis disertacijos reikšmingumas

Rankinis lengvųjų cementinių kompozitų maišymas sumažina aerogelio sutrupėjimą maišymo metu ir išlaiko šios medžiagos vientisumą cemento kompozituose. Sukurti lengvieji susitankinantys cementiniai kompozitai (LSSCK) atitinka ENFRAC 2005 keliamus reikalavimus susitankinantiems cementiniams mišiniams. Sukurti cementiniai kompozitai gali būti naudojami kaip šilumą izoliuojančios medžiagos, o jų savaiminio susitankinimo galimybė leidžia sutankinti sudėtingos konfigūracijos betonines konstrukcijas netaikant išorinės vibracijos poveikio. Savaiminio sutankinimo savybė leidžia padidinti LSSCK mišinio konsistenciją, pagerinti formų užpildymą ir mišinio sutankinimo lygį. Tyrimo metu sukurtos medžiagos šilumos laidumas buvo daug mažesnis nei įprasto betono ir gali būti pritaikytas statybų sektoriuje. Šio tyrimo metu cementinių kompozitų šilumos laidumas buvo apskaičiuotas taikant EN 1745:2012 standartą, kuris gali skirtis nuo laboratorijoje nustatyto šilumos laidumo koeficiento. Tyrimų metu sukurti racionalių sudėčių LSSCK taip pat gali būti naudojami kaip konstrukcinės medžiagos, nes jie atitinka reikalaujamą ACI-213R-03 (2003 ir 2014 m.) rekomendacijų gniuždomąjį stiprį. Praktinis šio tiriamojo darbo naujumas yra tai, kad sukurtas LSSB mažesnio nei 1400 kg/m^3 tankio, pakankamo stiprumo, gero šilumos laidumo ir jis gali būti potencialiai panaudotas statybų sektoriuje skirtingiems tikslams pasiekti.

Disertacijos teiginiai

1. Lengvieji cementiniai kompozitai su optimizuota mišinio sudėtimi gali pasiekti savaiminį sutankėjimą net esant mažesniam nei 1400 kg/m^3 tankiui ir SF2 bei SF3 pasklidos klasei.
2. Dėl aerogelio hidrofobinių savybių maišant šviežią cementinį kompozitą jis gali sulaikyti oro burbuliukus ir parodyti mažesnį sukibimą bei silpnesnę SRUKZ.
3. Naudojant anglies nanovamzdelius (ANV), grafeno nanoplokšteles (GNP), stireno ir butadieno kopolimero (SBK) ir parafino dangas, labai pagerėjo atsisluoksniavimo tarpai tarp aerogelio ir cementinio rišiklio. ANV ir GNP įdėjimas į lengvą cementinio kompozito mišinį pagerina atitinkamai 41,5 % bei 43,8 % gniuždomąjį stiprį ir sumažina 30,5 % bei 29 % vandens įgėrį.

Darbo struktūra ir apimtis

Ši daktaro disertacija parengta iš trijų skyrių, kuriuos sudaro įvadas, tyrimo rezultatai bei jų aptarimas ir išvados. Be to, pateikti cituojami literatūros šaltiniai, trumpa disertacijos santrauka lietuvių kalba, doktoranto gyvenimo aprašymas, publikacijų, susijusių su daktaro disertacija, sąrašas, taip pat papildomi disertacijos autoriaus publikuoti straipsniai ir padėka. Daktaro disertacijoje yra 52 paveikslai, 10 lentelių ir 50 cituojamų literatūros šaltinių.

Tyrimo rezultatų patvirtinimas

Atliktų tyrimų išvados buvo apibendrintos ir pateiktos iš viso penkiuose moksliniuose straipsniuose mokslo žurnaluose, kurie yra įtraukti į „Claritative

Analytics Web of Science“ duomenų bazes (su citavimo indeksu) ir priklauso Q1 ir Q2 kvartiliams.

Autoriaus indėlis

Medžiagas parinko ir tyrimų planą sudarė Suman Kumar Adhikary ir Žymantas Rudžionis. Medžiagas tyrimams pateikė Kauno technologijos universitetas ir Žymantas Rudžionis. Eksperimentus atliko, rinko duomenis ir rankraščius rašė doktorantas Suman Kumar Adhikary, vadovaujamas Žymanto Rudžionio. Simona Tučkutė padėjo atlikti SEM ir XRD bandymus, Danutė Vaičiukynienė – išanalizuoti SEM ir XRD rezultatus, o Deepankar Kumar Ashish – užbaigti ir kritiškai peržiūrėti rankraščius publikuojant straipsnius.

Mokslinių publikacijų disertacijos tema sąrašas

Šios disertacijos naujumas ir siekiami rezultatai buvo pasiekti penkių straipsnių rinkinyje. Siekiami rezultatai apibendrinami trimis etapais.

Pirmajame etape buvo atlikti pirminiai tyrimai betono mišinio savaiminio susitankinimo kriterijui ištirti. Pirmasis tyrimo etapas apima du straipsnius. Pirmasis straipsnis paskelbtas „Journal of Building Engineering“ žurnale, 2020, 101399 (Adhikary ir kt., 2020). Šio tyrimo etapo tikslas įgyvendintas dviem etapais. Iš pradžių buvo tiriamas rišiklių ir lengvųjų užpildų poveikis, ruošiant labai takų, lengvą cementinio kompozito mišinį. Vėliau, remiantis gautais rezultatais, buvo optimizuota mišinio sudėtis, kad atitiktų savaiminio sutankėjimo kriterijus. Šio žingsnio rezultatai paskelbti žurnale „Case Studies in Construction“, 2022, e00879 (Adhikary ir kt., 2022b).

Antrajame tyrimo etape buvo bandoma tobulinti ankstesnio etapo metu nustatytas problemas, susijusias su cemento kompozitais, pagamintais su putstiklio ir aerogelio užpildais. Tokias problemas kaip didesnis vandens sugertis ir silpnesnis sukibimas tarp aerogelio bei cementinių medžiagų buvo bandoma pagerinti polimerinėmis dangomis. Šio tyrimo rezultatai paskelbti žurnale „Materials Today Communications“, 2022, 103496 (Adhikary, 2022).

Trečiajame tyrimo etape nustatytas lengvo cementinio kompozito, paruošto su putstiklio ir aerogelio užpildais, problemas bandyta tobulinti panaudojant alternatyvias nanomedžiagas. Tokias problemas kaip prastesnės mechaninės savybės, silpnesnė SRUKZ tarp aerogelio bei cementinių medžiagų ir didesnė vandens absorbcijos rizika buvo bandoma spręsti naudojant naujos kartos nanomedžiagas, tokias kaip ANV ir GNP. Iš pradžių susitankinančio lengvojo betono mišinio paruošimui buvo naudojami anglies nanovamzdeliai; tyrimo rezultatai paskelbti žurnale „Scientific reports“, 2021, 2104 (S. K. Adhikary et al., 2021). Vėliau mechaninės, vandens įgėrio savybės ir SRUKZ tarp lengvųjų užpildų ir cementinių kompozitų buvo pagerintos įdedant nanografeno plokštelių (GNP) įmaišą. Tyrimo rezultatai paskelbti žurnale „Journal of Building Engineering“, 2022, 104870 (Adhikary et al., 2022c).

1. Tyrimo rezultatai ir jų aptarimas

1.1. Rišamųjų medžiagų, smulkiųjų dalelių ir lengvųjų užpildų koncentracijos įtakos tyrimai LSSCK fizikinėms, mechaninėms ir mikrostruktūros savybėms

Šio tyrimo tikslas buvo įgyvendintas dviem etapais. Pirmiausia buvo tiriamas rišamųjų medžiagų ir lengvųjų užpildų poveikis ruošiant takų lengvąjį cementinį kompozitą. Vėliau mišinio sudėtis buvo optimizuota, kad būtų sukurti LSSCK.

1.1.1. Pucolaninių priedų ir lengvųjų užpildų poveikio takių lengvųjų cementinių kompozitų savybėms tyrimai

Naudojant aerogelio ir putplasčio stiklo užpildus, buvo paruoštos dvi takių lengvųjų cementinių kompozitų sudėčių grupės. Pirmoji kompozito serija buvo skirta ištirti lakiųjų pelenų, kaip dalinio cemento pakaitalo, poveikį, kurioje nuo 0 iki 30 % cemento masės buvo pakeista lakiaisiais pelenais. Remiantis gautais kompozitų tyrimo rezultatais, kitai bandinių serijai buvo parinktas geriausias mišinys pagal mišinio konsistenciją, stiprumą ir vizualiai įvertintą mišinio išsisluoksniavimą. Antroje serijoje 1–2 mm dydžio putstiklio užpildų tūris buvo pakeistas 1–2 mm dydžio silicio aerogeliu atitinkamai 25 %, 50 %, 75 % ir 100 %. Kompozitų mišinio sudėtys pateiktos 1 lentelėje.

1 lentelė. Cementinio kompozito mišinių sudėtys (komponentų kiekis pateiktas kg 1 m^3 mišiniui paruošti) (I-A etapas)

LSSCK mišinio serija	Cementas	Aerogelis	Putstiklio užpildas (1/2+1/0,5+0,5/0,25 +0,01/0,3)	Lakieji pelenai	Superplastifikatorius, 1,8 %*	Stabilizatorius, 0,3 %*	Vanduo, (v/r = 0,65)
C100FA0	500	–	138+54+34+40	–	9	1,5	325
C90FA10	454,5	–	138+54+34+40	45,45	8,18	1,37	325
C80FA20	416,7	–	138+54+34+40	83,34	7,50	1,25	325
C70FA30	385	–	138+54+34+40	115,5	6,93	1,16	325
C90FA10AG25	454,5	10,5	103,5+54+34+40	45,45	8,18	1,37	325
C90FA10AG50	454,5	21	69+54+34+40	45,45	8,18	1,37	325
C90FA10AG75	454,5	31,5	34,5+54+34+40	45,45	8,18	1,37	325
C90FA10AG100	454,5	42	0+54+34+40	45,45	8,18	1,37	325

Pastaba: * – įmaišų kiekiai, proc. nuo cemento masės

Cementinio kompozito mišinio pasklidos tyrimo duomenys pateikti 2 lentelėje. Tyrimo rezultatai aiškiai rodo, kad cementinio kompozito mišinių pasklida mažėja didėjant aerogelio koncentracijai. O štai cementinio kompozito mišinių konsistencija pagerėjo įmaišius lakiuosius pelenus kaip cemento pakaitalą. Išmatuota C100FA0 bandinio mišinio pasklida buvo 21 cm, kuri padidėjo iki 23,4 cm, kai 30 % cemento buvo pakeista lakiasiais pelenais. C90FA10AG25 bandinio, kuriame yra 25 % 1–2 mm putstiklio užpildų tūrio, pakeista aerogeliu pasklida buvo 21 mm, o C90FA10AG100 kompozito, kuriame yra 100 % putstiklio užpildų tūrio, pakeista aerogeliu pasklida sumažėjo iki 18,4 mm. Cementinių kompozitų takumo

sumažėjimas pridėjus aerogelį gali būti siejamas su silicinio aerogelio sulaikytu oru ir didesniu vandens įgėriu. Tačiau kompozito klojumą galima pagerinti koreguojant vandens ir superplastifikatoriaus dozes.

2 lentelė. Lengvųjų cementinių kompozitų konsistencija (I-A etapas)

Serija	Pasklidos bandymas, cm	Serija	Pasklidos bandymas, cm
C100FA0	21	C90FA10AG25	21
C90FA10	21	C90FA10AG50	20
C80FA20	23	C90FA10AG75	18,9
C70FA30	23,4	C90FA10AG100	18,4

Šiame tyrimo etape kompozitų gniuždomasis ir lenkiamasis stipris f_c ir f_{fl} buvo išmatuoti po 7 ir 28 parų kietėjimo, jų duomenys pateikti 3 lentelėje. Tyrimo rezultatai rodo, kad padidėjus lakiųjų pelenų kiekiui, cementinio kompozito f_c mažėja. Taip pat pastebėta, kad padidėjus aerogelio koncentracijai sumažėja ir f_c, ir f_{fl}. 100 % 1–2 mm putstiklio užpildų pakeitus aerogeliu, po 28 parų kietėjimo betonas prarado apie 60,7 % gniuždomojo stiprio. Aerogelis yra trapi medžiaga, turinti labai mažą stiprumą; ir galbūt dėl šios priežasties, padidėjus aerogelio kiekiui kompozituose, sumažėjo gniuždomasis ir lenkiamasis stipris.

3 lentelė. Lengvųjų cementinių kompozitų gniuždomojo ir lenkiamojo stiprio tyrimo duomenys (I-A etapas)

Serija	Gniuždomasis ir lenkiamasis stipris po 7 parų kietėjimo, MPa		Gniuždomasis ir lenkiamasis stipris po 28 parų kietėjimo, MPa		Tankis esant sausos būsenos, kg/m^3
	f_c	f_{fl}	f_c	f_{fl}	
C100FA0	9,32	2,5	12,2	2,68	862,4
C90FA10	8,2	2,3	11,4	2,56	848
C80FA20	6,92	2,2	10	2,1	834,5
C70FA30	5,2	1,9	8	2,04	826,4
C90FA10AG25	5,72	1,7	6,52	2,38	816
C90FA10AG50	5,88	1,84	6,40	2,01	793
C90FA10AG75	3,32	1,11	4,8	1,61	774,5
C90FA10AG100	3,2	1,097	4,48	1,45	749,5

Išdžiovintų bandinių orasausis tankis buvo išmatuotas po 28 parų kietėjimo, tada apskaičiuotas kompozitų šilumos laidumas pagal EN 1745:2012. 3 lentelėje parodyta, kad padidėjus aerogelio koncentracijai kompozito tankis sumažėjo. Išdžiovinto kompozito C90FA10AG25 orasausis tankis buvo 816 kg/m^3; jis sumažėjo iki 749,5 kg/m^3 kompozitui C90FA10AG100, kuriame 100 % putstiklio užpildų fr. 1–2 mm buvo pakeista aerogelio užpildais. Dėl sumažėjusio kompozitų tankio sumažėja ir šilumos laidumas.

Aerogelis iš prigimties yra labai trapi medžiaga. Aerogelio užpildų SEM nuotraukos pateiktos 1 pav. Lygus ir švarus silicio aerogelio paviršius rodo, kad cemento hidratacijos metu jo irimas neįvyko. 1 pav. pateikti SEM vaizdai atskyrimo tarpų tarp hidrofobinio silicio aerogelio ir cementinio kompozito. Šis reiškinys rodo silpnesnį silicio aerogelio sukibimą su cementiniais kompozitais. Per tokius atskyrimo tarpus oras ar vanduo gali lengvai pernešti kenksmingas medžiagas ir paveikti kompozito ilgaamžiškumo savybes, ypač kompozito, veikiamo agresyvioje aplinkoje.

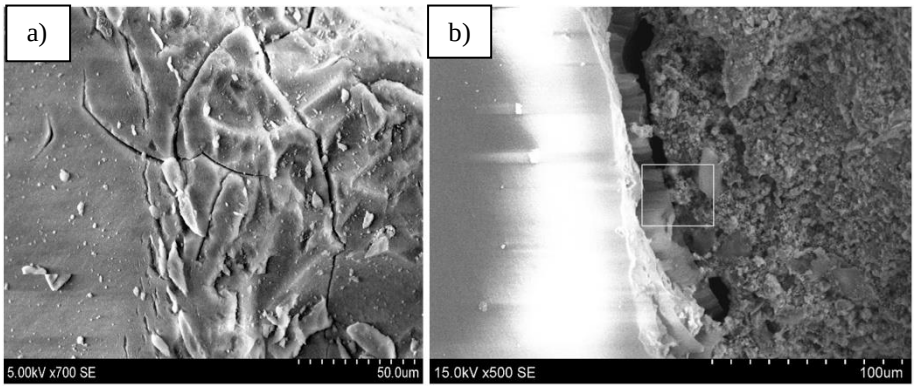

1 pav. a) Įtrūkimai aerogelio paviršiuje; b) atskyrimo tarpai tarp aerogelio ir cementinio kompozito kontaktinės zonos

1.1.2. Pucolaninių priedų ir lengvųjų užpildų poveikio savaime susitankinančių lengvųjų cementinių kompozitų savybėms tyrimai

Kompozito mišinys C100C100 buvo suformuotas natūralų smėlį derinant su įvairaus dydžio putstiklio užpildais (0,1–0,3 mm, 0,25–0,50 mm, 0,5–1 mm ir 1–2 mm) ir įvairiomis jų proporcijomis. C100S50 bandinyje pusė smėlio tūrio buvo pakeista labai smulkia 0,1–0,3 mm putstiklio užpildų frakcija, todėl tankis sumažėjo. Padidinus smulkiųjų dalelių kiekį, nežymiai padidėja vandens ir superplastifikatoriaus kiekis, reikalingas norimam kompozito takumo lygiui palaikyti. Kaip pucolaniniai priedai betono mišinių C90ZL10, C90FA10 ir C90ZL5FA5 sudėtims paruošti buvo panaudoti lakieji pelenai ir klinoptilolitas (gamtinis ceolitas) pakeičiant 10 % cemento dalį.

Bandinių serija C90ZL10 buvo naudojama kaip kontroliniai bandiniai. Buvo paruoštos dar keturios LSSCK bandinių serijos su skirtingais aerogelio kiekiais. 0,5–1 mm ir 1–2 mm dydžio putstiklio užpildai pakeisti aerogeliu (piltinis tankis 75 kg/m^3) 25 %, 50 %, 75 % ir 100 % kiekiais. Visuose kompozito bandiniuose vandens ir rišiklio santykis buvo 0,55. 4 lentelėje parodyta visų LSSCK mišinių sudėtys. Maišymo proceso metu putstiklio užpildai, ceolito milteliai ir cementas buvo kruopščiai sumaišyti sausos būsenos. Po to buvo įmaišyta 70 % viso vandens kiekio, kuris maišomas rankomis dar tris minutes. Tada superplastifikatorius ir stabilizatorius buvo sumaišyti su likusiu 30 % vandens kiekiu ir švelniai maišomi 2 minutes, prieš įdedant į kompozito mišinį. Paskutiniame etape į kompozito mišinį buvo pridėtas aerogelis, siekiant sumažinti aerogelio dalelių susmulkėjimą, paskui mišinys maišomas kitas dvi minutes.

4 lentelė. Lengvo savaime susitankinančio cementinio kompozito mišinių sudėtys (komponentų kiekis pateiktas kg 1 m^3 mišiniui paruošti) (I-B etapas)

LSSCK mišinio serija	Cementas	Smėlis	Putstiklio užpildas (1/2+1/0,5+0,5/0,25+0,01/0,3)	Aerogelis	Ceolitas	Lakieji pelenai	Stabilizatorius	Superplastifikato-rius	v/r santykis
C100S100	550	380	45+56+44+56	–	–	–	0,38	5,5	0,45
C100S50	530	183	43,4+54+42,4+ 43,6	–	–	–	0,38	6,9	0,58
C90ZL10	525	–	47,7+59,4+46,6+59,4+95,8	–	58,3		0,36	8,7	0,55
C90FA10	525	–	47,7+59,4+46,6+59,4+95,8	–	–	58	0,36	8,7	0,55
C90ZL5FA5	525	–	47,7+59,4+46,6+59,4+95,8	–	29,2	29,2	0,36	8,7	0,55
C90ZL10AG25	525	–	35,8+44,5+46,6+59,4+95,8	8	58,3	–	0,36	8,7	0,55
C90ZL10AG50	525	–	23,9+29,7+46,6+59,4+95,8	16	58,3	–	0,36	8,7	0,55
C90ZL10AG75	525	–	11,9+14,9+46,6+59,4+95,8	24	58,3	–	0,36	8,7	0,55
C90ZL10AG100	525	–	0+0+46,6+59,4+95,8	32	58,3	–	0,36	8,7	0,55

LSSCK mišinių konsistencijos bandymo rezultatai parodyti 5 lentelėje. Remiantis tyrimo rezultatais, kompozicinis mišinys su lakiaisiais pelenais turi didžiausią sklidumo skersmenį. C100S100, C100S50, C90ZL10, C90FA10 ir C90ZL5FA5 bandinių sklidumo skersmuo ir mažojo *V* piltuvo ištekėjimo trukmė buvo atitinkamai 247–258 mm ir 7,2–9 sekundės. Naudojant netaisyklingos dalelių formos smėlį, mažesnį vandens bei rišiklio santykį ir sumažintą superplastifikatoriaus kiekį, C100S100 mėginio sklidumo ir pasklidos skersmuo buvo mažiausias. Padidinus smulkaus pustiklio užpildo koncentraciją cemento ir kompozito mišinyje C100S50, padidėja vandens poreikis ir superplastifikatoriaus kiekis, kad LSSCK mišinio konsistencija būtų palaikoma savaiminio sutankėjimo lygio. Be to, putstiklio užpildai pasižymi didesne vandens absorbcijos geba nei natūralūs užpildai, todėl gali padidėti vandens ir superplastifikatoriaus poreikis. Antra vertus, kompozito mėginių C90ZL10, C90FA10 ir C90ZL5FA5 konsistencija žymiai pagerėjo, o tai galėjo būti siejama su pagerėjusia mišinio granuliometrine sudėtimi ir padidintu superplastifikatoriaus kiekiu.

Sklidumo ir pasklidos skersmuo šiek tiek sumažėja, kai LSSCK mišinyje didiname aerogelio koncentraciją, taip pat *V* formos piltuvo ištekėjimo laikas didėja. Pakeitus 100 % 2/1 mm ir 1/0,5 mm dydžio putstiklio užpildų tūrio aerogeliu, sklidumo skersmuo sumažėja beveik 4,3 %, o pasklidos skersmuo 12,5 %. Aerogelio paviršiuje esantys karboksilo (-COOH) ir hidroksilo (-OH) radikalai gali sugerti šiek tiek vandens, todėl sumažėja mišinio konsistencija (Adhikary et al., 2021a). Šiame tyrime stebimas kiek sumažėjęs LSSK klojumas, kurį galėjo lemti panašus veiksnys. Tačiau visi bandiniai atitiko EFNARC reikalavimus, kad jie būtų vadinami savaime susitankinančiais betono mišiniais. C90ZL10AG25 aerogelio cementinis

kompozitas atitinka SF3 pasklidos klasę, o C90ZL10AG50, C90ZL10AG75 ir C90ZL10AG100 – SF2 pasklidos klasę.

5 lentelė. LSSCK konsistencijos bandymo duomenys (I-B etapas)

Kompozito mišinys	Sklidumo skersmuo, mm	*V* piltuvo ištekėjimo trukmė, s (pagal EFNARC gaires *V* piltuvo matmenys skiediniui)	Slankumo kūgio pasklidos skersmuo, mm		*V* piltuvo laikas, sekundės (pagal EFNARC rekomendacijas *V* formos piltuvo matmenys betonui)	
C100S100	247	9	720	SF2	6	VF1
C100S50	248	8	725	SF2	5	VF1
C90ZL10	256	7,2	800	SF3	4	VF1
C90FA10	258	8	820	SF3	5	VF1
C90ZL5FA5	257	8,1	807	SF3	5	VF1
C90ZL10AG25	256	8	795	SF3	5	VF1
C90ZL10AG50	251	8,5	750	SF2	5,5	VF1
C90ZL10AG75	247	9,2	717	SF2	6,1	VF1
C90ZL10AG100	245	9,5	700	SF2	6,3	VF1

6 lentelėje pateikti visų LSSCK bandinių gniuždomojo ir lenkiamojo stiprio (f_c ir f_{fl}) bei tankio duomenys. LSSCK bandiniai nuo turi f_c ir f_{fl} atitinkamai nuo 7,9 MPa iki 21,3 MPa ir 1,7–5,5 MPa. LSSCK C100S100 bandinys, kuris buvo paruoštas naudojant smėlio ir putstiklio užpildų mišinį, pasižymi didžiausiais f_c ir f_{fl} rodikliais.

6 lentelė. Lengvųjų susitankinančių cementinių kompozitų fizinės ir mechaninės savybės

Pavyzdžiai	f_c, MPa	f_{fl}, MPa	Tankis, kg/m^3
C100S100	21,3	5,5	1343
C100S50	19,8	4,8	1178
C90ZL10	15,1	2,6	1126
C90FA10	12,8	3,5	1154
C90ZL5FA5	14,8	3	1146
C90ZL10AG25	13,6	2,3	1126
C90ZL10AG50	11	2,3	1076
C90ZL10AG75	9,1	2,0	1044
C90ZL10AG100	7,9	1,7	1019

Didėjant kompozite putsklio užpildų kiekiui, gniuždymo stipris mažėja. Poringos struktūros putstiklio užpildų mechaninis stipris yra mažesnis, o didelis jų kiekis betone mažina betono stiprumą. Nepaisant to, kompozito bandiniai C90ZL10 ir C90ZL5FA5 su ceolitu turi didesnes gniuždymo stiprio vertes nei bandinys C90FA10. Tai rodo, kad pridėjus ceolito į LSSCK, jo gniuždymo stiprumas bus didesnis. Kompozito bandinių C90ZL10, C90FA10 ir C90ZL5FA5 vandens ir rišiklio santykis buvo didesnis nei C100S100 bandinio, o tai galėjo turėti įtakos jų stiprumo sumažėjimui.

Remiantis gautais duomenimis, f_c ir f_{fl} sumažėjo didėjant aerogelio koncentracijai. f_c pablogėjimas buvo reikšmingesnis nei f_{fl} sumažėjimas. 1/0,5 mm ir 2/1 mm dydžio putstiklio užpildus pakeitus 100 % aerogeliu, f_c ir f_{fl} sumažėjo atitinkamai 49,2 % ir 34,6 %. Kontrolinio bandinio, C90ZL10AG25, C90ZL10AG50, C90ZL10AG75 ir C90ZL10AG100 f_c buvo išmatuotas atitinkamai 15,1; 13,6; 11,0; 9,1 ir 7,9 MPa. O štai bandinių C90ZL10AG25, C90ZL10AG50, C90ZL10AG75 ir C90ZL10AG100 f_{fl} svyravo nuo 2,3 iki 1,7 MPa. Aerogelio didelis trapumas ir mažas stiprumas turėjo didžiausią įtaką stiprio sumažėjimui. Naudojant aerogelio ir putstklio užpildų derinį, stipris sumažėja, ypač esant didesnei aerogelio koncentracijai. Pridėjus aerogelio į cementinį kompozitą, neabejotinai sumažės kompozito stipris, tačiau taip pat gali sumažėti jo tankis, kartu pagerėja medžiagos šilumos izoliacinės savybės (Adhikary et al., 2021a).

6 lentelėje parodytas visų LSSCK bandinių orasausis tankis, kuris svyruoja nuo 1343 iki 1019 kg/m^3. Remiantis gautais duomenimis, mažėjant natūralaus smėlio koncentracijai ir didėjant putstiklio užpildų koncentracijai, LSSCK tankis labai sumažėjo. Didelė putstiklio užpildų koncentracija cementiniame kompozite gali sumažinti tankį, nes putstiklis yra daug lengvesnė medžiaga už natūralų gamtinį smėlį. Tyrimo rezultatai taip pat parodė, kad padidėjus aerogelio koncentracijai žymiai sumažėja LSSCK tankis. Visiškai pakeitus 1/0,5 ir 2/1 mm stambumo putstiklio užpildus aerogeliu, LSSCK tankis sumažėjo 15,8 %. Orasausis C90ZL10AG25, C90ZL10AG50, C90ZL10AG75 ir C90ZL10AG100 tankis buvo atitinkamai apie 1126, 1076, 1044, 1019 ir 948 kg/m^3.

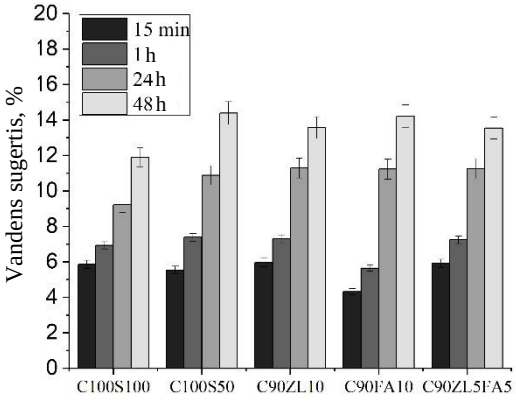

2 pav. Lengvojo cementinio kompozito bandinių, kuriuose nėra aerogelio, vandens sugertis

2 ir 3 paveiksluose pavaizduota visų LSSCK bandinių vandens įgėrio tyrimo duomenys. Po 48 valandų vandens įgėrio bandymo LSSCK bandinių nuo C100S100 iki C90ZL5FA5 WA įgerto vandens tūris svyravo nuo 11,9 iki 14,3 %. Kompozito bandinys, pagamintas naudojant mažesnį vandens bei rišiklio santykį ir putstiklio bei natūralaus smėlio užpildų mišinį, turi mažesnį vandens įgėrį nei kiti kompozito bandiniai. Iš tyrimo duomenų matome, kad LSSCK mišinių modifikavimui panaudojus pucolanines įmaišas vandens sugertis padidėja. Po 48 valandų mirkymo

išmatuotas bandinių C90ZL10AG25, C90ZL10AG50, C90ZL10AG75 ir C90ZL10AG100 vandens sugertis buvo 13,6 %, 15,7 % ir 17,7 %, 18,7 % ir 20,1 %. Dėl aerogelio užpildų didelio poringumo gali padidėti vandens įgėrio rizika.

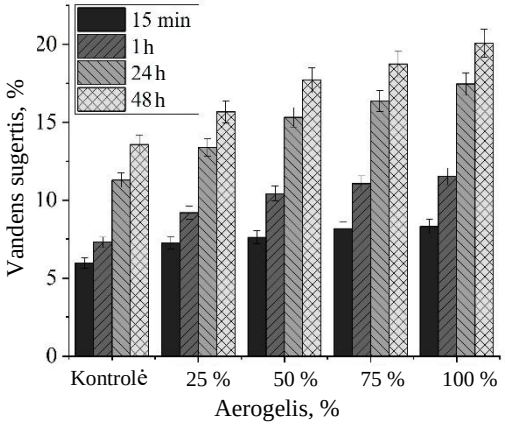

3 pav. Lengvojo cementinio kompozito bandinių, kuriuose yra aerogelio, vandens sugertis

4 paveiksle pateiktos LSSCK SEM nuotraukos rodo, kad aplink aerogelio daleles yra susiformavęs didesnis porų kiekis LSSCK. Galime teigti, kad maišant šviežius cementinius kompozitus aerogelis gali sulaikyti oro burbuliukus dėl didesnių paviršiaus įtempių. Ankstesniame tyrimo etape pastebėta, kad aerogelis taip pat silpniau sukimba su cementiniais rišikliais. Manome, kad LSSCK stiprumas sumažėja dėl silpnesnio aerogelio sukibimo su cementiniu rišikliu ir SRUKZ padidėjusio poringumo.

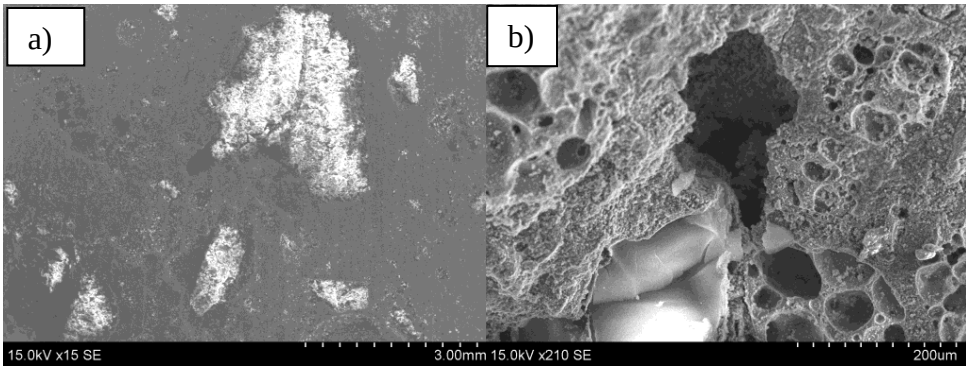

4 pav. a) ir **b)** Lengvojo betono skenuojamosios elektroninės mikroskopijos vaizdai, kuriuose matyti aplink aerogelio daleles padėjęs poringumas

1.2. LSSCK fizinių, mechaninių savybių ir SRUKZ gerinimas taikant lengvųjų užpildų paviršiaus padengimą polimerinėmis dangomis

Šiame eksperimentiniame tyrime kaip lengvieji užpildai buvo naudojamos kelios putstiklio užpildų frakcijos, o kaip polimerinės dangos – stireno ir butadieno

kopolimeras (SBK) ir skystas parafinas. Lengvųjų užpildų paviršiaus padengimui skystieji polimerai pirmiausia buvo supilami į indą, o lengvieji užpildai kuriam laikui panardinami jame. Maždaug po 20 sekundžių mirkymo lengvieji užpildai buvo išimami ir paskleidžiami ant plokščių paviršių džiovinimui. Antrasis dangos sluoksnis buvo pakartotinai padengiamas tuo pačiu būdu. Pirmajam LSSCK mėginiui (EGAC) paruošti naudotos šios putstiklio užpildų frakcijos: 0,1–0,3 mm, 0,25–0,5 mm, 0,5–1 mm, 1–2 mm, 2–4 mm ir 2–4 mm. Antrasis tyrimo bandinys buvo pavadintas A50; jame 50 % 2/1 mm ir 1/0,5 mm putstiklio užpildų tūrio buvo pakeista 2/0,5 mm aerogelio dalelėmis. Pirmieji du bandiniai, EGAC ir A50, buvo pagaminti be padengimo polimerinėmis dangomis. Vėliau tos pačios sudėties A50 mišinys buvo paruoštas naudojant jo užpildus ir padengiant skirtingomis polimerinėmis dangomis. SBR1 bandinys buvo paruoštas su 1/0,5 mm, 2/1 mm, 4/2 mm ir 8/4 mm stambumo putstiklio užpildais, kurių paviršius padengtas vienu SBK sluoksniu. PAR1 buvo paruoštas analogiškai SBR1 mišiniui su vienu skystojo parafino sluoksniu. SBR2 kompozito bandiniui paruošti naudoti putstiklio užpildai, kurių paviršius buvo padengtas dviem SBK dangos sluoksniais. SBR-PAR bandinys padengtas vienu SBK sluoksniu ir antru skystojo parafino dangos sluoksniu. Be to, aerogelio dalelės buvo padengtos SBK vienu sluoksniu ir naudojamos SBR1, PAR1, SBR2 ir SBR-PAR bandinių paruošimui. Vandens ir rišiklio santykis išlaikytas 0,48. 7 lentelėje pateiktos LSSCK bandinių mišinio sudėtys.

7 lentelė. Polimerais modifikuoto LSSCK mišinio sudėtys, kg/m^3 (II etapas)

Mišinio serija	Cementas	Užpildas (4/8+2/4+1/2+1/ 0,5+0,5/0,25+0, 01/0,3)	Aerogelis	Ceolitas	Superplastifika-torius	Vanduo, kg/m^3
EGAC	568,4	12,8+14,3+36,2+49,62+50,5+168,1	–	63,2	9,42	302,4
A50	568,4	12,8+14,3+36,2+49,62+50,5+168,1	11,8	63,2	9,42	302,4
SBR1	568,4	12,8+14,3+36,2+49,62+50,5+168,1	11,8	63,2	9,42	302,4
PAR1	568,4	12,8+14,3+ 36,2+49,62+50,5+168,1	11,8	63,2	9,42	302,4
SBR2	568,4	12,8+14,3+36,2+ 49,62+50,5+168,1	11,8	63,2	9,42	302,4
SBR-PAR	568,4	12,8+14,3+36,2+49,62+50,5+168,1	11,8	63,2	9,42	302,4

Pradinis maišymo etapas apima cemento, gamtinio ceolito ir putstiklio užpildų maišymą rankiniu būdu 2 minutes. Tada mišinys 3 minutes rankiniu būdu maišomas su 50 % vandeniu. Paskui superplastifikatorius sumaišomas su likusiu vandeniu ir įdedamas į kompozito mišinį. Aerogelis į kompozito mišinį buvo dedamas paskutinis, kad būtų išvengta aerogelio dalelių suskaldymo. Galutinis LSSCK mišinys maišomas 2 minutes ir atliekamas jo konsistencijos bandymas.

LSSCK mišinio konsistencijos bandymo duomenys pateikti 8 lentelėje. Tyrimo rezultatai rodo, kad į kompozito mišinį pridėjus aerogelio žymiai sumažėja jo pasklida. Aerogelis buvo naudojamas iš dalies pakeisti putstiklio užpildus LSSCK mišinyje, todėl pasklida sumažėjo nuo 81 cm iki 73,2 cm. Aerogelio paviršius gali sugerti vandenį, todėl cementinių mišinių klojumas sumažėja (Adhikary et al., 2021a; Venkateswara Rao et al., 2003).

8 lentelė. Polimerais modifikuoto LSSK mišinio klojumas (II etapas)

Mišinio serija	Pasklida, cm		T_{50}, s		*V* piltuvo ištekėjimo trukmė, s		*J* žiedo aukštis, cm
EGAC	81	SF3	5	VS2	6	VF2	9,4
A50	73,2	SF2	5,5	VS2	6,5	VF2	9
SBR1	74,5	SF2	5	VS2	5,4	VF2	9
PAR1	78,2	SF3	4,5	VS2	5	VF2	9,6
SBR2	75	SF2	5	VS2	6	VF2	8,5
SBR-PAR	76	SF3	5	VS2	6	VF2	9,5

Aerogelio įmaišymas į LSSCK mišinius sumažina mišinio konsistenciją. Tačiau vienu skystojo parafino ir SBK sluoksniu padengti putstiklio užpildai rodo nedidelį LSSCK mišinio konsistencijos padidėjimą. Iš tyrimo duomenų matome, kad vienu sluoksniu parafinu padengti putstiklio užpildai turi didesnį efektyvumą LSSCK mišinio konsistencijos padidėjimui nei SBK padengti putstiklio užpildai. PAR1 ir SBR1 mišinių pasklida padidėjo 6,9 % ir 1,8 % atitinkamai, lyginant su A50 bandiniu. T50 pasklidos trukmė iki 50 cm skersmens, kaip parodyta 8 lentelėje, kinta nuo 4,5 iki 5,5 sekundės. Pastebėta, kad EGAC mišinio pasklidos trukmė T50 yra 5 sekundės, o naudojant aerogelį kaip dalinį pustiklio užpildų pakaitalą (A50 mišinys), ji padidėjo iki 5,5 sekundės. T50 pasklidos trukmė buvo šiek tiek trumpesnė mišiniuose, kur užpildai buvo padengti vienu sluoksniu SBR ir skystu parafinu. Kompozito mišinių *J* žiedo bandymo aukštis svyravo nuo 8,5 cm iki 9,6 cm. Kompozito mišiniuose sluoksniavimosi požymių nebuvo. Tikėtina, kad dėl to polimerinėmis dangomis padengti putstiklio užpildai turėjo mažesnę vandens absorbciją; taip pat sumažėjo trinties jėgos tarp dalelių (Yashar ir Behzad, 2021), todėl pagerėjo klojumas. Tačiau visi LSSCK bandiniai atitiko EFNARC reikalavimus, kad būtų būti vadinami susitankinančiais mišiniais (SSB). Polimeru modifikuoto LSSCK pasklidos klasės buvo nustatytos SF2 ir SF3, o *V* piltuvo LSSCK klampos klasė buvo priskirta VF2.

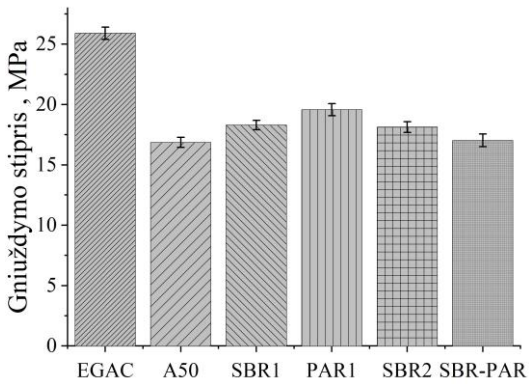

5 pav. Polimerais modifikuotų lengvųjų savaime susitankinančių cementinių kompozitų gniuždymo stipris (II etapas)

5 paveiksle pavaizduotas polimeru modifikuotų cementinių kompozitų bandinių gniuždymo stipris f_c. Bandymo rezultatai parodė, kad bandinių f_c svyravo nuo 25,9 MPa iki 17,03 MPa. Į LSSCK mišinį įdėjus aerogelį kaip dalinį putstiklio užpildų pakaitalą, f_c sumažėjo 38,9 %. Aerogelis iš prigimties yra hidrofobinis, todėl turi silpnesnį sukibimą su cementiniu akmeniu; dėl jo padidėja poringumas ir sumažėja mechaninis stipris (Adhikary et al., 2022b, 2021c; Lu et al., 2020). Šiame tyrime galima pastebėti nedidelį gniuždymo stiprio pagerėjimą iš anksto apdorojant lengvuosius užpildus polimerais. Kompozito stipris gniuždant pagerėjo 8,4 % ir 15,9 %, kai putstiklio užpildai buvo padengti vienu SBR arba parafino sluoksniu. Eksperimentinis tyrimas parodė, kad parafinu padengti putstiklio užpildai padidina betono stiprumą kiek daugiau nei su SBR padengtais užpildais pagamintas betonas. Galbūt polimeru dengtų kompozitų bandinių stipris padidėjo dėl SRUKZ pagerėjimo. Tačiau naudojant dvigubą polimerinių dangų sluoksnį ant putstiklio užpildų, sumažėjo gniuždymo stipris. Tikėtina, kad naudojant dviejų sluoksnių dangą ant lengvųjų užpildų maišymo metu į kompozitą pateko daugiau įtraukto oro, todėl padidėjo poringumas ir sumažėjo stipris.

6 paveiksle parodytas polimeru modifikuoto lengvojo savaime susitankinančio cementinio kompozito išdžiovintų bandinių tankis. Orasausis polimeru modifikuoto LSSCK tankis yra nuo 1164 iki 1065 kg/m^3. Išmatuotas 9,3 % tankio sumažėjimas, kai iš dalies putstiklio užpildai buvo pakeisti aerogeliu. Aerogelis yra lengvesnė medžiaga, palyginti su kitais lengvaisiais užpildais, todėl tikėtina, kad tankis sumažėja naudojant aerogelį kaip putstiklio užpildų pakaitalą.

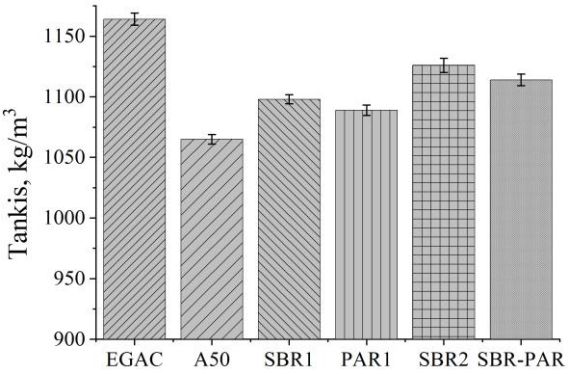

6 pav. Polimerais modifikuoto LSSCK tankis (II etapas)

7 paveiksle parodytas LSSCK vandens sugertis. Kompozitų vandens sugertis svyruoja nuo 8,25 % iki 13,16 % po 48 valandų panardinimo į vandenį. Naudojant aerogelį kaip dalinį putstiklio užpildų pakaitalą, vandens sugertis padidėjo 59,5 %. Tačiau polimeru dengti lengvieji užpildai galėjo sumažinti cementinio kompozito vandens sugertis. Cementinis kompozitas SBR1, padengtas vieno sluoksniu SBR, ir PAR1, padengtas vieno sluoksnio parafinu, po 48 valandų panardinimo į vandenį parodė 22,6 % ir 26 % mažesnį vandens įgėrį, palyginti su A50. Tačiau LSSCK, paruoštas su dvigubu polimeriniu sluoksniu padengtu pustiklio užpildu, turi panašų vandens įgėrį. Dvigubo sluoksnio danga padengtas putstiklio užpildas nežymiai

padidina vandens įgėrį, palyginti su vienu sluoksniu padengtu putstiklio užpildu. Šio atvejo priežastis gali būti padidėjęs LSSCK poringumas.

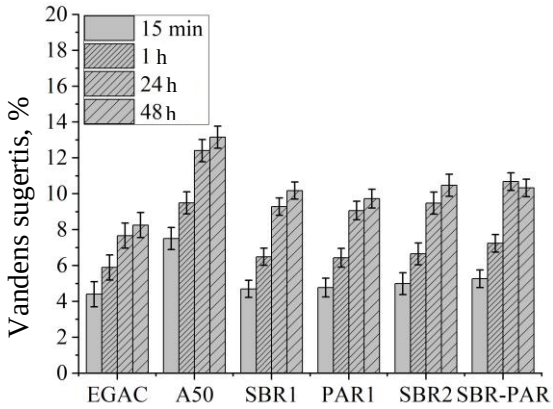

7 pav. Polimerais modifikuoto LSSCK vandens sugertis (II etapas)

Nepadengto putstiklio užpildo ir SBR polimerais padengto aerogelio SEM vaizdai pateikti 8 paveiksle. Iš SEM vaizdo matyti, kad aerogelio paviršius atrodo šiurkštus, matomas sutrūkinėjęs užpildo paviršius.

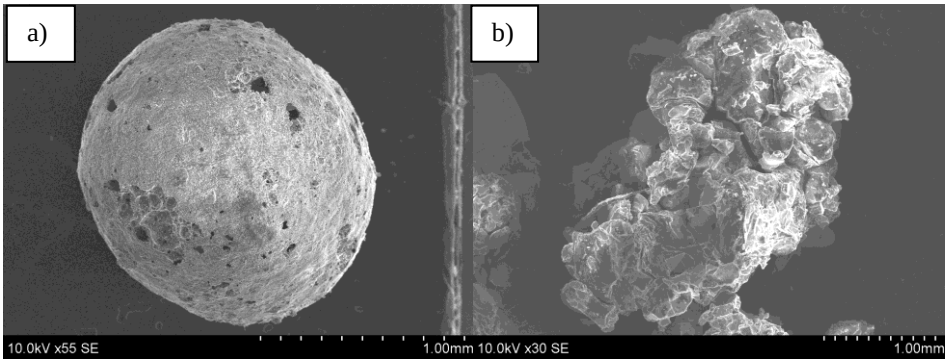

8 pav. Nepadengto danga putstiklio užpildo SEM vaizdas; b) SBR polimeru padengto aerogelio vaizdas

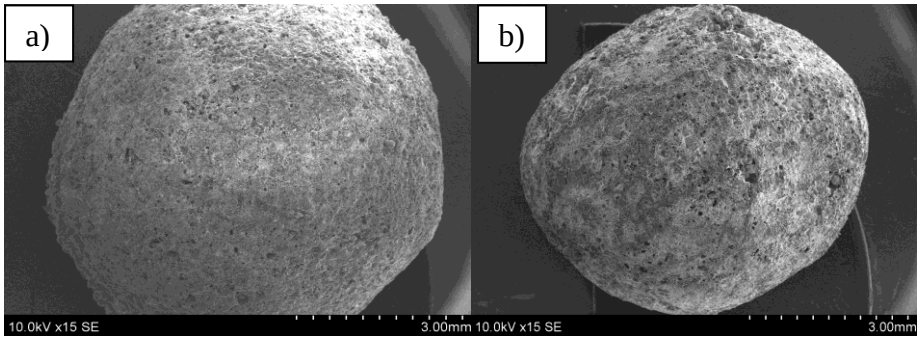

9 pav. a) SEM vaizdas, kuriame parodyta vienu sluoksniu parafinu dengto putstiklio užpildo paviršiaus tekstūra; b) SEM vaizdas, kuriame parodyta vienu sluoksniu SBR padengto putstiklio užpildo paviršiaus tekstūra

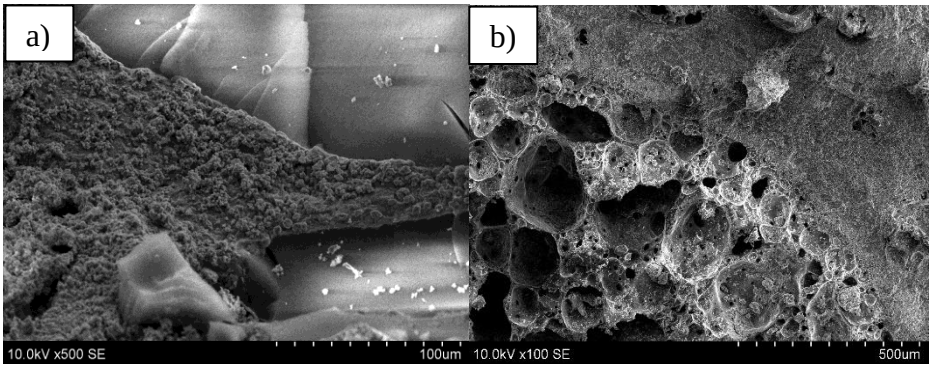

10 pav. a) SRUKZ tarp cementinio rišiklio ir polimeru dengto aerogelio SEM nuotrauka; b) SRUKZ polimeru dengto putstiklio užpildo SEM nuotrauka

Vieno sluoksnio parafinu padengtas putstiklio užpildo paviršius ir vieno sluoksnio SBR dengtas putstiklio užpildas parodytas 9 paveiksle. 10a) paveiksle parodytas nedidelis aerogelio ir cementinių medžiagų SRUKZ pagerėjimas. Taip pat šiame paveiksle parodyta, kad cementinės medžiagos kontaktinėje zonoje nepažeidė aerogelio dalelių. 10b) paveiksle parodyta putstiklio užpildo padengto SBR danga SRUKZ. Šioje nuotraukoje matomas geras putstiklio sukibimas su sukietėjusiu cementiniu akmeniu. Paveiksle taip pat parodyta, kad SRUKZ tarp cementinio rišiklio ir polimeru padengto putstiklio rišiklio turi neįprastai homogenišką ir tankią mikrostruktūrą. Atrodo, kad naudojant polimerines dangas pagerėja atskyrimo tarpai tarp aerogelio ir sukietėjusio cementinio rišiklio.

1.3. Lengvojo betono mechaninių, SRUKZ ir vandens įgėrio savybių gerinimas naudojant anglies nanovamzdelius (ANV) ir grafeno nanoplokšteles (GNP)

Šiame tyrime, naudojant tokias naujos kartos nanomedžiagas kaip ANV ir GNP, buvo bandoma spręsti tokias problemas: kaip padidinti lengvojo betono stiprumo savybes, pagerinti SRUKZ tarp aerogelio bei cemento rišiklio ir sumažinti vandens absorbcijos riziką.

1.3.1. Lengvųjų cemento kompozitų mechaninių, SRUKZ ir vandens įgėrio savybių gerinimas naudojant anglies nanovamzdelius

Šiame etape su aerogelio ir putstiklio užpildais pagaminti LSSCK buvo modifikuoti ANV, kurių buvo įdėta į mišinį iki 0,6 % nuo cemento masės. Pirmiausia cementas, gamtinis ceolitas (klinoptilolitas) ir putstiklio užpildai buvo maišomi sausomis sąlygomis 2 minutes. Po to į LSSCK mišinį pridėtas superplastifikatorius polikarboksilato pagrindu su 40 % bendru vandens kiekiu. Likę 60 % vandens įmaišyti į drėgną mišinį ir maišomi rankomis 2 minutes. ANV buvo įdėti į vandens tirpalą ir 3 minutes disperguoti ultragarsu. Taip apdorotas ANV tirpalas buvo įpiltas į LSSCK mišinį ir maišomas 3 minutes. Paskutiniame mišinio

paruošimo etape buvo įdėta aerogelio dalelių ir maišoma dar 2 minutes. ANV įmaiša modifikuoto cementinių kompozitų mišinio sudėtys pateiktos 9 lentelėje.

9 lentelė. LSSCK mišinio, modifikuoto anglies nanovamzdeliais, sudėtys, kg/m^3 (III-A etapas)

Mišinio serija	Cementas	Aerogelis	ANV %, %	Putstiklio užpildas (1/2+1/0,5+0,5/0,25+0,01/0,3)	Ceolitas	Superplastifikatorius	Stabilizatorius	Vanduo v/r = 0,65
LWC	454,5	31,5	0	34,5+54+34 + 40	45,45	8,181	1,3635	325
LWCCNT 0,04	454,5	31,5	0,04	34,5+54+34 +40	45,45	8,181	1,3635	325
LWCCNT 0,1	454,5	31,5	0,1	34,5+54+34 + 40	45,45	8,181	1,3635	325
LWCCNT 0,15	454,5	31,5	0,15	34,5+54+34 +40	45,45	8,181	1,3635	325
LWCCNT 0,30	454,5	31,5	0,30	34,5+54+34 +40	45,45	8,181	1,3635	325
LWCCNT 0,45	454,5	31,5	0,45	34,5+54+34 +40	45,45	8,181	1,3635	325
LWCCNT 0,60	454,5	31,5	0,60	34,5+ 54+ 3 4+ 40	45,45	8,181	1,3635	325

ANV modifikuotų LSSK bandinių f_c pateiktas 11 paveiksle. Tyrimo rezultatai rodo, kad ANV priedas turi reikšmingos įtakos LSSCK mechaninėms savybėms. LSSCK gniuždymo stipris f_c nuolat didėja, kai įdedama didesnė ANV dalis. LSSCK su 0,60 % ANV priedo nuo cemento masės padidino f_c 41,48 %. Tikėtina, kad dėl patobulintos LSSCK mikrostruktūros ir ANV kaip kristalizacijos centrų formavimo poveikio padidėja gniuždymo stipris. SEM vaizde buvo pastebėtas C-S-H naujadarų buvimas aplink ANV, iš kurio matyti ANV kaip kristalizacijos centro poveikis.

LSSK bandinių su iki 0,60 % ANV priedu vandens įgėrio kinetika parodyta 12 paveiksle. Išmatuotas kontrolinių mėginių vandens sugertis po 24 ir 48 valandų panardinimo į vandenį buvo 32,33 % ir 34,33 %, kuris sumažėjo iki 28,86 % ir 30,42 % esant 0,6 % ANV įmaišos kiekiui nuo cemento masės. Palyginti su kontroliniu bandiniu, ANV įmaiša sumažino vandens įgėrį iki 12 %. Sumažėjusį vandens įgėrį galima paaiškinti sumažėjusiu mikroporų kiekiu ir tankesne betono struktūra.

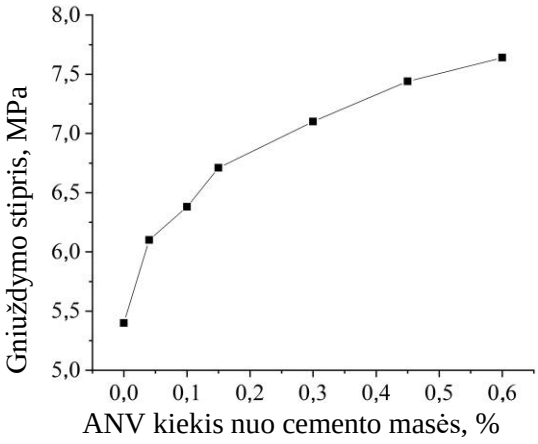

11 pav. LSSCK gniuždymo stiprio priklausomybė nuo ANV kiekio

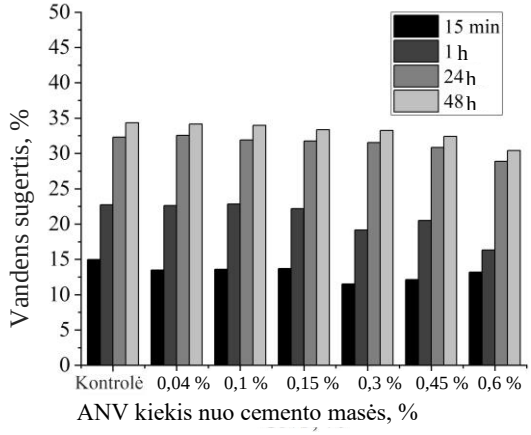

12 pav. LSSCK vandens sugertis priklausomybė nuo įdedamo ANV kiekio

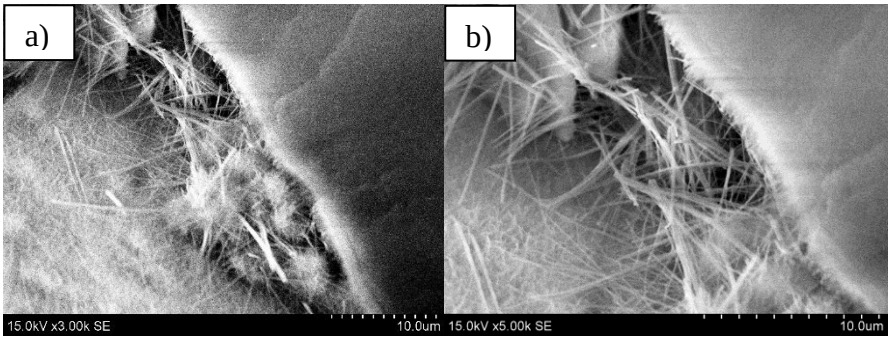

13 pav. SEM nuotraukos, parodančios hidratacijos produktų (adatos formos etringito bei kalcio hidrosilikatų) ir anglies nanovamzdelių buvimą aerogelio ir cementinės medžiagos SRUKZ

SEM tyrimo rezultatai rodo, kad ANV įmaišos panaudojimas nedideliais kiekiais padėjo pagerinti SRUKZ, kaip matyti 13 paveiksle. Cemento hidratacijos produktai ir ANV užpildė atskyrimo tarpus tarp hidrofobinio silicio aerogelio ir sukietėjusio cemento akmens. 14 paveiksle matyti, kad anglies nanovamzdeliai buvo homogeniškai išmaišyti LSSCK. Esant didelėms ANV koncentracijoms, kompozito struktūroje buvo pastebėtas į tinklą panašus pasiskirstymas. 14 paveiksle taip pat parodytas ANV kaip kristalizacijos centrų poveikis, o C-S-H naujadarų susidarymą galima aiškiai pastebėti aplink ANV daleles.

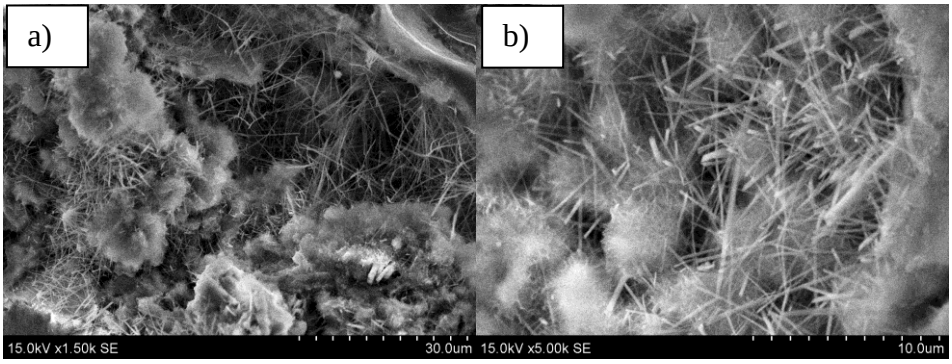

14 pav. SEM nuotraukos, parodančios ANV poveikį LSSCK mikrostruktūrai, taikant įvairų didinimą

1.3.2. LSSCK mechaninių, SRUKZ ir vandens įgėrio savybių gerinimas naudojant grafeno nanoplokšteles

LSSCK mišinių paruošimui buvo naudojami trys skirtingi GNP storiai, kurių dozavimo diapazonas buvo nuo 0,025 % iki 0,50 % cemento masės. LSSCK mišiniuose buvo palaikoma pastovi lengvojo užpildo koncentracija, o GNP kiekiai didinami nuo 0,025 % iki 0,5 % nuo cemento masės. Naudoti 0,1–0,3 mm, 0,25–0,5 mm, 0,5–1 mm, 1–2 mm, 2–4 mm, 4–8 mm frakcijų putstiklio užpildai, ir 0,5–2 mm dydžio aerogelio dalelės taip pat buvo naudojamos kaip lengvieji užpildai.

Vandens ir rišiklio santykis buvo išlaikomas pastovus – 0,48. Taikytas GNP storis buvo 2 nm, 6–8 nm ir 11–15 nm. LSSCK mišinių sudėtys pateiktos 10 lentelėje. Pirmajame etape GNP buvo išsklaidytas su visu vandens ir superplastifikatoriaus kiekiu, disperguojant ultragarsu 3 minutes. Paskui ceolito milteliai, cementas ir putstiklio užpildai buvo maišomi rankiniu būdu 2 minutes. Tada į mišinį buvo įpilas ultragarsu disperguotas GNP tirpalas ir švelniai maišomas dar 2 minutes. Paskutiniame maišymo etape buvo panaudota aerogelio dalis ir maišoma dar 1 minutę. Aerogelio dalelės buvo sumaišytos paskutiniame tyrimo etape, kad būtų išvengta maksimalaus aerogelio dalelių suskaldymo. Nustačius šviežio LSSCK mišinio savybes, iš kompozito buvo suformuoti 16,0 × 4,0 × 4,0 cm dydžio bandiniai ir vieną parą laikomi kambario temperatūroje kietėti. Įgavęs pirminį stiprumą kietėjantis cemento kompozitas buvo laikomas klimatinėje patalpoje 27 paras, išlaikant santykinę oro drėgmę ≥95 ir 20±1 °C temperatūrą.

10 lentelė. Lengvojo cemento kompozito, modifikuoto grafeno nanoplokštelėmis, mišinio sudėtis, kg/m^3 (III-B etapas)

Mišinio serija	Cementas	Putstiklio užpildas (4/8+2/4+1/2+1/0,5+0,5/0,25+0,01/0,3)	Aerogelis	Ceolitas	GNP %	Superplastiklis	Vanduo
Kontrolė	524,7	11,82+13,2+16,70+ 22,9+46,6+155,2	10,92	58,3	0	8,7	279,2
2 nm 0,025 %	524,7	11,82+13,2+16,70+ 22,9+46,6+155,2	10,92	58,3	0,025	8,7	279,2
2 nm 0,050 %	524,7	11,82+13,2+16,70+ 22,9+46,6+155,2	10,92	58,3	0,05	8,7	279,2
2 nm 0,1 %	524,7	11,82+13,2+16,70+ 22,9+46,6+155,2	10,92	58,3	0,1	8,7	279,2
2 nm 0,25 %	524,7	11,82+13,2+16,70+ 22,9+46,6+155,2	10,92	58,3	0,25	8,7	279,2
2 nm 0,50 %	524,7	11,82+13,2+16,70+ 22,9+46,6+155,2	10,92	58,3	0,5	8,7	279,2
6–8 nm 0,025 %	524,7	11,82+13,2+16,70+ 22,9+46,6+155,2	10,92	58,3	0,025	8,7	279,2
6–8 nm 0,050 %	524,7	11,82+13,2+16,70+ 22,9+46,6+155,2	10,92	58,3	0,05	8,7	279,2
6–8 nm 0,1 %	524,7	11,82+13,2+16,70+ 22,9+46,6+155,2	10,92	58,3	0,1	8,7	279,2
6–8 nm 0,25 %	524,7	11,82+13,2+16,70+ 22,9+46,6+155,2	10,92	58,3	0,25	8,7	279,2
6–8 nm 0,50 %	524,7	11,82+13,2+16,70+ 22,9+46,6+155,2	10,92	58,3	0,5	8,7	279,2
1115 nm 0,025 %	524,7	11,82+13,2+16,70+ 22,9+46,6+155,2	10,92	58,3	0,025	8,7	279,2
11–15 nm 0,050 %	524,7	11,82+13,2+16,70+ 22,9+46,6+155,2	10,92	58,3	0,05	8,7	279,2
11–15 nm 0.1 %	524,7	11,82+13,2+16,70+ 22,9+46,6+155,2	10,92	58,3	0,1	8,7	279,2
11–15 nm 0,25 %	524,7	11,82+13,2+16,70+ 22,9+46,6+155,2	10,92	58,3	0,25	8,7	279,2
11–15 nm 0,50 %	524,7	11,82+13,2+16,70+ 22,9+46,6+155,2	10,92	58,3	0,5	8,7	279,2

LSSCK gniuždymoir lenkimo stiprių f_c ir f_{fl} duomenys atitinkamai pateikti 15 ir 16 pav. Tyrimo rezultatai rodo, kad GNP įmaišos panaudojimas ir jos plokštelių storis turi didelę įtaką LSSCK mechaniniam stipriui; kad cementinio kompozito f_c pagerėjo padidinus GNP kiekį iki 0,25 % nuo cemento masės. Išmatuota kontrolinio bandinio f_c vertė buvo 11,32 MPa, kuri padidėjo iki 15,88 MPa, 15,52 MPa ir 14,92 MPa, panaudojant 0,25 % GNP įmaišos kiekį, kurios storis atitinkamai 2 nm, 6–8 nm ir 11–15 nm. Didžiausias išmatuotas gniuždymo stiprio padidėjimas buvo apie 43 %, palyginti su kontroliniu bandiniu, kai buvo panaudota 11–15 nm storio

GNP įmaiša. Tačiau smarkiai sumažėjo LSSCK gniuždymo stipris, kai GNP kiekis viršijo 0,25 %.

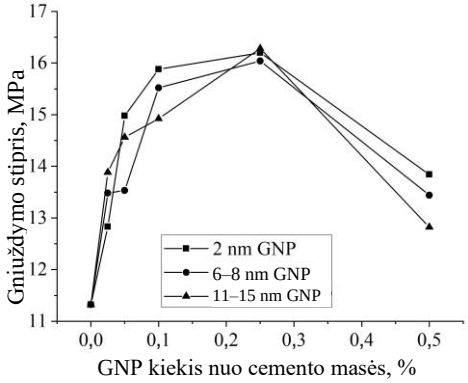

15 pav. LSSCK gniuždymo stiprio priklausomybė nuo GNP kiekio

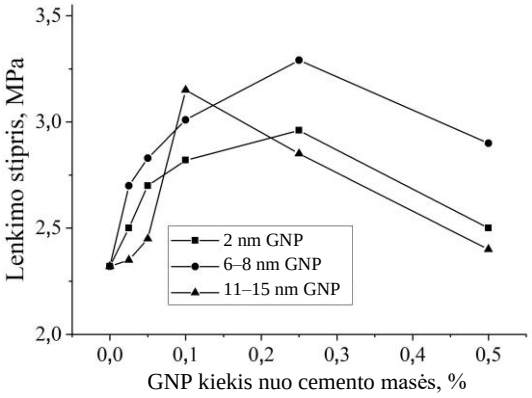

16 pav. LSSCK lenkimo stiprio priklausomybė nuo GNP kiekio

Lenkimo stipris kito panašiai kaip ir gniuždymo stipris, naudojant GNP įmaišas. Optimalus cementinių kompozitų, kuriuose panaudotas 2 nm ir 6–8 nm storio GNP priedas, stiprio lenkiant pagerėjimas buvo išmatuotas esant 0,25 % GNP kiekiui nuo cemento masės. O štai 11–15 nm GNP įmaiša sustiprintas LSSCK įgyja optimalų f_{fl} esant 0,1 % įmaišos kiekiui. Buvo nustatytas beveik 41,8 % cemento kompozito stiprio lenkiant pagerėjimas naudojant 6–8 nm storio 0,25 % GNP priedą. Literatūros tyrimai taip pat patvirtina, kad GNP naudojimas cementinėje sistemoje gali pagerinti mechanines savybes (Arslan et al., 2022; Cao et al., 2016). Mechaninės savybės gali pagerėti dėl GNP porų užpildymo ir kristalizacijos centrų susidarymo poveikio (Chen et al., 2019; Du ir Pang, 2015; Matalkah ir Soroushian, 2020). Tačiau šiame tyrime taip pat buvo pastebėtas cemento kompozitų su didesniu GNP kiekiu mechaninių savybių pablogėjimas; šį reiškinį galima paaiškinti nanomedžiagų hidrofilinėmis savybėmis (Arslan et al., 2022). Sugeriant vandenį nuo cemento paviršiaus, GNP hidrofiliškumas gali užkirsti kelią cemento hidratacijai (Barnard ir Snook, 2008; Nazari ir Riahi, 2011). Be to, naudojant didelius nanomedžiagų kiekius, vandens poreikis gali padidėti ir sutrikdyti tolygų

nanomedžiagų pasiskirstymą, todėl pablogėja mechaninės savybės (Chen et al., 2019). Tikriausiai dėl šių faktų cementinio kompozito mechaninės savybės pablogėja viršijant tam tikrus GNP kiekius.

Lengvojo cementinio kompozito vandens įgėrio (WA) po 24 valandų ir 48 valandų panardinimo į vandenį tyrimo duomenys atitinkamai pateikti 17 ir 18 paveiksluose. Tyrimo rezultatai parodė, kad padidėjus GNP kiekiui LSSCK, sumažėja lengvųjų cementinių kompozitų vandens sugertis. Po 48 valandų cemento kompozitas su 2 nm GNP turėjo mažiausią įgerto vandens kiekį. Po 24 valandų cemento kompozitų, kurių GNP storis yra 2 nm, 6–8 nm ir 11–15 nm, vandens sugertis sumažėjo atitinkamai maždaug 72,4 %, 56,7 % ir 64,4 %. Šis tyrimas parodė, kad GNP storis taip pat turi įtakos LSSCK vandens įgėriui WA. GNP dalelės užpildo cementinio kompozito poras, todėl pagerėja WA (Chen et al., 2019; Du ir Pang, 2015).

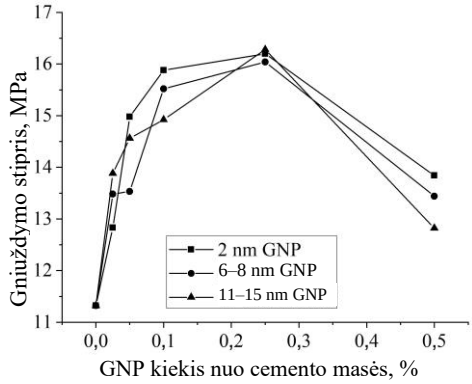

15 pav. LSSCK gniuždymo stiprio priklausomybė nuo GNP kiekio

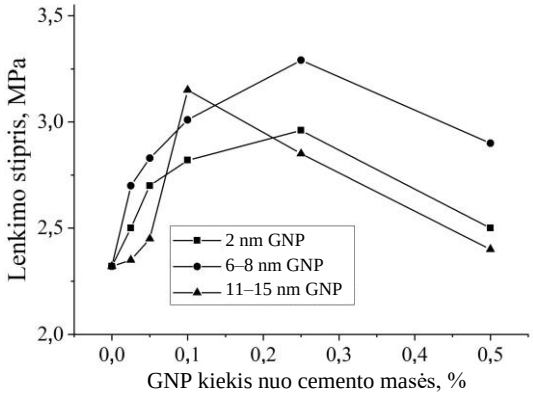

16 pav. LSSCK lenkimo stiprio priklausomybė nuo GNP kiekio

SRUKZ tarp aerogelio ir cementinių medžiagų be GNP įmaišos matoma 19a) paveiksle. Tačiau pastebimas SRUKZ pagerėjimas tarp aerogelio ir cementinių medžiagų su GNP įmaiša (žr. 19b) pav.). 20 paveiksle taip pat matoma, kad GNP

užtikrina porų / tuštumų užpildymo efektą. Tikriausiai dėl šių reiškinių pagerėjo cemento kompozito mechaninės ir vandens įgėrio savybės.

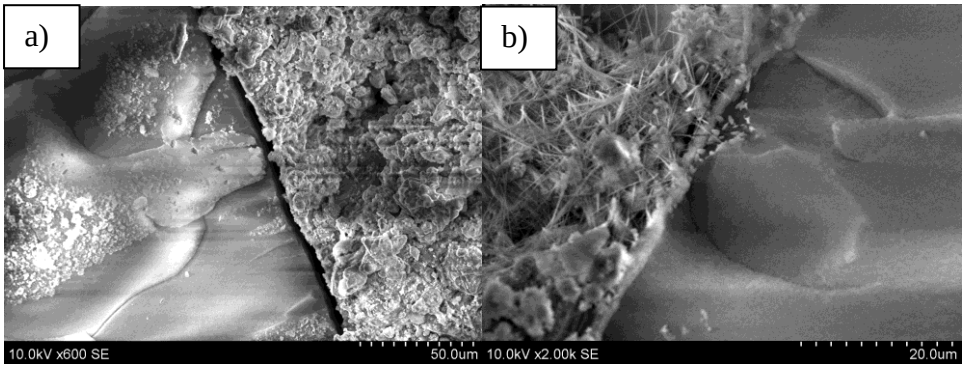

19 pav. SEM nuotraukos, kuriose parodyta: a) aerogelio SRUKZ be GNP įmaišos; b) aerogelio SRUKZ su GNP įmaiša

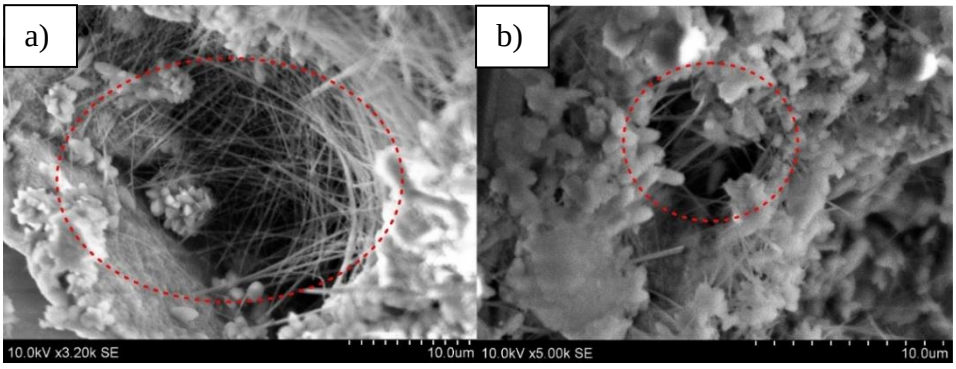

20 pav. SEM nuotraukos, kuriose parodomas porų / tuštumų užpildymo grafeno nanoplokštelėmis poveikis

2. Pagrindinės išvados

1 etapas. 1.1. Rišamųjų medžiagų, smulkiųjų dalelių ir lengvųjų užpildų koncentracijos įtakos tyrimai LSSCK fizikinėms, mechaninėms ir mikrostruktūros savybėms

Aerogelio naudojimas cementinėje sistemoje žymiai sumažina LSSCK tankį. Dalinis putstiklio užpildų pakeitimas aerogeliu (32,04 kg/m^3 kiekio) sumažina cemento kompozito tankį 15,8 %. Aerogelis yra lengvesnis nei putstiklio užpildai, o į cemento kompozitą įdėjus aerogelio, padidėja poringumas, todėl sumažėja tankis. Hidrofobinis aerogelis silpniau sukimba su cementinėmis medžiagomis, o naudojant 32,04 kg/m^3 ir 42 kg/m^3 silicinį aerogelį kaip dalinį putstiklio užpildo pakaitalą, gniuždymo stipris sumažėja atitinkamai 49,15 % ir 60,70 %.

Naudojant labai lengvus užpildus, tokius kaip putstiklis ir aerogelis, galima sukurti LSSCK tankio diapazone nuo 1343 iki 948 kg/m^3. Optimizuotas LSSCK

mišinys užtikrina klojumą diapazone nuo 700 iki 820 mm pasklidos ir atitinka EFNARC 2005 rekomenduojamas SF2 ir SF3 pasklidos klases tankio diapazone nuo 1400 iki 1000 kg/m^3. Be to, cementinio kompozito gniuždymo stipris yra nuo 21,3 iki 12,4 MPa, o tai taip pat rodo, kad jis atitinka rekomenduojamas ACI-213R-03-2003 (≥17 MPa) ir ACI-213R-2014 (≥17 MPa) CEB/RILEM (≥15 MPa) gniuždymo stiprio reikšmes. Tačiau LSSCK mikrostruktūros tyrimas parodė, kad aerogelio sukibimas su cementinėmis medžiagomis buvo silpnesnis, o SRUKZ buvo pastebėti atskyrimo tarpai. Be to, naudojant didelius aerogelio ir putstiklio užpildų kiekius cementinėse sistemose, padidėja vandens įgėrio rizika.

2 etapas. LSSCK fizinių, mechaninių savybių ir SRUKZ gerinimas taikant lengvųjų užpildų paviršiaus padengimą polimerinėmis dangomis

Pastebėta, kad lengvųjų užpildų paviršių padengus SBR ir skystojo parafino dangomis, LSSCK mišinių konsistencija kiek pagerėja. Pastebėtas beveik 6,8 % konsistencijos pagerėjimas, kai LSSK lengvieji užpildai iš anksto padengti polimerinėmis dangomis. Išmatuota pasklida buvo 810–732 mm, o tai atitinka SF2 ir SF3 pasklidos klasių keliamus reikalavimus. Lengvųjų užpildų padengimas polimerinėmis dangomis taip pat pagerina SRUKZ kokybę ir sumažina atskyrimo tarpus tarp aerogelio ir cementinio rišiklio. Be to, naudojant polimerines dangas, bendras poringumas sumažėja 2,9 %, o LSSCK vandens sugertis – apie 26 %. Nustatytas LSSCK gniuždymo stipris buvo nuo 25,9 MPa iki 17,03 MPa, ir tai atitinka CEB/RILEM, ACI-213R-03-2003 ir ACI-213R-2014 keliamus reikalavimus. Naudojant polimerines dangas LSSCK gniuždymo stipris padidėja 8,4 % ir 15,9 % atitinkamai, kai naudojamos vienasluoksnės SBR arba skysto parafino dangos.

3 etapas. 1.3. Lengvojo betono mechaninių, SRUKZ ir vandens įgėrio savybių gerinimas naudojant anglies nanovamzdelius (ANV) ir grafeno nanoplokšteles (GNP)

Pridėjus 0,6 % ANV įmaišos, LSSCK stipris gniuždant padidėjo beveik 41 %. Panaudojus ANV LSSK savybių modifikavimui, nustatyta, kad SRUKZ tarp aerogelio pagerėjo ir buvo pastebimas didesnis C-S-H naujadarų susidarymas. Taip pat pastebėta, kad ANV užpildo cementinio kompozito poras, todėl pagerėja LSSCK mechaninės ir vandens įgėrio savybės. ANV priedas sumažina LSSCK vandens įgėrį beveik 12 %.

Nustatyta, kad optimali yra 0,025 % nuo cemento masės GNP įmaiša, kuri pagerina LSSK gniuždymo stiprį. Įdėjus GNP, išmatuotas cementinio kompozito stipris gniuždant pagerėjo beveik 43 %, o vandens sugertis sumažėjo 72,4 % (po 24 valandų mirkymo). Be to, GNP priedas pagerina aerogelio ir cementinių rišiklių SRUKZ dėl porų užpildymo ir kristalizacijos centrų susidarymo.

REFERENCES

Adebayo Mujedu, K., Ab-Kadir, M.A., Ismail, M., 2020. A review on self-compacting concrete incorporating palm oil fuel ash as a cement replacement. Constr. Build. Mater. 258, 119541. https://doi.org/10.1016/j.conbuildmat.2020.119541

Adhikary, S.K., 2022. The influence of pre-coated EGA and aerogel on the properties of lightweight self-compacting cementitious composites. Mater. Today Commun. 31, 103496. https://doi.org/10.1016/j.mtcomm.2022.103496

Adhikary, Suman Kumar, Ashish, D.K., Rudžionis, Ž., 2021a. Aerogel based thermal insulating cementitious composites: A review. Energy Build. https://doi.org/10.1016/j.enbuild.2021.111058

Adhikary, S.K., Ashish, D.K., Sharma, H., Patel, J., Rudžionis, Ž., Mohammed, A.-A., Thomas, B.S., Khatib, J.M., 2022a. Lightweight self-compacting concrete : A review. Resour. Conserv. Recycl. Adv. 15. https://doi.org/10.1016/j.rcradv.2022.200107

Adhikary, S.K., Rudzionis, Z., 2020. Influence of expanded glass aggregate size, aerogel and binding materials volume on the properties of lightweight concrete. Mater. Today Proc. 32, 712–718. https://doi.org/10.1016/j.matpr.2020.03.323

Adhikary, S.K., Rudžionis, Ž., Tučkutė, S., 2022b. Characterization of novel lightweight self-compacting cement composites with incorporated expanded glass, aerogel, zeolite and fly ash. Case Stud. Constr. Mater. 16, e00879. https://doi.org/10.1016/j.cscm.2022.e00879

Adhikary, S.K., Rudžionis, Ž., Tučkutė, S., 2022c. Characterization of aerogel and EGA-based lightweight cementitious composites incorporating different thickness of graphene platelets. J. Build. Eng. 57. https://doi.org/10.1016/j.jobe.2022.104870

Adhikary, Suman Kumar, Rudžionis, Ž., Tučkutė, S., Ashish, D.K., 2021b. Effects of carbon nanotubes on expanded glass and silica aerogel based lightweight concrete. Sci. Rep. 11, 2104. https://doi.org/10.1038/s41598-021-81665-y

Adhikary, S.K., Rudžionis, Ž., Tučkutė, S., Ashish, D.K., 2021. Effects of carbon nanotubes on expanded glass and silica aerogel based lightweight concrete. Sci. Rep. 11. https://doi.org/10.1038/s41598-021-81665-y

Adhikary, S.K., Rudžionis, Ž., Vaičiukynienė, D., 2020. Development of flowable ultra-lightweight concrete using expanded glass aggregate, silica aerogel, and prefabricated plastic bubbles. J. Build. Eng. 31, 101399. https://doi.org/10.1016/j.jobe.2020.101399

Ahmad, F., Qureshi, M.I., Ahmad, Z., 2022. Influence of nano graphite platelets on the behavior of concrete with E-waste plastic coarse aggregates. Constr. Build. Mater. 316, 125980. https://doi.org/10.1016/j.conbuildmat.2021.125980

Altalabani, D., Linsel, S., Bzeni, D.K.H., 2020. Rheological Properties and Strength of Polypropylene Fiber-Reinforced Self-compacting Lightweight Concrete Produced with Ground Limestone. Arab. J. Sci. Eng. 45, 4171–4185. https://doi.org/10.1007/s13369-020-04410-z

Angelin, A.F., Cecche, R.C., Osório, W.R., Gachet, L.A., 2020. Evaluation of efficiency factor of a self-compacting lightweight concrete with rubber and expanded clay contents. Constr. Build. Mater. 257, 119573. https://doi.org/10.1016/j.conbuildmat.2020.119573

Arslan, S., Öksüzer, N., Gökçe, H.S., 2022. Improvement of mechanical and transport properties of reactive powder concrete using graphene nanoplatelet and waste glass aggregate. Constr. Build. Mater. 318. https://doi.org/10.1016/j.conbuildmat.2021.126199

Barnard, A.S., Snook, I.K., 2008. Thermal stability of graphene edge structure and graphene nanoflakes. J. Chem. Phys. 128. https://doi.org/10.1063/1.2841366

Barnat-Hunek, D., Góra, J., Andrzejuk, W., Lagód, G., 2018. The microstructure-

mechanical properties of hybrid fibres-reinforced self-compacting lightweight concrete with perlite aggregate. Materials (Basel). 11. https://doi.org/10.3390/ma11071093

Bumanis, G., Bajare, D., Locs, J., Korjakins, A., 2013. Alkali-silica reactivity of foam glass granules in structure of lightweight concrete. Constr. Build. Mater. 47, 274–281. https://doi.org/10.1016/j.conbuildmat.2013.05.049

Cao, M. li, Zhang, H. xia, Zhang, C., 2016. Effect of graphene on mechanical properties of cement mortars. J. Cent. South Univ. 23, 919–925. https://doi.org/10.1007/s11771-016-3139-4

Cheboub, T., Senhadji, Y., Khelafi, H., Escadeillas, G., 2020. Investigation of the engineering properties of environmentally-friendly self-compacting lightweight mortar containing olive kernel shells as aggregate. J. Clean. Prod. 249. https://doi.org/10.1016/j.jclepro.2019.119406

Chen, G., Yang, M., Xu, L., Zhang, Y., Wang, Y., 2019. Graphene nanoplatelets impact on concrete in improving freeze-thaw resistance. Appl. Sci. 9. https://doi.org/10.3390/app9173582

Da Silva, L.R.R., da Silva, J.A., Francisco, M.B., Ribeiro, V.A., de Souza, M.H.B., Capellato, P., Souza, M.A., Dos Santos, V.C., Gonçalves, P.C., Melo, M. de L.N.M., 2020. Polymeric waste from recycling refrigerators as an aggregate for self-compacting concrete. Sustain. 12, 1–19. https://doi.org/10.3390/su12208731

Du, H., Pang, S.D., 2015. Enhancement of barrier properties of cement mortar with graphene nanoplatelet. Cem. Concr. Res. 76, 10–19. https://doi.org/10.1016/j.cemconres.2015.05.007

Duplan, F., Abou-Chakra, A., Turatsinze, A., Escadeillas, G., Brule, S., Masse, F., 2014. Prediction of modulus of elasticity based on micromechanics theory and application to low-strength mortars. Constr. Build. Mater. 50, 437–447. https://doi.org/10.1016/j.conbuildmat.2013.09.051

El-Gamal, S.M.A., Hashem, F.S., Amin, M.S., 2017. Influence of carbon nanotubes, nanosilica and nanometakaolin on some morphological-mechanical properties of oil well cement pastes subjected to elevated water curing temperature and regular room air curing temperature. Constr. Build. Mater. 146, 531–546. https://doi.org/10.1016/j.conbuildmat.2017.04.124

Farooq, F., Akbar, A., Khushnood, R.A., Muhammad, W.L.B., Rehman, S.K.U., Javed, M.F., 2020. Experimental investigation of hybrid carbon nanotubes and graphite nanoplatelets on rheology, shrinkage, mechanical, and microstructure of SCCM. Materials (Basel). 13, 230. https://doi.org/10.3390/ma13010230

Gao, T., Jelle, B.P., Gustavsen, A., Jacobsen, S., 2014. Aerogel-incorporated concrete: An experimental study. Constr. Build. Mater. 52, 130–136. https://doi.org/10.1016/j.conbuildmat.2013.10.100

Juradin, S., Baloevi, G., Harapin, A., 2012. Experimental testing of the effects of fine particles on the properties of the self-compacting lightweight concrete. Adv. Mater. Sci. Eng. 2012. https://doi.org/10.1155/2012/398567

Kurt, M., Kotan, T., GüL, M.S., GüL, R., Aydin, A.C., 2016a. The effect of blast furnace slag on the self-compactability of pumice aggregate lightweight concrete. Sadhana - Acad. Proc. Eng. Sci. 41, 253–264. https://doi.org/10.1007/s12046-016-0462-2

Kurt, M., Said, M., Gül, R., Cüneyt, A., Kotan, T., 2016b. The effect of pumice powder on the self-compactability of pumice aggregate lightweight concrete. Constr. Build. Mater. 103, 36–46. https://doi.org/10.1016/j.conbuildmat.2015.11.043

Kwasny, J., Sonebi, M., Taylor, S.E., Bai, Y., Owens, K., Doherty, W., 2012. Influence of the Type of Coarse Lightweight Aggregate on Properties of Semilightweight Self-Consolidating Concrete. J. Mater. Civ. Eng. 24, 1474–1483.

https://doi.org/10.1061/(asce)mt.1943-5533.0000527

Leonavičius, D., Pundienė, I., Girskas, G., Pranckevičienė, J., Kligys, M., Kairytė, A., 2018. The effect of multi-walled carbon nanotubes on the rheological properties and hydration process of cement pastes. Constr. Build. Mater. 189, 947–954. https://doi.org/10.1016/j.conbuildmat.2018.09.082

Liu, Z. hui, Wang, F., Deng, Z. ping, 2016. Thermal insulation material based on SiO2 aerogel. Constr. Build. Mater. 122, 548–555. https://doi.org/10.1016/j.conbuildmat.2016.06.096

Lu, J., Jiang, J., Lu, Z., Li, J., Niu, Y., Yang, Y., 2020. Pore structure and hardened properties of aerogel/cement composites based on nanosilica and surface modification. Constr. Build. Mater. 245, 118434. https://doi.org/10.1016/j.conbuildmat.2020.118434

Matalkah, F., Soroushian, P., 2020. Graphene nanoplatelet for enhancement the mechanical properties and durability characteristics of alkali activated binder. Constr. Build. Mater. 249, 118773. https://doi.org/10.1016/j.conbuildmat.2020.118773

Nazari, A., Riahi, S., 2011. The effects of zinc dioxide nanoparticles on flexural strength of self-compacting concrete. Compos. Part B Eng. 42, 167–175. https://doi.org/10.1016/j.compositesb.2010.09.001

Nguyen, H.D., Truong, K.X.T., Nguyen, N.M., Do, T.T., 2018. Self-compacting lightweight aggregate concrete in Vietnam. IOP Conf. Ser. Mater. Sci. Eng. 365. https://doi.org/10.1088/1757-899X/365/3/032030

Ranjbar, M.M., Mousavi, S.Y., 2015. Strength and durability assessment of self-compacted lightweight concrete containing expanded polystyrene. Mater. Struct. Constr. 48, 1001–1011. https://doi.org/10.1617/s11527-013-0210-6

Schönlein, M., Plank, J., 2018. A TEM study on the very early crystallization of C-S-H in the presence of polycarboxylate superplasticizers: Transformation from initial C-S-H globules to nanofoils. Cem. Concr. Res. 106, 33–39. https://doi.org/10.1016/j.cemconres.2018.01.017

T.Ch, M., Pavithra.P, Singh, S.B., Raj, S.B.V., Paul, S., 2012. Effect of Multiwalled Carbon Nanotubes On Mechanical Properties of Concrete. Int. J. Sci. Res. 2, 166–168. https://doi.org/10.15373/22778179/june2013/53

Ting, T.Z.H., Rahman, M.E., Lau, H.H., Ting, M.Z.Y., 2019. Recent development and perspective of lightweight aggregates based self-compacting concrete. Constr. Build. Mater. 201, 763–777. https://doi.org/10.1016/j.conbuildmat.2018.12.128

Venkateswara Rao, A., Kulkarni, M.M., Amalnerkar, D.P., Seth, T., 2003. Surface chemical modification of silica aerogels using various alkyl-alkoxy/chloro silanes. Appl. Surf. Sci. 206. https://doi.org/10.1016/S0169-4332(02)01232-1

Wan, L.Y., Stefan, D., Aslani, F., Ma, G., 2018. Lightweight Self-Compacting Concrete Incorporating Perlite, Scoria, and Polystyrene Aggregates. J. Mater. Civ. Eng. 30, 04018178. https://doi.org/10.1061/(asce)mt.1943-5533.0002350

Westgate, P., Paine, K., Ball, R.J., 2018. Physical and mechanical properties of plasters incorporating aerogel granules and polypropylene monofilament fibres. Constr. Build. Mater. 158. https://doi.org/10.1016/j.conbuildmat.2017.09.177

Yashar, M., Behzad, V., 2021. Effect of pre-coating lightweight aggregates on the self-compacting concrete 1–12. https://doi.org/10.1002/suco.202000744

Yu, Q.L., Spiesz, P., Brouwers, H.J.H., 2013. Development of cement-based lightweight composites - Part 1: Mix design methodology and hardened properties. Cem. Concr. Compos. 44, 17–29. https://doi.org/10.1016/j.cemconcomp.2013.03.030

Yu, Z., Tang, R., Cao, P., Huang, Q., Xie, X., Shi, F., 2019. Multi-axial test and failure criterion analysis on self-compacting lightweight aggregate concrete. Constr. Build. Mater. 215, 786–798. https://doi.org/10.1016/j.conbuildmat.2019.04.236

Zhu, P., Brunner, S., Zhao, S., Griffa, M., Leemann, A., Toropovs, N., Malekos, A., Koebel, M.M., Lura, P., 2019. Study of physical properties and microstructure of aerogel-cement mortars for improving the fire safety of high-performance concrete linings in tunnels. Cem. Concr. Compos. 104. https://doi.org/10.1016/j.cemconcomp.2019.103414

Zhu, P., Yu, S., Cheng, C., Zhao, S., Xu, H., 2020. Durability of silica aerogel cementitious composites - Freeze-thaw resistance, water resistance and drying shrinkage. Adv. Cem. Res. 32, 527–536. https://doi.org/10.1680/jadcr.18.00145

Zhu, X., Kang, X., Deng, J., Yang, K., Yu, L., Yang, C., 2021. A comparative study on shrinkage characteristics of graphene oxide (GO) and graphene nanoplatelets (GNPs) modified alkali-activated slag cement composites. Mater. Struct. Constr. 54, 1–15. https://doi.org/10.1617/s11527-021-01695-w

Zhu, Y., Cui, H., Tang, W., 2016. Experimental investigation of the effect of manufactured sand and lightweight sand on the properties of fresh and hardened self-compacting lightweight concretes. Materials (Basel). 9. https://doi.org/10.3390/ma9090735

CURRICULUM VITAE

Suman Kumar Adhikary
Suman.adhikary@kru.edu

Education:

2012 – 2016	Bachelor of Technology in Civil Engineering Maulana Abul Kalam Azad University of Technology, India
2016 – 2018	Master in Civil Engineering, Kaunas University of Technology, Kaunas, Lithuania
2018 – 2022	PhD in Civil Engineering, Kaunas University of Technology, Kaunas, Lithuania

Awards:

2019	Most active PhD student, Faculty of Civil Engineering, Kaunas University of Technology
2020	Most active PhD student, Faculty of Civil Engineering, Kaunas University of Technology
2021	Most active PhD student, Faculty of Civil Engineering, Kaunas University of Technology
2019	Academic Excellence of PhD Students, Research Council of Lithuania
2020	Academic Excellence of PhD Students, Research Council of Lithuania
2022	Academic Excellence of PhD Students, Research Council of Lithuania

Research Interests: Lightweight concrete, self-compacting concrete, geopolymers, recycling, sustainable concrete, sustainability.

LIST OF PUBLICATIONS

Peer-reviewed publications forming the basis of this dissertation: Indexed in the Web of Science with Impact Factor

1. Adhikary, Suman Kumar; Rudžionis, Žymantas; Vaičiukynienė, Danutė. Development of flowable ultra-lightweight concrete using expanded glass aggregate, silica aerogel, and prefabricated plastic bubbles // Journal of building engineering. Amsterdam: Elsevier. ISSN 2352-7102. 2020, vol. 31, art. No. 101399, p. 1-10. DOI: 10.1016/j.jobe.2020.101399. [Science Citation Index Expanded (Web of Science); Scopus] [IF: 5.318; AIF: 4.248; IF/AIF: 1.251; Q1 (2020, InCites JCR SCIE)] [CiteScore: 5.50; SNIP: 2.305; SJR: 0.974; Q1 (2020, Scopus Sources)].
2. Adhikary, Suman Kumar; Rudžionis, Žymantas; Tučkutė, Simona. Characterization of novel lightweight self-compacting cement composites with incorporated expanded glass, aerogel, zeolite and fly ash //Case studies in construction materials. Amsterdam: Elsevier. ISSN 2214-5095. 2022, vol. 16, art. No. e00879, p. 1-19. DOI: 10.1016/j.cscm.2022.e00879. [Science Citation Index Expanded (Web of Science); Scopus] [IF: 4.934; AIF: 5.545; IF/AIF: 0.889; Q1 (2021, InCites JCR SCIE)] [CiteScore: 5,20; SNIP: 1.932; SJR: 1.009; Q1 (2021, Scopus Sources)].
3. Adhikary, Suman Kumar. The influence of pre-coated EGA and aerogel on the properties of lightweight self-compacting cementitious composites // Materials today communications. Amsterdam: Elsevier. ISSN 2352-4928. 2022, vol. 31, art. No. 103496, p. 1-8. DOI: 10.1016/j.mtcomm.2022.103496. [Science Citation Index Expanded (Web of Science); Scopus] [IF: 3.662; AIF: 6.504; IF/AIF: 0.563; (2021, InCites JCR SCIE)]
4. Adhikary, Suman Kumar; Rudžionis, Žymantas; Tučkutė, Simona; Ashish, Deepankar Kumar. Effects of carbon nanotubes on expanded glass and silica aerogel based lightweight concrete // Scientific reports. London: Nature research. ISSN 2045-2322. 2021, vol. 11, iss. 1, art. No. 2104, p. 1-11. DOI: 10.1038/s41598-021-81665-y. [Science Citation Index Expanded (Web of Science); Scopus; MEDLINE] [IF: 4.996; AIF: 7.700; IF/AIF: 0.648; Q2 (2021, InCites JCR SCIE)] [CiteScore: 6.90; SNIP: 1.389; SJR: 1.005; Q1 (2021, Scopus Sources)].
5. Adhikary, Suman Kumar; Rudžionis, Žymantas; Tučkutė, Simona. Characterization of aerogel and EGA-based lightweight cementitious composites incorporating different thickness of graphene platelets // Journal of building engineering. Amsterdam: Elsevier. ISSN 2352-7102. 2022, vol. 57, art. No 104870, p. 1-14. DOI: 10.1016/j.jobe.2022.104870. [Science Citation Index Expanded (Web of Science); Scopus] [IF: 7.144; AIF: 5.065;

IF/AIF: 1.410; Q1 (2021, InCites JCR SCIE)] [CiteScore: 6.40; SNIP: 2.147; SJR: 1.164; Q1 (2021, Scopus Sources)].

Peer-reviewed publications other than the dissertation: Indexed in the Web of Science with Impact Factor

1. Abbara, Abbas Abdulalim; Al-Ajamee, Abdelrahman Abdelhalim, Mohammed; Ahmed, Omer; Adhikary, Suman Kumar; Ahmed, Mohamedel Mustafa. Uniaxial compressive stress-strain relationship for rubberized concrete with coarse aggregate replacement up to 100% //Case studies in construction materials. Amsterdam: Elsevier. ISSN 2214-5095. 2022, vol. 17, art. No e01336, p. 1-15. DOI: 10.1016/j.cscm.2022.e01336. [Science Citation Index Expanded (Web of Science); Scopus] [IF: 4.934; AIF: 5.545; IF/AIF: 0.889; Q1 (2021, InCites JCR SCIE)] [CiteScore: 5.20; SNIP: 1.932; SJR: 1.009; Q1 (2021, Scopus Sources)].
2. Adhikary, Suman Kumar; Ashish, Deepankar Kumar; Rudžionis, Žymantas. A review on sustainable use of agricultural straw and husk biomass ashes: transitioning towards low carbon economy // Science of the total environment. Amsterdam: Elsevier. ISSN 0048-9697. eISSN 1879-1026. 2022, vol. 838, pt. 3, art. No. 156407, p. 1-16. DOI: 10.1016/j.scitotenv.2022.156407. [Science Citation Index Expanded (Web of Science); Scopus; MEDLINE] [IF: 10.753; AIF: 6.309; IF/AIF: 1.704; Q1 (2021, InCites JCR SCIE)] [CiteScore: 14.10; SNIP: 2.175; SJR: 1.806; Q1 (2021, Scopus Sources)].
3. Adhikary, Suman Kumar; Ashish, Deepankar Kumar. Turning waste expanded polystyrene into lightweight aggregate: towards sustainable construction industry // Science of the total environment. Amsterdam: Elsevier. ISSN 0048-9697. eISSN 1879-1026. 2022, vol. 837, art. No. 155852, p. 1-15. DOI: 10.1016/j.scitotenv.2022.155852. [Science Citation Index Expanded (Web of Science); Scopus; MEDLINE] [IF: 10.753; AIF: 6.309; IF/AIF: 1.704; Q1 (2021, InCites JCR SCIE)] [CiteScore: 14.10; SNIP: 2.175; SJR: 1.806; Q1 (2021, Scopus Sources)].
4. Rudžionis, Žymantas; Adhikary, Suman Kumar; Manhanga, Fallon Clare; Ashish, Deepankar Kumar; Ivanauskas, Remigijus; Stelmokaitis, Gediminas; Navickas, Arūnas Aleksandras. Natural zeolite powder in cementitious composites and its application as heavy metal absorbents // Journal of building engineering. Oxford: Elsevier. ISSN 2352-7102. 2021, vol. 43, art. No. 103085, p. 1-12. DOI: 10.1016/j.jobe.2021.103085. [Science Citation Index Expanded (Web of Science); Scopus] [IF: 7.144; AIF: 5.065; IF/AIF: 1.410; Q1 (2021, InCites JCR SCIE)] [CiteScore: 6.40; SNIP: 2.147; SJR: 1.164; Q1 (2021, Scopus Sources)].
5. Adhikary, Suman Kumar; Ashish, Deepankar Kumar; Rudžionis, Žymantas. Expanded glass as light-weight aggregate in concrete – a review // Journal

of cleaner production. Oxford: Elsevier. ISSN 0959-6526. eISSN 1879-1786. 2021, vol. 313, art. No. 127848, p. 1-20. DOI: 10.1016/j.jclepro.2021.127848. [Science Citation Index Expanded (Web of Science); Scopus] [IF: 11.072; AIF: 7.953; IF/AIF: 1.392; Q1 (2021, InCites JCR SCIE)] [CiteScore: 15.80; SNIP: 2.444; SJR: 1.921; Q1 (2021, Scopus Sources)].

6. Adhikary, Suman Kumar; Ashish, Deepankar Kumar; Rudžionis, Žymantas. Aerogel based thermal insulating cementitious composites: a review // Energy and buildings. Lausanne: Elsevier. ISSN 0378-7788. eISSN 1872-6178. 2021, vol. 245, art. No. 111058, p. 1-25. DOI: 10.1016/j.enbuild.2021.111058. [Science Citation Index Expanded (Web of Science); Scopus; Academic Search Complete] [IF: 7.201; AIF: 6.047; IF/AIF: 1.190; Q1 (2021, InCites JCR SCIE)] [CiteScore: 11.50; SNIP: 2.069; SJR: 1.682; Q1 (2021, Scopus Sources)].
7. Adhikary, Suman Kumar; Rudžionis, Žymantas; Rajapriya, R. The effect of carbon nanotubes on the flowability, mechanical, microstructural and durability properties of cementitious composite an overview// Sustainability. Basel : MDPI. ISSN 2071-1050. 2020, vol. 12, iss. 20, art. No. 8362, p. 1-25. DOI: 10.3390/su12208362. [Science Citation Index Expanded (Web of Science); Scopus; DOAJ] [IF: 3.251; AIF: 3.985; IF/AIF: 0.815; Q2 (2020, InCites JCR SSCI); IF: 3.251; AIF: 5.860; IF/AIF: 0.554; Q2 (2020, InCites JCR SCIE)] [CiteScore: 3.90; SNIP: 1.247; SJR: 0.612; Q1 (2020, Scopus Sources)].

Indexed in the Web of Science or Scopus without Impact Factor

1. Adhikary, Suman Kumar; Rudzionis, Zymantas; Zubrus, Marijus. Investigations of the influence of polystyrene foamed granules on the properties of lightweight concrete // Journal of applied engineering sciences. Warsaw: Sciendo. ISSN 2247-3769. eISSN 2284-7197. 2019, vol. 9, iss. 1, art. No. 248, p. 19-24. DOI: 10.2478/jaes-2019-0002. [Emerging Sources Citation Index (Web of Science)].
2. Adhikary, Suman Kumar; Rudzionis, Zymantas; Balakrishnan, Arvind; Jayakumar, Vignesh. Investigation on the mechanical properties and post-cracking behavior of polyolefin fiber reinforced concrete //Fibers. Basel: MDPI. ISSN 2079-6439. 2019, vol. 7, iss. 1, art. No. 8, p. 5-15. DOI: 10.3390/fib7010008. [Emerging Sources Citation Index (Web of Science); Scopus; INSPEC] [CiteScore: 2.70; SNIP: 1.018; SJR: 0.442; Q2 (2019, Scopus Sources)].

Articles in peer-reviewed conference proceedings

1. Das, Mahadeb; Adhikary, Suman Kumar; Rudžionis, Žymantas. Effectiveness of fly ash, zeolite, and unburnt rice husk as a substitute of cement in concrete // Materials today: proceedings. Amsterdam: Elsevier.

ISSN 2214-7853. 2022, vol. 61, pt. 2, p. 237-242. DOI: 10.1016/j.matpr.2021.09.005. [Conference Proceedings Citation Index - Science (Web of Science)] [CiteScore: 2.30; SNIP: 0.575; SJR: 0.355; Q3 (2021, Scopus Sources)].

2. Adhikary, Suman Kumar; Rudžionis, Žymantas; Ghosh, Ranjit. Influence of CNT, graphene nanoplate and CNT-graphene nanoplate hybrid on the properties of lightweight concrete // Materials today: proceedings: 11th international conference on materials, processing & characterization, December 15-17, 2020, Indore, India/ edited by: S.K. Singh, M. Gupta, E.P. Korimilli, A. Parey. Amsterdam: Elsevier. ISSN 2214-7853. 2021, vol. 44, pt. 1, p. 1979-1982. DOI: 10.1016/j.matpr.2020.12.115. [Conference Proceedings Citation Index – Science (Web of Science); Scopus] [CiteScore: 2.30; SNIP: 0.575; SJR: 0.355; Q3 (2021, Scopus Sources)].
3. Adhikary, Suman Kumar; Rudzionis, Zymantas. Influence of expanded glass aggregate size, aerogel and binding materials volume on the properties of lightweight concrete // Materials today: proceedings: 3rd international conference on innovative technologies for clean and sustainable development, 19-21 February, Chandigarh, India. Oxford: Elsevier. ISSN 2214-7853. 2020, vol. 32, pt. 4, p. 712-718. DOI: 10.1016/j.matpr.2020.03.323. [Conference Proceedings Citation Index – Science (Web of Science); Scopus] [CiteScore: 1.80; SNIP: 0.650; SJR: 0.341; Q3 (2020, Scopus Sources)].
4. Adhikary, Suman Kumar; Rudžionis, Žymantas. Investigations on lightweight concrete prepared by combinations of rubber particles and expanded glass aggregate // 13th international conference *Modern building materials, structures and techniques*, 16–17 May, 2019, Vilnius, Lithuania. Vilnius: Faculty of Civil Engineering, Vilnius Gediminas Technical University, 2019. eISBN 9786094761973. eISSN 2029-9915. p. 9-14. DOI: 10.3846/mbmst.2019.007.

Presentation of research results at conferences

1. Das, Mahadeb; Adhikary, Suman Kumar; Rudzionis, Zymantas. Effectiveness of unburnt rice husk, fly ash, and zeolite as a substitute of cement in concrete // The F-EIR conference 2021 on Environment concerns and its remediation, Chandigarh, India, October 18–22, 2021.
2. Adhikary, Suman Kumar; Rudzionis, Zymantas. Lightweight concrete containing fly ash and prefabricated air bubbles // The F-EIR conference 2021 on Environment concerns and its remediation, Chandigarh, India, October 18–22, 2021.
3. Adhikary, Suman Kumar; Rudzionis, Zymantas; Rajapriya, R. Influences of carbon nanotubes on the flowability, mechanical and microstructural

properties of cementitious composite: an overview // Advanced construction and architecture: proceedings of 1st international scientific conference, 23–25 September 2020, Kaunas, Lithuania.

4. Adhikary, Suman Kumar; Rudžionis, Zymantas. Influence of expanded glass aggregate size, aerogel and binding materials volume on the properties of lightweight concrete // ITCSD 2020: 3rd international conference on innovative technologies for clean and sustainable development, 19–21 February, 2020 Chandigarh, India.
5. Adhikary, Suman Kumar; Rudžionis, Žymantas. Influence of fly ash and prefabricated plastic bubbles on the properties of expanded glass aggregates incorporating sustainable flowable lightweight concrete // SBE19 Malta: international conference *Sustainability & Resilience*, 21–22 November 2019, Malta / Editors R.P. Borg, C.S. Staines. Msida: University of Malta, 2019.
6. Adhikary, Suman Kumar; Rudžionis, Žymantas. Investigations on lightweight concrete prepared by combinations of rubber particles and expanded glass aggregate // 13th international conference *Modern building materials, structures and techniques*, 16–17 May 2019, Vilnius, Lithuania.

COPIES OF THE PUBLICATIONS

Article 1.

Authors: Suman Kumar Adhikary, Žymantas Rudžionis, Danutė Vaičiukynienė

Title of article: Development of flowable ultra-lightweight concrete using expanded glass aggregate, silica aerogel, and prefabricated plastic bubbles

Citation: Journal of Building Engineering, Volume 31, September 2020, 101399; https://doi.org/10.1016/j.jobe.2020.101399

Journal of Building Engineering 31 (2020) 101399

Contents lists available at ScienceDirect

Journal of Building Engineering

journal homepage: http://www.elsevier.com/locate/jobe

Development of flowable ultra-lightweight concrete using expanded glass aggregate, silica aerogel, and prefabricated plastic bubbles

Suman Kumar Adhikary *, Žymantas Rudžionis, Danute Vaičiukynienė

Faculty of Civil Engineering and Architecture, Kaunas University of Technology, Kaunas, LT-44249, Lithuania

ARTICLE INFO

Keywords:
Expanded glass aggregates
Prefabricated plastic bubbles
Silica aerogel
Thermography
SEM and XRD

ABSTRACT

Low energy consumption buildings is one of effective responses to the challenge of climate change. Lightweight cement-based composites with excellent thermal insulation and mechanical properties are sustainable building materials for energy-efficient buildings. In this study three different types of lightweight thermal insulating materials, namely expanded glass aggregates, silica-aerogel, and prefabricated plastic bubbles, were tested as aggregates and fine fillers. Four different series of concrete samples were prepared using expanded glass aggregates, fly ash, prefabricated plastic bubbles, and aerogel to investigate the mechanical properties of lightweight/ultra-lightweight concrete. Scanning microscopy, thermography, semi-adiabatic calorimetry tests and XRD analysis of concrete samples were performed to analyse the effect of aerogel particles on the hydration process of lightweight/ultra-lightweight concrete. The results show that replacement of up to 15% of cement by aerogel particles cause the compressive strength of concrete to drop by more than 42%. Less than 800 kg/m^3 density of concrete can be reached when a higher content of aerogel particles is used in combination with expanded glass aggregate. Separation gaps observed between the aerogel and surrounding cementitious materials indicate lower bonding of aerogel particles. Fly ash and prefabricated plastic bubbles were found to be very beneficial for the production of flowable lightweight/ultra-lightweight concrete.

1. Introduction

A growing concern about the environment and the global warming demand for more sustainable and energy saving building materials. Various researchers have estimated that energy consumption in buildings in some countries reaches 35–40% [1,2], and that justifies the need for high building insulation standards. The building sector also is one of the major producers of greenhouse gasses [3], which have tremendous negative effects on the environment. According to the global status report of 2017, the annual global building-related carbon emissions were estimated around 9.0 gigatons of CO_2 in 2016, where 2.8 Gt CO_2 was emitted directly from buildings and 3.7 Gt CO_2 was emitted from building construction. Heat preservation and building insulation are the most effective ways to reduce the total energy consumption in buildings. Various insulating materials are used for the thermal insulation of buildings and also for the preparation of lightweight thermal insulating concrete. The type of fillers and aggregates used, and the unit weight of cementitious materials are the key factors determining the thermal behaviour of insulation [4]. A lower unit weight of cement-based material leads to better performance of thermal insulation [5]. Therefore, the choice of suitable lightweight aggregates/fillers for producing lightweight cement-based composites is of prime importance. In the last decades, a lot of studies investigated the lightweight/ultra-lightweight concrete and thermal insulation materials containing expanded polystyrene [6–10], polyurethane [11–13], expanded glass aggregates [14,15] pumice [16–18], diatomite [19–22], scoria [23,24], expanded clay [25,26], etc. Fly ash is a lightweight pozzolanic material having a lower loose density than cement, thus it is very useful for producing lightweight concrete. Recently, many studies have been carried out on fly ash based lightweight concrete [27,28]. Nowadays, aerogel is gaining popularity in the construction sector for its excellent thermal insulation properties. There are various types of aerogel: graphene aerogel [29], silica aerogel [30,31], carbon aerogel [32], cellulose aerogel [33]; of these silica aerogel is more easily and widely available in the market. In the 1930s, Samuel Stephens Kistler first produced silica aerogels [34]. Aerogel is a highly insulated and lightweight material that can be used in buildings for many purposes. Aerogel is almost three times

* Corresponding author.
E-mail addresses: suman.adhikary@ktu.edu (S.K. Adhikary), zymantas.rudzionis@ktu.lt (Ž. Rudžionis), danute.vaiciukyniene@ktu.lt (D. Vaičiukynienė).

https://doi.org/10.1016/j.jobe.2020.101399
Received 11 December 2019; Received in revised form 31 March 2020; Accepted 1 April 2020
Available online 9 April 2020

denser than air and has very high porosity; this material, can have porosity above 95%. Large aerogel particles consist of a network of mesoporous (~50 nm in diameter) and microporous (5–10 nm in diameter) particles; to put it simply, large aerogel particles are aggregations of small nanoparticles [35]. According to the data, 30% of heat losses of buildings occur due to inappropriate thermal insulation techniques [36]. Traditionally, extruded polystyrene board, expanded polystyrene panels, glass felts, polyurethane foam, etc. are used for the thermal insulation purposes of building envelopes, which have lower fire resistance, lower strength properties, but poor hydrophobicity [37]. Therefore, ultra-lightweight/lightweight aerogel concrete can be the best alternative for traditionally used thermal insulation of building envelopes. In the last few years various researchers conducted studies to develop different forms of aerogel insulating materials for the improvement of building insulation. Ibrahim et al. showed in his study that aerogel insulating coating for the exterior wall had better performance than any other thermally insulating materials [38]. Sughwan Kim et al. achieved thermal conductivity of 0.135 W/(m K) by incorporating aerogel into cement paste [39]. Normally, aerogel has thermal conductivity of about 0.010–0.020 W/m·K depending on the preparation conditions [40,41]. However, in contrast to good thermal properties, aerogel has poor mechanical properties and is a very brittle material. Some large aerogel particles might be broken during the mixing process [42]. Therefore, it is very hard to achieve a higher strength in low density aerogel concrete. Fickler et al. [43] used silica aerogel granules and achieved 3.0 MPa and 23.6 MPa compressive strength with 0.16 W/m·K and 0.37 W/m·K thermal conductivity respectively. Gao et al. developed aerogel concrete containing 60% of aerogel with compressive strength of ~8.3 MPa and thermal conductivity of ~0.26 W/m·K [35]. Aerogel particles can be mixed reasonably well with cement before and after water is added, and that contradicts to the requirement to pre-treat aerogel particles with methanol reported by Kim et al. [39]. Hanif et al. reports the findings of research into the microstructure of cementitious composites incorporating aerogel and fly ash and proves that the composites have a porous inner structure [27].

In this study, a series of concrete samples were prepared to observe the effect of the quantity of fly ash, prefabricated plastic bubbles and aerogel particles on the properties of ultra-lightweight concrete. As the flowability and strength of concrete were given priority in this study, all types of concrete samples were made flowable. Besides the mechanical properties, the chemical analysis was also carried out to investigate the influence of aerogel particles on lightweight concrete.

2. Experimental details

2.1. Materials used in lightweight concrete

Ordinary Portland cement of grade CEM I 42.5R, satisfying the requirements of standard EN 197-1:2011 [44], and fly ash, satisfying the requirements of standard EN 450-1:2012 [45], were used as binding materials for the preparation of lightweight/ultra-lightweight concrete. Expanded glass aggregates, which satisfied the requirements of standard EN 13055-1:2002 + AC:2004 [46], 1–2 mm irregularly shaped silica aerogel with bulk density of 70 kg/m^3 and holding the approval No. Z-3.212-1948 from German Institute of Construction Technology (DIBt), and Acrylonitrile-Polymer based prefabricated plastic bubbles with 135 kg/m^3 bulk density were used as aggregates. Combinations of four different sizes of 0.01–0.3 mm, 0.25–0.5 mm, 0.5–1.0 mm and 1–2 mm of expanded glass aggregates were used in the concrete mixture. The physical properties of expanded glass aggregates are given in Table 1. Polycarboxylate ether polymer-based superplasticizer MasterGlenium SKY 8700 and stabilizer MasterMatrix SDC 100 were used as a chemical admixture in this study. Superplasticizer and stabilizer were added to all types of concrete samples by weight of cement at 1.8% and 0.3% respectively.

Table 1
Physical properties of expanded glass aggregate used in lightweight concrete.

Designation	Standard	Expanded glass aggregate size			
		0.1–0.3 mm	0.25–0.50 mm	0.5–1 mm	1–2 mm
Bulk density in kg/m^3	EN 1097-3	400	340	270	230
Compressive strength (±15%)	EN 13055-1, A annex	2.8	2.5	2.3	2
Thermal conductivity in W/(m-k) (±0.02)	EN 12939:2002	0.0767	0.0767	0.0713	0.0663
Water absorption % by mass (absorption % after 24 h submerged in water)	EN 1097-6:2002 C annex	25	25	20	20
Specific density		2.3	2.3	2.3	2.3
pH value		9–11			
Softening point		700 °C/1300 °F (approximately)			
Color		Cream white			

2.2. Preparation of lightweight concrete

Four series A, B, C, D of concrete samples were prepared maintaining a constant water/binder ratio of 0.65. Series A samples were prepared to investigate the influence of fly ash content in the preparation of lightweight concrete. Fly ash was used as cement replacement ranging from 0 to 30% by weight of cement and the best result was used in the preparation of series B, C, and D of concrete samples. Similarly, series B and C were prepared to investigate the effect of prefabricated plastic bubbles and aerogel particles on the properties of ultra-light concrete. In series B samples prefabricated plastic bubbles were replaced by 0.01–0.3 mm expanded glass aggregate, the amount of which ranged from 0 to 10 kg/m^3. In series C samples 1–2 mm expanded glass aggregates were replaced by aerogel. The aerogel particles were added to the mixture at 15%, 30%, 45%, and 60% by volume of total aggregate content. In series D samples the best quantity of fly ash and prefabricated plastic bubbles were used. All concrete samples were mixed by hand. The composition of concrete samples is shown in Table 2. At first, expanded glass aggregate, cement, fly ash and prefabricated plastic bubbles were mixed together. Then, 90% of the total water was mixed into the concrete mixture for 1 min, thereafter, the rest 10% of the water mixed with superplasticizer and stabilizer was added to concrete mixture and mixed for 40 s. Afterwards flowability tests of the paste were done. Aerogel particles are very brittle in nature and can easily break into pieces during the mixing process. For this reason aerogel particles were mixed in the last stage of the mixing process. At first, the aggregates, the binding material, water, and chemical admixtures were mixed thoroughly by hand and then aerogel particles were gently mixed in for another 20–30 s by hand. The mixing process was immediately followed by flowability tests of all concrete mixtures. Thereafter, concrete samples were molded into 16.0 × 4.0 × 4.0 cm size prisms and kept for 24 h at room temperature to set. After the setting process, all concrete samples were demolded and kept water immersed in the climatic chamber (Temperature: 20 ± 1 °C, RH: more than 95%) until the 28th day of the hardening process.

Table 2
Mixing composition of lightweight concrete samples, Materials for 1 m^3 of concrete.

Series	Cement	Aerogel	Air solid	Aggregate (1/2 + 1/0.5 + 0.5/0.25 + 0.01/0.3)	Fly ash	Super plasticiser 1.8%	Stabilizer 0.3%	Water (w/b = 0.65)
A-1	500	–	–	138 + 54 + 34 + 40	–	9	1.5	325
A-2	454.5	–	–	138 + 54 + 34 + 40	45.45	8.181	1.3635	325
A-3	416.7	–	–	138 + 54 + 34 + 40	83.34	7.50	1.25	325
A-4	385	–	–	138 + 54 + 34 + 40	115.5	6.93	1.155	325
B-1	454.5	–	2	138 + 54 + 34 + 34	45.45	8.181	1.3635	325
B-2	454.5	–	4	138 + 54 + 34 + 28	45.45	8.181	1.3635	325
B-3	454.5	–	6	138 + 54 + 34 + 22	45.45	8.181	1.3635	325
B-4	454.5	–	8	138 + 54 + 34 + 16	45.45	8.181	1.3635	325
B-5	454.5	–	10	138 + 54 + 34 + 10	45.45	8.181	1.3635	325
C-1	454.5	10.5	–	103.5 + 54 + 34 + 40	45.45	8.181	1.3635	325
C-2	454.5	21	–	69 + 54 + 34 + 40	45.45	8.181	1.3635	325
C-3	454.5	31.5	–	34.5 + 54 + 34 + 40	45.45	8.181	1.3635	325
C-4	454.5	42	–	0+54 + 34 + 40	45.45	8.181	1.3635	325
D-1	454.5	10.5	8	103.5 + 54 + 34 + 16	45.45	8.181	1.3635	325
D-2	454.5	21	8	69 + 54 + 34 + 16	45.45	8.181	1.3635	325
D-3	454.5	31.5	8	34.5 + 54 + 34 + 16	45.45	8.181	1.3635	325
D-4	454.5	42	8	0+54 + 34 + 16	45.45	8.181	1.3635	325

3. Results and discussion

3.1. Flowability test of lightweight concrete

The selection of aggregates plays a predominant role in achieving the desired slump flow, rheological parameters and plastic viscosity of concrete. Ostrowski et al. showed in his studies that the shape of coarse aggregate remarkably influences the rheological parameters of concrete. Coarse aggregates of regular shape and low friction angle lead to higher flowability concrete compared to coarse aggregates of irregular shape and bigger friction angle [47]. Harini et al. showed that mortar made of irregular shape fine aggregates increased the uncompacted void content. A higher percentage of uncompacted voids decrease the slump flow of the mortar. The mortar with high fine aggregate content also has lower flowability [48]. The flowability of concrete was determined using the flow table test, satisfying the requirements of standards EN 12350-5:2009 [49] and GOST (23789-85), and Stuart viscometer. The dimensions of the flow table and cylindrical Stuart viscometer are given in Fig. 1. Both tests were performed three times for each concrete sample and the mean value was taken as a result. The study revealed that the flowability of concrete increases with the increase of fly ash and prefabricated plastic bubble content in the mixture. The results of the flowability test of concrete samples are shown in Table 3. It has been proven by research that fly ash increases the flowability of concrete and slows down the hydration process [50]. Aerogel particles (of irregular shape) incorporated in concrete sample of Series C reduce the flowability of lightweight concrete, whereas the combination of aerogel particles and prefabricated plastic bubbles (of regular shape) mixed into lightweight concrete samples of Series D give better flowability results compared to Series C concrete samples.

3.2. Strength, density and thermal conductivity of lightweight concrete

Compressive and flexural strength is one of the most important properties of concrete. Compressive and flexural strength of lightweight concrete samples was measured on the 7^{th} and 28^{th} days of the curing process according to the requirements of standard EN 196-1:2016 [51]. The resistance demonstrated by the material without undergoing failure or changing its shape or form under the compressive/flexural loading is termed as compressive/flexural strength. Normal conventional concrete subjected to heavy loading has high strength properties. Concrete density and the type of materials used are some of the most important factors for the compressive strength of lightweight concrete. Usually, concrete strength decreases with density [52]. In the study described herein the lightweight/ultra-lightweight concrete was prepared using aerogel particles and expanded glass aggregates. Both materials are lightweighted and have lower strength properties. These factors directly affect the strength properties of lightweight concrete. The compressive strength of Series A concrete samples decreased with the higher content of fly ash used to replace cement. The flexural strength of concrete samples also decreased with the addition of fly ash. The strength drops with the addition of fly ash because fly ash delays the hydration process. 30% replacement of fly

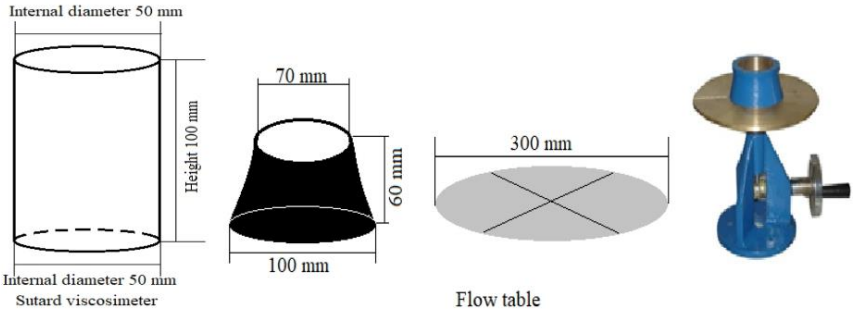

Fig. 1. Dimensions of Sutard viscometer and flow table.

Table 3
Flowability of lightweight concrete samples.

Series		Sutard viscosimeter test, cm	Flow table test, cm	Series		Sutard viscosimeter, cm	Flow table test, cm
Series A	A-1	16.5	21	Series C	C-1	16.5	21
	A-2	16.9	21		C-2	16.5	20
	A-3	20	23		C-3	15.5	18.9
	A-4	20.5	23.4		C-4	14.5	18.4
Series B	B-1	17	21	Series D	D-1	19	22
	B-2	17	21.2		D-2	18.5	22.1
	B-3	17.8	22		D-3	17.5	20.5
	B-4	18	22.4		D-4	17	20
	B-5	18.5	22.9				

ash reduced the compressive strength by 44.2% and 34.4% on the 7th and 28th days of the hydration process respectively. Concrete samples of Series B also showed very similar results: the compressive strength decreased with the addition of a higher amount of prefabricated plastic bubbles. Interestingly, prefabricated plastic bubbles showed better results on the flexural strength properties: the flexural strength value decreased less than the compressive strength value. The addition of prefabricated plastic bubbles at 10 kg/m^3 reduced the compressive strength of the samples by almost 23.15% and the density by 4.7% on the 28th day of hydration process. The replacement of cement by both fly ash and prefabricated plastic bubbles in concrete samples helps to produce concrete with lower density. Aerogel added from 15% to 60% into lightweight concrete reduces the compressive strength from 42.8% to 60.7% and density from 3.7% to 11.6% on the 28th day of the hydration process. The compressive strength drops more than density in concrete samples of Series D, where both aerogel and prefabricated plastic bubbles are used. The results show that a higher content of aerogel in concrete can decrease the density to less than 800 kg/m^3. The results of compressive strength, flexural strength, and dry density of lightweight concrete samples on the 7th and 28th day of curing are given in Table 4. Fig. 2 illustrates that the strength properties of lightweight concrete incorporating aerogel reduced drastically with the decreasing density of concrete. Literature studies confirm that lightweight cementitious composites incorporating aerogel have very low strength properties [34,53–55]. The specific strength of concrete sample A-1 was calculated 14.15 kN m/kg and it drops to 9.68 kN m/kg by using 30% replacement volume of fly ash. Similarly, from 2 kg/m^3 to 10 kg/m^3 prefabricated plastic bubbles added lightweight concrete reduces specific strength from 13.9 kN m/kg to 10.84 kN m/kg. Interestingly, aerogel added from 15% to 60% into lightweight concrete reduces specific strength from 7.99 kN m/kg to 5.98 kN m/kg due to its lower strength and adhesive properties. Thermal conductivity of concrete samples was calculated according to EN 1745:2012. The thermal conductivity of lightweight concrete decreased along with decreasing dry density of concrete. The thermal conductivity results of lightweight concrete samples are given in Table 4. Thermal conductivity of lightweight concrete depends on

Table 4
Investigation results of compressive strength, flexural strength and density of lightweight concrete samples.

Series		7th day strength test		28th day strength test		Dry density, kg/m^3	Thermal conductivity [W/(m.K)]
		Compressive strength, MPa	Flexural strength, MPa	Compressive strength, MPa	Flexural strength, MPa		
Series A	A-1	9.32	2.5	12.2	2.68	862.4	0.356
	A-2	8.2	2.3	11.4	2.56	848.0	0.348
	A-3	6.92	2.2	10	2.1	834.5	0.345
	A-4	5.2	1.9	8	2.04	826.4	0.342
Series B	B-1	7.9	2.36	11.6	2.69	834.8	0.348
	B-2	7.6	2.31	11.1	2.58	829	0.342
	B-3	7.0	2.27	10.22	2.52	823	0.340
	B-4	6.41	2.2	9.33	2.48	818.6	0.338
	B-5	5.93	1.9	8.76	2.12	808.3	0.333
Series C	C-1	5.72	1.7	6.52	2.38	816	0.337
	C-2	5.88	1.84	6.40	2.01	793	0.328
	C-3	3.32	1.11	4.8	1.61	774.5	0.322
	C-4	3.2	1.097	4.48	1.45	749.5	0.314
Series D	D-1	5.66	1.91	7.88	2.01	815	0.336
	D-2	4.58	1.19	5.06	1.64	743.3	0.312
	D-3	3	1.06	4.04	1.4	733.4	0.310
	D-4	2.56	0.89	3.72	1.29	713.5	0.302

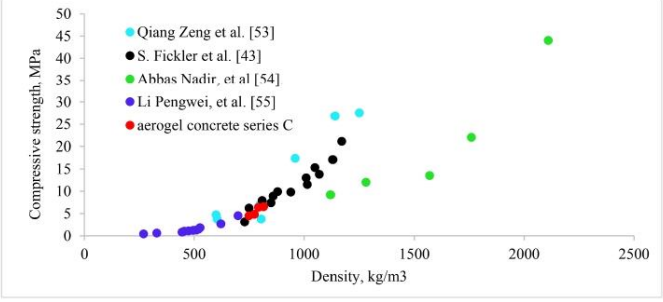

Fig. 2. Relationship between compressive strength and density of cementitious materials incorporating aerogel.

various parameters, such as moisture content, aerogel content, porosity, cement content, etc. [56]. The results show that the thermal conductivity of aerogel incorporated lightweight concrete samples C-1, C-2, C-3 and C-4 are 0.337 W/m·K, 0.328 W/m·K, 0.322 W/m·K, and 0.318 W/m·K. While the thermal conductivity of without aerogel content concrete sample A-1, A-2, A-3 and A-4 are 0.356 W/m·K, 0.348 W/m·K, 0.345 W/m·K and 0.342 W/m·K. The study infer that the thermal insulation properties of lightweight concrete enhanced with aerogel and prefabricated plastic bubbles.

3.3. Semi-adiabatic calorimetry test of lightweight concrete

Fig. 3 shows a semi-adiabatic temperature rise of cement mortar samples with and without fly ash with various doses of aerogel particles. The test was carried out to understand the influence of aerogel particles on the hydration process of concrete. Table 5 shows the mixing composition of cement paste samples. The setting time of Portland cement retarded when fly ash was mixed in the cement paste (samples S2, S5 and S6). The longer setting time could be explained by the rate of pozzolanic reaction. Similar results were obtained by Yılmaz et al. [57]. The addition of aerogel particles did not have a significant effect on the setting time of Portland cement (samples S3 and S4). The setting times on unmodified cement paste remain almost stable, but the setting time is slightly retarded when a portion of cement is replaced by fly ash. This finding indicates that aerogel particles are slightly reactive with cementitious materials (see Fig. 4).

3.4. Simultaneous thermal analysis of lightweight concrete

Simultaneous thermal analysis was performed on a thermal analyser LINSEIS STA PT-1000 (Germany), which analyses the weight change and heat flow of the sample as a function of time or temperature under controlled atmosphere. The following DSC-TGA parameters were used: the rate of temperature increase was 10 °C/min, the temperature range was 25–945 °C, the standard platinum crucible was used, the atmosphere in the furnace was nitrogen, the weight of the sample was 10 mg, the accuracy of measurement was ± 3 °C. DSC-TGA was performed for samples A-1, A-2, C-1, C-2, C-3 and C-4 on the 28th day of concrete hydration process. A-1 is the designation of concrete prepared without fly ash and A-2 is the designation of concrete prepared with fly ash. Concrete samples C-1, C-1, C-2, C-3, and C-4 have various doses of aerogel particle with a constant fly ash content. Concrete series B and D were prepared with prefabricated plastic bubbles; therefore, DSC-TGA analysis was done only with series A and C. Fig. 5 and Fig. 6 show the DSC and TGA curves of lightweight concrete samples. The first endothermic peak observed at 102.1 °C, 100.9 °C, 98.6 °C, 102.1 °C, 98.5 °C and 102.1 °C for concrete samples A-1, A-2, C-1, C-2, C-3, and C-4 indicates the drying process of concrete when physically bound water is driven out. The second endothermic peak indicates the formation of calcium silicate hydrate by the loss of water at the peak of 140.7 °C, 138.9 °C, 140.6 °C, 140.3 °C, 137.7 °C, and 139.2 °C. The weight loss of samples A-1, A-2, C-1, C-2, C-3 and C-4 due to water loss was 11.2%, 10.6%, 8.05%, 7.09%, 7.5%, and 7.8% respectively. The endothermic peak of concrete samples at 443.3 °C, 442.4 °C, 446.6 °C, 450.3 °C, 449 °C, 452.8 °C indicates the dehydration of calcium hydroxide (portlandite). The weight loss due to dehydration of portlandite was 1.71%, 1.52%, 2.15%, 2.63%, 2.36% and 2.80% for samples A-1, A-2, C-1, C-2, C-3, and C-4 respectively. The endothermic peak ranging from 620.3°C to 688.7 °C denotes the dehydration of calcium carbonate ($CaCO_3$). The weight loss in concrete samples due to dehydration of calcium carbonate was 1.04%, 1.82%, 1.80%, 2,0%, 1.77% and 2.04%. The peak at 830 °C in lightweight concrete samples incorporating aerogel indicates the presence of C–S–H. The peak of C–S–H at 830 °C was observed when aerogel was used in the lightweight concrete and the temperature increased with the increasing volume of aerogel particles.

3.5. X-ray diffraction analysis of lightweight concrete

The X-ray diffraction analysis was performed with X-ray diffractometer DRON-6 with Bragg-Brentano geometry using Ni-filtered Cu Kα radiation and graphite monochromator, operating with the voltage of 30 kV and emission current of 20 mA. The step-scan was performed from the angular range 2°–70° (2θ) and each step of 2θ was 0.02°. Concrete samples A-1, A-2, C-1, C-2, C-3, and C-4, made of cement, fly ash, aerogel, and expanded glass, were crushed and converted to powder to perform the X-ray diffraction analysis. Figs. 6 and 7, Fig. 8, Fig. 9, and Fig. 10 show the X-ray diffraction patterns of aerogel, Portland cement, fly ash, expanded glass aggregate and lightweight concrete samples A-1, A-2, C-1, C-2, C-3, and C-4. X-ray diffraction pattern of silica aerogel confirmed the amorphous nature of silica aerogel. In the range of 20°–30° one broad peak was observed in the pattern without any narrow peaks. X-ray diffraction of concrete samples shows that the intensity of ettringite near 8° decreased with the increasing content of aerogel in the concrete samples. Similarly, the intensity of hydrotalcite near 12° reduces after the aerogel particles are incorporated in concrete samples. This reduction of ettringite and hydrotalcite peaks could be explained by the partial dissolving and reaction of aerogel during Portland cement hydration. Aerogel of amorphous nature is expected to be reactive and it can partially dissolve in contact with Portland cement paste. Literature studies confirm that aerogel particles partially dissolve and react with cement during the hydration process [58].

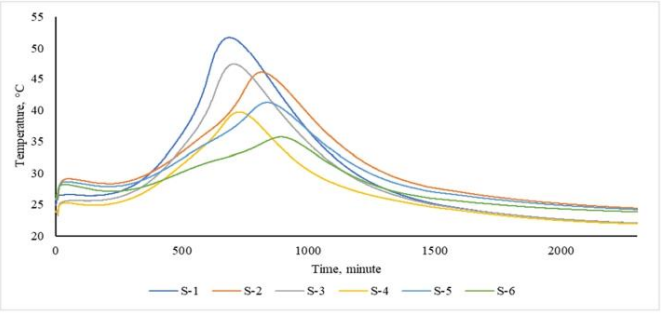

Fig. 3. Hydration of cement paste containing fly ash and aerogel.

Table 5
Mixing composition of cement paste for the semi-adiabatic calorimetry test.

Sample	Cement, g	Aerogel, g	Fly ash, g	Water, g
S-1	100	–		35
S-2	100	–	10	35
S-3	100	2.1	–	35
S-4	100	4.2	–	35
S-5	100	2.1	10	35
S-6	100	4.2	10	35

3.6. Scanning electronic microscopy (SEM) of lightweight concrete

Scanning electronic microscopy analysis was carried out for aerogel particles and concrete samples A-1, A-2, C-2, C-4, and D-1. A high-resolution electronic microscope FEI Quanta 200 FEG with Schottky field emission gun (FEG), an energy-dispersive X-ray spectrometer (EDS) with a silicon type drift droplet detector were used for this analysis. The image of plain aerogel in Fig. 11 clearly illustrates that it is a very brittle material having cracks on the surface in the nanoscale, which lead to lower strength properties. The compositional analysis of aerogel revealed that those particles are mainly silica/silicates. The SEM image of concrete incorporating aerogel particles clearly shows the distribution of irregular shaped aerogel particles. Clean and smooth aerogel particles in concrete samples also indicate that no degradation of aerogel particles occurs in the hydration process of the binding materials. During the hydration process of cementitious materials, aerogel particles are found to be fairly stable. A similar phenomenon was observed by Gao et al. [35]. However, semi-adiabatic calorimetry test and XRD analysis confirmed that aerogel reacts slightly with cementitious materials. Literatures studies show that aerogel particles partially dissolve in alkaline environment due to the hydration of cement mortar, aerogel reacts with pore solution and forms C–S–H with low Ca/Si ratio [58]. Interestingly, several separation gaps between aerogel particles and surrounding concrete materials were identified in lightweight concrete samples on the nanoscale level. That indicates lower binding properties of aerogel particles. The separation gap of aerogel particles and the surrounding cementitious material are shown in Fig. 11 (b). Water and/or air can be easily transported through the gap between aerogel and surrounding cementitious materials. Needles of ettringite and honeycomb structure of C–S–H can be clearly seen in the microscopy of concrete samples. This can be explained by the presence of silica in aerogel. It should be noted that a higher amount of C–S–H phase was found in concrete sample C-4. The presence of C–S–H phase in concrete helps to develop better strength properties. Concrete sample microscopy image in Fig. 12 also shows the sizes and good binding properties of prefabricated plastic bubbles in lightweight concrete. The distribution of aerogel particles and minerals in concrete sample are shown in Fig. 13 and Fig. 14.

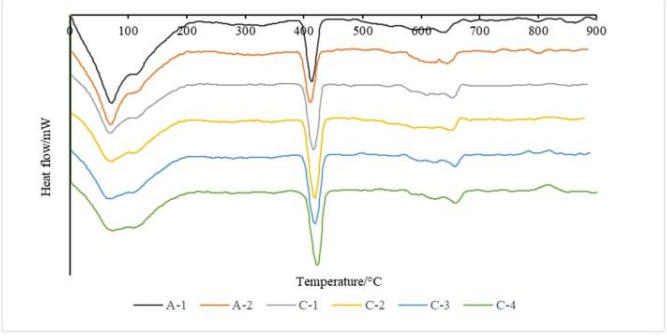

Fig. 4. DSC curves of lightweight concrete made of reference material and containing aerogel.

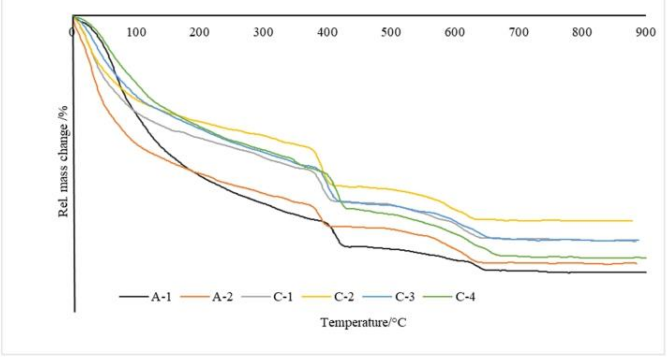

Fig. 5. DTG curves of lightweight concrete made of reference material and containing aerogel.

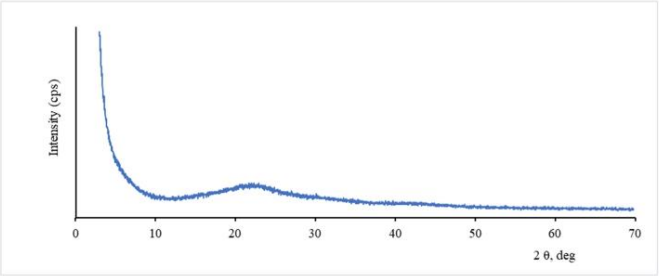

Fig. 6. X-ray diffraction pattern of silica aerogel.

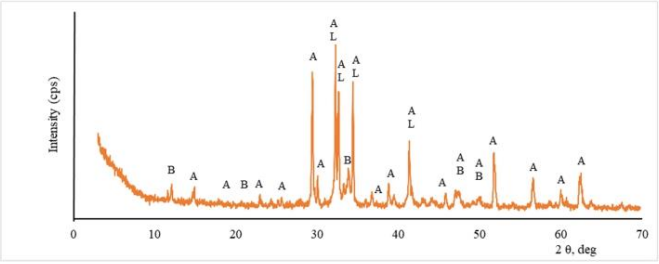

Fig. 7. X-ray diffraction pattern of Portland cement. *Notes:* A-alite $Ca_{54}MgAl_2Si_{16}O_{90}$ (13–272); L—belite Ca_2SiO_4 (33–302); B—brownmillerite Ca_2 (Al, Fe)$_2$ O_5 (30–226).

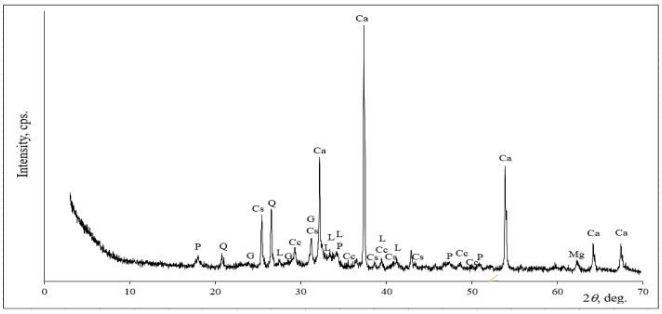

Fig. 8. X-ray diffraction pattern of fly ash. *Notes:* Ca – (CaO) calcium oxide (82–1690), Mg – (MgO) magnesium oxide (78–430), Q – (SiO_2) quartz (83–539), Cs – ($Ca(SO)_4$) calcium sulfate (80–787), P – ($Ca(OH)_2$) portlandite (1–837), Cc – ($Ca(CO)_3$) calcium carbonate (1–837), G – (Ca_2 $Al(AlSiO_7)$) gehlenite (79–1726), L – (Ca_2SiO_4) belite (24–37).

4. Conclusions

This study analyses the feasibility of using aerogel particles, fly ash and prefabricated plastic bubbles to produce lightweight/ultralight-weight flowable concrete. The following conclusions can be drawn on the basis of the results obtained:

1. The content of fly ash in concrete plays an important role in the production of lightweight flowable concrete. Fly ash increases the flowability, slows down the hydration process and reduces the strength properties of concrete. Fly ash added to the concrete mixture at 30% by weight of cement reduces the compressive strength of lightweight concrete incorporating expanded glass aggregates by almost 34.42%.
2. Proper utilization of prefabricated plastic bubbles can be very beneficial to produce flowable lightweight/ultra-lightweight concrete. They help to improve the workability and slightly decrease the density of lightweight concrete.
3. Aerogel is a lightweight and excellent insulating material, which is beneficial to produce lightweight concrete with good thermal insulation properties. Combinations of expanded glass, prefabricated plastic bubbles and aerogel can be used as lightweight aggregates in the construction industry to produce thermally insulating lightweight/ultra-lightweight flowable concrete. The thermal conductivity of lightweight concrete series-

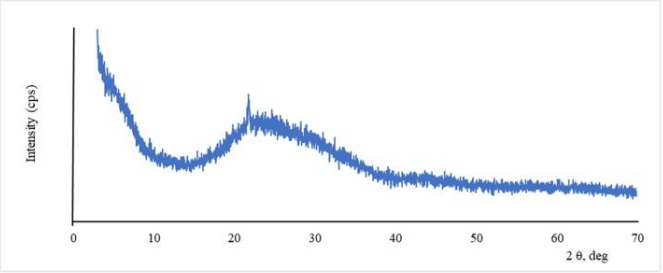

Fig. 9. X-ray diffraction pattern of expanded glass aggregates.

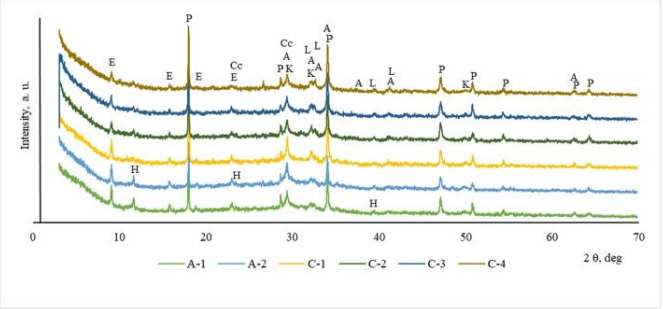

Fig. 10. X-ray diffraction pattern of lightweight concrete samples containing aerogel particles.
Notes: P – $Ca(OH)_2$ portlandite (1–837), K –$Ca_{1.5}Si\ O_{3.5}$•x H_2O calcium silicate hydrate (33–306), Cc – $Ca(CO)_3$ calcite (24–27), A – alite $Ca_{54}MgAl_2Si_{16}O_{90}$ (13–272); L – Ca_2SiO_4 belite (33–302), E – ettringite $Ca_6Al_2(SO_4)_3(OH)_{12}$·$26H_2O$ (41–1451), H – hydrotalcite $Mg_4Al_2CO_9$•$(OH)_{12}CO_3$ $(H_2O)_3)_{0.5}$ (70–2151).

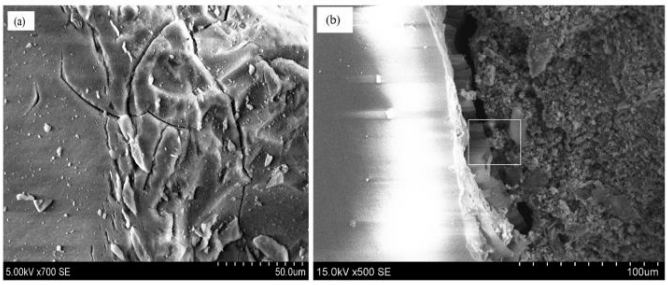

Fig. 11. (a) Cracks in aerogel particles on microscale level; (b) separation gap between aerogel particle and cementitious material, concrete sample C-2.

A without aerogel content varies 0.356 W/m·K to 0.342 W/m·K. While the thermal conductivity of lightweight concrete enhanced by the addition of aerogel and prefabricated plastic bubbles. Concrete sample D-4 made with high volume of aerogel particle and prefabricated plastic bubbles show the lowest thermal 0. 302 W/m·K.

4. A higher volume of aerogel particles in the concrete reduces the concrete density and strength properties. 60% content of aerogel particles reduces the compressive strength of lightweight concrete by almost 60.7% and density by 11.6%. The results show specific strength of the lightweight concrete is decreased by the addition of aerogel content due to its lower strength and adhesive properties. The specific strength of concrete sample A-1 was calculated 14.5 kN m/kg while specific strength of 60% aerogel incorporated concrete sample C-4 reduced to 5.98 kN m/kg.
5. Aerogel of amorphous nature is expected to be reactive and it partially dissolves in contact with Portland cement paste. It helps to gain more C–S–H during the hydration process of concrete. It is possible to detect aerogel particles in the cement matrix through SEM analysis. A separation gap is found between aerogel and the surrounding material on microscale level. This gap indicates lower adhesive properties of aerogel particles with cement matrix. Aerogel particles remain almost stable during the hydration process of concrete.

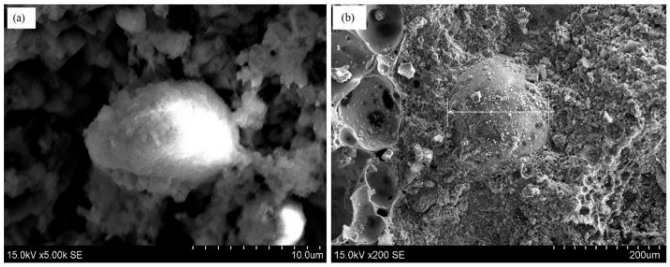

Fig. 12. (a) Fly ash particles and (b) prefabricated plastic bubbles in lightweight concrete sample D-1.

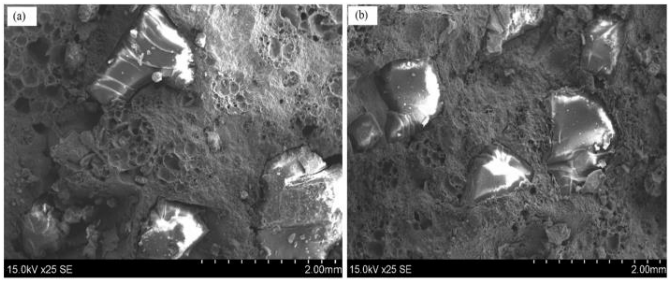

Fig. 13. Distribution of aerogel particles in lightweight concrete samples (a) C-2 and (b) C-4.

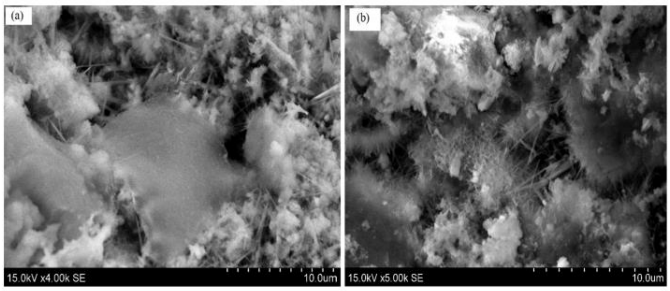

Fig. 14. Microscopic image of lightweight concrete samples (a) C-2 and (b) C-4.

Declaration of competing interestCOI

The authors declare that they have no known competing financial interests or personal relationships that could have appeared to influence the work reported in this paper.

CRediT authorship contribution statement

Suman Kumar Adhikary: Data curation, Writing - original draft. **Žymantas Rudžionis:** Data curation, Writing - original draft. **Danute Vaičiukynienė:** Data curation, Writing - original draft.

Appendix A. Supplementary data

Supplementary data to this article can be found online at https://doi.org/10.1016/j.jobe.2020.101399.

References

[1] D.Y. Li, J. He, L. Li, A review of renewable energy applications in buildings in the hot-summer and warm-winter region of China, Renew. Sustain. Energy Rev. 57 (2016) 327–336, https://doi.org/10.1016/j.rser.2015.12.124.
[2] G. Samson, A. Phelipot-Mardelé, C. Lanos, A review of thermomechanical properties of lightweight concrete, Mag. Concr. Res. 69 (4) (2016) 201–216, https://doi.org/10.1680/jmacr.16.00324.
[3] Y. Li, L. Yang, B. He, D. Zhao, Green building in China: needs great promotion, Sustain. Cities Soc. 11 (2014) 1–6, https://doi.org/10.1016/j.scs.2013.10.002.
[4] M. Khan, Factors affecting the thermal properties of concrete and applicability of its prediction models, Build. Environ. (2002), https://doi.org/10.1016/S0360-1323(01)00061-0.
[5] K.-H. Kim, S.-E. Jeon, J.-K. Kim, S. Yang, An experimental study on thermal conductivity of concrete, Cement Concr. Res. 33 (2003) 363–371, https://doi.org/10.1016/S0008-8846(02)00965-1.
[6] D.M.K.W. Dissanayake, C. Jayasinghe, M.T.R. Jayasinghe, A comparative embodied energy analysis of a house with recycled expanded polystyrene (EPS) based foam concrete wall panels, Energy Build. 135 (2017) 85–94, https://doi.org/10.1016/j.enbuild.2016.11.044.
[7] S.K. Adhikary, Z. Rudzionis, M. Zubrus, Investigations of the influence of polystyrene foamed granules on the properties of lightweight concrete, Appl. Eng.

Sci. 9 (1) (2019) 19–24, https://doi.org/10.2478/jaes-2019-0002.
[8] Y. Xie, J. Li, Z. Lu, J. Jiang, Y. Niu, Preparation and properties of ultra-lightweight EPS concrete based on pre-saturated bentonite, Construct. Build. Mater. 195 (2019) 505–514, https://doi.org/10.1016/j.conbuildmat.2018.11.091.
[9] A. Dixit, S.D. Pang, S.-H. Kang, J. Moon, Lightweight structural cement composites with expanded polystyrene (EPS) for enhanced thermal insulation, Cement Concr. Compos. 102 (2019) 185–197, https://doi.org/10.1016/j.cemconcomp.2019.04.023.
[10] N. Liu, B. Chen, Experimental study of the influence of EPS particle size on the mechanical properties of EPS lightweight concrete, Construct. Build. Mater. 68 (2014) 227–232, https://doi.org/10.1016/j.conbuildmat.2014.06.062.
[11] I.K. Harith, Study on polyurethane foamed concrete for use in structural applications, Case stud. construct. mater. 8 (2018) 79–86, https://doi.org/10.1016/j.cscm.2017.11.005.
[12] B. Chen, M. He, Z. Huang, Z. Wu, Long-tern field test and numerical simulation of foamed polyurethane insulation on concrete dam in severely cold region, Construct. Build. Mater. 212 (2019) 618–634, https://doi.org/10.1016/j.conbuildmat.2019.04.016.
[13] M. Major, K. Kuliński, I. Major, Thermal and dynamic numerical analysis of a prefabricated wall construction composite element made of concrete-polyurethane, Procedia eng. 190 (2017) 231–236, https://doi.org/10.1016/j.proeng.2017.05.331.
[14] M. Limbachiya, M. Seddik Meddah, S. Fotiadou, Performance of granulated foam glass concrete, Construct. Build. Mater. 28 (1) (2012) 759–768, https://doi.org/10.1016/j.conbuildmat.2011.10.052.
[15] A. Kashani, T.D. Ngo, A. Hajimohammadi, Effect of recycled glass fines on mechanical and durability properties of concrete foam in comparison with traditional cementitious fines, Cement Concr. Compos. 99 (2019) 120–129, https://doi.org/10.1016/j.cemconcomp.2019.03.004.
[16] K.M.A. Hossain, Blended cement using volcanic ash and pumice, Cement Concr. Res. 33 (10) (2003) 1601–1605, https://doi.org/10.1016/S0008-8846(03)00127-3.
[17] K.M.A. Hossain, Volcanic ash and pumice as cement additives: pozzolanic, alkali-silica reaction and autoclave expansion characteristics, Cement Concr. Res. 35 (6) (2005) 1141–1144, https://doi.org/10.1016/j.cemconres.2004.09.025.
[18] S. Green, N. Brooke, L. McSaveney, Pumice aggregates for structural lightweight and internally cured concretes, N. Z. Concr. Construct 4 (2010) 183–195.
[19] K. Pimraksa, P. Chindaprasirt, Lightweight bricks made of diatomaceous earth, lime and gypsum, Ceram. Int. 35 (1) (2009) 471–478, https://doi.org/10.1016/j.ceramint.2008.01.013.
[20] J.E. Kogel, N.C. Trivedi, J.M. Barker, S.T. Krukowski (Eds.), Industrial Minerals & Rocks: Commodities, Markets, and Uses, SME, 2006.
[21] D. Fragoulis, M.G. Stamatakis, D. Papageorgiou, E. Chaniotakis, The physical and mechanical properties of composite cements manufactured with calcareous and clayey Greek diatomite mixtures, Cement Concr. Compos. 27 (2) (2005) 205–209, https://doi.org/10.1016/j.cemconcomp.2004.02.008.
[22] P. Posi, S. Lertmimoolchai, V. Sata, T. Phoo-ngernkham, P. Chindaprasirt, Investigation of properties of lightweight concrete with calcined diatomite aggregate, KSCE J. Civ. Eng. 18 (5) (2014) 1429–1435, https://doi.org/10.1007/s12205-014-0637-5.
[23] W.H.J. Tchamdjou, T. Cherradi, M. Larbi Abidi, A. Luiz, Pereira-de-Oliveira, Mechanical properties of lightweight aggregates concrete made with cameroonian volcanic scoria: destructive and non-destructive characterization, J. Build. Eng. 16 (2018) 134–145, https://doi.org/10.1016/j.jobe.2018.01.003.
[24] A. Kılıç, C.D. Atiş, E. Yaşar, F. Özcan, High-strength lightweight concrete made with scoria aggregate containing mineral admixtures, Cement Concr. Res. 33 (10) (2003) 1595–1599, https://doi.org/10.1016/S0008-8846(03)00131-5.
[25] M.R. Ahmad, B. Chen, S.F. Ali Shah, Investigate the influence of expanded clay aggregate and silica fume on the properties of lightweight concrete, Construct. Build. Mater. 220 (2019) 253–266, https://doi.org/10.1016/j.conbuildmat.2019.05.171.
[26] A.M. Rashad, Lightweight expanded clay aggregate as a building material–An overview, Construct. Build. Mater. 170 (2018) 757–775, https://doi.org/10.1016/j.conbuildmat.2018.03.009.
[27] A. Hanif, P. Parthasarathy, Z. Li, Utilizing fly ash cenosphere and aerogel for lightweight thermal insulating cement-based composites, ICGBMCE 2017: 19th International Conference on Green Building, Materials and Civil Engineering, London, 2017.
[28] X. Huang, R. Ranade, Q. Zhang, W. Ni, V.C. Li, Mechanical and thermal properties of green lightweight engineered cementitious composites, Construct. Build. Mater. 48 (2013) 954–960, https://doi.org/10.1016/j.conbuildmat.2013.07.104.
[29] Y. Lin, G.J. Ehlert, C. Bukowsky, H.A. Sodano, Superhydrophobic functionalized graphene aerogels, ACS Appl. Mater. Interfaces 3 (7) (2011) 2200–2203, https://doi.org/10.1021/am200527j.
[30] A.S. Dorcheh, M.H. Abbasi, Silica aerogel; synthesis, properties and characterization, J. Mater. Process. Technol. 199 (1–3) (2008) 10–26, https://doi.org/10.1016/j.jmatprotec.2007.10.060.
[31] M. Schmidt, F. Schwertfeger, Applications for silica aerogel products, J. Non-Cryst. Solids 225 (1998) 364–368, https://doi.org/10.1016/S0022-3093(98)00054-4.
[32] Y.J. Lee, J.C. Jung, J. Yi, S.-H. Baeck, Jung Rag Yoon, and in Kyu Song. "Preparation of carbon aerogel in ambient conditions for electrical double-layer capacitor, Curr. Appl. Phys. 10 (2) (2010) 682–686, https://doi.org/10.1016/j.cap.2009.08.017.
[33] H. Sehaqui, Z. Qi, L.A. Berglund, High-porosity aerogels of high specific surface area prepared from nanofibrillated cellulose (NFC), Compos. Sci. Technol. 71 (13) (2011) 1593–1599, https://doi.org/10.1016/j.compscitech.2011.07.003.
[34] S.S. Kistler, Method of making aerogels, U.S. Patent 2 (767) (1941) 249 July 22.
[35] T. Gao, B. Petter Jelle, A. Gustavsen, S. Jacobsen, Aerogel-incorporated concrete: an experimental study, Construct. Build. Mater. 52 (2014) 130–136, https://doi.org/10.1016/j.conbuildmat.2013.10.100.
[36] K. Goulouti, J. De Castro, T. Keller, Aramid/glass fiber-reinforced thermal break–thermal and structural performance, Compos. Struct. 136 (2016) 113–123, https://doi.org/10.1016/j.compstruct.2015.10.001.
[37] B.P. Jelle, Traditional, state-of-the-art and future thermal building insulation materials and solutions–Properties, requirements and possibilities, Energy Build. 43 (10) (2011) 2549–2563, https://doi.org/10.1016/j.enbuild.2011.05.015.
[38] M. Ibrahim, P. Henry Biwole, E. Wurtz, P. Achard, A study on the thermal performance of exterior walls covered with a recently patented silica-aerogel-based insulating coating, Build. Environ. 81 (2014) 112–122, https://doi.org/10.1016/j.buildenv.2014.06.017.
[39] S. Kim, J. Seo, J. Cha, S. Kim, Chemical retreating for gel-typed aerogel and insulation performance of cement containing aerogel, Construct. Build. Mater. 40 (2013) 501–505, https://doi.org/10.1016/j.conbuildmat.2012.11.046.
[40] A.C. Pierre, G.M. Pajonk, Chemistry of aerogels and their applications, Chem. Rev. 102 (11) (2002) 4243–4266, https://doi.org/10.1021/cr0101306.
[41] H. Thorne-Banda, T. Miller, Aerogel by cabot corporation: versatile properties for many applications, Aerogels Handbook, Springer, New York, NY, 2011, pp. 847–856, https://doi.org/10.1007/978-1-4419-7589-8_38.
[42] T. Woignier, J. Phalippou, Mechanical strength of silica aerogels, J. Non-Cryst. Solids 100 (1–3) (1988) 404–408, https://doi.org/10.1016/0022-3093(88)90054-3.
[43] S. Fickler, B. Milow, L. Ratke, M. Schnellenbach-Held, T. Welsch, Development of high-performance aerogel concrete, Energy Procedia 78 (2015) 406–411, https://doi.org/10.1016/j.egypro.2015.11.684.
[44] EN, BS, "197-1: 2011." Cement, Composition, Specifications and Conformity Criteria for Common Cements, British Standard Institution (BSI), London, England, 2011.
[45] EN, BS. "450-451 (2012) Fly Ash for concrete." Definition, Specifications and Conformity Criteria. British Standards Institute (BSI), London.
[46] EN 13055-1:2002/AC:2004: Lightweight Aggregates- Part 1: Lightweight Aggregates for Concrete, Mortar and Grout.
[47] K. Ostrowski, The influence of coarse aggregate shape on the properties ofhigh-performance, self-compacting concrete, Tech. Trans. Civ. Eng. 5 (2017) 25–33, https://doi.org/10.4467/2353737xct.17.066.6423.
[48] M. Harini, G. Shaalini, G. Dhinakaran, Effect of size and type of fine aggregates on flowability of mortar, KSCE J. Civ. Eng. 16 (1) (2012) 163–168.
[49] EN, DIN, "12350-5: 2009 "Testing Fresh Concrete-Part 5." Flow Table Test", German version EN, 2009, pp. 12350–12355.
[50] J.M. Khatib, Performance of self-compacting concrete containing fly ash, Construct. Build. Mater. 22 (9) (2008) 1963–1971, https://doi.org/10.1016/j.conbuildmat.2007.07.011.
[51] EN, B, 196-1: 2016. Methods of Testing Cement, Determination of Strength, 2016.
[52] P. Li, et al., Preparation and optimization of ultra-light and thermal insulative aerogel foam concrete, Construct. Build. Mater. 205 (2019) 529–542.
[53] Q. Zeng, T. Mao, H. Li, Y. Peng, Thermally insulating lightweight cement-based composites incorporating glass beads and nano-silica aerogels for sustainably energysaving buildings, Energy Build. (2018), https://doi.org/10.1016/j.enbuild.2018.06.031.
[54] N. Abbas, et al., Silica aerogel derived from rice husk: an aggregate replacer for lightweight and thermally insulating cement-based composites, Construct. Build. Mater. 195 (2019) 312–322.
[55] P. Li, et al., Preparation and optimization of ultra-light and thermal insulative aerogel foam concrete, Construct. Build. Mater. 205 (2019) 529–542, https://doi.org/10.1016/j.conbuildmat.2019.01.212.
[56] S. Iffat, Relation between density and compressive strength of hardened concrete, Concr. Res. Lett. 6 (4) (2015) 182–189.
[57] B. Yılmaz, A. Olgun, Studies on cement and mortar containing low-calcium fly ash, limestone, and dolomitic limestone, Cement Concr. Compos. 30 (3) (2008) 194–201.
[58] P. Zhu, et al., Study of physical properties and microstructure of aerogel-cement mortars for improving the fire safety of high-performance concrete linings in tunnels, Cement Concr. Compos. 104 (2019) 103414.

Article 2.

Authors: Suman Kumar Adhikary, Žymantas Rudžionis, Simona Tučkutė

Title of article: Characterization of novel lightweight self-compacting cement composites with incorporated expanded glass, aerogel, zeolite and fly ash

Citation: Case studies in construction materials, Volume 16, June 2022, e00879; https://doi.org/10.1016/j.cscm.2022.e00879

Case Studies in Construction Materials 16 (2022) e00879

Contents lists available at ScienceDirect

Case Studies in Construction Materials

journal homepage: www.elsevier.com/locate/cscm

Case study

Characterization of novel lightweight self-compacting cement composites with incorporated expanded glass, aerogel, zeolite and fly ash

Suman Kumar Adhikary [a,*], Žymantas Rudžionis [a], Simona Tučkutė [b]

[a] Faculty of Civil Engineering and Architecture, Kaunas University of Technology, Kaunas LT - 44249, Lithuania
[b] Center for Hydrogen Energy Technologies, Lithuanian Energy Institute, Breslaujos st. 3, 44403 Kaunas, Lithuania

ARTICLE INFO

Keywords:
Aerogel
Self-compacting cement composite
Expanded glass
Lightweight concrete
Microscopy
Porosity

ABSTRACT

This study is aimed at preparing thermal insulating lightweight self-compacting cement composites (LWSCCC) below the density of 1400 kg/m^3 by using lightweight minerals and aggregates. Study results showed that incorporation of porous-structured expanded glass aggregate (EGA) enhances the demand for water to maintain the workability and increases the risk of higher water absorption capacity. The use of a portion of aerogel as a replacement of EGA increases porosity by 7.3%, resulting in lowering of compressive strength by 49% and a 7% increase in water absorption capacity. However, the use of aerogel in combination with EGA cement composite can reach a density of less than 1000 kg/m^3, maintaining self-compaction ability and adequate strength. The gaps between the cementitious materials and aerogel shown in SEM indicate poor aerogel particle adhesion with cementitious materials. Additionally, X-ray diffraction analysis and thermal conductivity results were analyzed in this study.

1. Introduction

An intense rise in energy consumption and growing waste disposal problem has attracted researchers worldwide to consume waste materials for the sustainable growth of economy and the society. One of the interesting topic is thermal insulating composites that emerges from the use of waste materials, EGA is one such thermal insulating material usually prepared from waste/recycled glass [1]. These highly porous granules are primarily used to prepare lightweight composites bearing superior thermal and acoustic resistance, and much lighter density over conventional concrete [2]. During the last ten years, plenty of research has been carried out on normal weight SCC, while only a few studies have been conducted on the characterization of thermal insulating LWSCCC [3,4]. it is an optimized product of SCC and LWAC that facilitates the zero-required vibration energy for molding and casting. The development of LWSCC/LWSCCC not only provides great quality of product, but it significantly enhances the productivity and working environment. Therefore, the design of thermal insulating LWSCCC is imperative as an engineering and scientific incentive for future applications in energy-efficient buildings.

In past, some studies have been performed to evaluate the characteristics of lightweight aggregate concrete. Choi et al. [5] prepared high-strength LWSCC with a density range of 2000–2300 kg/m^3, and reported the correlation between strength and workability. The authors observed that increasing the concentration of fine LWA has a significant negative impact on obtaining adequate workability.

* Corresponding author.
E-mail address: sumankradk9s@gmail.com (S.K. Adhikary).

https://doi.org/10.1016/j.cscm.2022.e00879
Received 16 October 2021; Received in revised form 5 January 2022; Accepted 8 January 2022
Available online 12 January 2022

Nomenclature

LWSCCC	lightweight self-compacting cement composites
LWA	lightweight aggregate
LWAC	lightweight aggregate concrete
EGA	expanded glass aggregates
OPC	Ordinary Portland cement
ITZ	Interfacial transition zone
EFNARC	European federation of national associations representing for concrete
SEM	Scanning electronic microscopy
XRD	X-ray diffraction analysis

Kwasny et al. [6] reported that in the case of semilightweight self-compacting concrete, larger grain LWA might float at the top and impact the homogeneous distribution of aggregates, resulting in segregation problems. Similar phenomena were observed by Adhikary and Rudzionis [7]. Yu et al. [8] prepared LWSCCC with a density range of 1280–1290 kg/m^3 using EGA and reported that the composite sample containing greater concentrations of EGA enhances the total permeable porosity. The authors also noticed that the selection of finer EGA has lower thermal conductivity and a more homogeneous aggregate distribution than coarse EGA. Interestingly, Adhikary et al. reported that fine EGA particles have higher strength properties relative to coarse particles. Lightweight concrete generally tends to have lower strength properties, depending on the lightweight aggregate used. Owing to low thermal and high strength properties, fine EGA particles become an interesting material to be used in lightweight concrete [7]. Aerogel is another thermal insulating material that has gained plentiful recognition for its applications in cementitious composites [9–11]. Gao et al. [12] prepared LWAC using aerogel and reported a weaker ITZ between the aerogel and cementitious composites, which might be attributed to the hydrophobic surface of aerogel. Adhikary et al. [13,14] reported that the presence of the gaps in the weaker ITZ of aerogel might enhance the porosity of the composites, leading to weaker strength and a risk of higher water absorption properties.

The literature studies suggest the detailed mechanical and durability properties of EGA and aerogel concrete. Aerogel and EGA both lightweight thermal insulating materials, and in the past, there were limited studies conducted evaluating the properties of EGA-aerogel cement composites. EGA has a thermal conductivity of about 0.052–0.077 W/(m-k) [1], whereas aerogel is much lighter and a thermal insulator than EGA, with a thermal conductivity of about 0.01–0.020 W/(m-k) [13]. The combination of aeorogel and EGA significantly might lower the density of the cement composite and improves the thermal resistance performance. This kinds of thermal insulating cement composite can be a useful product to use in different thermal bridges of buildings to improve the thermal insulation properties. It is very difficult to compact and transport the conventional thermal insulating cement composites in the conjuected part of buildings, while self-compacting thermal insulating cement composites might be a beneficial product to tackle these problems. Besides, aerogel is a highly fire and heat-resistant material, and the use of aerogel-based cement composites might provide protection from fire and heat [15–17]. Several studies in the literature indicate the presence of various materials-based thermal insulating lightweight cement composites; however, no studies have been conducted to evaluate the properties of EGA-aerogel-based thermal insulating self-compacting cement composites. So, this study is aimed at preparing lightweight thermal insulating self-compacting composites using EGA and aerogel below the density of 1400 kg/m^3. Aerogel is much lighter than EGA, and the replacement of a partial amount of EGA with aerogel might significantly lower the density. To achieve the objective of the study, 1–2 mm and 0.5–1 mm of EGA were replaced with 0.5–2 mm of silica aerogel by 25%, 50%, 75%, and 100%. Aerogel is still a high-cost product on the market today, and using a higher concentration in cement composite could significantly increase production costs. This experimental study aims at the detailed analysis of self-compacting cement composites prepared using EGA and an adequate amount of aerogel with the use of supplementary cementitious materials.

Table 1
Physical properties of expanded glass.

Designation	Standard	Expanded glass aggregate size			
		1–2 mm	0.5–1 mm	0.25–0.50 mm	0.1–0.3 mm
Particle density in Mg/m^3	EN 1097-6:2003, C annex	0.37	0.42	0.52	0.57
Bulk density in kg/m^3	EN 1097-3	230	270	340	400
WATER absorption % by mass (absorption % after 24 h submerged in water)	EN 1097-6:2002 C annex	18	18	15	10
Compression strength (±15%)	EN 13055–1,A annex	2	2.3	2.5	2.8
Thermal conductivity in W/(m-k) (±0.02)	EN 12939:2002	0.0663	0.0713	0.0767	0.0767
pH value		9–11			
Softening point		700 °C/1300°F (approximately)			
Color		Cream white			

Table 2
Chemical properties of cement, zeolite, fly ash and EGA.

Chemical composition	CaO	MgO	SiO_2	Al_2O_3	Fe_2O_3	K_2O	Na_2O	SO_3	TiO_2	Cl	Na_2O eq	LOI	Insoluble residue	Free Lime	Lime paste	Other
Cement	63	2.9	20.4	4.1	3.5	0.7	0.23	3.2	–	0.03	0.74	2.5	0.5	1.2	3.9	—
Zeolite	2.8	0.7	58.7	9.0	1.4	2.6	—	0.1	0.2	—	—	5.1	—	—	—	—
Fly ash	3.68	1.7	49.7	27.45	7.38	4.54	0.95	0.92	1.65		—	—	—	—	—	2.03
EGA	8–10.5		71–73	1.5–2	<0.3	—	13–14		—	—	—	—	—	—	—	<0.5

Table 3
Mixing composition of LWSCCC, kg/m^3.

Mix	Cement	Sand	Aggregate (1/2 +1/0.5 +0.5/0.25 +0.01/0.3)	Aerogel	Zeolite	Fly ash	mva		Super plasticiser		Water	
							%	Kg/m^3	%	Kg/m^3	Kg/m^3	w/b
A	550	380	45 + 56 + 44 + 56	–	–	–	1.8	0.327	1	5.5	247	0.45
B	530.2	183.16	43.4 + 54 + 42.4 + 43.6	–	–	–	1.73	0.327	1.30	6.9	308.5	0.58
C/Control	524.7	–	47.7 + 59.4 + 46.6 + 155.2	–	58.3		1.9	0.362	1.658	8.7	321	0.55
D	524.7	–	47.7 + 59.4 + 46.6 + 155.2	–	–	58.3	1.9	0.362	1.658	8.7	321	0.55
E	524.7	–	47.7 + 59.4 + 46.6 + 155.2	–	29.15	29.15	1.9	0.362	1.658	8.7	321	0.55
A25	524.7	–	35.8 + 44.5 + 46.6 + 155.2	8.01	58.3	–	1.9	0.362	1.658	8.7	321	0.55
A50	524.7	–	23.9 + 29.7 + 46.6 + 155.2	16.02	58.3	–	1.9	0.362	1.658	8.7	321	0.55
A75	524.7	–	11.9 + 14.9 + 46.6 + 155.2	24.03	58.3	–	1.9	0.362	1.658	8.7	321	0.55
A100	524.7	–	0 + 0 + 46.6 + 155.2	32.04	58.3	–	1.9	0.362	1.658	8.7	321	0.55

2. Materials and methods

2.1. Materials

OPC (CEM I 42.4R), fly ash, and zeolite powder (50 μm) were used as mineral admixtures, and expanded glass and aerogel were used as LWA to produce LWSCCC. The physical properties of EGA and the chemical composition of fly ash, zeolite, cement, and EGA are presented in Tables 1 and 2, respectively. In the LWSCCC, MasterMatrix SDC 100 stabilizer and polycarboxylate based superplasticizer MasterGlenium SKY 8700 were used as chemical admixtures.

2.2. Sample preparation

The composite samples were prepared using mxing and trial methods. Composite mixture A was prepared using combinations of natural sand and 0.1–0.3 mm, 0.25–0.50 mm, 0.5–1 mm, and 1–2 mm size EGA. To prepare the composite specimen A, SCLC1 sample composition was taken as a reference sample from the experimental study by Yu et al. [8]. To lower the density of the composite, natural sand was replaced with 0.1–0.3 mm EGA. Due to the increase in fine content, the demand for water increased to maintain the desired workability. For the composite samples C, D, and E, a small amount of SCM such as zeolite and fly was used to improve the workability of the composite.

From the visual inspection of workability and analysis of strength, density, and water absorption results, zeolite was chosen as the SCM to prepare the next aerogel-added composite specimens. Composite sample C was considered as the control sample, and 0.5–1 and 1–2-mm EGA aggregates were replaced with 0.5–2 mm of aerogel particles (70 kg/m^3 bulk density) by volumes of 25%, 50%, 75%, and 100%. The water/binder ratio of all composite samples was maintained at 0.55. The mixing composition of all LWSCCC is presented in Table 3**.** During the mixing process, first EGA, zeolite powder, and cement were carefully mixed in the dry state. Then 70% of the total water content was added to the mixture and manually mixed for 3 min. Thereafter, the superplasticizer and stabilizer are mixed with the remaining water and added to the composite mixture. At the last stage, aerogel was added to the composite mixture to minimize the crushing of aerogel particles, then mixed for another 2 min.

2.3. Workability test

The fresh properties of lightweight self-compacting cement composite, such as mini-slump flow, slump flow, mini v-funnel, and V-funnel time, were immediately measured according to the EFNARC guidelines [18]. A slump cone with a 30 cm height, a 20 cm bottom diameter and a 10 cm top diameter used to test slump flow. While performing mini-slump flow on a flow table with a 6 cm height, a 10 cm bottom diameter, and a 7 cm top diameter was used. In the slump-flow and mini-slump flow tests, the slump cone and flow table cone were lifted vertically. After the flow stopped, the mean diameter of the composite base was taken as a result. V-funnel test of the composite was performed using a V-shaped funnel satisfying dimensions of the EFNARC guidelines for concrete and mortar. After filling the fresh composite bottom opening of the V-funnel was opened after 10 s and flow out time was measured. Subsequently, samples were molded into 16.0 × 4.0 × 4.0 cm size prisms for the hardening process and kept in the open air for 24 h. Hardened composite specimens were demolded and kept in water for the hydration process in the climatic chamber (RH: more than 95%, room temperature 20 ± 1 °C) for 28 days.

2.4. Compression and flexural strength

Compression and flexural strength of LWSCCC were tested on the 28th day of hydration satisfying the EN 196-1:2016 standard. On the 28th day, water immersed composite specimens were taken out from the climatic chamber and kept at room temperature for 6 h for the natural dying process and afterwards, used in the mechanical strength test. A total of 6 specimens for each sample were tested, and the average value was considered as a result.

2.5. Density and water absorption

After the hydration process on the 28th day, the composite specimens were taken out of the water and kept in the oven at 105 °C for 24 h. After 24 h of the oven drying process, the dry density of each type of composite specimen was measured. Afterward, the composite specimens were immersed in water for 15 min, 1 h, 24 h, and 48 h to measure the water absorption capacity of the composite specimens. The average value of six specimens of each type of composite sample was taken as the final result.

2.6. Porosity

The porosity of LWSCCC samples was calculated after 28 days of hydration according to the GOST 127304 standard. To determine the porosity of the composite, first the composite samples were oven dried at 105 °C for 24 h. The mass of the oven-dried samples was measured using highly accurate equipment. Afterwards, composite samples were kept in water, immerged for 15 min, 1 h, 24 h, and 48 h; the subsequent mass of the water-immerged samples was measured after 15 min, 1 h, 24 h, and 48 h, respectively. Finally, after 48 h of water absorption, the masses of the samples were measured under the water, and using a flowing formula, the total and open porosity of the composite were calculated.

*Ordinary density (kg/m3) = {Mass of oven dried sample/(mass of the water immerged sample after 48 h watere absorption – mass of the sample under water)}*1000.…(1).*

*Massive water absorption (%), Wp = (mass of the water immerged sample after 48 h of water absorption-mass of the over dried sample)/mass of the oven dried sample}*100.(2).*

*Open porosity (%) = (massive water absorption*ordinary density)/1000.(3).*

Total porosity= {1-(ordinary density/2690)} 100 ……..(4).*

Closed porosity = total porosity-open porosity. ……..(5).

2.7. Thermal conductivity

The thermal conductivity of LWSCCC specimens was calculated by EN 1745:2012 standards. On a side note, this calculation is based on the density of lightweight aggregate concrete. The aggregate-matrix transition zone, type of aggregates, and presence of fly ash and zeolite might have notable impacts on the thermal conductivity of the composite. Aerogel is a highly thermal insulating material, having greater thermal resistance than EGA. The actual thermal conductivity of the aerogel-added lightweight cement composite tested in the laboratory is expected to have a lower thermal conductivity than the obtained results from the calculation.

2.8. Scanning microscopy

SEM of LWSCCC specimens was analyzed by a high-resolution electronic microscope Hitachi S-3400 N with a Bruker Quad 5040 EDS detector (123 eV). A thin layer of concrete slice was cut from the cement composite using a rotary blade cutter at the age of 28 days for the microscopic analysis.

2.9. X-RD

The DRON-6 X-ray diffractometer was used to perform the X-ray diffraction analysis of cement, fly ash, zeolite, and LWSCCC composite specimens. The operating voltage of the equipment was 30 Kv with 20 mA current emission, and each step scan of 2θ was 0.02°. Fracture pieces of the cement composite generated from the compressive strength test were selected for the XRD analysis at the age of 28 curing days. Fragmented pieces of the cement composites were powdered manually using ceramic-made apparatus, and the samples were sent for the XRD test.

3. Results

3.1. Workability

The workability results of LWSCCC are presented in Table 4. Study results indicate that composite mixture D, prepared with fly ash, shows the highest flow diameter. While LWSCCC mixture A shows the lowest workability compared to other specimens. Mini-slump flow and mini-V-funnel time of samples A, B, C, D, and E lay between 247 and 258 mm and 7.2 to 9 s. The increase in fine EGA content in composite mixture B increases the demand for water and superplasticizer doses to maintain the workability of LWSCC. Also, EGA has a higher water absorption capacity than natural aggregates, which might lead to an increase in demand forwater/superplasticizer doses [1,19–21]. However, composite samples C, D, and E showed improved workability, and this might be due to the addition of fine pozzolans and increased superplasticizer doses. Guneyisi et al. [22] and Ting et al. [23] reported the enhanced workability effects of fly ash added LWSCC. The addition of fly ash might have a dilution effect that diminishes the flocculation of the cement particles. Besides, spherical-shaped FA particles provide ball-bearing effects by facilitating the movement of neighboring particles. Perhaps due to a similar mechanism, enhanced workability was observed in this study.

The inclusion of aerogel and its concentration slightly negatively impacted the fresh properties of LWSCCC. With the rising concentration of aerogel replacement, the slump flow diameter is slightly reduced and the V-funnel time increases. At 100% replacement volume of aerogel by of 2/1- and 1/0.5-mm size EGA, the mini-slump flow diameter is almost lowered by 4.3%. A similar reduction in

Table 4
Workability of LWSCCC.

Composite Mix	Flow table diameter, mm	V-funnel time, seconds (according to EFNARC guideline V-funnel dimensions for mortar)	Slump cone diameter, mm	V-funnel time, seconds (EFNARC guideline V-funnel dimensions for concrete)
A	247	9	720	6
B	248	8	725	5
C/Control	256	7.2	800	4
D	258	8	820	5
E	257	8.1	807	5
A25	256	8	795	5
A50	251	8.5	750	5.5
A75	247	9.2	717	6.1
A100	245	9.5	700	6.3

flowability of the aerogel added composite was observed in a previous studies [24,25]. Kim et al. [26] used aerogel powder in a thermal insulating mortar and reported a 37.8% reduction in flow. The surface chemicals of aerogel, carboxylic (–COOH), and hydroxyl (–OH), can also absorb some water, leading to a decrease in workability [13,27]. Perhaps due to a similar reason, a slight decline in workability of LWSCCC was noticed in this study. According to the EFNARC recommendations, mortars should have a flow diameter (flow table method) of 240–260 mm with a V-funnel time of 7–11 s. To satisfy the SCC criteria, concrete must have a 550–850 mm slump flow diameter and an 8–25 s V-funnel time. In the present study, all the prepared composite samples fulfilled the self-compactability criteria.

3.2. Porosity

The porosity of LWSCCC is an important factor that might have notable impacts on the strength and durability properties of the composite. Fig. 1 shows the general and open porosity of all LWSCCC specimens. The general (total) porosity and open porosity of the composites A to E lie between 50% and 56.93%; and 16% and 17%, respectively. The increase in water/binder ratio and EGA concentration increases the porosity of B, C, D, and E. EGA is a porous structured material, and incorporation of EGA at a high volume might enhance the total porosity of concrete [1,28,29]. Adhikary et al.[1] reported that after the evaporation of free water in cement composites, pores were created that enhanced the porosity of concrete. Due to the use of EGA and a higher water/binder ratio, the porosity of LWSCCC increased and led to lower strength properties. However, the addition of pozzolan materials didn't have a significant impact on the porosity of LWSCC.

The general and open porosity of all the aerogel added LWSCCCs was increased by the increases in the aerogel concentration. The general porosity of the control samples, A25, A50, A75, and A100, was measured at 56.93%, 58.77%, 60.22%, 62.08%, and 64.23%, respectively. The open porosity of the control samples, A25, A50, A75, and A100 was measured at 15.72%, 17.38%, 18.9%, 19.1%, and 19.32%, respectively. Figs. 1 and 2 show a clear relationship between the aerogel concentration, porosity, and strength. With the increase in aerogel content in the LWSCCC, the porosity increases, and the strength decreases. The enhancement in porosity of aerogel added LWSCCC can be explained as during the mixing process, hydrophobic aerogel entrapped some air bubbles, leading to a rise in porosity and a decline in strength [13]. It was [12,13] reported that due to its hydrophobic characteristic, aerogel has lower adhesion with cement paste, leading to microscopic separation gaps in the ITZ between aerogel and cementitious materials. Because of these phenomena, the porosity of the aerogel-based thermal insulating LWSCCC of this study can be enhanced. Lu et al. [30] reported that the use of 66 vol% of aerogel in cement composite could reach a porosity of around 72.8%. A similar increase in the porosity of aerogel added concrete was noticed by several authors [9,30,31]. EGA is a porous structured material and the use of it significantly increases the porosity of concrete [1,32,33]. Agreeing with previous literature, combinations of aerogel and EGA might lead to achieving such high porosity.

3.3. Density

Fig. 3 shows the density of all LWSCCC samples. The dry density of the composites A to E lies between 1343 and 1126 kg/m^3. Study results show that the decrease in natural sand concentrations and the rise in EGA in the composite significantly decreased the density. EGA is a much more lightweight material than natural aggregate, and incorporation of a high concentration of EGA in a cement composite might lead to a decrease in density [8,34,35].

Study results also show the significant decrease in density of LWSCCC by the rise in aerogel concentration. The addition of aerogel as a 100% replacement of 1/0.5 and 2/1 mm EGA reduced the density of LWSCCC by 15.8%. The oven-dry density of the control samples, A25, A50, A75, and A100, was measured 1126, 1076, 1044, 1019, and 948 kg/^{3}. From the Fig. 4, it can be clearly understood that the concentration of aerogel, density, strength, and porosity share a close relationship. As the concentration of aerogel increases, the porosity also increases, leading to a decrease in the density and strength of LWSCCC. Zhu et al. [36] prepared lightweight concrete and measured a density of 1740 kg/m^3 without aerogel content that decreased to 582 kg/m^3 containing 80 vol% of aerogels. Similarly,

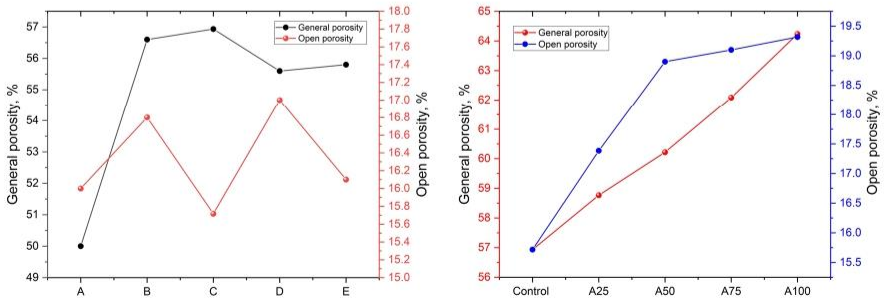

Fig. 1. General and open porosity of LWSCCC.

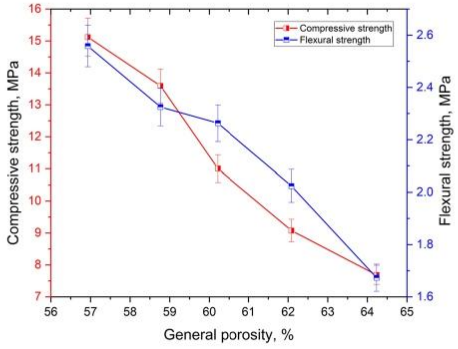

Fig. 2. Relationship between the general porosity and mechanical strength of aerogel added LWSCCC.

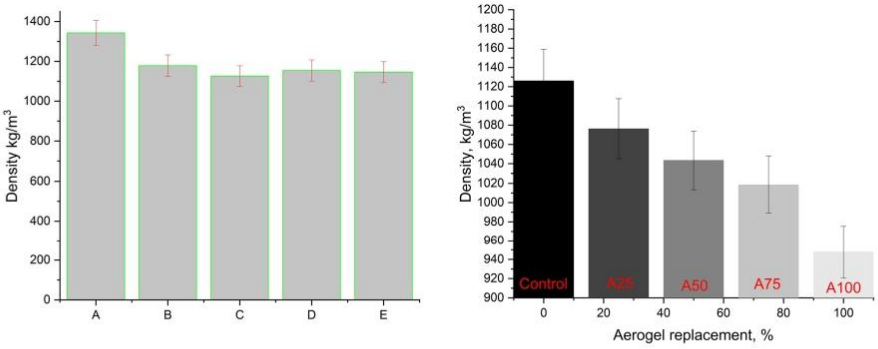

Fig. 3. Oven dry density of all LWSCCC.

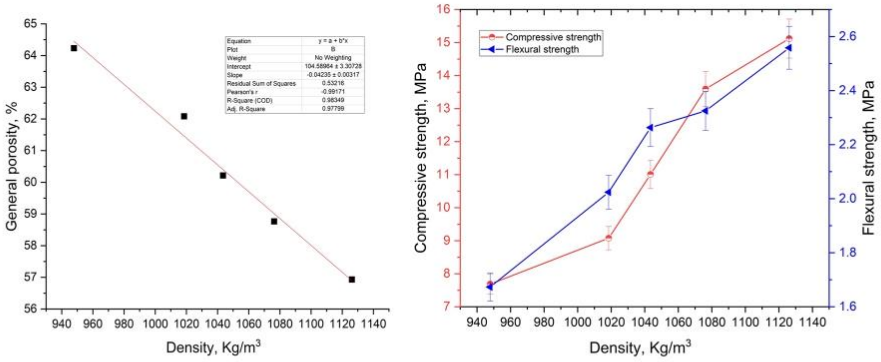

Fig. 4. Relationship between the porosity and density; and density vs mechanical strength of aerogel added LWSCCC.

Liu et al. [37] reported that the use of 60 vol% of aerogel in mortar could decrease the density by about 38.9%. A similar decrease in density of aerogel added concrete was reported by several researchers [12,38–40]. EGA is also a very lightweight aggregate, and the use of EGA as LWA can significantly decrease the density of concrete [1,35,41].

3.4. Compression and flexural strength

The compression and flexural strengths of all LWSCCC samples are presented in Fig. 5. The compression and flexural strength of the composites A to E lie between 21.3 and 12.4 MPa; and 5.5 and 2.56 MPa, respectively. The LWSCCC sample A, prepared with the combination of sand and EGA, achieves the highest compressive and flexural strength. Increasing the EGA concentration in the composite decreases the mechanical strength. This phenomenon can be explained as a combination of sand and EGA showing better compatibility, leading to higher strength development. Besidesporous structured EGA has lower mechanical strength, and a high volume of EGA in the concrete leads to a decrease in strength. [1,42–44]. Composite sample D prepared with fly ash shows slightly lower strength. This might be due to the retardation in the hydration of cement, leading to lower strength development at an early age [45]. However, zeolite-added composites show greater strength characteristics than fly ash-added composite D. Ahmadi and Shekarchi [46] reported that the use of 20% zeolite powder as a replacement for cement might enhance the compressive strength by 25%. A imilar enhanced strength of zeolite added concrete was reported by Chan and Ji [47]. A comparatively higher water/binder ratio was used in the composite specimens B to E, and that could also be a reason for the decrease in strength. A similar decrease in the strength of foamed glass concrete by enhancing the water/binder ratio was observed by Limbachiya et al. [43] and Zach et al. [28].

The results of LWSCCC also indicate that with the rise in aerogel concentration, both compression and flexural strength were decreased. The decrease in compression strength was more significant compared to flexural strength. Adding 100% aerogel as a replacement of 1/0.5 and 2/1 mm EGA shows almost a 49.2% and 34.6% decrease in compression and flexural strength, respectively. The compression strength of the control samples, A25, A50, A75, and A100 was measured 15.12, 13.59, 11.01, 9.08, and 7.69 MPa respectively. The flexural strength of A25, A50, A75, and A100 was measured at 2.56, 2.33, 2.26, 2.02, and 1.67, respectively. The decline in the strength of aerogel added LWSCCC can be attributed to the brittleness of aerogel. Because of its fragile nature, aerogel cannot withstand sufficient loads [12,13,48]. A similar decrease in the strength of aerogel added concrete was reported by several researchers [12,24,38,49,50]. Besides, SEM images suggest that aerogel has lower adhesion with cement composites and that aerogel might entrap some airbubbles. Those phenomena might lead to an increase in porosity and a decline in strength. However, in a previous study [51], it was observed that the use of 0.6% nanotube in aerogel concrete could enhance the strength by 41.48%.

3.5. Water absorption

Water absorption of concrete is an important durability factor. Higher water absorption of concrete can allow unwanted substances into concrete that might hamper the durability characteristic of concrete. Lightweight aggregate concrete is mainly a porous material having with a higher porosity than conventional normal weight concrete. Fig. 6 suggests that the water absorption capacity of the composites A to E shows about 11.9–14.39% after a 48-hour absorption test. Composite specimens prepared with greater EGA concentrations shows higher water absorption. EGA is a porous-structured LWA that can absorb 20–25% of water, and the use of a high volume of EGA in concrete might enhance the water absorption [1]. Besides, the higher w/b of the cement composites might also lead to enhanced water absorption. After the evaporation, free water makes pores in the composite, leading to an enhancement in porosity and water absorption [1]. However, there was no significant impact of pozzolanic materials observed in this study.

Fig. 6 also revealed that the water absorption of the composites increases as the aerogel content increases.The final water absorption after 48 h of the control samples, A25, A50, A75, and A100, was measured at 13.57%, 15.67%, 17.70%, 18.74%, and 20.06%, respectively. This enhanced water absorption of aerogel-added cement composites might be attributed to the entrapped air bubbles by aerogel. Besides, aerogel has weaker adhesion with cementitious materials, and those entrapped air bubbles and separation gaps in ITZ might enhance the porosity of the composites, leading to an increase in water absorption [9,13,30,52,53]. The relationships of porosity

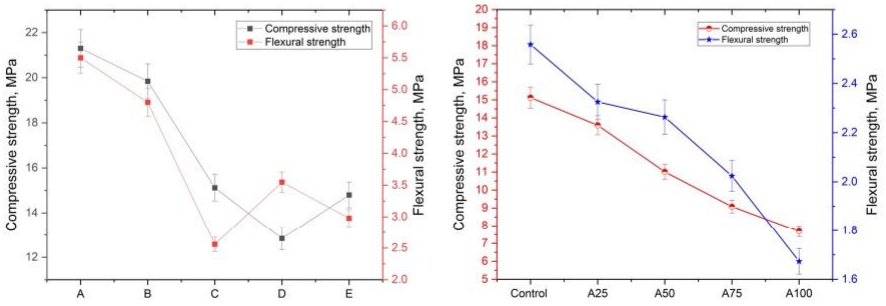

Fig. 5. Compression and flexural strength of LWSCCC.

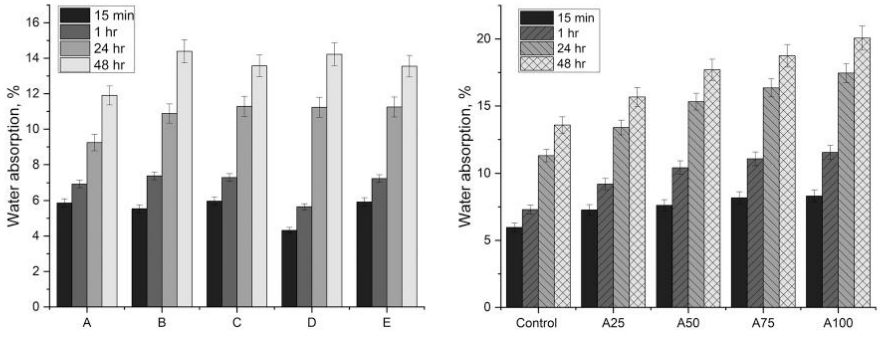

Fig. 6. Water absorption of all LWSCCC.

and water absorption of the aerogel cement composite presented in Fig. 7 satisfy those statements. Soares et al. [53] used aerogel in their study and reported an almost 56% increase in the open porosity of aerogel added cement mortar, leading to an enhancement in capillary water absorption. However, previous study results [51] suggested that the use of carbon nanotubes effectively enhances the adhesion between aerogel and cement paste in the ITZ, leading to improvement in the water absorption capacity of concrete.

3.6. Scanning microscopy

Aerogel is a brittle material, and Fig. 8 shows clearly visible cracks on the aerogel surface.Due to its hydrophobic nature, aerogel doesn't have good adhesion with cement paste resulting in a separation gap in the ITZ of aerogel and cementitious materials. The microscope image doesn't show any cracks or separation gaps in the ITZ between EGA and cement paste. The ITZ of aerogel and EGA are presented in Fig. 9**.** SEM images suggest that EGA has greater adhesion with cementitious materials compared to agerogel. Some pores were observed surrounding the aerogel particles in the LWSCCC as presented in Fig. 10. This can be attributed to the entrapped air bubbles by the aerogel during the mixing of fresh concrete [13]. The presence of pores and gaps in the ITZ of aerogel might increase the porosity of the composite and lower the strength. Besides, it allows harmful substances into the cement composites and impacts the durability characteristics. Some studies have reported that the use of silica fume and carbon nanotubes might improve the microstructure and ITZ of aerogel concrete [51,59]. A study [54] reported that a rim of air bubbles in the transition zone between EGA and the cement paste might have occurred during the exchange of air and water during the water absorption. However, in this study, it is evident that no rim of air bubbles were created in the ITZ of EGA. Fig. 9 also shows the presence of crystals of ettringites in the pores of EGA and in the ITZ. A similar observation was noticed by Bumanis et al. [55]. The authors also reported that during the mixing process, the outer shell of EGA might easily collapse due to its lower strength characteristics, leading to acceleration of the ASR mechanism. The presence of ettringite might promote the recrystallization of ettringite or leach out alkalis leading to deterioration and expansion of composite. Needle-shaped hydration products (ettringite) were observed in the aerogel added LWSCCC as shown in Fig. 11. However,

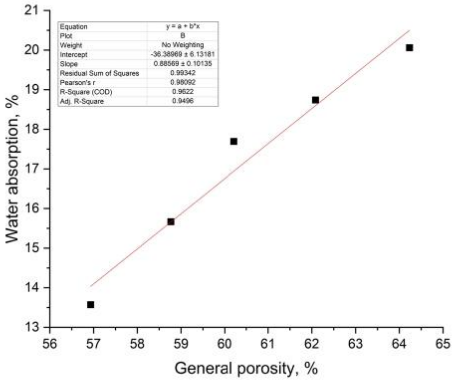

Fig. 7. Relationship between water absorption and general porosity of aerogel added LWSCCC.

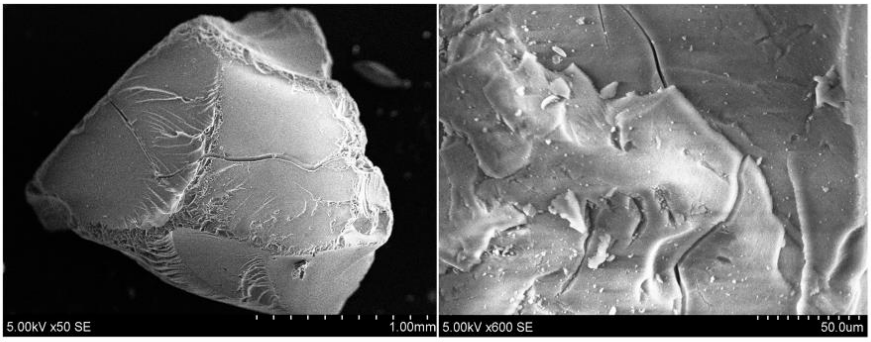

Fig. 8. Microscopic image of silica aerogel showing its cracked surface.

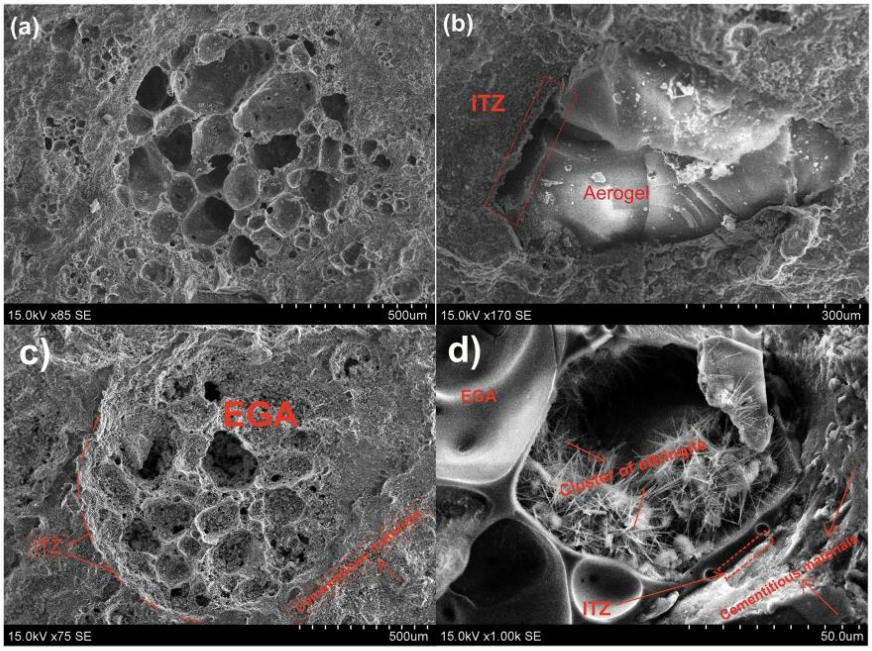

Fig. 9. Microscopic image of EGA and aerogel added cement composite showing the ITZ between the aggregate and cementitious composites.

the smooth and clean surface of the aerogel in composite specimen also indicates no degradation of aerogel due to the hydration of cementitious materials as presented in Fig. 9 (b) and Fig. 10 (d). This occurrence is indicates that the aerogel particles might stay fairly stable during the hydration process of cement. Gao et al. [12] also observed a similar occurrence in their study. However, Zhu et al. [56] reported that aerogel particles might slightly dissolve in the alkaline environment provided by cement hydration and form C-S-H with a low Ca/Si ratio. Hai-li et al.[57] and De Fátima Júlio et al. [58] reported that the presence of amorphous silica in silica aerogel might lead to ASR due to the reactions between alkali presence in cement and the hydroxyl ions of aerogel.

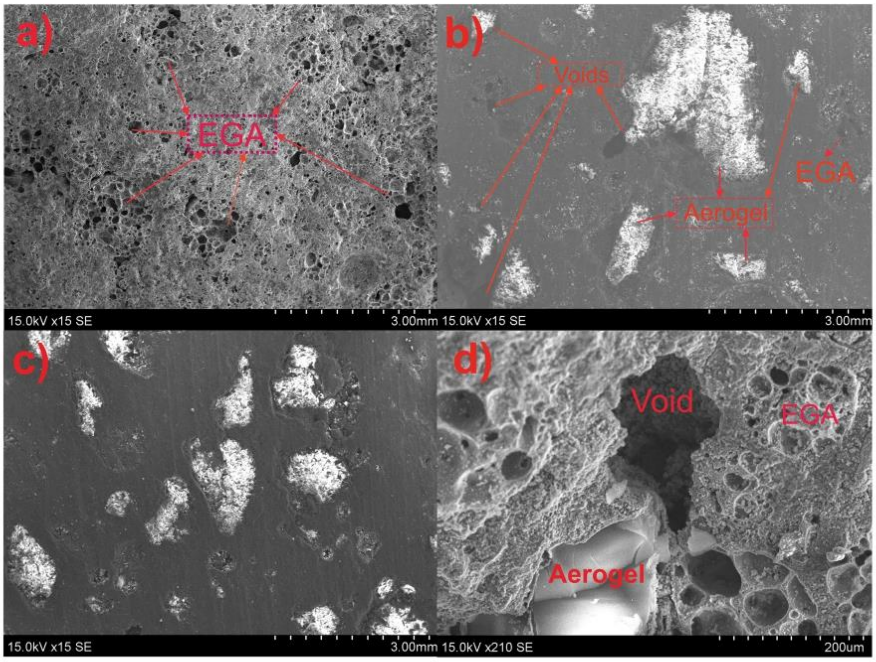

Fig. 10. Microscopic image of EGA and aerogel added cement composite showing the distribution of LWA and the entrapped voids surrounding to the aerogel particles.

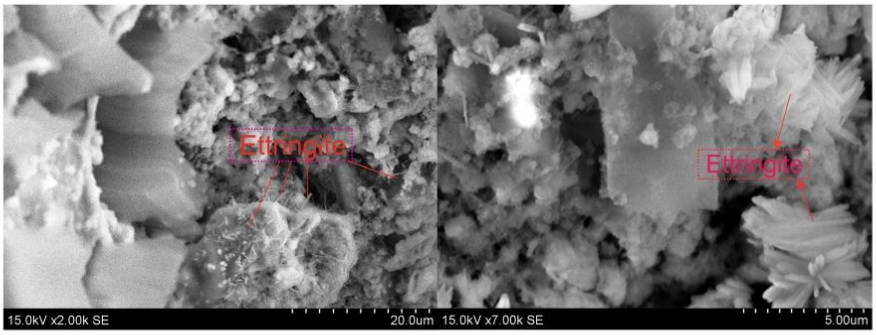

Fig. 11. Microscopic image of aerogel added cement composite (28 days) showing the growth of hydration products.

3.7. XRD analysis

X-ray diffraction patterns of OPC, fly ash, zeolite, and EGA are presented in Figs. 12, 13, 14, and 15. An XRD of EGA and aerogel confirms its amorphous characteristics, near 23° a hump was noticed. The XRD of LWSCCC samples A to E; and samples containing aerogel is presented in Figs. 16 and 17. The XRD of LWSCCC revealed that ettringite, portlandite, calcite, calcium aluminum silicate hydrate, calcite, brownmillerite, and lawsonite are the main hydration products of LWSCCC. It was observed that the intensity of ettringite near 8° for LWSCCC mix B was reduced compared to mix A. This reduction in ettringite content can be attributed to a higher

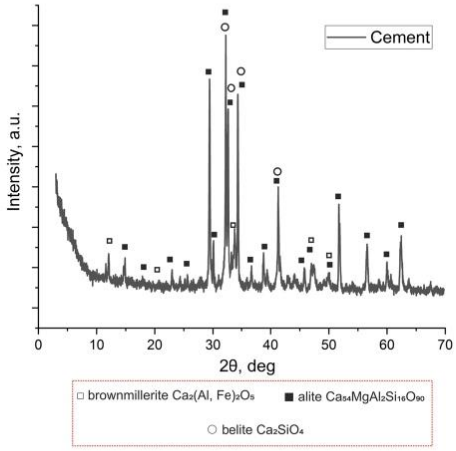

Fig. 12. XRD pattern of OPC cement.

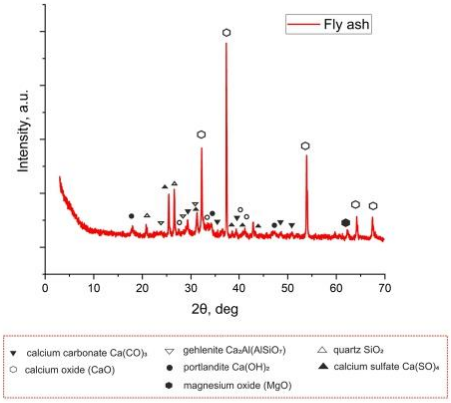

Fig. 13. XRD pattern of fly ash.

water/binder ratio.

Zuo et al. [60] reported a similar higher ettringite content at a lower water/cement ratio. The author also reported that higher growth of ettringite might help to enhance the compression strength of the composite. the reduced intensity of the LWSCCC mix can be attributed due to the delay in hydration provided by higher doses of PCES [61]. The peaks of portlandite near 18° and 34° were observed for all LWSCCC samples, while compared to fly ash added LWSCCC, a higher intensity of portlandite was observed for LWSCCC containing zeolite. The combination of fly ash and zeolite shows slightly higher peaks than the fly ash added composite samples. This can be attributed to the acceleration in pozzolanic reactivity due to the presence of zeolite. However, the enhanced peak of ettringite shows that the addition of zeolite might accelerate the formation of ettringite. A similar appearance of ettringite in zeolite added cement was observed by Snellings et al. [62]. The XRD image also shows higher peaks of ettringite and calcium aluminum silicate hydrate till 75% replacement volume of aerogel. A reduction peak was noticed for A100, containing a higher volume of aerogel. These phenomena suggest that aerogel might partially dissolve and react with OPC. Similar phenomena were observed by Zhu et al. [56].

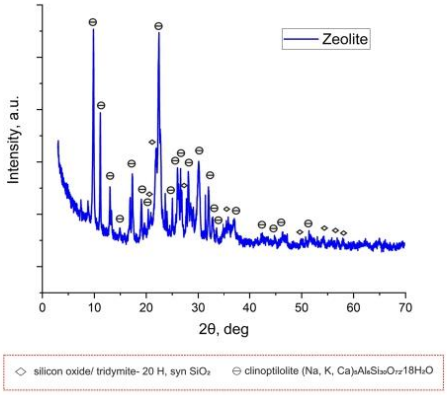

Fig. 14. XRD pattern of zeolite.

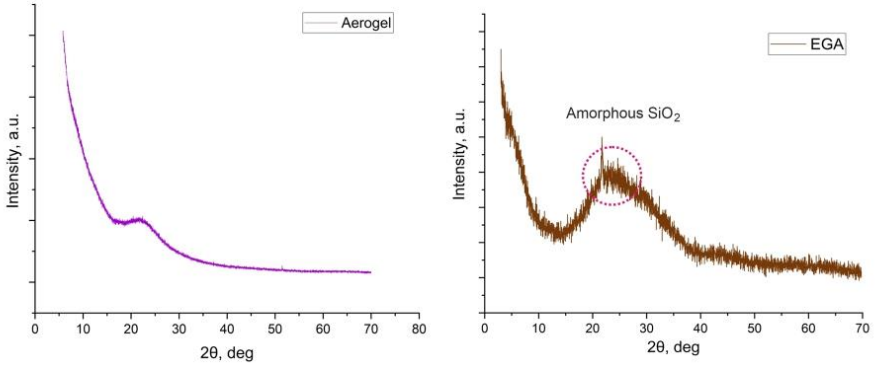

Fig. 15. XRD pattern of EGA and silica aerogel.

3.8. Thermal conductivity

The thermal conductivity coefficient of concrete is mainly density-dependent [8]. The thermal conductivity of normal weight concrete is about 1.6 W/m·K at 2200 kg/m^3 density. The thermal conductivity of all LSWCCC is shown in Fig. 18A higher concentration of EGA combined with zeolite lowers the density and enhances the total porosity of composite, leading to an improvement in thermal conductivity. It was also observed that an increase in aerogel content in the LWSCCC thermal conductivity of the composite specimen decreases. The thermal conductivity coefficient of the control samples, A25, A50, A75, and A100, was calculated as 0.47, 0.45, 0.427, 0.418, and 0.382 W/m·K, respectively. The addition of EGA and aerogel to LWSCCC significantly lowers the density due to a rise in porosity and their lightweight density [13,63,64].

Abbas et al.reported that the use of aerogel in lightweight thermal insulating composites could lower the thermal conductivity by 46% by adding 62.34 vol% of aerogel to the composite [9]. Similarly, Gao et al. [12] reported that with the addition of 60 vol% aerogel to the cement composite, 50% of the density of the composite was reduced and the thermal conductivity was reduced by around 7 times.A similar decrease in thermal conductivity of aerogel added cement composite/concrete was observed by several authors [9,49, 50,64–66]. Fig. 18 and Fig. 19 show that aerogel content, porosity, density, mechanical strength, and thermal conductivity share a close relationship, as the aerogel content rises in the composite, porosity increases, whereas density, compressive strength, and thermal conductivity decrease.

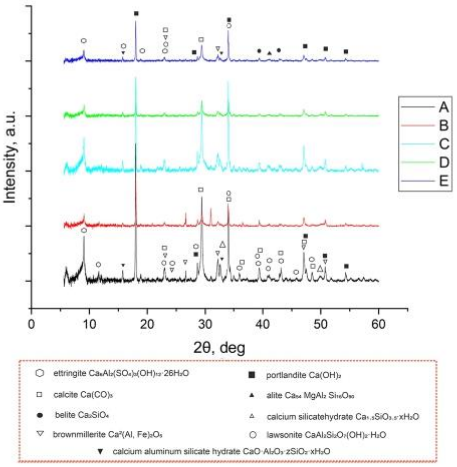

Fig. 16. XRD pattern of LWSCC composite specimen A to E.

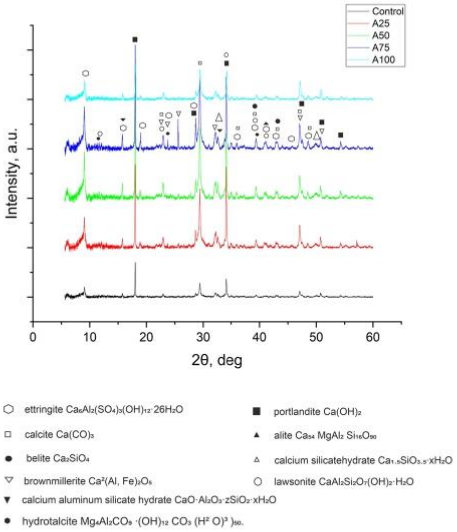

Fig. 17. XRD pattern of LWSCC composite specimens containing aerogel.

3.9. Discussion

EGA is a porous structured lightweight aggregate containing a high volume of pores within its structure. Because of the porous structure, EGA has very low strength and density compared to conventional natural aggregates. EGA's mechanical and physical properties might vary according to size, degree of porosity, and manufacturing process [51]. Due to the lightweight density, LWA might float to the top of the concrete mixture, impacting the homogeneous distribution of aggregates and leading to segregation [15, 16]. A study result reported that the use of fine particles and greater binding materials could improve the flowability of concrete [67]. Also, it was observed in a previous study that the use of combinations of fine EGA shows a greater homogeneous distribution of

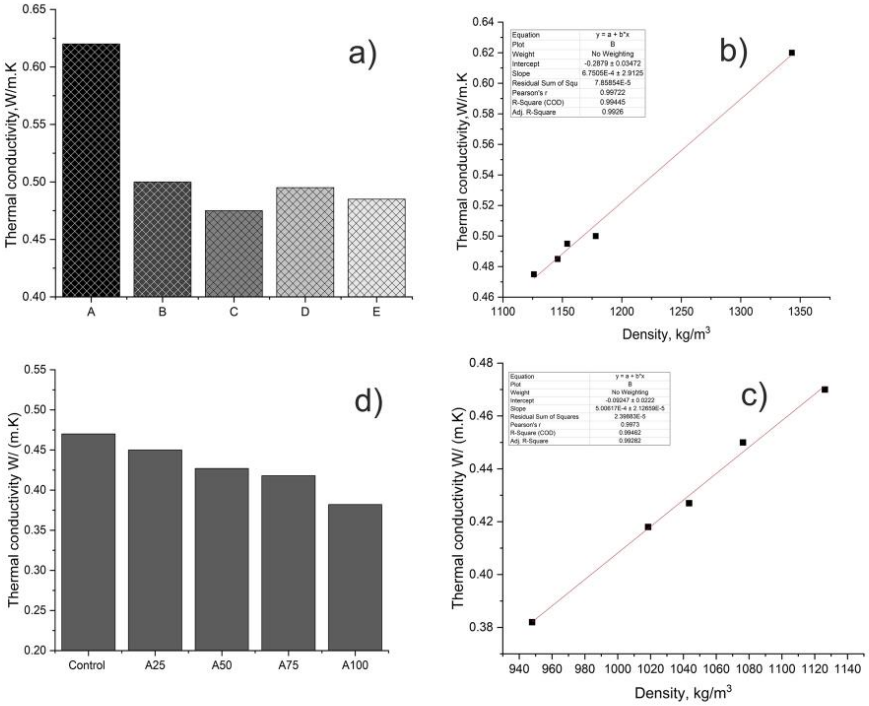

Fig. 18. a) thermal conductivity of LWSCCC samples A to E; b) relationship between density and thermal conductivity of LWSCCC samples A to E. c) thermal conductivity of LWSCCC samples containing aerogel; d) relationship between density and thermal conductivity of LWSCCC samples containing aerogel.

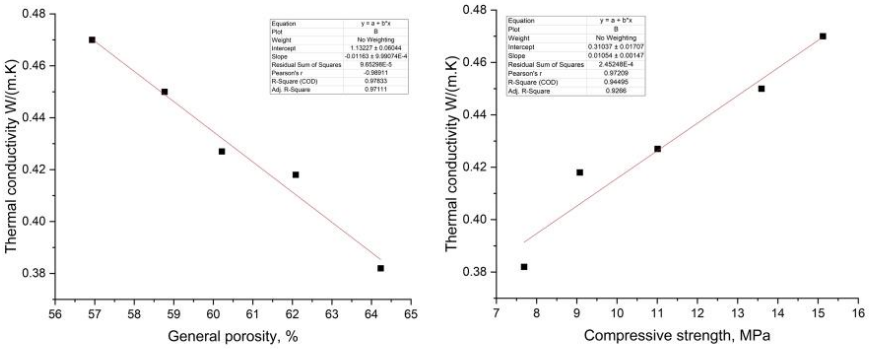

Fig. 19. Relationship between general porosity, compressive strength, and thermal conductivity LWSCCC containing aerogel.

aggregates and strength [7]. Agreeing with the previous studies and literature, the combinations of fine EGA were used to achieve higher workability with sufficient strength characteristics. Previously, Yu et al. [28] developed LWSCCC using EGA having a density of 1280–1490 kg/m^3 with 23.3 and 30.2 MPa compressive strength. They measured the mini-slump value about 300 mm with a

4–11 s V-funnel flow time. This study shows that it is possible to prepare LWSCCC even at a lower than 1000 kg/m^3, having achieved adequate mechanical strength. Aerogel and expanded glasses are lightweight materials and the use of these materials in cement composite could significantly reduce the density of the cement composite. A higher concentration of aerogel in a composite could lead to a sudden drop in strength due to its poor mechanical performance. Some researchers observed that the use of 80 vol% of aerogel in concrete could lead to a drastic reduction in compression strength to 1 MPa [36,38,59]. Due to the very lightweight density, LWA can float to the top and face segregation problems [6,68]. Li et al. [67] suggested that greater content of fine particle and binding materials could enhance the mortar film thickness leading to improvement in workability. Agreeing with the previous literature, a higher content of binding materials and fine grains of EGA and aerogel were used in the LWSCCC. Due to the use of a high volume of fine particles, there was no visual segregation, and some floating of aerogel particles was observed. However, the addition of aerogel slightly decreased the workability of the composite, but greatly lowered the density and improved the thermal conductivity of the composite. Perhaps entrapped air bubbles by aerogel in the composite mixture enhance the viscosity of LWSCCC, leading to an increase in V-funnel time.

3.10. Conclusion

The experimental study investigates the suitability of aerogel particles to produce LWSCCC From the analysis of the obtained results, the following conclusions can be drawn.

- The increase in fine EGA concentration enhanced the water and superplasticizer demand to maintain the workability of the composite. The W/B ratio and superplasticizer doses play a dominant role in enhancing the workability of LWSCCC, while pozzolanic additions show marginal impacts. The addition of aerogel decreased the slump flow of the composite. It is evident from SEM and porosity results that the inclusion of aerogel in LWSCCC might entrap some air bubbles that might increase the viscosity of the composite, leading to an enhancement in flow time.
- The composite samples containing EGA show a higher risk of water absorption. The inclusion of aerogel increases the total and open porosity of LWSCCC. The total and open porosity of the control sample were calculated 56.93% and 15.72%, respectively which increased to 64.23%, and 19.32% for the A100 sample.
- The porous structured EGA has low strength, and the addition of a greater amount of EGA reduces the strength of the composite. However, the addition of a small amount of natural sand might improve the strength of the composite. As expected, the compressive and flexural strength of aerogel added LWSCCC declined with the enhancement in aerogel concentrations. Almost 49.2% and 34.6% reduction compressive and flexural strength was measured by the addition of aerogel as a replacement of EGA. The lower strength of aerogel weakened adhesion with cement, and increased porosity might lead to a reduction in the strength of aerogel added LWSCCC.
- As expected, the zeolite and fly ash reacted with the cement and slightly impacted the hydration. The presence of ettringite was observed for all LWSCCC samples, but a lower water/binder ratio and the inclusion of zeolite might have accelerated the ettringite formation. XRD and SEM images of the LWSCCC clearly shows the presence of ettringite in the LWSCCC.
- An amorphous aerogel might partially dissolve in the alkaline environment of OPC and perhaps accelerate the growth of hydration products. Through the SEM analysis, aerogel particles and some pores surrounding the aerogel in the composite mixture can be clearly detected. Separation gaps in the ITZ between aerogel and cement paste suggested weaker adhesion of aerogel, while greater adhesion of EGA with cement paste was observed. The separation gaps and pores might enhance the porosity and water absorption of LSWCC.
- The use of expanded glass aggregates combined with aerogel significantly lowers the density of the composite, leading to a decrease in the thermal conductivity of LWSCCC.

Declaration of Competing Interest

The authors declare that they have no known competing financial interests or personal relationships that could have appeared to influence the work reported in this paper.

References

[1] S.K. Adhikary, D.K. Ashish, Ž. Rudžionis, Expanded glass as light-weight aggregate in concrete – a review, J. Clean. Prod. 313 (2021), 127848, https://doi.org/10.1016/j.jclepro.2021.127848.
[2] Y. Wu, J.Y. Wang, P.J.M. Monteiro, M.H. Zhang, Development of ultra-lightweight cement composites with low thermal conductivity and high specific strength for energy efficient buildings, Constr. Build. Mater. 87 (2015) 100–112, https://doi.org/10.1016/j.conbuildmat.2015.04.004.
[3] T. Cheboub, Y. Senhadji, H. Khelafi, G. Escadeillas, Investigation of the engineering properties of environmentally-friendly self-compacting lightweight mortar containing olive kernel shells as aggregate, J. Clean. Prod. 249 (2020), 119406, https://doi.org/10.1016/j.jclepro.2019.119406.
[4] Q.L. Yu, H.J.H. Brouwers, Development of a self-compacting gypsum-based lightweight composite, Cem. Concr. Compos. 34 (2012) 1033–1043, https://doi.org/10.1016/j.cemconcomp.2012.05.004.
[5] Y.W. Choi, Y.J. Kim, H.C. Shin, H.Y. Moon, An experimental research on the fluidity and mechanical properties of high-strength lightweight self-compacting concrete, Cem. Concr. Res. 36 (2006) 1595–1602, https://doi.org/10.1016/j.cemconres.2004.11.003.
[6] J. Kwasny, M. Sonebi, S.E. Taylor, Y. Bai, K. Owens, W. Doherty, Influence of the type of coarse lightweight aggregate on properties of semilightweight self-consolidating concrete, J. Mater. Civ. Eng. 24 (2012) 1474–1483, https://doi.org/10.1061/(asce)mt.1943-5533.0000527.
[7] S.K. Adhikary, Z. Rudzionis, Influence of expanded glass aggregate size, aerogel and binding materials volume on the properties of lightweight concrete, Mater. Today Proc. 32 (2020) 712–718, https://doi.org/10.1016/j.matpr.2020.03.323.

[8] Q.L. Yu, P. Spiesz, H.J.H. Brouwers, Development of cement-based lightweight composites - part 1: mix design methodology and hardened properties, Cem. Concr. Compos. 44 (2013) 17–29, https://doi.org/10.1016/j.cemconcomp.2013.03.030.
[9] N. Abbas, H.R. Khalid, G. Ban, H.T. Kim, H.K. Lee, Silica aerogel derived from rice husk: an aggregate replacer for lightweight and thermally insulating cement-based composites, Constr. Build. Mater. 195 (2019) 312–322, https://doi.org/10.1016/j.conbuildmat.2018.10.227.
[10] G. Jia, Z. Li, Influence of the aerogel/expanded perlite composite as thermal insulation aggregate on the cement-based materials: Preparation, property, and microstructure, Constr. Build. Mater. 273 (2021), 121728, https://doi.org/10.1016/j.conbuildmat.2020.121728.
[11] K.L. Huang, S.J. Li, P.H. Zhu, Effect of early curing temperature on the tunnel fire resistance of self-compacting concrete coated with aerogel cement paste, Materials 14 (2021) 5782, https://doi.org/10.3390/ma14195782.
[12] T. Gao, B.P. Jelle, A. Gustavsen, S. Jacobsen, Aerogel-incorporated concrete: an experimental study, Constr. Build. Mater. 52 (2014) 130–136, https://doi.org/10.1016/j.conbuildmat.2013.10.100.
[13] S.K. Adhikary, D.K. Ashish, Ž. Rudžionis, Aerogel based thermal insulating cementitious composites: a review, Energy Build. 245 (2021), 111058, https://doi.org/10.1016/j.enbuild.2021.111058.
[14] S.K. Adhikary, Ž. Rudžionis, S. Tučkutė, D.K. Ashish, Effects of carbon nanotubes on expanded glass and silica aerogel based lightweight concrete, Sci. Rep. 11 (2021) 2104, https://doi.org/10.1038/s41598-021-81665-y.
[15] X. Wang, P. Zhu, S. Yu, H. Liu, Y. Dong, X. Xu, Effect of moisture content on tunnel fire resistance of self-compacting concrete coated with aerogel mortar, Mag. Concr. Res. 73 (2021) 1071–1080, https://doi.org/10.1680/jmacr.19.00436.
[16] P. Zhu, Z. Jia, X. Wang, C. Chen, H. Liu, X. Xu, Density dependence of tunnel fire resistance for aerogel-cement mortar coatings, J. Wuhan. Univ. Technol. Mater. Sci. Ed. 35 (2020) 598–604, https://doi.org/10.1007/s11595-020-2296-3.
[17] P. Zhu, X. Xu, H. Liu, S. Liu, C. Chen, Z. Jia, Tunnel fire resistance of self-compacting concrete coated with SiO2 aerogel cement paste under 2.5h HC fire loading, Constr. Build. Mater. 239 (2020), 117857, https://doi.org/10.1016/j.conbuildmat.2019.117857.
[18] Specification and Guidelines for Self-Compacting Concrete, EFNARC, Rep. from EFNARC, (2002) 32.
[19] M.L. Torres, P.A. García-Ruiz, Lightweight pozzolanic materials used in mortars: evaluation of their influence on density, mechanical strength and water absorption, Cem. Concr. Compos. 31 (2009) 114–119, https://doi.org/10.1016/j.cemconcomp.2008.11.003.
[20] Q.L. Yu, P. Spiesz, H.J.H. Brouwers, Ultra-lightweight concrete: conceptual design and performance evaluation, Cem. Concr. Compos. 61 (2015) 18–28, https://doi.org/10.1016/j.cemconcomp.2015.04.012.
[21] G. Bumanis, D. Bajare, J. Locs, A. Korjakins, Alkali-silica reactivity of expanded glass granules in structure of lightweight concrete, IOP Conf. Ser. Mater. Sci. Eng. 47 (2013) 12022, https://doi.org/10.1088/1757-899x/47/1/012022.
[22] R.W. Floyd, W.M. Hale, J.C. Bymaster, Effect of aggregate and cementitious material on properties of lightweight self-consolidating concrete for prestressed members, Constr. Build. Mater. 85 (2015) 91–99, https://doi.org/10.1016/j.conbuildmat.2015.03.084.
[23] T.Z.H. Ting, M.E. Rahman, H.H. Lau, Sustainable lightweight self-compacting concrete using oil palm shell and fly ash, Constr. Build. Mater. 264 (2020), 120590, https://doi.org/10.1016/j.conbuildmat.2020.120590.
[24] S.K. Adhikary, Ž. Rudžionis, D. Vaičiukynienė, Development of flowable ultra-lightweight concrete using expanded glass aggregate, silica aerogel, and prefabricated plastic bubbles, J. Build. Eng. 31 (2020), 101399, https://doi.org/10.1016/j.jobe.2020.101399.
[25] S.N. Shah, K.H. Mo, S.P. Yap, M.K.H. Radwan, Effect of micro-sized silica aerogel on the properties of lightweight cement composite, Constr. Build. Mater. 290 (2021), 123229, https://doi.org/10.1016/j.conbuildmat.2021.123229.
[26] S. Kim, J. Seo, J. Cha, S. Kim, Chemical retreating for gel-typed aerogel and insulation performance of cement containing aerogel, Constr. Build. Mater. 40 (2013) 501–505, https://doi.org/10.1016/j.conbuildmat.2012.11.046.
[27] A. Venkateswara Rao, M.M. Kulkarni, D.P. Amalnerkar, T. Seth, Surface chemical modification of silica aerogels using various alkyl-alkoxy/chloro silanes, Appl. Surf. Sci. 206 (2003), https://doi.org/10.1016/S0169-4332(02)01232-1.
[28] J. Zach, M. Sedlmajer, J. Hroudova, A. Nevaril, Technology of concrete with low generation of hydration heat, Procedia Eng. 65 (2013) 296–301, https://doi.org/10.1016/j.proeng.2013.09.046.
[29] K. Gorospe, E. Booya, H. Ghaednia, S. Das, Effect of various glass aggregates on the shrinkage and expansion of cement mortar, Constr. Build. Mater. 210 (2019) 301–311, https://doi.org/10.1016/j.conbuildmat.2019.03.192.
[30] J. Lu, J. Jiang, Z. Lu, J. Li, Y. Niu, Y. Yang, Pore structure and hardened properties of aerogel/cement composites based on nanosilica and surface modification, Constr. Build. Mater. 245 (2020), 118434, https://doi.org/10.1016/j.conbuildmat.2020.118434.
[31] C. Lian, Y. Zhuge, S. Beecham, The relationship between porosity and strength for porous concrete, Constr. Build. Mater. 25 (2011) 4294–4298, https://doi.org/10.1016/j.conbuildmat.2011.05.005.
[32] P. Spiesz, Q.L. Yu, H.J.H. Brouwers, Development of cement-based lightweight composites - part 2: durability-related properties, Cem. Concr. Compos. 44 (2013) 30–40, https://doi.org/10.1016/j.cemconcomp.2013.03.029.
[33] M. Kurpińska, T. Ferenc, Effect of porosity on physical properties of lightweight cement composite with foamed glass aggregate, ITM Web Conf. 15 (2017) 06005.
[34] A. Yousefi, W. Tang, M. Khavarian, C. Fang, S. Wang, Thermal and mechanical properties of cement mortar composite containing recycled expanded glass aggregate and nano titanium dioxide, Appl. Sci. 10 (2020) 2246, https://doi.org/10.3390/app10072246.
[35] D. Rumsys, E. Spudulis, D. Bacinskas, G. Kaklauskas, Compressive strength and durability properties of structural lightweight concrete with fine expanded glass and/or clay aggregates, Materials 11 (2018), https://doi.org/10.3390/ma11122434.
[36] P. Zhu, S. Yu, C. Cheng, S. Zhao, H. Xu, Durability of silica aerogel cementitious composites - Freeze-thaw resistance, water resistance and drying shrinkage, Adv. Cem. Res. 32 (2020) 527–536, https://doi.org/10.1680/jadcr.18.00145.
[37] Z. hui Liu, F. Wang, Z. ping Deng, Thermal insulation material based on SiO2 aerogel, Constr. Build. Mater. 122 (2016) 548–555, https://doi.org/10.1016/j.conbuildmat.2016.06.096.
[38] S. Ng, B.P. Jelle, L.I.C. Sandberg, T. Gao, Ó.H. Wallevik, Experimental investigations of aerogel-incorporated ultra-high performance concrete, Constr. Build. Mater. 77 (2015) 307–316, https://doi.org/10.1016/j.conbuildmat.2014.12.064.
[39] F. Chen, Y. Zhang, J. Liu, X. Wang, P.K. Chu, B. Chu, N. Zhang, Fly ash based lightweight wall materials incorporating expanded perlite/SiO2 aerogel composite: towards low thermal conductivity, Constr. Build. Mater. 249 (2020), 118728, https://doi.org/10.1016/j.conbuildmat.2020.118728.
[40] A. Hanif, P. Parthasarathy, Z. Li, ⟨2017-Utilizing Fly Ash Cenosphere and Aerogel for. pdf⟩, 11 (2017) 84–90.
[41] S.Y. Chung, P. Sikora, D.J. Kim, M.E. El Madawy, M. Abd Elrahman, Effect of different expanded aggregates on durability-related characteristics of lightweight aggregate concrete, Mater. Charact. 173 (2021), 110907, https://doi.org/10.1016/j.matchar.2021.110907.
[42] S.Y. Chung, M. Abd Elrahman, J.S. Kim, T.S. Han, D. Stephan, P. Sikora, Comparison of lightweight aggregate and foamed concrete with the same density level using image-based characterizations, Constr. Build. Mater. 211 (2019) 988–999, https://doi.org/10.1016/j.conbuildmat.2019.03.270.
[43] M. Limbachiya, M.S. Meddah, S. Fotiadou, Performance of granulated foam glass concrete, Constr. Build. Mater. 28 (2012) 759–768, https://doi.org/10.1016/j.conbuildmat.2011.10.052.
[44] M. Kurpinska, L. Kułak, Predicting performance of lightweight concrete with granulated expanded glass and ash aggregate by means of using artificial neural networks, Materials 12 (2019), https://doi.org/10.3390/ma12122002.
[45] T. Hemalatha, A. Ramaswamy, A review on fly ash characteristics – towards promoting high volume utilization in developing sustainable concrete, J. Clean. Prod. 147 (2017) 546–559, https://doi.org/10.1016/j.jclepro.2017.01.114.
[46] B. Ahmadi, M. Shekarchi, Use of natural zeolite as a supplementary cementitious material, Cem. Concr. Compos. 32 (2010) 134–141, https://doi.org/10.1016/j.cemconcomp.2009.10.006.
[47] S.Y.N. Chan, X. Ji, Comparative study of the initial surface absorption and chloride diffusion of high performance zeolite, silica fume and PFA concretes, Cem. Concr. Compos. 21 (1999) 293–300, https://doi.org/10.1016/S0958-9465(99)00010-4.

[48] K. Guo, H. Song, X. Chen, X. Du, L. Zhong, Graphene oxide as an anti-shrinkage additive for resorcinol-formaldehyde composite aerogels, Phys. Chem. Chem. Phys. 16 (2014) 11603–11608, https://doi.org/10.1039/c4cp00592a.
[49] L. Wang, P. Liu, Q. Jing, Y. Liu, W. Wang, Y. Zhang, Z. Li, Strength properties and thermal conductivity of concrete with the addition of expanded perlite filled with aerogel, Constr. Build. Mater. 188 (2018) 747–757, https://doi.org/10.1016/j.conbuildmat.2018.08.054.
[50] H. Li, P. Zang, H. Liu, K. Cao, X. Liao, D. Wei, B. Zhang, H. Li, J. Wang, Preparation and heat insulation of Geminihalloysite aerogel/concrete composites, J. Polym. Eng. 41 (2021) 387–396, https://doi.org/10.1515/polyeng-2020-0317.
[51] S.K. Adhikary, Ž. Rudžionis, S. Tučkutė, D.K. Ashish, Effects of carbon nanotubes on expanded glass and silica aerogel based lightweight concrete, Sci. Rep. 11 (2021) 2104, https://doi.org/10.1038/s41598-021-81665-y.
[52] P.-H. Zhu, Y.-Q. Sun, Experimental study on the influence of particle size of the SiO2 aerogel on properties of silica aerogel tunnel fireproof mortar, DEStech Trans. Mater. Sci. Eng. (2017) 2–7, https://doi.org/10.12783/dtmse/icmsea/mce2017/10858.
[53] A. Soares, M. Julio, I. Flores-Colen, L. Ilharco, J. De Brito, J. Gaspar Martinho, Water-resistance of mortars with lightweight aggregates, Key Eng. Mater. 634 (2015) 46–53, https://doi.org/10.4028/www.scientific.net/KEM.634.46.
[54] B.H. Spratt, Lightweight Aggregate Concrete, Civ. Eng., London, 1984, https://doi.org/10.1016/0016-0032(45)90197-9.
[55] G. Bumanis, D. Bajare, J. Locs, A. Korjakins, Alkali-silica reactivity of foam glass granules in structure of lightweight concrete, Constr. Build. Mater. 47 (2013) 274–281, https://doi.org/10.1016/j.conbuildmat.2013.05.049.
[56] P. Zhu, S. Brunner, S. Zhao, M. Griffa, A. Leemann, N. Toropovs, A. Malekos, M.M. Koebel, P. Lura, Study of physical properties and microstructure of aerogel-cement mortars for improving the fire safety of high-performance concrete linings in tunnels, Cem. Concr. Compos. 104 (2019), 103414, https://doi.org/10.1016/j.cemconcomp.2019.103414.
[57] C. Hai-li, Influence on the Performances of Foamed Concrete by Silica Aerogels, Am. J. Civ. Eng. 3 (2015) 183, https://doi.org/10.11648/j.ajce.20150305.18.
[58] M. de Fátima Júlio, L.M. Ilharco, A. Soares, I. Flores-Colen, J. de Brito, Silica-based aerogels as aggregates for cement-based thermal renders, Cem. Concr. Compos. 72 (2016) 309–318, https://doi.org/10.1016/j.cemconcomp.2016.06.013.
[59] S. Ng, B.P. Jelle, T. Stæhli, Calcined clays as binder for thermal insulating and structural aerogel incorporated mortar, Cem. Concr. Compos. 72 (2016) 213–221, https://doi.org/10.1016/j.cemconcomp.2016.06.007.
[60] J. ping Zuo, Z. jie Hong, Z. qiang Xiong, C. Wang, H. qiang Song, Influence of different W/C on the performances and hydration progress of dual liquid high water backfilling material, Constr. Build. Mater. 190 (2018) 910–917, https://doi.org/10.1016/j.conbuildmat.2018.09.146.
[61] M.D.M. Alonso, M. Palacios, F. Puertas, Effect of polycarboxylate-ether admixtures on calcium aluminate cement pastes. Part 1: compatibility studies, Ind. Eng. Chem. Res. 52 (2013) 17323–17329, https://doi.org/10.1021/ie401615t.
[62] R. Snellings, G. Mertens, Ö. Cizer, J. Elsen, Early age hydration and pozzolanic reaction in natural zeolite blended cements: Reaction kinetics and products by in situ synchrotron X-ray powder diffraction, Cem. Concr. Res. 40 (2010) 1704–1713, https://doi.org/10.1016/j.cemconres.2010.08.012.
[63] A. Lamy-Mendes, A.D.R. Pontinha, P. Alves, P. Santos, L. Durães, Progress in silica aerogel-containing materials for buildings' thermal insulation, Constr. Build. Mater. 286 (2021), 122815, https://doi.org/10.1016/j.conbuildmat.2021.122815.
[64] S.N. Shah, K.H. Mo, S.P. Yap, M.K.H. Radwan, Towards an energy efficient cement composite incorporating silica aerogel: a state of the art review, J. Build. Eng. 44 (2021), 103227, https://doi.org/10.1016/j.jobe.2021.103227.
[65] A. Hanif, S. Diao, Z. Lu, T. Fan, Z. Li, Green lightweight cementitious composite incorporating aerogels and fly ash cenospheres - mechanical and thermal insulating properties, Constr. Build. Mater. 116 (2016) 422–430, https://doi.org/10.1016/j.conbuildmat.2016.04.134.
[66] P.F. Bergmann Becker, C. Effting, A. Schackow, Lightweight thermal insulating coating mortars with aerogel, EPS, and vermiculite for energy conservation in buildings, Cem. Concr. Compos. 125 (2022), 104283, https://doi.org/10.1016/j.cemconcomp.2021.104283.
[67] J. Li, Y. Chen, C. Wan, A mix-design method for lightweight aggregate self-compacting concrete based on packing and mortar film thickness theories, Constr. Build. Mater. 157 (2017) 621–634, https://doi.org/10.1016/j.conbuildmat.2017.09.141.
[68] S.K. Adhikary, Z. Rudzionis, Influence of expanded glass aggregate size, aerogel and binding materials volume on the properties of lightweight concrete, Mater. Today Proc. 32 (2020) 712–718, https://doi.org/10.1016/j.matpr.2020.03.323.

Article 3.

Authors: Suman Kumar Adhikary

Title of article: The influence of pre-coated EGA and aerogel on the properties of lightweight self-compacting cementitious composites

Citation: Materials Today Communications, Volume 31, June 2022, 103496; https://doi.org/10.1016/j.mtcomm.2022.103496

Materials Today Communications 31 (2022) 103496

Contents lists available at ScienceDirect

Materials Today Communications

journal homepage: www.elsevier.com/locate/mtcomm

The influence of pre-coated EGA and aerogel on the properties of lightweight self-compacting cementitious composites

Suman Kumar Adhikary *

Faculty of Civil Engineering and Architecture, Kaunas University of Technology, Kaunas LT-44249, Lithuania

ARTICLE INFO

Keywords:
Polymer coatings: treated lightweight aggregate
Aerogel
Lightweight self-compacting cementitious composites
Microscopy

ABSTRACT

Aerogel and porous lightweight aggregates have adverse impacts on the fresh, mechanical, and water absorption characteristics of concrete. In this study, styrene-butadiene rubber (SBR) and Paraffin were used to coat the lightweight aggregates. The lightweight aggregates were coated in single and double layers. Besides, aerogel particles were also coated with SBR. The properties of the cementitious composites, such as slump flow, T50 flow time, V-funnel flow time, J-ring height, compressive strength, water absorption, porosity, and microstructural analysis, were evaluated. It was observed that single-layer coatings of polymers on EGA improved the slump flow by 6.9% and lowered the water absorption by 26%. The compressive strength of the cementitious composites incorporating polymer coated EGA also improved by 15.9%. Scanning microscopy was used to evaluate the microstructure of EGA, aerogel, and lightweight cementitious composites. A uniform, denser structure of polymer coated EGA was observed in the interfacial transition zone.

1. Introduction

Lightweight concrete is one of the prime topics in the building industry, and it is a topic that researchers are very interested in. The primary advantage of LWC is that it reduces the weight of the structure [1]. Owing to its high porosity, LWC has a lower heat conductivity than conventional concrete [2,3]. In recent years, lightweight self-compacting concrete has been gaining attention for its several benefits. However, in the last decade, several studies were carried out to understand and improve the characteristics of conventional self-compacting concrete [4,5] but only limited studies were done on lightweight thermal insulating LWSCC and LWSCCC [6,7]. LWSCC/LWSCCC is a refined product of LWAC and SCC that enables molding and casting without using any vibration energy. It not only results in a high-quality product, but it also considerably improves productivity and working conditions. The use of lightweight aggregate to produce LWSCC or LWSCCC might cause a risk of higher water absorption than conventional SCC [7]. Most lightweight aggregates are porous-structured, having up to 45% of water absorption capacity, while aggregates used in conventional concrete have up to less than 10% water absorption [8,9]. In this context, modification and pre-treatment of aggregates might be useful to improve the water absorption capacity, strength, and durability characteristics [8,10,11].

Vahabi et al. [8] utilized SBR and PVR latex to coat scoria and expanded clay. The authors reported that due to the reduction in WA of aggregates, the slump of LWSCC improved by 2–10%. The slump flow of LWSCC's sump improved due to the increase in coating layers of polymers. Additionally, polymer membrane layers reduce frictional forces, which reduces flow time and blocks resistance in LWSCC. The compressive strength of treated scoria and LECA-based LWSCC was improved by almost 21% and 13.5%, respectively. A similar phenomena was observed by Güneyisi et al. [10]. The author used water glass-treated FAA and observed improved workability of LWSCC. The water absorption and cohesion forces of FAA were reduced owing to the hydrophobic water glass coating, which improved slump flow, decreased flow time, and decreased the blockage resistance of LWSCC. Moreover, the author reported a 32–44% enhancement in the compressive strength of concrete incorporating water glass treated FAA. According to Assaad and Mir [12], SBR latex might increase the bond strength by enhancing monolithic interlayer bonding and inhibiting microcrack propagation. Li et al. [13] studied the characteristics of concrete incorporating pozzolanic material-coated aggregates. The authors observed that treated aggregates improved the slump and mechanical properties of the concrete. Bidesi et al. [14] observed improved strength of concrete incorporating polymer-coated lightweight aggregates.

Literature studies indicate that the use of polymer coatings on the

* Corresponding author.
E-mail address: sumankradk9s@gmail.com.

https://doi.org/10.1016/j.mtcomm.2022.103496
Received 20 March 2022; Received in revised form 2 April 2022; Accepted 4 April 2022
Available online 6 April 2022

Nomenclature

LWC	Lightweight concrete
LWSCC	Lightweight self-compacting concrete
LWAC	Lightweight aggregate concrete
LWSCCC	Lightweight self-compacting cementitious composites
SCC	Self-compacting concrete
SP	Superplasticiser
WA	Water absorption
C_S	Compressive strength

self-compatibility of the cementitious composites below 1200 kg/m^3 density and to investigate the impacts of polymer-coated aerogel and EGA on the characteristics of self-compacting cementitious composites.

2. Materials and methods

2.1. Materials

In this experimental study, OPC of grade 42.4 R and an average 50 μm diameter zeolite powder were used as mineral admixtures. While aerogel and different grades of EGA were used as lightweight aggregates, the physical and chemical properties of EGA, OPC, and zeolite are presented in Tables 1 and 2. The aerogel and EGA aggregates were

Table 1
Physical properties of EGA.

EGA size, mm	Bulk density, kg/m^3	Compressive strength, MPa	Water absorption, %	Thermal conductivity, W/ (m-K)	pH value	Softening point	Color
0.1–0.3	400	4	18	–	9–11	Approx. 700 °C	Cream white
0.25–0.5	340	2.5	20	0.0767			
0.5–1	270	1.7	18	0.0713			
1–2	230	2.0	18	0.0663			
2–4	200	1.4	15	0.0639			
4–8	190	1.2	10	0.0661			

Table 2
Chemical compositions of cement, zeolite and EGA.

Chemical composition	CaO	MgO	SiO_2	Al_2O_3	Fe_2O_3	K_2O	Na_2O	SO_3	TiO_2	Cl	Na_2O eq	LOI	Insoluble residue	Free lime	Lime paste	Other
Cement	63	2.9	20.4	4.1	3.5	0.7	0.23	3.2	–	0.03	0.74	2.5	0.5	1.2	3.9	—
Zeolite	2.8	0.7	58.7	9.0	1.4	2.6	—	0.1	0.2	—	—	5.1	—	—	—	—
EGA	8–10.5		71–73	1.5–2	< 0.3	—	13–14		—	—	—	—	—	—	—	< 0.5

aggregates effectively improves the fresh, mechanical, and microstructural properties of cementitious systems. Aerogel and EGA are both lightweight aggregates and are used to prepare thermally insulating cementitious composites [15–17]. In the past, only a few studies have examined the performance of aerogel and EGA-based light-weight thermal insulating cementitious composites [7,18–20]. EGA aggregates absorb a sufficient amount of water and enhance the required amount of water to get the desired workability [7,21–23]. Moreover, use of higher volume EGA and a greater w/b ratio enhances the risk of rise in water absorption. This study aimed to lower the water absorption capacity of the EGA-based cementitious composites by coating the EGA with polymers. Besides, aerogel has weaker adhesion with cement-based systems. Aerogel was also coated with SBR polymers, aiming to enhance the adhesion of aerogel with cementitious composites. Moreover, most developed lightweight self-compacting concrete/cementitious composites have more than 1400 kg/m^3 density. In the past, there were no studies investigating the characteristics of self-compacting cementitious composites incorporating aerogel and EGA. Also, the impacts of polymers coated on expanded glass aggregate cementitious composites weren't deeply studied. This study also aimed to obtain purchased from "CABOT" and "Stikloporas", respectively. SBR and Paraffin were used for the pre-coating of aerogel and EGA. To maintain the fresh properties of LWSCCC, MasterGlenium SKY 8700 and MasterMatrix SDC 100 stabilizer were used as chemical admixtures.

2.2. Coating of lightweight aggregates

To coat the lightweight aggregates first, the polymer liquids were poured into containers and the lightweight aggregates were dropped for a short period of time. Afterward, lightweight aggregates were taken out and kept on the flat surface for 48 h for the dying process. A similar process was repeated for the second layer of coatings.

2.3. Sample preparation

The mixing and trial methods were used to prepare the LWSCCC samples. The first composite sample EGAC was prepared with 4–8 mm, 2–4 mm, 1–2 mm, 0.5–1 mm, 0.25–0.5 mm, and 0.1–0.3 mm EGA aggregates. For the second sample A50, half of the volume of 2–1 mm and 1–0.5 mm EGA was replaced with 2–0.5 mm aerogel particles. The first

Table 3
Mixing composition of lightweight self-compacting cementitious composites, kg/m^3.

Mix	Cement	Aggregate (4/8 + 2/4 + 1/2 + 1/0.5 + 0.5/0.25 + 0.01/0.3)	Aerogel, kg/m^3	Zeolite	SP		Water	
					%	Kg/m^3	Kg/m^3	w/b
EGAC	568.4	12.8 + 14.3 + 36.2 + 49.62 + 50.5 + 168.1	–	63.2	1.8	9.42	302.4	0.48
A50	568.4	12.8 + 14.3 + 18.1 + 24.8 + 50.5 + 168.1	11.8	63.2	1.8	9.42	302.4	0.48
SBR1	568.4	12.8 + 14.3 + 18.1 + 24.8 + 50.5 + 168.1	11.8	63.2	1.8	9.42	302.4	0.48
PAR1	568.4	12.8 + 14.3 + 18.1 + 24.8 + 50.5 + 168.1	11.8	63.2	1.8	9.42	302.4	0.48
SBR2	568.4	12.8 + 14.3 + 18.1 + 24.8 + 50.5 + 168.1	11.8	63.2	1.8	9.42	302.4	0.48
SBR-PAR	568.4	12.8 + 14.3 + 18.1 + 24.8 + 50.5 + 168.1	11.8	63.2	1.8	9.42	302.4	0.48

two samples, EGAC and A50, were prepared without any pre-coated lightweight aggregates. The rest of the samples were prepared with pre-coated lightweight aggregates. For the sample, SBR1, 8–4 mm, 4–2 mm, 2–1 mm, and + 1–0.5 mm of EGA were coated with a single layer of SBR. While Paraffin coated 4–8 mm, 2–4 mm, 1–2 mm, 0.5–1 mm, EGA was used to prepare PAR1. Similarly, for the SBR2, a double-layer coating of SBR is used. For the composite sample SBR-PAR, the first layer of SBR and the second layer of Paraffin were employed on the EGA. In addition, the aerogel particles used in the concrete samples (except EGAC and A50) were also coated with Styrene-butadiene rubber. All composite samples were kept at a w/b ratio of 0.48. The mixing composition of the composite samples is presented in Table 3. At the first stage of the mixing process, cement, zeolite, and EGA were gently mixed by hand for two minutes. Subsequently, the mixture was manually stirred for three minutes with 50% of the total water content. After that, the SP and stabilizer are blended with the leftover water and mixed to the composite mixture. Aerogel was incorporated into the composite mixture at the very end to prevent the aerogel particles from being crushed. The final composite mixture was mixed for another two minutes.

2.4. Workability test

To evaluate the fresh characteristics of LWSCCC, slump flow, T50 time, V-funnel time, and J-ring height were measured to satisfy EFNARC guidelines. To measure the slump flow, a 30-centimeter-high cone with a 20-centimeter-wide bottom and a 10-centimeter-wide top is utilized. Slump-flow tests were carried out by raising the slump cone vertically and taking the average diameter of the LWSCCC base as a result. An EFNARC-compliant concrete V-funnel was used for the testing of the composite. After 10 s of filling, the bottom of the V-funnel was opened to evaluate flow out time. After that, samples were molded into 100×100×100 mm cubes for hardening and left at room temperature for 24 h. Hardened composite specimens were demoulded and hydrated in water for 28 days.

2.5. Compressive strength test

The C_S of LWSCCC was measured on the 28th day of hydration in accordance with EN 196-1:2016. Six specimens were analyzed for each sample, and the mean values were used as the result.

2.6. Porosity

After 28 days of hydration in accordance with GOST 127304, the porosity of LWSCCC samples was measured. Samples of the composites were then oven-dried for 24 h at 105 °C. The mass of the oven-dried samples was accurately measured. After that, the mass of the composite samples was measured after they had been submerged in water for 15 min, an hour, 24 h, and 48 h. Underwater mass measurements were made after 48 h of WA and the porosity of the composite samples was calculated using the formula stated in the previous paper [7]. However, the accuracy of this calculation might differ from that of the mercury intrusion porosimetry (MIP) method.

2.7. Density and water absorption

In order to estimate each specimen's dry density, on the 28th day, the LWSCCC specimens were removed from the water and dried for 24 h at 105 °C. Following that, the composite specimens were evaluated for 15 min, 1 h, 24 h, and 48 h for water absorption. The average of six specimens from each composite sample type was considered as a result.

2.8. Scanning electron microscopy

The Hitachi S-3400 N high-resolution electronic microscope with a Bruker Quad 5040 EDS detector was used to conduct SEM analysis on LWSCCC specimens. A rotary blade cutter was used to slice a thin layer of concrete from the LWSCC specimens at 28 days of age for microscopic examination.

Table 4
Workability of lightweight self-compacting cementitious composites.

Mix	Slump flow, cm	T_{50}, s	V-funnel time, s	J-ring height, cm
EGAC	81	5	6	9.4
A50	73.2	5.5	6.5	9
SBR1	74.5	5	5.4	9
PAR1	78.2	4.5	5	9.6
SBR2	75	5	6	8.5
SBR-PAR	76	5	6	9.5

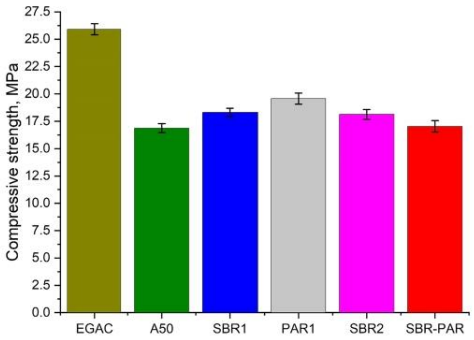

Fig. 1. Compressive strength of lightweight self-compacting cementitious composites.

3. Results

3.1. Workability

Table 4 shows the workability of LWSCCC. Study results show that the incorporation of aerogel significantly lowers the slump flow of the composite. The slump flow of the EGAC without aerogel was measured at 81 cm, which was reduced to 73.2 cm by incorporating aerogel as a partial replacement of EGA. Several studies [7,20,24–26] found a similar decrease in slump flow of a cementitious system incorporating aerogel. Water can be absorbed by the aerogel's surface chemicals, resulting in a decline in workability [24,27]. Besides, it was also observed that the incorporation of aerogel might entrap some air bubbles [7]. Ma et al. [28] used aerogel in 3D printable concrete and reported an almost 37.65% reduction in slum flow of concrete incorporating aerogel. In accordance with previous findings and literature, the incorporation of aerogel may have a negative impact on workability due to its surface chemistry and super hydrophobic properties. However, it was observed that a single layer of polymer coated EGA with SBR and Paraffin slightly enhances the workability. A single layer Paraffin.

-coated EGA was shown to be more workable than a single layer SBR-coated EGA in the study. When compared to A50, the slump flow of SBR1 and PAR1 improved by 1.8% and 6.9%, respectively. Table 4 further reveals that the T50 flow time of LWSCCC is between 4.5 and 5.5 s. T50 flow time of EGAC was measured 5 s, that increased to 5.5 incorporating aerogel. The composite samples containing single-layer SBR and paraffin-coated EGA showed a slight decrease in T50 flow time. The composites' V-funnel time was also found to exhibit the same phenomenon. The J-ring height of the composite samples was

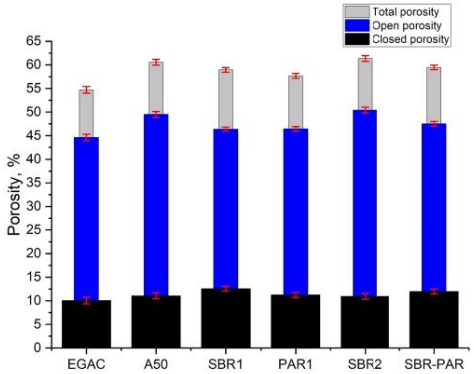

Fig. 2. Porosity of lightweight self-compacting cementitious composites.

somewhere between 8.5 and 9.6 cm. There was no blockage observed for the composite samples. Polymer coating may reduce water absorption and reduce frictional forces between aggregates, which leads to better workability [8]. Similar phenomena were observed by Rostami et al. [29]. However, in this study, the effectiveness in improving workability was declined when double layers of polymer coatings were employed for the composite samples SBR2 and SBR-PAR.

3.2. Compressive strength

The C_S of the composite samples was presented in Fig. 1. The compressive strength of the samples was found to lie between 25.9 MPa and 17.03 MPa. Study results reveal that incorporation as partial replacement of EGA lowers the C_S by 38.9%. The reduction in strength of cementitious composites incorporating aerogel might be due to the lower strength of aerogel [20,30]. Furthermore, aerogel had weaker adhesion with cementitious materials and increased porosity, resulting in a decrease in strength [7,18,30]. Gao et al. [31] reported a 9-times decrease in the C_S of concrete containing 60 vol% of aerogel over a control sample. Several authors [32–34] reported similar decreases in C_S of aerogel-based cementitious composites. However, polymer coatings on the lightweight aggregates slightly enhance the strength of the LWSCCC. Almost 8.4% and 15.9% increases in the compressive strength of the composite were measured for the EGA coated with single layer SBR and single layer Paraffin. According to the findings of the study, Paraffin coated EGA concrete gains more strength than SBR coatings. Microscopy images of the LWSCCC reveal that polymer coatings effectively improve the adhesion of LWA with cementitious composites. A dense structure in the ITZ of EGA was observed for the composites coated with polymers. Besides, in this study, polymer-coated aerogel also showed slightly improved adhesion with cementitious materials. Probably due to this phenomenon, an improvement in the strength of the polymer coated composite samples was observed. However, when a double layer of polymer coatings was employed on the EGA, the effectiveness in increasing compressive strength declined. Probably double-layered coated lightweight aggregates probably entrapped some air bubbles during the mixing process, leading to a slight increase in porosity and a decline in strength. Rostami et al. [29] reported that polymer coating might prevent hydration product adhesion, leading to a decrease in strength. Similar observations were made by Akyuncu and Sanliturk [35].

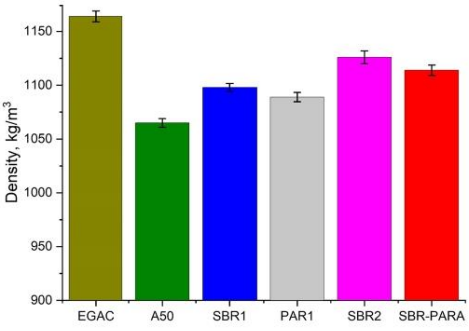

Fig. 3. Density of lightweight self-compacting cementitious composites.

3.3. Porosity

Any cementitious system's porosity has a significant effect on the composite's strength and long-term durability. Fig. 2 shows the porosity of the cementitious composite samples. The total porosity of the composite samples lies between 54.7% and 61.37%. The open and closed porosity of the composite ranged from 44.36% to 50.4% and 10.06–12.57%, respectively. The incorporation of aerogel as a partial replacement of EGA in the A50 sample enhances the total porosity and closed porosity by 5.87% and 4.87%, respectively. Previous studies [7, 24]. observed a similar phenomenon of increased porosity of cementitious system by incorporating aerogel. Hydrophobic nature of aerogel might entrap some air bubbles during the mixing of fresh cementitious composite, leading to an increase in porosity [31]. It was observed that large aerogel particles are an aggregation of nanoparticles and consist of substantial voids (~50 nm in diameter, mesoporous). It also comprises of a "pearl-necklace' like a network of mesoporous and secondary particles with 5–10 nm diameter [24,31]. Apart from having weaker adhesion with the cementitious system, several authors reported separation gaps in the ITZ between cementitious materials and aerogel [7,24, 31]. The incorporation of aerogel probably enhances the porosity of the composite A50. However, single-layer coatings of SBR and Paraffin on EGA show a slight improvement in porosity. Compared to A50, almost 1.63% and 2.9% reductions in total porosity and a 3.1% decrease in closed porosity were observed for the composite samples SBR1 and PAR1. On the other hand, a double layer of polymer coating on EGA was not found to be effective in lowering the porosity of the composites. This is most likely due to composite samples with double layer coating entrapping some air bubbles, leading to an increase in porosity.

3.4. Density

The oven dried density of the composite samples was presented in Fig. 3. The oven dried density of the LWSCCC samples was found to lie between 1164 and 1065 kg/m3. Study results suggested that incorporation of aerogel as a partial replacement of EGA reduced the density by 9.3%. Aerogel is a lightweight material having a bulk density of about 70 kg/m3, and incorporation of aerogel as a replacement for EGA leads to a decline in density [7,36]. Besides, incorporation of aerogel enhances the porosity of the LWSCCC, leading to a decline in porosity [36]. However, the use of polymer coatings on the aerogel and EGA slightly enhances the density of the composite samples SBR1, PAR1, SBR2 and SBR-PAR. The oven dried density of the composite sample SBR1, PAR1, SBR2 and SBR-PAR was measured at 1098, 1089, 1126 and 1114 kg/m3. The polymer coatings on the lightweight aggregates slightly enhance the density, leading to an enhancement in the density of the composite samples [8].

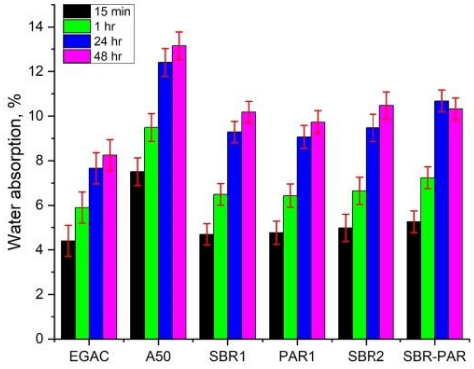

Fig. 4. Water absorption of lightweight self-compacting cementitious composites.

3.5. Water absorption

Among concrete's many useful properties, water absorption is crucial for long-term durability. An increase in concrete's water absorption may allow toxic elements to penetrate the concrete's structure [37]. WA of the cementitious systems is presented in Fig. 4. The WA of composites lies between 8.25% and 13.16% after 48 h of water immersion. Study results clearly show that the use of aerogel as a partial replacement of EGA enhances the water absorption capacity by 59.5%. This phenomenon might be associated with the enhancement in porosity of the LWSCCC by the addition of aerogel. Similar phenomena were noticed in previous studies [7,30]. However, polymer coatings on the lightweight aggregates were observed to be effective in improving the water absorption capacity of the cementitious composites. Single layer coatings of polymer coatings on EGA were observed to be more effective in improving the water absorption of the lightweight cementitious composites. The study's findings also indicate that paraffin-coated expanded glass has a lower water absorption capacity than SBR-coated EGA. Compared to A50, composite samples SBR1 and PAR1 show 22.6% and 26% improved water absorption after 48 h of water immersion, respectively. However, the double layer of polymers on the EGA doesn't show improvement in water absorption. In contrast, composite samples incorporating double-layer coated EGA show a slight increase in water absorption over single-layer coated EGA. This phenomenon might be associated with the increase in porosity. Double-coated LWA might entrap some air bubbles and slightly enhance the porosity, leading to an increase in WA.

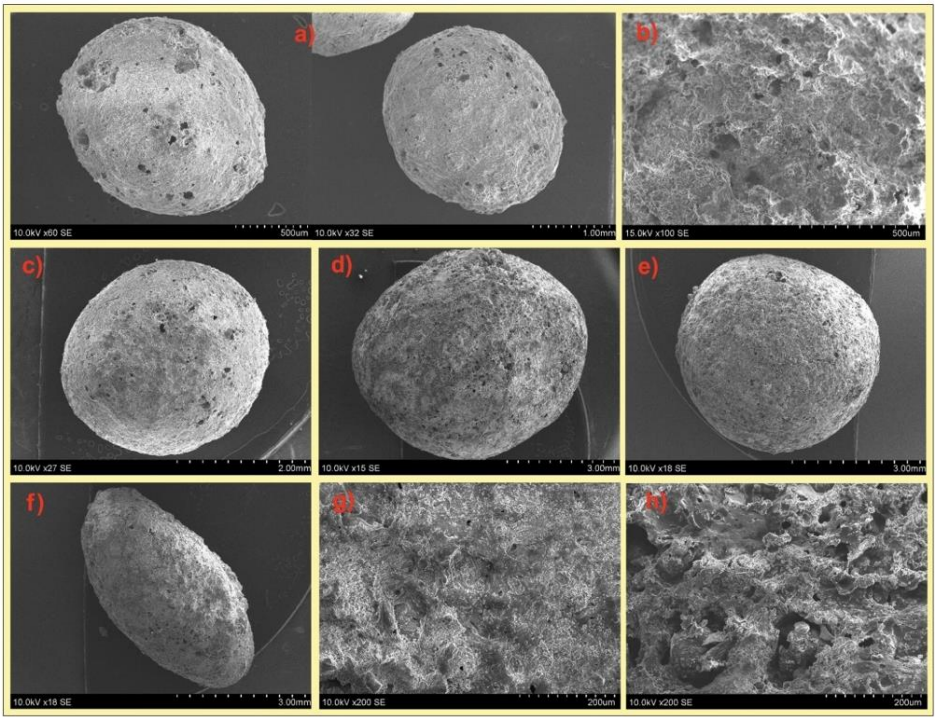

Fig. 5. a) SEM image of non-coated EGA, b) microscopic surface texture of non-coated EGA, c) single layer SBR coated EGA, d) single layer Paraffin coated EGA, e) double layer SBR coated EGA, f) combined SBR and Paraffin coated EGA (first layer of SBR and second layer of Paraffin), g) microscopic surface texture of Paraffin coated EGA, h) microscopic surface texture of SBR coated EGA.

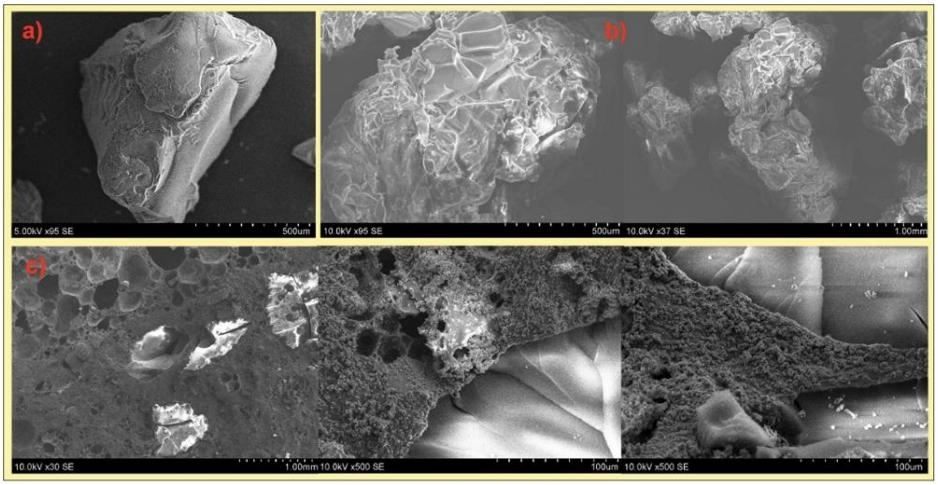

Fig. 6. a) SEM image of non-coated aerogel, b) SBR coated aerogel, c) adhesion of SBR coated aerogel with cementitious materials.

3.6. Scanning electron microscopy

Scanning microscopy of EGA and polymers coated with EGA is presented in Fig. 5. Fig. 5a) and b) show that EGA has a rough surface structure at the microscope level and some broken shell pores were observed on the surface of EGA. Fig. 5c), d), e), and f) depict EGA with single layer SBR coating, single layer Paraffin coating, double layer SBR coatings, and combined SBR and Paraffin (first layer of SBR and second layer of Paraffin) coatings, respectively. Fig. 5(g) and h) show that the polymer layer on the surface of EGA is well bonded and that the pores are mostly filled with polymers. Fig. 6 shows the microscope image of the aerogel and SBR coated aerogel. Fig. 6**a)** clearly shows the evident fragile nature of aerogel. Multiple cracks on the surface of the aerogel at microscope level are clearly visible. Similar cracks on the aerogel surface and its fragile nature were observed in previous studies [7,20]. Fig. 6**(b)** depicts the surface of an SBR-coated aerogel. Fig. 6c) shows the ITZ of aerogel and cementitious materials is moderately improved. The figures suggest that aerogel particles were intact with cementitious materials, but some crack surfaces of aerogel were also visible. The ITZ of non-coated EGA is depicted in Fig. 7(a) and (b). that EGA particles were nicely bonded in the cementitious system. Fig. 7c), d), and e) show that polymer coated EGA has an exceptionally uniform and denser microstructure at the ITZ between cementitious materials and polymer coated EGA. Similarly, improved ITZ of polymer coated aggregates was reported by Vahabi et al. [8]. According to the authors the thickness of polymer-coated light weight aggregates improved by 50–150 μm.

4. Applicability and future prospect

Aerogel-based cementitious composites are gaining popularity due to their unique properties and Shah et al. [38] reported that the number of aerogel-based cement composite studies has significantly increased since 2020. Recently published articles suggested the wider scope of applicability of aerogel cementitious composites. Ghazi Wakili et al. [39] used applied aerogel-based render to a building façade. Similarly, real-time applicability of aerogel-based render was studied by Ibrahim et al. [40] and Stahl et al. [41]. Buratti et al. [42] and Ibrahim et al. [43] reported on the effective thermal insulation properties of aerogel-based mortar used in building envelope. An aerogel-based cement composite having adequate strength and thermal insulation characteristics might also be a useful product. The developed cement composite in this study might be used for flooring and casting walls. Self-compacting lightweight cement composites might be used to improve thermal bridges. In addition, self-compacting properties will enable us to reach the products in congested areas where reaching vibration equipment is difficult. The improved strength and water absorption characteristics of polymer modified concrete will also increase the applicability of the product. According to ACI-213R-03 (2003 and 2014) recommendations, the compressive strength of lightweight concrete $\geq$ 17 MPa can be used as a structural application. In addition, improved water absorption properties of the composite will prevent moisture damage. Aerogel-based cement products have been researched for the past few years. However, most of the research is focused only on the development of aerogel-based products. More studies are required to use such developed materials in real-time building applications. The pre-treated aerogel and lightweight aggregates were observed to be beneficial in improving the characteristics of the cement composite. Unfortunately, there are only limited methods of pre-treatment of aggregates studied, and further detailed studies are required to identify the optimum efficiency products at a low cost. Some studies are required to investigate the long-term behavior of polymer-modified lightweight aggregate concrete.

5. Conclusion

The present study investigates the influence of polymer coatings of EGA and aerogel on the fresh, microstructural, and mechanical properties of lightweight concrete. The fresh properties of the LWSCCC were within the range of EFNARC recommendations. Single layer coatings of polymers on the EGA show improved workability compared to double layer coatings. Paraffin-coated lightweight aggregates possessed greater workability than SBR. The use of polymer coated EGA slightly improves the porosity of the lightweight cementitious composites. Use of single layer SBR and paraffin coatings lowers the total porosity by 1.63% and 2.9%. The water absorption of lightweight cementitious composites is significantly increased by the incorporation of aerogel. Using polymer coated EGA and aerogel reduces water absorption by 22–26%. Paraffin-coated EGA was observed to be more effective than SBR-coated EGA. Microstructural analysis revealed that SBR coated aerogel possessed

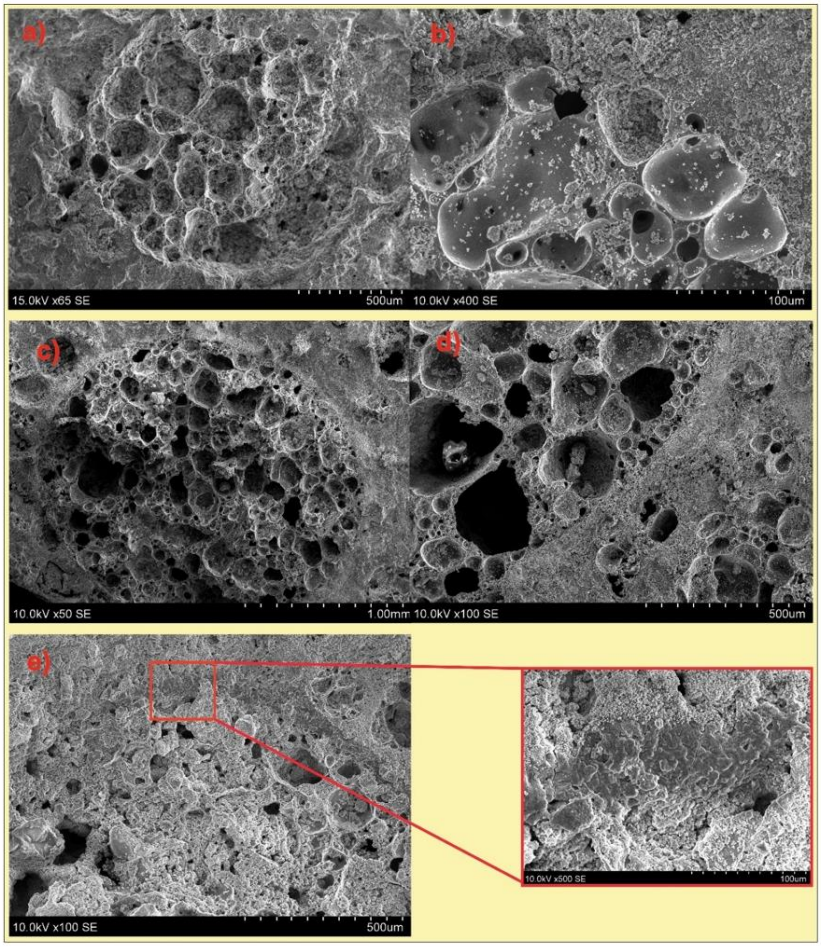

Fig. 7. a) Adhesion of non-coated EGA with cementitious materials, b) ITZ of non-coated EGA, c) adhesion of SBR coated EGA, d) adhesion of Paraffin coated EGA, e) ITZ of polymer coated EGA.

improved adhesion with cementitious materials. On the other hand, SBR and Paraffin coated EGA show uniformly denser ITZ. The compressive strength of the LWSCCC was significantly decreased by the inclusion of aerogel. The use of single layer polymer coated EGA in the aerogel based cementitious composites was observed to be effective in improving the compressive strength by 8.4–15.9%. Paraffin coated EGA possessed a greater improvement in strength over SBR coated EGA.

Declaration of Competing Interest

The authors declare that they have no known competing financial interests or personal relationships that could have appeared to influence the work reported in this paper.

References

[1] B. wan Jo, S. kook Park, J. bin Park, Properties of concrete made with alkali-activated fly ash lightweight aggregate (AFLA), Cem. Concr. Compos. 29 (2007) 128–135, https://doi.org/10.1016/j.cemconcomp.2006.09.004.
[2] S. Real, C. Maia, J.A. Bogas, M. Da Gl ria Gomes, Thermal conductivity modelling of structural lightweight aggregate concrete, Mag. Concr. Res. 73 (2021) 798–809, https://doi.org/10.1680/jmacr.19.00320.
[3] R. Demirboğa, R. Gül, The effects of expanded perlite aggregate, silica fume and fly ash on the thermal conductivity of lightweight concrete, Cem. Concr. Res. 33 (2003) 723–727, https://doi.org/10.1016/S0008-8846(02)01032-3.
[4] T. Cheboub, Y. Senhadji, H. Khelafi, G. Escadeillas, Investigation of the engineering properties of environmentally-friendly self-compacting lightweight mortar containing olive kernel shells as aggregate, J. Clean. Prod. 249 (2020), https://doi.org/10.1016/j.jclepro.2019.119406.
[5] Q.L. Yu, H.J.H. Brouwers, Development of a self-compacting gypsum-based lightweight composite, Cem. Concr. Compos. 34 (2012) 1033–1043, https://doi.org/10.1016/j.cemconcomp.2012.05.004.
[6] H.K. Kim, J.H. Jeon, H.K. Lee, Workability, and mechanical, acoustic and thermal properties of lightweight aggregate concrete with a high volume of entrained air,

Constr. Build. Mater. 29 (2012) 193–200, https://doi.org/10.1016/j.conbuildmat.2011.08.067.
[7] S.K. Adhikary, Ž. Rudžionis, S. Tučkutė, Characterization of novel lightweight self-compacting cement composites with incorporated expanded glass, aerogel, zeolite and fly ash, Case Stud. Constr. Mater. 16 (2022), e00879, https://doi.org/10.1016/j.cscm.2022.e00879.
[8] M. Yashar, V. Behzad, Effect of pre-coating lightweight aggregates on the self-compacting concrete (2021) 1–12. https://doi.org/10.1002/suco.202000744.
[9] L. Domagała, The effect of lightweight aggregate water absorption on the reduction of water-cement ratio in fresh concrete, Procedia Eng. 108 (2015) 206–213, https://doi.org/10.1016/j.proeng.2015.06.139.
[10] E. Güneyisi, M. Gesoglu, O.A. Azez, H.Ö. Öz, Effect of nano silica on the workability of self-compacting concretes having untreated and surface treated lightweight aggregates, Constr. Build. Mater. 115 (2016) 371–380, https://doi.org/10.1016/j.conbuildmat.2016.04.055.
[11] E. Güneyisi, M. Gesoglu, O.A. Azez, H.Ö. Öz, Physico-mechanical properties of self-compacting concrete containing treated cold-bonded fly ash lightweight aggregates and SiO2 nano-particles, Constr. Build. Mater. 101 (2015) 1142–1153, https://doi.org/10.1016/j.conbuildmat.2015.10.117.
[12] J.J. Assaad, A.El Mir, Durability of polymer-modified lightweight flowable concrete made using expanded polystyrene, Constr. Build. Mater. 249 (2020), 118764, https://doi.org/10.1016/j.conbuildmat.2020.118764.
[13] J. Li, H. Xiao, Y. Zhou, Influence of coating recycled aggregate surface with pozzolanic powder on properties of recycled aggregate concrete, Constr. Build. Mater. 23 (2009) 1287–1291, https://doi.org/10.1016/j.conbuildmat.2008.07.019.
[14] A. Bideci, A.H. Gültekin, H. Yildirim, S. Oymael, Ö.S. Bideci, Internal structure examination of lightweight concrete produced with polymer-coated pumice aggregate, Compos. Part B Eng. 54 (2013) 439–447, https://doi.org/10.1016/j.compositesb.2013.06.004.
[15] G. Bumanis, D. Bajare, A. Korjakins, Mechanical and thermal properties of lightweight concrete made from expanded glass, J. Sustain. Archit. Civ. Eng. 2 (2013), https://doi.org/10.5755/j01.sace.2.3.2790.
[16] E. Namsone, G. Sahmenko, E. Namsone, A. Korjakins, Thermal conductivity and frost resistance of foamed concrete with porous aggregate, Vide Tehnol. Resur. Environ. Technol. Resour. 3 (2017) 222–228, https://doi.org/10.17770/etr2017vol3.2625.
[17] J. Šeputytė-Jucikė, M. Sinica, The effect of expanded glass and polystyrene waste on the properties of lightweight aggregate concrete, Eng. Struct. Technol. 8 (2016) 31–40, https://doi.org/10.3846/2029882x.2016.1162671.
[18] S.K. Adhikary, Ž. Rudžionis, S. Tučkutė, D.K. Ashish, Effects of carbon nanotubes on expanded glass and silica aerogel based lightweight concrete, Sci. Rep. 11 (2021) 2104, https://doi.org/10.1038/s41598-021-81665-y.
[19] S.K. Adhikary, Z. Rudzionis, Influence of expanded glass aggregate size, aerogel and binding materials volume on the properties of lightweight concrete, Mater. Today Proc. 32 (2020) 712–718, https://doi.org/10.1016/j.matpr.2020.03.323.
[20] S.K. Adhikary, Ž. Rudžionis, D. Vaičiukynienė, Development of flowable ultra-lightweight concrete using expanded glass aggregate, silica aerogel, and prefabricated plastic bubbles, J. Build. Eng. 31 (2020), 101399, https://doi.org/10.1016/j.jobe.2020.101399.
[21] S.K. Adhikary, D.K. Ashish, Ž. Rudžionis, Expanded glass as light-weight aggregate in concrete – a review, J. Clean. Prod. 313 (2021), https://doi.org/10.1016/j.jclepro.2021.127848.
[22] P. Chakartnarodom, P. Ineure, Foam glass development using glass cullet and fly ash or rice husk ash as the raw materials, Key Eng. Mater. 608 (2014) 73–78, https://doi.org/10.4028/www.scientific.net/KEM.608.73.
[23] M.H.N. Yio, Y. Xiao, R. Ji, M. Russell, C. Cheeseman, Production of foamed glass-ceramics using furnace bottom ash and glass, Ceram. Int. (2020), https://doi.org/10.1016/j.ceramint.2020.11.103.
[24] S.K. Adhikary, D.K. Ashish, Ž. Rudžionis, Aerogel based thermal insulating cementitious composites: a review, Energy Build. (2021), https://doi.org/10.1016/j.enbuild.2021.111058.
[25] S.N. Shah, K.H. Mo, S.P. Yap, M.K.H. Radwan, Effect of micro-sized silica aerogel on the properties of lightweight cement composite, Constr. Build. Mater. 290 (2021), 123229, https://doi.org/10.1016/j.conbuildmat.2021.123229.
[26] S. Kim, J. Seo, J. Cha, S. Kim, Chemical retreating for gel-typed aerogel and insulation performance of cement containing aerogel, Constr. Build. Mater. 40 (2013) 501–505, https://doi.org/10.1016/j.conbuildmat.2012.11.046.
[27] A. Venkateswara Rao, M.M. Kulkarni, D.P. Amalnerkar, T. Seth, Surface chemical modification of silica aerogels using various alkyl-alkoxy/chloro silanes, Appl. Surf. Sci. 206 (2003), https://doi.org/10.1016/S0169-4332(02)01232-1.
[28] G. Ma, R. A, P. Xie, Z. Pan, L. Wang, J.C. Hower, 3D-printable aerogel-incorporated concrete: anisotropy influence on physical, mechanical, and thermal insulation properties, Constr. Build. Mater. 323 (2022), 126551, https://doi.org/10.1016/j.conbuildmat.2022.126551.
[29] J. Rostami, O. Khandel, R. Sedighardekani, A.R. Salneh, S.A. Ghahari, Enhanced workability, durability, and thermal properties of cement-based composites with aerogel and paraffin coated recycled aggregates, J. Clean. Prod. 297 (2021), 126518, https://doi.org/10.1016/j.jclepro.2021.126518.
[30] J. Lu, J. Jiang, Z. Lu, J. Li, Y. Niu, Y. Yang, Pore structure and hardened properties of aerogel/cement composites based on nanosilica and surface modification, Constr. Build. Mater. 245 (2020), 118434, https://doi.org/10.1016/j.conbuildmat.2020.118434.
[31] T. Gao, B.P. Jelle, A. Gustavsen, S. Jacobsen, Aerogel-incorporated concrete: an experimental study, Constr. Build. Mater. 52 (2014) 130–136, https://doi.org/10.1016/j.conbuildmat.2013.10.100.
[32] S. Ng, B.P. Jelle, L.I.C. Sandberg, T. Gao, Ó.H. Wallevik, Experimental investigations of aerogel-incorporated ultra-high performance concrete, Constr. Build. Mater. 77 (2015) 307–316, https://doi.org/10.1016/j.conbuildmat.2014.12.064.
[33] L. Wang, P. Liu, Q. Jing, Y. Liu, W. Wang, Y. Zhang, Z. Li, Strength properties and thermal conductivity of concrete with the addition of expanded perlite filled with aerogel, Constr. Build. Mater. 188 (2018) 747–757, https://doi.org/10.1016/j.conbuildmat.2018.08.054.
[34] H. Li, P. Zang, H. Liu, K. Cao, X. Liao, D. Wei, B. Zhang, H. Li, J. Wang, Preparation and heat insulation of Geminihalloysite aerogel/concrete composites, J. Polym. Eng. 41 (2021) 387–396, https://doi.org/10.1515/polyeng-2020-0317.
[35] V. Akyuncu, F. Sanliturk, Investigation of physical and mechanical properties of mortars produced by polymer coated perlite aggregate, J. Build. Eng. 38 (2021), 102182, https://doi.org/10.1016/j.jobe.2021.102182.
[36] P. Zhu, S. Yu, C. Cheng, S. Zhao, H. Xu, Durability of silica aerogel cementitious composites - freeze-thaw resistance, water resistance and drying shrinkage, Adv. Cem. Res. 32 (2020) 527–536, https://doi.org/10.1680/jadcr.18.00145.
[37] S.P. Zhang, L. Zong, Evaluation of relationship between water absorption and durability of concrete materials, Adv. Mater. Sci. Eng. 2014 (2014), https://doi.org/10.1155/2014/650373.
[38] S.N. Shah, K.H. Mo, S.P. Yap, M.K.H. Radwan, Towards an energy efficient cement composite incorporating silica aerogel: a state of the art review, J. Build. Eng. 44 (2021), 103227, https://doi.org/10.1016/j.jobe.2021.103227.
[39] K. Ghazi Wakili, C. Dworatzyk, M. Sanner, A. Sengespeick, M. Paronen, T. Stahl, Energy efficient retrofit of a prefabricated concrete panel building (Plattenbau) in Berlin by applying an aerogel based rendering to its façades, Energy Build. 165 (2018) 293–300, https://doi.org/10.1016/j.enbuild.2018.01.050.
[40] M. Ibrahim, E. Wurtz, P.H. Biwole, P. Achard, H. Sallee, Hygrothermal performance of exterior walls covered with aerogel-based insulating rendering, Energy Build. 84 (2014), https://doi.org/10.1016/j.enbuild.2014.07.039.
[41] T. Stahl, K. Ghazi Wakili, S. Hartmeier, E. Franov, W. Niederberger, M. Zimmermann, Temperature and moisture evolution beneath an aerogel based rendering applied to a historic building, J. Build. Eng. 12 (2017), https://doi.org/10.1016/j.jobe.2017.05.016.
[42] C. Buratti, E. Moretti, E. Belloni, F. Agosti, Development of innovative aerogel based plasters: preliminary thermal and acoustic performance evaluation, Sustainability 6 (2014), https://doi.org/10.3390/su6095839.
[43] M. Ibrahim, L. Bianco, O. Ibrahim, E. Wurtz, Low-emissivity coating coupled with aerogel-based plaster for walls' internal surface application in buildings: energy saving potential based on thermal comfort assessment, J. Build. Eng. 18 (2018), https://doi.org/10.1016/j.jobe.2018.04.008.

Article 4.

Authors: Suman Kumar Adhikary, Žymantas Rudžionis, Simona Tučkutė, Deepankar Kumar Ashish

Title of article: Effects of carbon nanotubes on expanded glass and silica aerogel based lightweight concrete

Citation: Scientific reports, Volume 11, January 2021, 2104 (2021); https://doi.org/10.1038/s41598-021-81665-y

scientific reports

Check for updates

OPEN

Effects of carbon nanotubes on expanded glass and silica aerogel based lightweight concrete

Suman Kumar Adhikary[1]✉, Žymantas Rudžionis[1], Simona Tučkutė[2] & Deepankar Kumar Ashish[3,4]

This study is aimed to investigate the effect of carbon nanotubes on the properties of lightweight aggregate concrete containing expanded glass and silica aerogel. Combinations of expanded glass (55%) and hydrophobic silica aerogel particles (45%) were used as lightweight aggregates. Carbon nanotubes were sonicated in the water with polycarboxylate superplasticizer by ultrasonication energy for 3 min. Study results show that incorporating multi-wall carbon nanotubes significantly influences the compressive strength and microstructural performance of aerogel based lightweight concrete. The addition of carbon nanotubes gained almost 41% improvement in compressive strength. SEM image of lightweight concrete shows a homogeneous dispersal of carbon nanotubes within the concrete structure. SEM image of the composite shows presence of C–S–H gel surrounding the carbon nanotubes, which confirms the cites of nanotubes for the higher growth of C–S–H gel. Besides, agglomeration of carbon nanotubes and the presence of ettringites was observed in the transition zone between the silica aerogel and cementitious materials. Additionally, flowability, water absorption, microscopy, X-ray powder diffraction, and semi-adiabatic calorimetry results were analyzed in this study.

Nowadays, the use of carbon nanotubes in cementitious materials is getting attention for the improvement of physical and mechanical characteristics. Carbon nanotubes (CNTs) are an allotrope of carbon composed of coaxial hexagonal carbon rings, cylindrical in shape having around 132,000,000:1 length–diameter ratio. The nanoscale diameters and smooth surfaces of CNT's could affect the early age hydration of cementitious materials[1]. Carbon nanotubes can be categorized into single-wall carbon nanotube (SWCNT) and multiwall carbon nanotube (MWCNT). Inclusion of small doses of MWCNT can effectively improve the mechanical properties of cementitious composites improving early age and long-term durability[2]. The reinforcing efficiency of carbon nanotubes can be influenced by several parameters such as type of CNTs[3], the concentration of CNT[4], dispersion surfactants[5], treatment of CNTs[6,7], dispersion technique[8], the interaction with cementitious materials and bond strength[9], the water–cement ratio[10,11] and geometry of CNTs[12,13]. Zou et al.[8] and Collins et al.[10] reported that ultrasonication energy and polycarboxylate-based superplasticizer could significantly influence the mechanical and microstructural properties of CNT incorporated cementitious composites by optimally dispersing the CNTs within a concrete structure[8,10]. Han et al.[14] reported that polycarboxylate-based superplasticizer plays a double dispersion mechanism to disperse the cement and CNTs within the composite. Without proper dispersion technique, agglomeration of CNTs can be noticed in the concrete structure due to the strong van der Waals forces and can influence the mechanical and microstructural properties. The improvement in cementitious composites were found different for cement mortar, cement paste, and concrete. The highest improvement in compressive and flexural strength was observed 83.33%[15] and 30%[16] for cement paste; ~ 35%[3] and 28.04%[17] for mortar; 38.62% and 38.63% for concrete[18], respectively.

The strength development of cementitious composite also depends on the properties of aggregates and what kind of pozzolanic materials were used. With the increase in the consumption of natural aggregates, researchers are mainly focused on conserving the natural eco-system that leads to the use of lightweight aggregates such as expanded glass aggregates, silica aerogel[19]. Silica aerogel is a lightweight thermal insulating material having low density and high specific surface area, allowing its application in many areas[20]. Expanded glass aggregates is

[1]Faculty of Civil Engineering and Architecture, Kaunas University of Technology, 44249 Kaunas, Lithuania. [2]Center for Hydrogen Energy Technologies, Lithuanian Energy Institute, Breslaujos st. 3, 44403 Kaunas, Lithuania. [3]Civil Engineering Department, Maharaja Agrasen Institute of Technology, Maharaja Agrasen University, Baddi 174 103, India. [4]Civil Engineering Department, Punjab Engineering College (Deemed to be University), Chandigarh 160012, India. ✉email: sumankradk9s@gmail.com

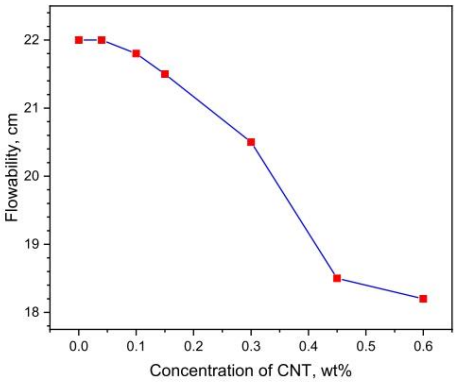

Figure 1. Flowability of sonicated CNT-LWAC specimens.

also a thermal conducting material with porous structure[21]. Lightweight aggregates are 25–35% lighter than the conventionally used aggregates[19]. However, the strength properties of lightweight aggregates are also much lower than the conventional aggregates; due to this fact, cement composites utilizing lightweight aggregates generally achieve lower mechanical properties and densities[22]. Mechanical properties of lightweight aggregate concrete also depend on the desired density of the composite; decreasing the density reduces the mechanical properties of composite[23]. Kurpińska and Ferenc[24,25] investigated the importance of grading of lightweight aggregates. They reported that an optimal graduating of lightweight aggregates could reduce the porosity of lightweight aggregate concrete and improve mechanical performance. Major studies have been presented on the use of lightweight aggregate such as fly ash[26,27], expanded glass aggregate[28], silica aerogel[21] in cement mortar. A study conducted by Yousefi et al.[21] reported a decrease in compressive strength of cement mortar containing expanded glass aggregates, however inclusion of nano titanium dioxide as nanomaterials increased compressive strength by 39.02%.

Similarly, hydrophobic silica aerogel is also a very lightweight and brittle material, and its incorporation in concrete results in a decrease in mechanical performance[29,30]. In addition, hydrophobic silica aerogel has lower adhesive properties with water-rich cementitious materials. Several researchers observed the separation gaps between the aerogel and cementitious materials in the transition zone[20,31]. CNT is a well-known material for improving mechanical performance and cracks bridging mechanism[32]. The incorporation of CNT not only bridges the cracks and voids; it can also change the microstructure of hydration products[33]. Singh et al.[34] identified new compounds due to the chemical bonds between the hydrates and carbon nanotubes. Liew et al.[35], in their study, suggested that CNTs also provide sites for the growth of C–S–H, and CNT can coat the calcium silicate hydrate and provide a larger contact area between the hydration product and CNT. As a result, stronger bonds are created between them, which significantly helps to improve the mechanical properties of cementitious composites[35].

In this study, several lightweight concrete samples were prepared with different doses of CNTs. Expanded glass aggregates and hydrophobic silica aerogel were used as lightweight aggregates. Microscopy of the composite was deeply analyzed, especially surrounding the hydrophobic aerogel particles. The main aim was to improve the strength property of aerogel concrete by reducing the separation gaps between silica aerogel and cementitious materials. This is the first study that presents the use of CNTs to enhance the compressive strength property of lightweight concrete prepared with expanded glass aggregates and hydrophobic silica aerogel. The study also investigates fluidity, water absorption, and microstructural analysis.

Results and discussion

Flowability test of CNT-LWAC. The flowability of cementitious composites containing CNT depends on several parameters like ultrasonication energy[8], treatment of CNTs[36], water-cement ratio[37], the concentration of CNTs[38], and types of fine fillers[39]. Mostly studied literature[10,38,40,41] illustrates that the incorporation of CNTs reduced the flowability of cementitious composites. While there are several studies that indicate the increase in flowability of CNT incorporated cementitious composites[36,39,42]. Besides, the incorporation of silica aerogel also reduces the flowability of cementitious composites[20]. The results of the present study revealed that the flowability of CNT-LWAC was influenced by the quantity of CNT. The flowability of CNT-LWAC decreases with the escalating doses of CNTs. Almost a 17% reduction in flowability was measured for lightweight concrete specimen prepared with 0.6 wt% CNT. The flowability of CNT-LWAC specimens is shown in Fig. 1. The possible reason for the reduction in flowability can be the high surface area and the elongated shape of nanoparticles. Higher doses of superplasticizer can adjust the flowability of the concrete, high specific gravity of CNTs also demands for the large amount of superplasticizer to overcome the intermolecular forces. Besides, nanoparticles enhance the packing density of concrete by filling up the micro and mesopores, significantly influencing the demand for superplasticizer[32].

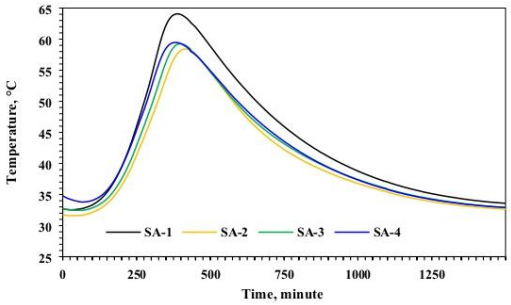

Figure 2. Hydration of cement mortar containing aerogel and sonicated and un-sonicated CNTs.

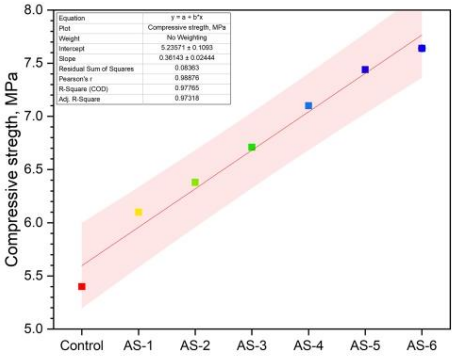

Figure 3. Compressive strength of sonicated CNT-LWAC specimens.

Semi-adiabatic calorimetry test of CNT-LWAC. Figure 2 demonstrates the semi-adiabatic temperature rise of CNT incorporated cement mortar. Study results revealed that the incorporation of silica aerogel slightly retarded the setting time of the cement mortar and produced lower heat of hydration than the plain cement mortar. Study results also confirm the reactivity of silica aerogel with cementitious materials. Similar phenomena were noticed in the previous study[20]. The addition of CNTs to the cement paste having aerogel produced slightly higher heat as indicated in samples SA-3 and SA-4 and shortened setting time compared to sample SA-2. Besides, by increasing the concentration of CNTs, slightly high heat of the exothermic reaction was noticed.

Strength of CNT-LWAC. Figure 3 shows the compressive strength of CNT-LWAC specimens. The average compressive strength of the control sample was measured 5.4 MPa. Study results show that the addition of CNTs to the lightweight concrete significantly influences the mechanical strength of concrete. An increase in the concentration of CNTs showed a gradual increase in the compressive strength; however, the sonicated LWAC specimens showed better improvement in compressive strength against the control concrete sample. The compressive strength of the sonicated concrete specimens was increasing by the increasing doses of CNTs. The highest improvement in compressive strength was measured at 41.48% for AS-6 containing 0.60 wt% CNT. As aerogel is a lightweight, fragile material, the literature confirms the reduction in the mechanical performance of aerogel incorporated cementitious composites[43–45]. However, the incorporation of small doses of CNTs to the aerogel based lightweight concrete significantly increased the compressive strength. The increase in compressive strength can be attributed to the nucleating effects and improvement in the microstructure of CNT-LWAC. The C–S–H gel was identified surrounding the CNTs, moreover, hydration products and CNTs fill the micro crack/gaps of the lightweight concrete to provide additional support and increase compressive strength. Detailed discussion is given in section "*Scanning electronic microscopy (SEM) of CNT-LWAC*". The literature studies confirm that the incorporation of nanoparticles improves the microstructure and provides a denser concrete structure[32]. The confidence intervals for compressive strength are presented in Fig. 3 which shows the example of the straight-line correlation until 0.6% of CNTs use from cement mass. X is the type of CNT-LWAC, and mean compressive strength is given as Y variable values obtained on cubes.

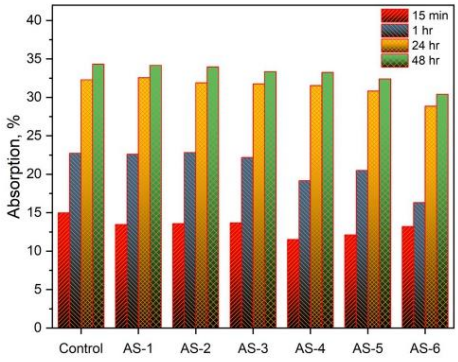

Figure 4. Water absorption of CNT-LWAC specimen.

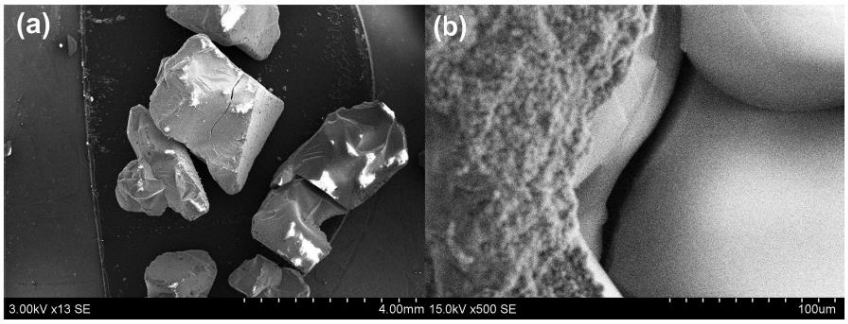

Figure 5. (**a**) Cracks on the surface of native silica aerogel; (**b**) cracks aerogel in the hydrated concrete specimen.

Water absorption. Figure 4 illustrates the water absorption kinetics of the CNT-LWAC specimens containing up to 0.60 wt% CNTs. Water absorption rate of control sample was measured 14.98%, 22.74%, 32.33% and 34.33% at 15 min, 1 h, 24 h and 48 h that decreased to 13.20%, 16.31%, 28.86% and 30.42% respectively. Madhavi et al.[46], and Leonavičius et al.[47] reported that at a lower concentration of CNTs, total pore volume was observed reducing attributed to filling of voids that lead to a reduction in water absorption. According to Leonavičius et al.[47] and Kordkheili et al.[48] high concentration of CNTs in concrete results in a more porous structure and reduces the mechanical performance of concrete[47,48]. In the present study, all nanocomposite concrete specimens showed a marginal decrease in water absorption rate by an increase in the concentration of CNTs. The reduction in water absorption can be attributed to the association of CNTs with the lightweight concrete that helped in decreasing the micropores and produced the denser concrete structure. Besides, a comparatively higher water absorption rate was observed than Leonavičius et al.[47] and Kordkheili et al.[48] due to the use of expanded glass aggregates in the study. Expanded glass aggregates are porous in structure that can absorb water up to 20–25%, attributed to an increase in water absorption.

Scanning electronic microscopy (SEM) of CNT-LWAC. The plain image of hydrophobic silica aerogel in Fig. 5a suggested that it is a very brittle material with cracks on the surface that can easily break into pieces during the mixing process and lead to lower mechanical properties. Moreover, in Fig. 5b, the cracked surface of aerogel particles in the hydrated concrete specimens can be clearly noticed. Literatures[20,49,50] also indicate the brittleness of aerogel and a decrease in the mechanical performances with the incorporation of aerogel.

Due to the hydrophobic nature of silica aerogel, it do not develop chemical bonds with the hydrophilic cement matrix. Figure 6a clearly shows the separation gaps between aerogel and surrounding cementitious material in the transition zone of the control sample. This phenomenon indicates the lower adhesion properties of hydrophobic silica aerogel. Similar separation gaps were identified by Gao et al.[31] and Adhikary et al.[20]. While better adhesion was observed for expanded glass aggregates with cementitious materials, as indicated in Fig. 6b. Through the

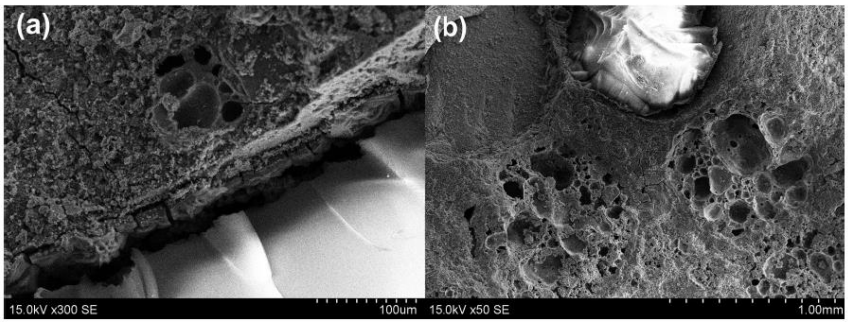

Figure 6. (**a**) Separation gaps between aerogel and cementitious material in the transition zone, (**b**) good adhesion of expanded glass aggregates with cementitious material.

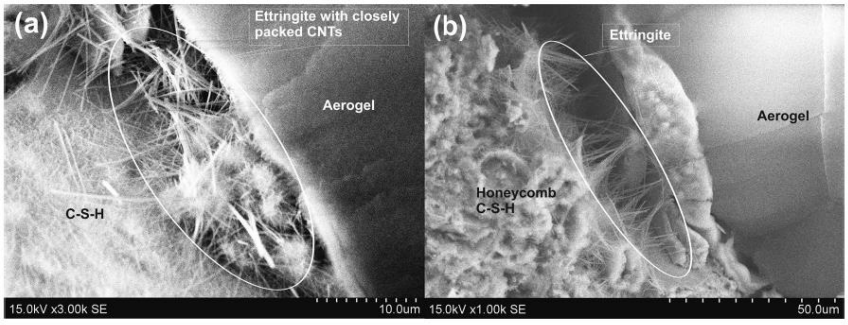

Figure 7. Agglomeration of CNTs and presence of ettringite and honeycomb structure of C–S–H gel in the transition zone of aerogel and cementitious material.

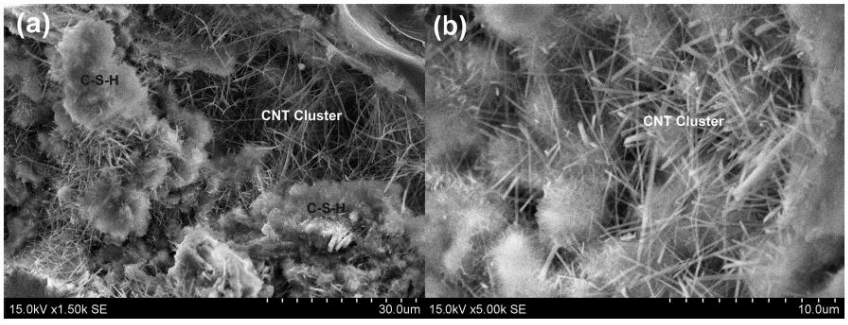

Figure 8. The well-dispersed concrete sample under high concentration of CNT at different magnification; the presence of C–S–H gel surrounding to the CNTs.

separation gaps, air and/or water can easily transport and makes concrete weaker. Interestingly the separation gaps were reduced by utilizing carbon nanotubes as indicated in Fig. 7. Separation gaps between hydrophobic silica aerogel and surrounding cement-based materials were filled by hydration products and CNTs.

SEM image of CNT-LWAC, as shown in Fig. 8 indicates that the CNTs were almost dispersed uniformly within the concrete structure. At the high concentration of CNTs, a network-like distribution within the composite

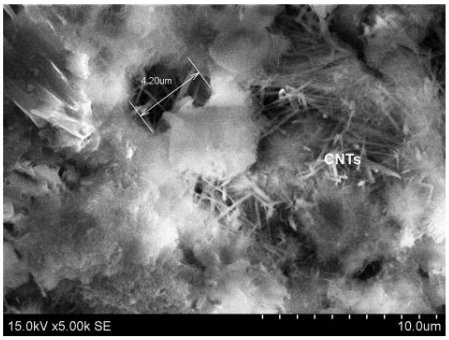

Figure 9. CNTs filling the micropores of the lightweight concrete structure.

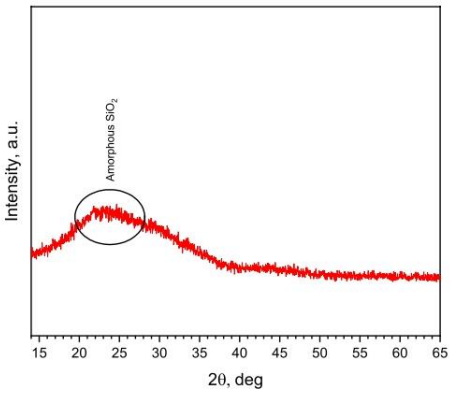

Figure 10. X-ray diffraction pattern of expanded glass aggregates.

structure was noticed. Zou et al.[8], Vesmawala et al.[5], and Collins et al.[10] also reported that CNTs could be effectively dispersed within the concrete structure by ultrasonication energy and polycarboxylate superplasticizer, may be due to this fact high agglomeration of CNTs was not noticed. Unlikely in the present study, the needle-like structure of ettringite was observed along with the agglomeration of CNTs in the transition zone of aerogel, as shown in Fig. 7. However, increasing the duration of ultrasonication and concentration of superplasticizer can effectively help to improve the dispersion of CNTs without agglomeration. Moreover, CNTs were found to reinforce the concrete structure's micropores, as indicated in Fig. 9.

Zhu et al.[45] suggested that due to the hydration process of cementitious materials, aerogel particles can slightly react with the pore solution and get partially dissolved in an alkaline environment to form C–S–H with a low Ca/Si ratio. de Fátima Júlio et al.[51] and Hai-li et al.[52] reported that aerogel particles could promote hydration due to high surface activity that leads to ASR, and Si–O–Si might form C–S–H. Incorporation of CNTs to the cement composite also provides sites for the formation of calcium silicate hydrate (C–S–H) by acting as a nucleating agent[53,54]. The honeycomb structure of C–S–H gel and its presence near to the CNTs can easily be observed in Figs. 7a and 8b, which illustrates the nucleating effects of CNTs.

X-ray diffraction analysis of CNT-LWAC. Figures 10, 11, and 12 show the X-ray diffraction analysis of expanded glass aggregates, silica aerogel, and LWAC specimens (control, AS-1, AS-3, and AS-6), respectively. X-ray diffraction pattern of silica aerogel reveals the amorphous nature of silica aerogel and expanded glass aggregates. In Figs. 10 and 11, a hump was observed for the amorphous matrix of SiO_2 at around $2\theta = 22$ and 23 °C for silica aerogel and expanded glass aggregates, respectively. In Fig. 12, CNT-LWAC concrete specimen illustrates that the intensity of portlandite near about 34° and 47° increases with the increasing concentration

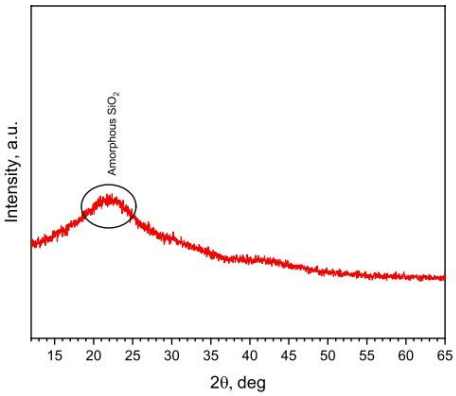

Figure 11. X-ray diffraction pattern of silica aerogel.

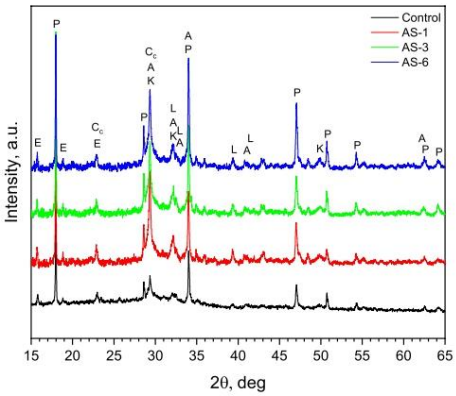

Figure 12. X-ray diffraction pattern of sonicated CNT-LWAC specimens. A—alite $Ca_{54}MgAl_2Si_{16}O_{90}$ (13–272); E—ettringite $Ca_6Al_2(SO_4)_3(OH)_{12}{\cdot}26H_2O$ (41–1451); L—Ca_2SiO_4 belite (33–302); K—$Ca_{1.5}Si\,O_{3.5}{\cdot}\times\,H_2O$ calcium silicate hydrate (33–306), Cc—$Ca(CO)_3$ calcite (24–27); P—$Ca(OH)_2$ portlandite (1–837).

of CNT. The increasing peak of calcium silicate hydrate near 29°, 32°, and 50° explained the nucleation effects of carbon nanotubes. Moreover, CNT-LWAC shows a slightly higher amount of calcite and ettringite than the control specimen. However, a higher amount of hydration products was observed for CNT incorporated LWAC specimens. A higher concentration of CNTs within the concrete structure leads to higher growth of hydration products. A similar increasing peak of hydration products by incorporating CNT in the cementitious composite was identified by El-Gamal et al.[55].

Materials and methods

Materials used in CNT-LWAC. For the preparation of lightweight concrete specimens, ordinary Portland cement (OPC) of grade CEM I 42.4R was used as binding materials according to EN 197-1:2011[56] standard, and 50 µm size (average particle size) zeolite powder was used as a pozzolanic additive. A total of 500 kg/m^3 binding materials was used to prepare lightweight concrete samples, where 90% volume consists of cement and 10% consists of zeolite. The chemical composition of cement and zeolite are shown in Table 1. The standard EN 13055-1:2002/AC:2004[57] was followed for the combinations of four different sizes of expanded glass aggregates, and 1–2 mm size irregular shaped hydrophobic silica aerogel particles with bulk density 70 kg/m^3 holding the approval No. Z-3.212-1948 from the DIBt—German Institute of Construction Technology were used as lightweight aggregates. The concrete specimens were prepared with 45% volume of total aggregates of silica

Chemical composition	CaO	SiO_2	Al_2O_3	Fe_2O_3	MgO	K_2O	Na_2O	Na_2O eq	SO_3	CI	TiO_2	LOI	Insoluble residue	Free Lime	Lime stone
OPC	63	20.4	4.1	3.5	2.9	0.7	0.23	0.74	3.2	0.03	–	2.5	0.5	1.2	3.9
Zeolite	2.8	58.7	9.0	1.4	0.7	2.6	–	–	0.1		0.2	5.1	–	–	–

Table 1. Chemical properties of OPC and zeolite.

Designation	Standard	Expanded glass aggregate size			
		0.1–0.3 mm	0.25–0.50 mm	0.5–1 mm	1–2 mm
Bulk density in kg/m^3	EN 1097–3	400	340	270	230
Compressive strength (± 15%)	EN 13055-1, A annex	2.8	2.5	2.3	2
Thermal conductivity in W/(m–k) (± 0.02)	EN 12939:2002	0.0767	0.0767	0.0713	0.0663
WATER absorption % by mass (absorption % after 24 h submerged in water)	EN 1097-6:2002, C annex	25	25	20	20
Specific density		2.3	2.3	2.3	2.3
pH value		9–11			
Softening point		~ 700 °C/1300 °F			
Color		Cream white			

Table 2. Physical properties of expanded glass aggregates.

Material type	Appearance	Purity	Inner diameter	Outer diameter	Length	Specific surface area	Density	Actual density	Resistivity	Preparation method
MWCNT	Black powder	> 95 wt%	3–5 nm	8–15 nm	3–12 μm	> 233 m^2/g	0.15 g/cm^3	2.1 g/cm^3	1412 μΩm	CVD

Table 3. Properties of multiwalled carbon nanotubes (MWCNTs).

aerogel having 70 kg/m^3 bulk density while the rest of 55% of aggregate contains a combination of 1–2 mm, 0.5–1 mm, 0.25–0.50 mm, and 0.1–0.3 mm size expanded glass aggregates. The physical properties of expanded glass aggregates are shown in Table 2. Polycarboxylate ether polymer-based superplasticizer (1.8% of cement mass) and stabilizer (0.3% of cement mass) were used as chemical admixtures. Powder-type MWCNT supplied by Advanced 2D Materials Co. Ltd. was used in the study. The MWCNT was black in color with an inner diameter of 3–5 nm and the outer diameter of 8–15 nm; and lengths of 3–12 μm. The specific surface area was higher than 233 m^2/g, and density was approximately 0.15 g/cm^3. Resistivity was observed at 1412 μΩm. MWCNT was synthesized by the chemical vapor deposition (CVD) technique. Multiwall-carbon nanotubes (MWCNTs) were used as nanofibers to enhance the mechanical performance of the lightweight aggregate concrete. The properties of MWCNTs are shown in Table 3.

Dispersion of CNTs and specimen preparation. The dispersion of carbon nanotubes in the cement matrix is more challenging than in the conventional concrete mixture. Due to the reliable van der Waals forces between carbon nanotubes, it is necessary to maintain the separation of aggregated carbon nanotube bundles to protect cement composites from defects. In this study, carbon nanotubes were sonicated separately in water by ultrasonication energy (in 40% of total water content) with polycarboxylate based superplasticizer for 3 min. Ultrasonic treatment was carried out by Bandelin Electronic ultrasonic converter UW 3400 of 200 W power and 20 kHz frequency. After mixing lightweight concrete composition with 60% total water, sonicated carbon nanotubes liquid was added to the concrete mixture and manually mixed for another 5 min. After the final mixing process, the flowability test was carried out, and concrete samples were molded into 16 × 4 × 4 cm size prisms and kept at room temperature for 24 h for the hardening process. After the setting process, concrete samples were demolded and kept immersed in water until the 28th day of the hydration process in the climatic chamber, having more than 95% RH and 20 ± 1 °C temperature. The mixing composition of the lightweight concrete samples is shown in Table 4.

Methods. The flowability of the CNT-LWAC was performed by flow table test satisfying EN 12350-5:2009[58] standard requirements. For each type of concrete specimen, three times a flow table test was performed, and the mean value was taken as a result.

Compressive strength of CNT-LWAC was measured on the 28th day of the curing process, satisfying BS EN 196-1:2016[59] standard requirements. The mean value of three specimens was taken as a result of each type of concrete sample.

Series	Cement, kg	Aerogel, kg	CNT%	CNT, kg	Aggregate (1/2 + 1/0.5 + 0.5/0.25 + 0.01/0.3), kg	Zeolite, kg	Superplasticizer, kg	Stabilizer, kg	Water w/b = 0.65	Sonication time (min)
Control	454.5	31.5	0	–	34.5 + 54 + 34 + 40	45.45	8.181	1.3635	325	–
AS-1	454.5	31.5	0.04	0.1818	34.5 + 54 + 34 + 40	45.45	8.181	1.3635	325	3
AS-2	454.5	31.5	0.10	0.4544	34.5 + 54 + 34 + 40	45.45	8.181	1.3635	325	3
AS-3	454.5	31.5	0.15	0.6816	34.5 + 54 + 34 + 40	45.45	8.181	1.3635	325	3
AS-4	454.5	31.5	0.30	1.3632	34.5 + 54 + 34 + 40	45.45	8.181	1.3635	325	3
AS-5	454.5	31.5	0.45	2.0453	34.5 + 54 + 34 + 40	45.45	8.181	1.3635	325	3
AS-6	454.5	31.5	0.60	2.7264	34.5 + 54 + 34 + 40	45.45	8.181	1.3635	325	3

Table 4. Mixing composition of lightweight concrete samples, materials for 1 m^3 of concrete.

Sample	Cement (g)	CNT (g)	Water (g)	Aerogel (g)
SA-1	100	–	35	
SA-2	100	–	35	31.5
SA-3	100	0.04	35	31.5
SA-4	100	0.15	35	31.5

Table 5. Mixing composition of CNT-cement paste for the semi-adiabatic calorimetry test.

Water absorption kinetics observation of the lightweight aggregate concrete specimens reveals the increase in water absorption rate on the 28th day of hydration. LWAC specimens were oven-dried at 105 °C after the 28 days of hydration and immersed in water for 15 min, 1 h, 24 h, and 48 h to observe water absorption in the LWAC specimens.

To perform a semi-adiabatic calorimetry test, several mortar samples were prepared with cement and aerogel containing different concentrations of CNTs. CNTs were sonicated in water for 3 min before mixing with the cement. Table 5 shows the mixing composition of cement paste.

Scanning electronic microscopy of CNT-LWAC was analyzed by a high-resolution electronic microscope FEI Quanta 200 FEG with Schottky field emission gun (FEG), an energy-dispersive X-ray spectrometer (EDS) with a silicon type drift droplet detector.

The X-ray diffraction analysis of the composite specimens was performed with X-ray diffractometer DRON-6 with Bragg–Brentano geometry using Ni-filtered Cu Kα radiation and graphite monochromator, operating with the voltage of 30 kV and emission current of 20 mA. The step-scan was performed from the angular range 2°–70° (2θ), and each step of 2θ was 0.02°.

Conclusion

Study results analyses the viability of using MWCNTs to improve the compressive strength of lightweight aggregate concrete prepared by silica aerogel and expanded glass aggregates. The following conclusions can be drawn based on the obtained results.

- The flowability of CNTLWAC was decreased by increasing the concentration of CNTs. At 0.6 wt% of CNT loading, an almost 17% reduction in flowability was measured for the lightweight concrete specimen.
- The utilization of CNTs significantly improved the compressive strength of the aerogel added lightweight concrete. Almost 41% improvement in the strength of lightweight concrete was observed at 0.6 wt% CNTs loading.
- The dispersion technique of CNTs by sonication with water and polycarboxylate based superplasticizer worked almost effectively to disperse the CNTs within the concrete structure. However, some agglomerations were identified in the transition zone of aerogel.
- CNTs were found to promote the growth of C–S–H, portlandite, and calcite. The study revealed the presence of more hydration products surrounding the CNTs.
- Separation gaps were identified in the transition zone between the hydrophobic silica aerogel and cementitious materials for the control specimen. The utilization of CNTs effectively helped to reduce the separation gaps by filling the voids and gaps. Moreover, the nucleating effects of CNTs were noticed; separations gaps and voids were not only filled by CNTs, but hydration products were also found in the gaps.

Received: 18 November 2020; Accepted: 11 January 2021
Published online: 22 January 2021

References

1. Makar, J. M., Margeson, J. C. & Luh, J. Carbon nanotube/cement composites—early results and potential applications. In *3rd International Conference on Construction Materials: Performance, Innovation and Structural Implications [Proceedings]* 1–10 (2005).
2. Konsta-Gdoutos, M. S., Metaxa, Z. S. & Shah, S. P. Multi-scale mechanical and fracture characteristics and early-age strain capacity of high performance carbon nanotube/cement nanocomposites. *Cem. Concr. Compos.* **32**, 110–115 (2010).
3. Ruan, Y., Han, B., Yu, X., Zhang, W. & Wang, D. Carbon nanotubes reinforced reactive powder concrete. *Compos. Part A Appl. Sci. Manuf.* **112**, 371–382 (2018).
4. Zhan, M., Pan, G., Zhou, F., Mi, R. & Shah, S. P. In situ-grown carbon nanotubes enhanced cement-based materials with multi-functionality. *Cem. Concr. Compos.* **108**, 103518 (2020).
5. Vesmawala, G. R., Vaghela, A. R., Yadav, K. D. & Patil, Y. Effectiveness of polycarboxylate as a dispersant of carbon nanotubes in concrete. *Mater. Today Proc.* **28**, 1170–1174 (2020).
6. Li, G. Y., Wang, P. M. & Zhao, X. Mechanical behavior and microstructure of cement composites incorporating surface-treated multi-walled carbon nanotubes. *Carbon N. Y.* **43**, 1239–1245 (2005).
7. Kang, S.-T., Seo, J.-Y. & Park, S.-H. The characteristics of CNT/cement composites with acid-Treated MWCNTs. *Adv. Mater. Sci. Eng.* **2015**, 308725 (2015).
8. Zou, B. *et al.* Effect of ultrasonication energy on engineering properties of carbon nanotube reinforced cement pastes. *Carbon N. Y.* **85**, 212–220 (2015).
9. Yazdanbakhsh, A., Grasley, Z. C., Tyson, B. & Al-Rub, R. K. A. Carbon nano filaments in cementitious materials: Some issues on dispersion and interfacial bond. *ACI Symp. Publ.* **267**, 21–34 (2009).
10. Collins, F., Lambert, J. & Duan, W. H. The influences of admixtures on the dispersion, workability, and strength of carbon nanotube–OPC paste mixtures. *Cem. Concr. Compos.* **34**, 201–207 (2012).
11. Yazdani, N. & Mohanam, V. Carbon nano-tube and nano-fiber in cement mortar: Effect of dosage rate and water–cement ratio. *Int. J. Mater. Sci.* **4**, 45–52 (2014).
12. Mohsen, M. O. *et al.* Effect of nanotube geometry on the strength and dispersion of CNT-cement composites. *J. Nanomater.* **2017**, 6927416 (2017).
13. Manzur, T., Yazdani, N. & Emon, M. A. B. Effect of carbon nanotube size on compressive strengths of nanotube reinforced cementitious composites. *J. Mater.* **2014**, 960984 (2014).
14. Han, B., Zhang, K., Yu, X., Kwon, E. & Ou, J. Fabrication of piezoresistive CNT/CNF cementitious composites with superplasticizer as dispersant. *J. Mater. Civ. Eng.* **24**, 658–665 (2012).
15. Nasibulina, L. I. *et al.* Effect of carbon nanotube aqueous dispersion quality on mechanical properties of cement composite. *J. Nanomater.* **2012**, 169262 (2012).
16. Xu, S., Liu, J. & Li, Q. Mechanical properties and microstructure of multi-walled carbon nanotube-reinforced cement paste. *Constr. Build. Mater.* **76**, 16–23 (2015).
17. Irshidat, M. R., Al-Nuaimi, N., Salim, S. & Rabie, M. Carbon nanotubes dosage optimization for strength enhancement of cementitious composites. *Proced. Manuf.* **44**, 366–370 (2020).
18. Barodawala, Q. I., Shah, S. G. & Shah, S. G. Modifying the strength and durability of self compacting concrete using carbon nanotubes. In *UKIERI Concrete Congress-Concrete: The Global Builder* (ed. Singh, S. P.) (UKIERI Concrete Congress, 2019).
19. Palanisamy, M. *et al.* Permeability properties of lightweight self-consolidating concrete made with coconut shell aggregate. *J. Mater. Res. Technol.* **9**, 3547–3557 (2020).
20. Adhikary, S. K., Rudžionis, Ž. & Vaičiukynienė, D. Development of flowable ultra-lightweight concrete using expanded glass aggregate, silica aerogel, and prefabricated plastic bubbles. *J. Build. Eng.* **31**, 20 (2020).
21. Yousefi, A., Tang, W., Khavarian, M., Fang, C. & Wang, S. Thermal and mechanical properties of cement mortar composite containing recycled expanded glass aggregate and nano titanium dioxide. *Appl. Sci.* **10**, 20 (2020).
22. Nahhab, A. H. & Ketab, A. K. Influence of content and maximum size of light expanded clay aggregate on the fresh, strength, and durability properties of self-compacting lightweight concrete reinforced with micro steel fibers. *Constr. Build. Mater.* **233**, 117922 (2020).
23. Chung, S.-Y. *et al.* Comparison of lightweight aggregate and foamed concrete with the same density level using image-based characterizations. *Constr. Build. Mater.* **211**, 988–999 (2019).
24. Kurpińska, M. & Ferenc, T. Effect of porosity on physical properties of lightweight cement composite with foamed glass aggregate. *ITM Web Conf.* **15**, 06005 (2017).
25. Kurpińska, M. & Ferenc, T. Experimental and numerical investigation of mechanical properties of lightweight concretes (LWCs) with various aggregates. *Materials (Basel)* **13**, 3474 (2020).
26. Ashish, D. K. & Verma, S. K. Cementing efficiency of flash and rotary calcined metakaolin in concrete. *J. Mater. Civ. Eng.* **31**, 4019307 (2019).
27. Ashish, D. K. & Verma, S. K. Determination of optimum mixture design method for self-compacting concrete: Validation of method with experimental results. *Constr. Build. Mater.* **217**, 664–678 (2019).
28. Mehta, A. & Ashish, D. K. Silica fume and waste glass in cement concrete production: A review. *J. Build. Eng.* https://doi.org/10.1016/j.jobe.2019.100888 (2019).
29. Wang, Y. *et al.* Experimental investigation on thermal conductivity of aerogel-incorporated concrete under various hygrothermal environment. *Energy* **188**, 115999 (2019).
30. Zhu, P., Yu, S., Cheng, C., Zhao, S. & Xu, H. Durability of silica aerogel cementitious composites—freeze–thaw resistance, water resistance and drying shrinkage. *Adv. Cem. Res.* **32**, 527–536 (2020).
31. Gao, T., Jelle, B. P., Gustavsen, A. & Jacobsen, S. Aerogel-incorporated concrete: An experimental study. *Constr. Build. Mater.* **52**, 20 (2014).
32. Farooq, F. *et al.* Experimental investigation of hybrid carbon nanotubes and graphite nanoplatelets on rheology, shrinkage, mechanical, and microstructure of SCCM. *Materials* **13**, 230 (2020).
33. Shi, T., Li, Z., Guo, J., Gong, H. & Gu, C. Research progress on CNTs/CNFs-modified cement-based composites—a review. *Constr. Build. Mater.* **202**, 290–307 (2019).
34. Singh, A. P. *et al.* Multiwalled carbon nanotube/cement composites with exceptional electromagnetic interference shielding properties. *Carbon N. Y.* **56**, 86–96 (2013).
35. Liew, K. M., Kai, M. F. & Zhang, L. W. Carbon nanotube reinforced cementitious composites: An overview. *Compos. Part A Appl. Sci. Manuf.* **91**, 301–323 (2016).
36. Hawreen, A. & Bogas, J. A. Creep, shrinkage and mechanical properties of concrete reinforced with different types of carbon nanotubes. *Constr. Build. Mater.* **198**, 70–81 (2019).
37. Kim, H. K., Park, I. S. & Lee, H. K. Improved piezoresistive sensitivity and stability of CNT/cement mortar composites with low water–binder ratio. *Compos. Struct.* **116**, 713–719 (2014).
38. Naeem, F., Lee, H. K., Kim, H. K. & Nam, I. W. Flexural stress and crack sensing capabilities of MWNT/cement composites. *Compos. Struct.* **175**, 86–100 (2017).
39. Aydın, A. C., Nasl, V. J. & Kotan, T. The synergic influence of nano-silica and carbon nano tube on self-compacting concrete. *J. Build. Eng.* **20**, 467–475 (2018).

40. Ha, S.-J. & Kang, S.-T. Flowability and strength of cement composites with different dosages of multi-walled CNTs. *J. Korea Concr. Inst.* **28**, 67–74 (2016).
41. Parveen, S., Rana, S., Fangueiro, R. & Paiva, M. C. Microstructure and mechanical properties of carbon nanotube reinforced cementitious composites developed using a novel dispersion technique. *Cem. Concr. Res.* **73**, 215–227 (2015).
42. MacLeod, A. J. N. *et al.* Enhancing fresh properties and strength of concrete with a pre-dispersed carbon nanotube liquid admixture. *Constr. Build. Mater.* **247**, 118524 (2020).
43. Li, P. *et al.* Preparation and optimization of ultra-light and thermal insulative aerogel foam concrete. *Constr. Build. Mater.* **205**, 20 (2019).
44. Abbas, N., Khalid, H. R., Ban, G., Kim, H. T. & Lee, H. K. Silica aerogel derived from rice husk: An aggregate replacer for lightweight and thermally insulating cement-based composites. *Constr. Build. Mater.* **195**, 20 (2019).
45. Zhu, P. *et al.* Study of physical properties and microstructure of aerogel-cement mortars for improving the fire safety of high-performance concrete linings in tunnels. *Cem. Concr. Compos.* **104**, 20 (2019).
46. Madhavi, T. C., Pavithra, P., Singh, S. B., Raj, S. B. V. & Paul, S. Effect of multiwalled carbon nanotubes on mechanical properties of concrete. *Int. J. Sci. Res.* **2**, 166–168 (2013).
47. Leonavičius, D. *et al.* The effect of multi-walled carbon nanotubes on the rheological properties and hydration process of cement pastes. *Constr. Build. Mater.* **189**, 947–954 (2018).
48. Kordkheili, H. Y., Hiziroglu, S. & Farsi, M. Some of the physical and mechanical properties of cement composites manufactured from carbon nanotubes and bagasse fiber. *Mater. Des.* **33**, 395–398 (2012).
49. Westgate, P., Paine, K. & Ball, R. J. Physical and mechanical properties of plasters incorporating aerogel granules and polypropylene monofilament fibres. *Constr. Build. Mater.* **158**, 20 (2018).
50. Liu, Z., Wang, F. & Deng, Z. Thermal insulation material based on SiO_2 aerogel. *Constr. Build. Mater.* **122**, 548–555 (2016).
51. de Fátima Júlio, M., Ilharco, L. M., Soares, A., Flores-Colen, I. & de Brito, J. Silica-based aerogels as aggregates for cement-based thermal renders. *Cem. Concr. Compos.* **72**, 20 (2016).
52. Hai-li, C., Fei-hua, Y., Yi, W. & Li-wei, H. Influence on the performances of foamed concrete by silica aerogels. *Am. J. Civ. Eng.* **3**, 183–188 (2015).
53. Makar, J. M. & Chan, G. W. Growth of cement hydration products on single-walled carbon nanotubes. *J. Am. Ceram. Soc.* **92**, 1303–1310 (2009).
54. Guan, X., Bai, S., Li, H. & Ou, J. Mechanical properties and microstructure of multi-walled carbon nanotube-reinforced cementitious composites under the early-age freezing conditions. *Constr. Build. Mater.* **233**, 117317 (2020).
55. El-Gamal, S. M. A., Hashem, F. S. & Amin, M. S. Influence of carbon nanotubes, nanosilica and nanometakaolin on some morphological-mechanical properties of oil well cement pastes subjected to elevated water curing temperature and regular room air curing temperature. *Constr. Build. Mater.* **146**, 531–546 (2017).
56. BS EN 197-1:2011. *Cement—Part 1: Composition, Specifications and Conformity Criteria for Common Cements*. http://106.38.59.21:8080/userfiles/d46365fdde004ea0a5da5d9701142815/files/teckSolution/2019/10/EN197-1-2011_3750.pdf (2011).
57. EN 13055-1:2002/AC:2004. *Lightweight Aggregates. Lightweight Aggregates for Concrete, Mortar and Grout*. (2004).
58. EN DIN 12350-5:2009. *Testing Fresh Concrete—Part 5. Flow Table Test*. (2009).
59. BS EN 196-1:2016. *Methods of Testing Cement. Determination of Strength*. (2016).

Author contributions

S.K.A. and Ž.R. designed, coordinated this research, carried out experiments and data analysis and finally prepared a draft the manuscript. S.T. participated in research coordination of the study. D.K.A. finalized and critically revised the manuscript as well as contributed to the final approval of the article. The authors read and approved the final manuscript.

Funding

This work is financially supported by the Grant of Kaunas University of Technology, Kaunas, Lithuania.

Competing interests

The authors declare no competing interests.

Additional information

Correspondence and requests for materials should be addressed to S.K.A.

Reprints and permissions information is available at www.nature.com/reprints.

Publisher's note Springer Nature remains neutral with regard to jurisdictional claims in published maps and institutional affiliations.

Article 5.

Authors: Suman Kumar Adhikary, Žymantas Rudžionis, Simona Tučkutė

Title of article: Characterization of aerogel and EGA-based lightweight cementitious composites incorporating different thickness of graphene platelets

Citation: Journal of Building Engineering, Volume 57, October 2022, 104870; https://doi.org/10.1016/j.jobe.2022.104870

Journal of Building Engineering 57 (2022) 104870

Contents lists available at ScienceDirect

Journal of Building Engineering

journal homepage: www.elsevier.com/locate/jobe

Characterization of aerogel and EGA-based lightweight cementitious composites incorporating different thickness of graphene platelets

Suman Kumar Adhikary [a,*], Žymantas Rudžionis [a], Simona Tučkutė [b]

[a] Faculty of Civil Engineering and Architecture, Kaunas University of Technology, Kaunas, LT, 44249, Lithuania
[b] Center for Hydrogen Energy Technologies, Lithuanian Energy Institute, Breslaujos st. 3, 44403, Kaunas, Lithuania

ARTICLE INFO

Keywords:
Graphene nanoplatelets
Microstructure
Water absorption
Cementitious composite
Aerogel
Lightweight cement composite

ABSTRACT

The use of nanomaterials in cement composites isn't new in concrete research. Due to the refined microstructure and extraordinary mechanical characteristics, fabrication of graphene nanoplatelets (GNP) is gaining popularity. However, the impact of the thickness of GNP on the characteristics of lightweight cement composite hasn't been completely studied yet. In this experimental study, 2 nm, 6–8 nm, and 11–15 nm GNP were incorporated into the aerogel and expanded glass-based lightweight cementitious composite at a concentration of 0.025, 0.05, 0.1%, 0.25%, and 0.5%, respectively. Workability, semi-adiabatic calorimetry, compressive and flexural strength, water absorption, microscopy, and XRD analysis of the cement composite were carefully studied. Study results reveal that the thickness of GNP has a notable impact on cement hydration. Incorporation of GNP almost improved the compressive and flexural strength by 43.8% and 41.8%, respectively. Water absorption and microstructure analysis suggest that GNP improves the ITZ of aerogel and densifies the microstructure of the cement composite.

1. Introduction

Graphene is widely considered to be the strongest material yet discovered by humans. The unique properties of graphene may be harnessed by integrating it into composite materials [1,2]. For future references, the fabrication of graphene into concrete might enable the higher toughness, mechanical performance, and durability of the material. The nanomodification of cement composites will undoubtedly have a major impact on construction materials and the construction field. Recently published, several articles demonstrate the promising benefits of graphene-incorporated cementitious composites [2–6]. However, research into graphene nanoplatelet reinforced cementitious composites is just getting started.

Graphene is a new generation of functional fillers for cement-based systems, which is a single-layer hexagonal plane carbon. Du and co-workers [3,7] introduced GNP in cement mortar and reported improved chloride ingress and water absorption characteristics. Wang et al. [8] observed that inclusion of 0.5% GNP in a cement composite might enhance the compressive (C_S) and flexural strength (F_S) by 24% and 8%, respectively. Similarly, Ranjbar et al. [9] reported that incorporation of GNP in geopolymer concrete might enable improvement of the C_S and F_S by 1.44 and 2.16 times, respectively. A study by Peyvandi et al. [10] stated that GNP has greater chemical interactions with the cementitious system and has the ability to transfer the stress. Similarly, Jiang et al. [11] used graphene in cement composites and reported that composites containing more than 5% GNP exhibited improved piezoresistive behaviour.

* Corresponding author.
E-mail address: sumankradk9s@gmail.com (S.K. Adhikary).

https://doi.org/10.1016/j.jobe.2022.104870
Received 18 March 2022; Received in revised form 30 May 2022; Accepted 22 June 2022
Available online 25 June 2022

Table 1
Physical properties of EGA.

EGA Size, mm	Bulk density, kg/m^3	Compressive strength, MPa	Water absorption, %	Thermal conductivity, W/(m-K)	pH value	Softening point	Colour
0.1–0.3	400	4	18	–	9–11	Approx. 700°C	Cream white
0.25–0.5	340	2.5	20	0.0767			
0.5–1	270	1.7	18	0.0713			
1–2	230	2.0	18	0.0663			
2–4	200	1.4	15	0.0639			
4–8	190	1.2	10	0.0661			

The literature studies suggest that GNP is a promising material and has several beneficial aspects. However, the impact of the thickness of GNP on the cementitious system isn't completely understood yet. Besides, the impacts of GNP in lightweight cement composites haven't been fully investigated either. Aerogel is also a widely used material in the construction industry, having lower mechanical performance and adhesion with cementitious systems [12]. Aerogel is a lightweight thermal insulating fire resistance material and, due to the impressive characteristics of aerogel, it is used in the construction sector for various purposes like 3D printable thermal insulation concrete [13], thermal insulation rendering [14–16], thermal insulation plaster [17,18], thermal insulation concrete [19], aerogel based wall panels [20], fire safety mortars [21], and fire resistance concrete [22]. Adhikary et al. [23,24] reported that cementitious composites incorporating aerogel possessed lower mechanical performance and lower ITZ of aerogel. In addition, due to the entrapped air, aerogel-based cementitious composites might have higher porosity [24]. Previous research has suggested that GNP has reinforcing and crack-filling properties [25]. In addition, GNP is also provide nucleation effects for the growth of hydration products [26]. The inclusion of GNP might enable the improvement in mechanical properties, microstructure, and ITZ of the aerogel cement composite. There was no detailed study published in the past studying the impacts of GNP on aerogel-based cementitious composites. Moreover, the impacts of the thickness of GNP on lightweight cement composites also need to be investigated. For those reasons, the study of GNP reinforced lightweight cementitious composite could be worthwhile for future references.

In this study, 2 nm, 6–8 nm, and 11–15 nm GNP were incorporated into lightweight cement composites at a concentration of 0.025%, 0.05%, 0.1%, 0.25%, and 0.5%, respectively. Ultrasonication energy and a polycarboxylate-based superplasticiser were used to uniformly disperse the nano particles. Except the GNP, other mixing compositions remained constant for all lightweight cementitious composite samples. Workability, semi-adiabatic calorimetry, microstructure, water absorption, mechanical properties, and XRD analysis were investigated. The findings of the study enable the detailed analysis of the impact of GNP diameter and its concentrations on the aerogel-based lightweight cementitious composites, which might open the gate for future smart cementitious composites.

2. Materials and methods

2.1. Materials

The mineral admixtures utilized in this experiment were OPC grade OPC grade 42.5 R R and an average 50-m thickness zeolite powder. Different grades of EGA and silica aerogel were used as LWA in these experimental studies. The physical characteristics of the EGA and chemical characteristics of the EGA, zeolite and OPC are presented in Table 1 and Table 2. Three different thickness ranges of graphene platelets were used as nano reinforcement of the cementitious composites. The GNP was purchased from 'io-li-tech'. The properties of GNP are presented in Table 3. A MasterGlenium SKY 8700 superplasticiser was used as a chemical admixture to disperse the nanomaterials and maintain the workability of the composites.

2.2. Sample preparations and dispersion of nano materials

The mixing and trial methods were used to prepare the nano-reinforced cementitious composite samples. All the composite samples contained similar volumes of 4–8 mm, 2–4 mm, 1–2 mm, 0.5–1 mm, 0.25–0.5 mm, and 0.1–0.3 mm of EGA and 0.5–2 mm of silica aerogel as aggregates. The first sample, termed the "control sample," was prepared without any nano reinforcement. The rest of the samples were prepared with three different sizes (2 nm, 6–8 nm, and 11–15 nm) of graphene platelets at doses of 0.025%, 0.05%, 0.1%, 0.25%, and 0.50% of cement mass. The water/binder ratio of all the composite samples was kept constant at 0.48. The mixing composition of all nano-reinforced cementitious composites is presented in Table 4. In the first stage of the experiments, nanomaterials were ultrasonically dispersed. As compared to a normal concrete mixture, dispersing nanomaterials into the cementitious composite is more challenging. In order to prevent the defects of cement composites, it is necessary to keep the bundles of graphene nanoplatelets apart from one another due to the strong van der Waals interactions between nanomaterials. The GNP was separated using ultrasonication energy in the aqueous solution of a polycarboxylate-based superplasticiser. The total amount of water of each type of cementitious composite mixture was mixed with 1.66% of superplasticiser. Afterwards, GNP was added to the solution and sonicated for 3 min. The ultrasonically dispersed GNP solution is shown in Fig. 1. To prepare the fresh composites, OPC, zeolite and EGA were manually mixed at the dry stage for 2 min. Subsequently, the dispersed GNP solution was mixed into the cement mixture and gently mixed for another 2 min. At the last stage of the mixture, aerogel was incorporated to prevent the maximum crushing of aerogel and mixed for another 1 min. Prepared fresh nano-reinforced samples were sent for the workability test, and afterwards, the samples were moulded into 16.0 × 4.0 × 4.0 cm size prisms for the different property evolutions. Freshly moulded samples were kept at room temperature for 24 h for the hardening process. After that, hardened samples were demoulded and kept water-immersed for 28 days.

Table 2
Chemical composition of cement, zeolite and expanded glass aggregates.

Chemical composition	CaO	MgO	SiO_2	Al_2O_3	Fe_2O_3	K_2O	Na_2O	SO_3	TiO_2	Cl	Na_2O eq	LOI	Insoluble residue	Free Lime	Lime paste	Other
Cement	63	2.9	20.4	4.1	3.5	0.7	0.23	3.2	–	0.03	0.74	2.5	0.5	1.2	3.9	–
Zeolite	2.8	0.7	58.7	9.0	1.4	2.6	–	0.1	0.2	–	–	5.1	–	–	–	–
EGA	8–10.5		71–73	1.5–2	<0.3	–	13–14		–	–	–	–	–	–	–	<0.5

Table 3
Physical properties of GNP.

Thickness, nm	SSA, m2/g	Purity
~2	750	99.5%
6–8	120–150	99.5%
11–15	50–80	99.5%

Table 4
Mixing composition of nano reinforced lightweight cementitious composites, materials for 1 m^3 of concrete.

Mix	Cement	Aggregate (4/8 + 2/4 + 1/2 + 1/0.5 + 0.5/0.25 + 0.01/0.3)	Aerogel, kg/m^3	Zeolite	Graphene		Super plasticiser		Water	
					%	Kg/m^3	%	Kg/m^3	Kg/m^3	w/b
Control	524.7	11.82 + 13.2+16.70 + 22.9+46.6 + 155.2	10.92	58.3	0	0	1.658	8.7	279.2	0.48
2nm0.025	524.7	11.82 + 13.2+16.70 + 22.9+46.6 + 155.2	10.92	58.3	0.025	0.131	1.658	8.7	279.2	0.48
2nm0.050	524.7	11.82 + 13.2+16.70 + 22.9+46.6 + 155.2	10.92	58.3	0.05	0.262	1.658	8.7	279.2	0.48
2nm0.1	524.7	11.82 + 13.2+16.70 + 22.9+46.6 + 155.2	10.92	58.3	0.1	0.524	1.658	8.7	279.2	0.48
2nm0.25	524.7	11.82 + 13.2+16.70 + 22.9+46.6 + 155.2	10.92	58.3	0.25	1.311	1.658	8.7	279.2	0.48
2nm0.50	524.7	11.82 + 13.2+16.70 + 22.9+46.6 + 155.2	10.92	58.3	0.5	2.623	1.658	8.7	279.2	0.48
6–8nm0.025	524.7	11.82 + 13.2+16.70 + 22.9+46.6 + 155.2	10.92	58.3	0.025	0.131	1.658	8.7	279.2	0.48
6–8nm0.050	524.7	11.82 + 13.2+16.70 + 22.9+46.6 + 155.2	10.92	58.3	0.05	0.262	1.658	8.7	279.2	0.48
6–8nm0.1	524.7	11.82 + 13.2+16.70 + 22.9+46.6 + 155.2	10.92	58.3	0.1	0.524	1.658	8.7	279.2	0.48
6–8nm0.25	524.7	11.82 + 13.2+16.70 + 22.9+46.6 + 155.2	10.92	58.3	0.25	1.311	1.658	8.7	279.2	0.48
6–8nm0.50	524.7	11.82 + 13.2+16.70 + 22.9+46.6 + 155.2	10.92	58.3	0.5	2.623	1.658	8.7	279.2	0.48
11–15nm0.025	524.7	11.82 + 13.2+16.70 + 22.9+46.6 + 155.2	10.92	58.3	0.025	0.131	1.658	8.7	279.2	0.48
11–15nm0.050	524.7	11.82 + 13.2+16.70 + 22.9+46.6 + 155.2	10.92	58.3	0.05	0.262	1.658	8.7	279.2	0.48
11–15nm0.1	524.7	11.82 + 13.2+16.70 + 22.9+46.6 + 155.2	10.92	58.3	0.1	0.524	1.658	8.7	279.2	0.48
11–15nm0.25	524.7	11.82 + 13.2+16.70 + 22.9+46.6 + 155.2	10.92	58.3	0.25	1.311	1.658	8.7	279.2	0.48
11–15nm0.50	524.7	11.82 + 13.2+16.70 + 22.9+46.6 + 155.2	10.92	58.3	0.5	2.623	1.658	8.7	279.2	0.48

Fig. 1. Ultrasonically dispersed GNP.

3. Methods

The workability of the nano-reinforced cementitious materials was tested using a flow table in accordance with EN 12350–5:2009 standard requirements. The mean value of three times the permed flow table spread was recorded as the final result.

To perform the semi-adiabatic calorimetry test, mortar samples were prepared using similar concentrations of GNP, maintaining a

Table 5
Mixing composition of the nano-reinforced cement paste for the semi-adiabatic calorimetry test.

Mix	Cement, g	GNP, g	Superplasticiser, g	Water, g
Control	100	0	1.658	40
2nm0.025	100	0.025	1.658	40
2nm0.050	100	0.05	1.658	40
2nm0.1	100	0.1	1.658	40
2nm0.25	100	0.25	1.658	40
2nm0.50	100	0.5	1.658	40
6–8nm0.025	100	0.025	1.658	40
6–8nm0.050	100	0.05	1.658	40
6–8nm0.1	100	0.1	1.658	40
6–8nm0.25	100	0.25	1.658	40
6–8nm0.50	100	0.5	1.658	40
11–15nm0.025	100	0.025	1.658	40
11–15nm0.050	100	0.05	1.658	40
11–15nm0.1	100	0.1	1.658	40
11–15nm0.25	100	0.25	1.658	40
11–15nm0.50	100	0.5	1.658	40

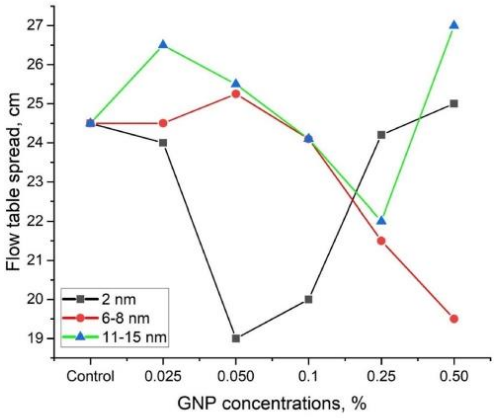

Fig. 2. Workability of GNP reinforced lightweight cementitious composites.

0.40 water-cement ratio. The GNP was ultrasonically dispersed for 3 min with water containing 1.66% superplasticiser. The mixing composition of the cement mortars for the semi-adiabatic calorimetry test is presented in Table 5.

After the 28 days of curing, water-immerged GNP reinforced cement samples were taken out and dried in the open air for 24 h before proceeding to the mechanical strength test. The C_S and F_S of the composite samples were performed in accordance with EN 196–1:2016 standards.

After the 28-day hydration, GNP reinforced cementitious composites were oven dried at 105 °C for 24 h. In order to calculate the water absorption of cementitious composites, oven-dried cement composites were immerged in water for 24 and 48 h. The mean value of three specimens was recorded as a result.

For SEM of GNP reinforced cementitious composites, the FEI Quanta 200 FEG with Schottky emission gun (FEG) and an energy-dispersive X-ray spectrometer (EDS) with silicon type drift droplet detector were used for SEM.

A DRON-6 X-ray diffractometer with Bragg–Brentano geometry, Ni-filtered Cu K radiation, and a graphite monochromator operating at 30 kV and a 20 mA emission current analyzed X-ray diffraction of used materials and GNP reinforced cementitious composites. In the 2°–70° (2) angular range, the step-scan was carried out in steps of 0.02°.

4. Results

4.1. Workability

The workability of any cementitious system is critical to its ease of placement and compacting. Lightweight aggregates having porous structures such as expanded glass and expanded clay absorb some water during the mixing process, leading to a higher demand for water to maintain the desired flowability [27,28]. However, in this contest, prewetting of such aggregates might be beneficial. GNP

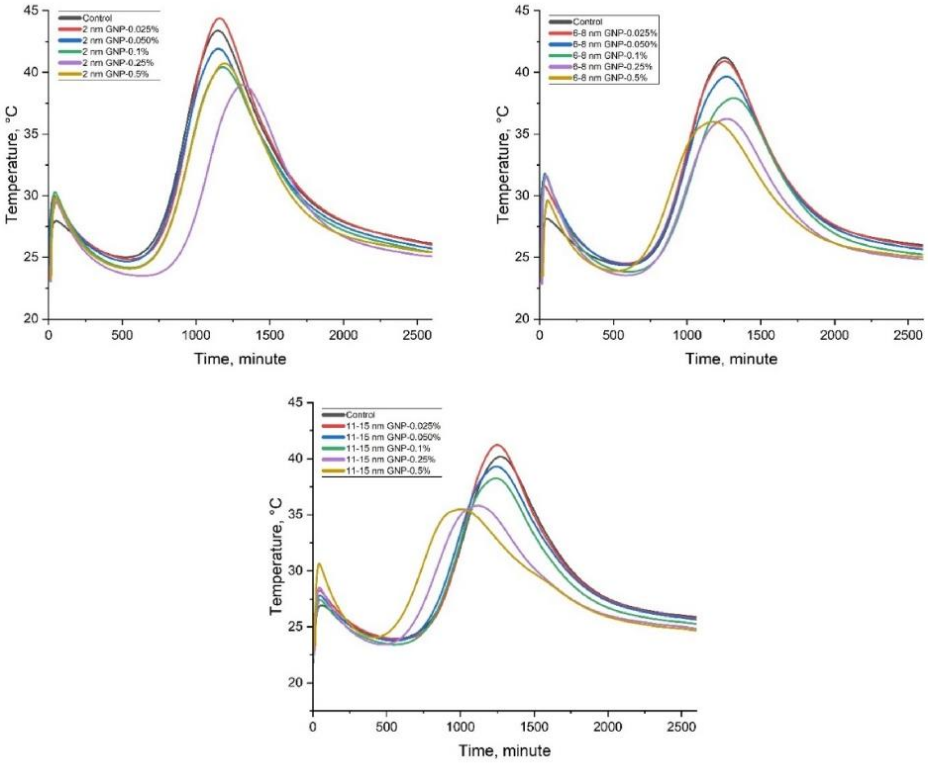

Fig. 3. Hydration of nano reinforced cement paste.

has a higher surface area that enhances the required water demand; a higher amount of water is required to cover the GNP particle, leading to a decline in free water content [29]. In addition, adding GNP might increase the frictional forces between GNP and cementitious particles, leading to a decline in workability [30,31]. In this study, EGA was used at large concentrations and GNP was used as reinforcement. Workability of the prepared samples is shown in Fig. 2. Study results indicated that the thickness of GNP has a notable impact on the workability of lightweight cementitious composites. Composite samples incorporating different thickness of GNP show inconsistent workability behaviour. Composite samples incorporating 2 nm GNP show adverse effects up to 0.05% concentrations and show a 22.4% reduction in workability. While afterwards, workability is enhanced with a rise in GNP concentrations. At 0.5% GNP reinforcement, the composite sample shows a 2% increase in flow. While the 6–8 nm GNP reinforced cementitious composite samples show completely different behaviours, the workability of the composite samples wasn't much impacted until 0.1% GNP reinforcement. A 3% increase in workability of a 0.05% GNP reinforced cement composite was measured, and afterwards, workability decreased with the rise in GNP content. At 0.25% and 0.5%, 6–8 nm, GNP reinforcement composite samples show a 12.2% and 20.4% decline in workability over control samples. On the other hand, the 11–15 nm GNP reinforced cementitious composite shows an 8.1% increase in workability at 0.025% GNP reinforcement and subsequently workability decreases till 0.25% GNP concentration. A 9.2% decline in workability was measured, incorporating 0.25% of GNP. Interestingly, the composite sample at 0.5% reinforcement shows a notable increase in flow and a 10.2% enhancement in flow over the control sample was measured. The flow table spread of some GNP-reinforced cementitious composites is shown in Fig. 3. Guo et al. [26] used GNP in their study and reported a 20.6% reduction in workability incorporating 0.1% GNP. However, the authors observed a slight enhancement in the workability of silane-treated GNP concrete compared to the concrete samples containing non-treated GNP. Similarly, Ahmad et al. [32] reported a 22.58% decline in the workability of concrete reinforced with 5% GNP. composites in greater depth. GNP concentrations up to 0.050%, the composite sample prepared with a 2 nm thickness of GNP loses its workability the most. Up to 0.25% GNP concentration, 6–8 nm GNP reinforced cement composite shows slightly lower workability than 11–15 nm of GNP reinforcement. It can be observed that at optimum doses of GNP, the thinner the GNP shows a greater rate of decline in workability. The inconsistence behaviour in workability

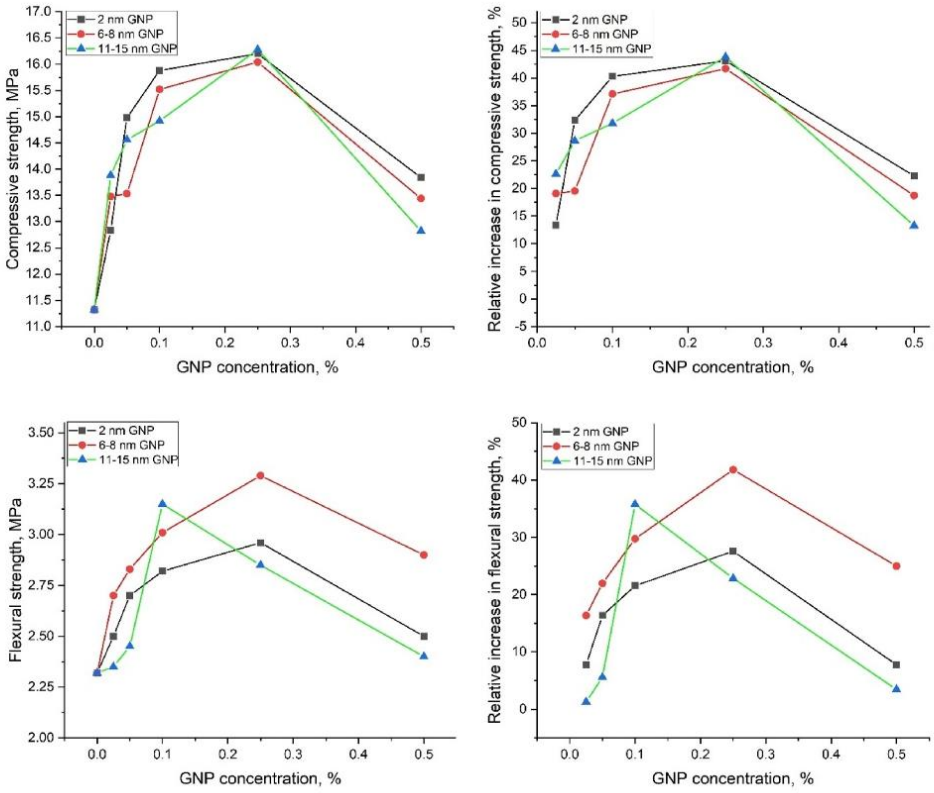

Fig. 4. C_S and F_S of GNP-reinforced lightweight cement composites.

of varied thicknesses of GNP could be associated with the surface area of GNP. The GNP with a smaller thickness has a larger surface area that might enhance the requirement for water, leading to a higher rate of decline in workability. However, the reduced workability of 2 nm and 11–15 nm GNP reinforced cement composite was observed up to certain doses; afterwards, it was increasing. The sudden improvement in workability at high doses of GNP might be associated with the agglomerations of nano particles.

4.2. Semi-adiabatic calorimetry analysis

The semi-adiabatic temperature of different thickness GNP reinforced cementitious systems is presented in Fig. 3, and it clearly demonstrates that the hydration of the cement composite is notably impacted by the thickness of GNP. Cementitious composites incorporating 2 nm GNP effectively retard the hydration of cement paste. However, there were no stable relationships observed between the retardation of cement hydration and GNP concentration. Cement paste samples reinforced with 0.025% GNP show slight retardation in hydration and show comparatively higher exothermic heat than the control samples. Other composite samples gain less exothermic heat than control samples. Sample containing 0.25% nm GNP shows the highest level of retardation in cement hydration. While the 0.5% GNP reinforced cement composite shows significant accelerated heat of hydration and produced heat over the 0.25% GNP reinforced cement paste, On the other hand, all the composite samples reinforcing 6–8 nm GNP show lower production of exothermic heat than the control sample. The cement hydration of the cement paste was retarded up to 0.1% GNP reinforcement, and afterwards, cement hydration was accelerated by the rise in GNP concentrations. Cement paste containing 0.025% 11–15 nm GNP gains more produced heat than the control sample, and the rest of the samples gain comparatively lower exothermic heat. Interestingly, the cement hydration incorporating 11–15 nm GNP accelerated the cement hydration. In the experimental study, it was observed that the thickness of GNP plays an important role in the hydration of the cementitious system. The larger the thickness of the GNP reinforced cementitious system, the better the cement hydration. The delay in cement hydration might be attributed to the surface anionic charge density of GNP. Higher anionic charge density might also delay the transformation of C–S–H [33,34]. Schönlein and

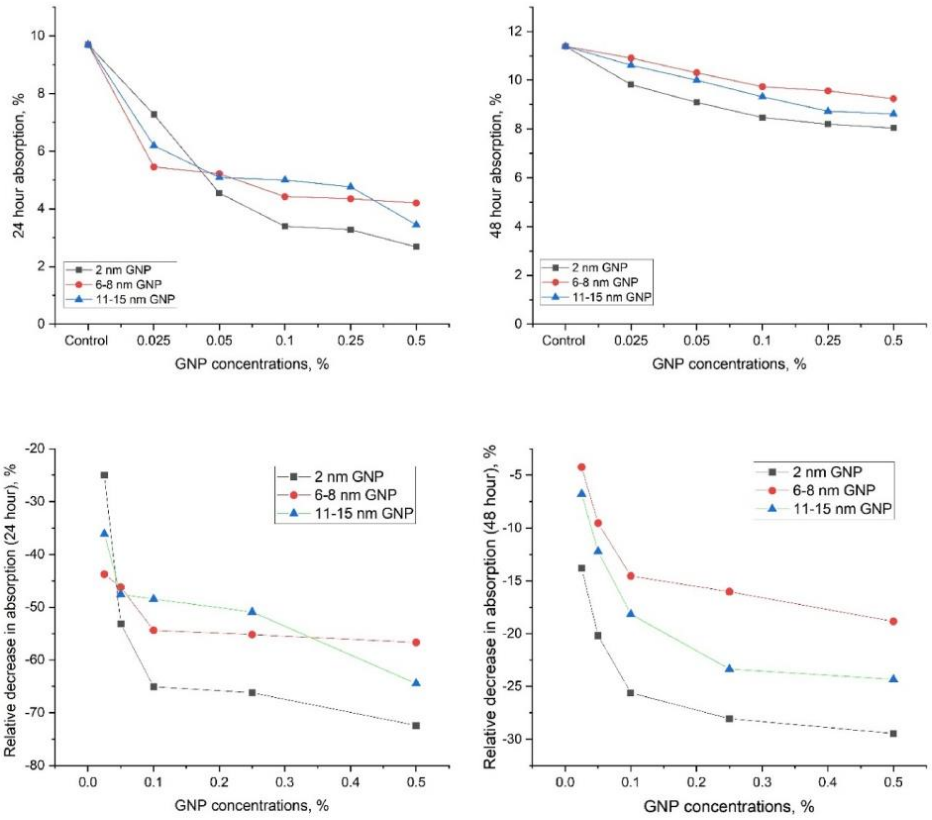

Fig. 5. W_A strength of GNP-reinforced lightweight cement composites.

Plank reported that the surface area of nanomaterials might initially hold back the growth of C–S–H [33]. The growth of hydration products and nucleation effects are primarily influenced by the early age of the hydration cementitious system. It is probably that higher-thickness GNP initially accelerated the formation of hydration products, leading to an acceleration in hydration. The heat of hydration was tested for cement paste containing various doses of GNP to understand the impact of GNP on cement hydration. However, the impact of GNP combining with lightweight aggregates such as aerogel might be slightly impacted. Adhikary et al. [23] observed that aerogel might slightly lower the produced exothermic heat and slightly retard the hydration time of cement paste.

4.3. Compressive and flexural strength

In Fig. 4, the Cs and Fs of the lightweight GNP reinforcement cementitious composite at different thickness and concentrations are presented in Fig. 5. It is clearly observed that the thickness of GNP has an important role in the mechanical strength of the grain of the GNP reinforced cementitious system. The C_S of the cementitious composite was increased up to a 0.25% concentration, but afterwards it decreased. All of the composite samples, however, gain greater C_S than the control sample. The optimum C_S gain was observed at a 0.25% concentration of different thickness of GNP. The C_S of the control sample, 2 nm, 6–8 nm, and 11–15 nm GNP reinforced cement composites at 0.25% concentration was measured at 11.32 MPa, 15.88 MPa, 15.52 MPa, and 14.92 MPa, respectively. Similarly, the F_S of the GNP reinforced cement composite was increased up to a certain concentration, but subsequently started decreasing. However, all of the nano-reinforced cement composites outperform the control sample in terms of F_S. The optimum F_S gain of the 2 nm and 6–8 nm GNP reinforced cement composites was measured at 0.25%. While 11–15 nm GNP reinforced cement composite gains optimum flexural strength at 0.1% concentration, the flexural strength of the control sample, 2 nm, 6–8 nm, and 11–15 nm GNP reinforced cement composites at 0.25% concentration was measured at 2.32 MPa, 2.96 MPa, 3.29 MPa, and 2.85 MPa, respectively. This experimental investigation showed that the mechanical performance of the cementitious system was remarkably improved by

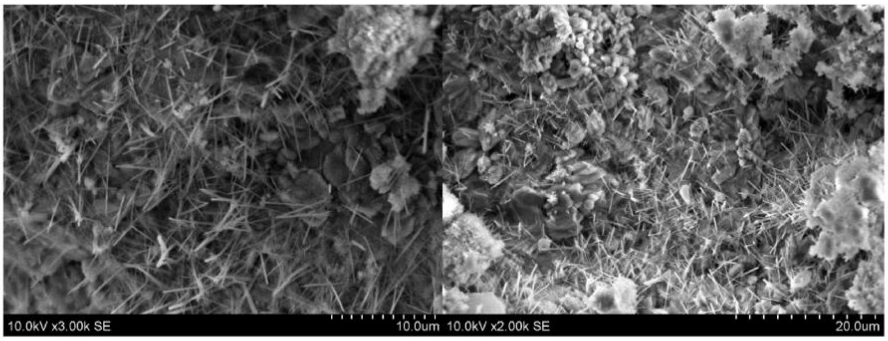

Fig. 6. Dispersion of GNP within the cementitious composites.

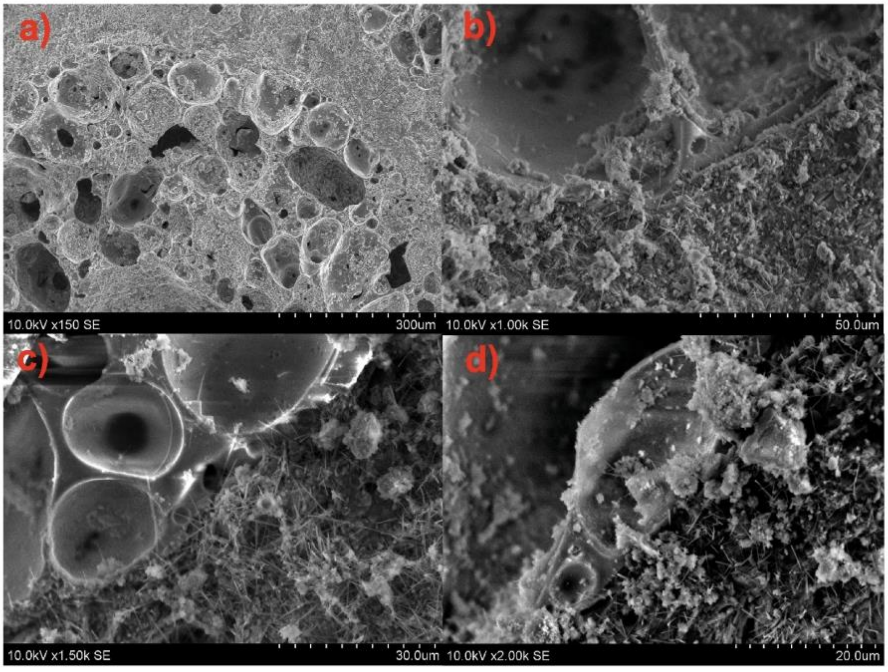

Fig. 7. a) ITZ of EGA without GNP reinforcements, b), c) and d) ITZ of EGA with GNP reinforcements.

incorporating GNP. 11–15 nm thickness GNP reinforced cement composite gains greater compressive strength at its optimum level (43% increased Cs at 0.25% GNP reinforcement). While 6–8 nm in thickness, GNP reinforced cement composites gain greater flexural strength at their optimum level (41.8% increased Fs at 0.25% GNP reinforcement). Similar improved mechanical performances of GNP reinforced cementitious systems have been reported in the literature [35–37]. The GNP might provide pore filing and nucleation effects, leading to improvement in microstructure and mechanical performance [3,38,39]. In addition, GNP also has a reinforcement capability [25]. It is probably due to those reasons that the mechanical performance of the GNP reinforced cement composite was improved. However, after certain doses, a drop in mechanical performance is also noticed. Previously published literature suggested that the drop in mechanical performance after certain doses of nano materials might be attributed to the hydrophilic behaviour of nano

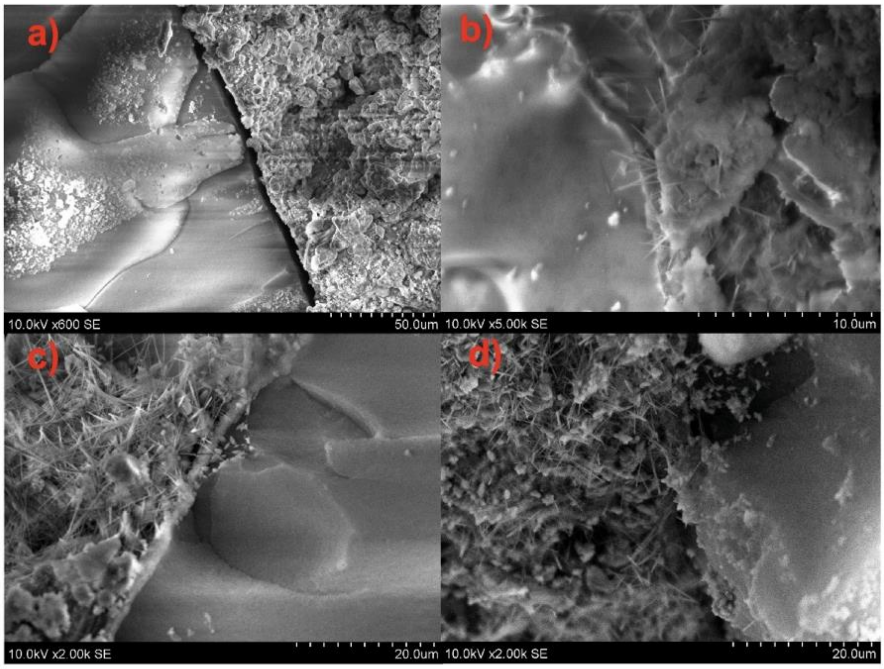

Fig. 8. a) ITZ of aerogel without GNP reinforcements, b), c) and d) ITZ of aerogel with GNP reinforcements.

materials [37]. The hydrophilic behaviour of GNP might prevent cement hydration by absorbing water on the cement surface [36,40,41]. The higher doses of GNP might enhance the required water and disrupt the homogeneous distribution of GNP in the cementitious composite [39]. This phenomenon might lower the mechanical performance of the GNP reinforced cementitious system [40]. Jiang et al. [42] also reported a drop in the mechanical performance of GNP-reinforced concrete after certain doses. The authors state that at large concentrations, GNP may agglomerate and reduce the nucleation sites accessible for hydration, resulting in a reduction in the weak zone inside concrete, leading to a decline in strength. Gao et al. [45] used different diameters of carbon-based nanomaterials and reported that the smaller diameter of nanomaterials provides better pore felling effects while larger diameter nanomaterials provide better dispersions. The effectiveness of GNP for the improvement in mechanical strength after 28 days of curing of different thicknesses of GNP might be associated with its surface area and its impacts on cement hydration and pore felling effects.

4.4. Water absorption

The WA of the GNP reinforced cementitious composite is presented in Fig. 5. WA of the lightweight cement composite was measured after 24 and 48 h of water immersion. Study results showed that the water absorption of the composite decreased with the rise in GNP reinforcement concentrations. The lowest water absorption after 48 h was measured for the cement composite incorporating 2 nm GNP. After 48 h of water immersion, the water absorption of the control sample, 2 nm GNP, 6–8 nm GNP, and 11–15 nm GNP reinforced cement composite at 0.5% concentration was measured at 11.4%, 8.04%, 9.24%, and 8.62%, respectively. The rate of improvement in water absorption after 24 and 48 h at 0.5% concentration was measured at 72.4%, 56.7%, and 64.4%, and 29.45%, 18.85%, and 24.32% for the 2 nm GNP, 6–8 nm GNP, and 11–15 nm GNP reinforced cement composite samples, respectively. This experimental study also showed that the thickness of GNP also has an impact on the WA of the cementitious system. The incorporation of GNP and other nano particles fills the pores and voids of the cementitious composite and provides nucleation effects for the growth of hydration products [3,38,39]. This improvement in microstructure led to an improvement in water absorption of cement composite. A similar improvement in water absorption of graphene reinforced cementitious systems was observed by several authors [32,43]. A study [44] reported that incorporation of graphene in cementitious composites provides nanoscale reinforcement and reduces the porosity and densifies the composite matrix, leading to an improvement in water absorption. The effectiveness of carbon based nano materials for the improvement in water absorption of the cement composite might be associated with the impacts of pore filling effects, improvement in porosity, and degree of dispersion [45].

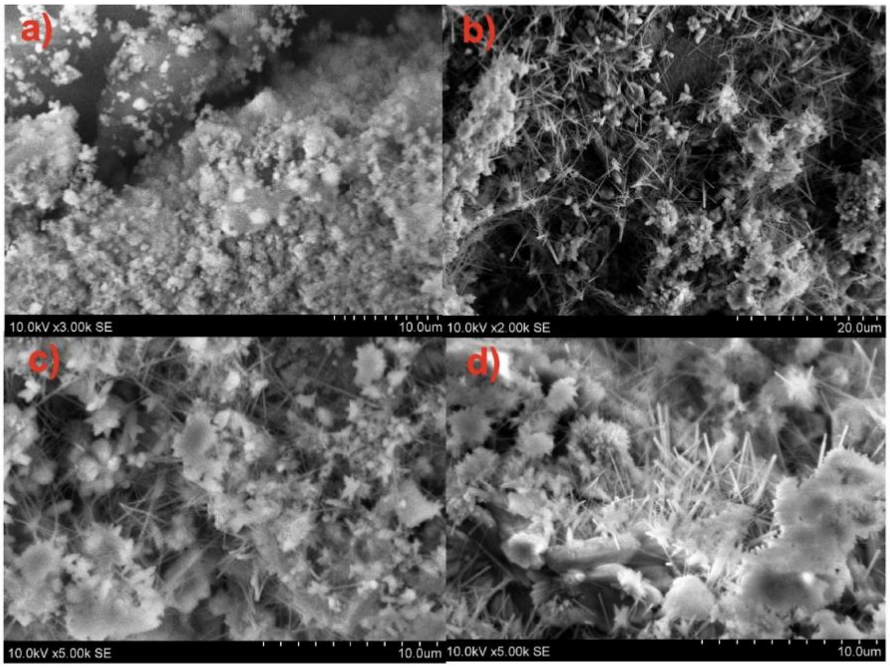

Fig. 9. a) Microstructure of cement composite without GNP reinforcements, b), c) and d) Microstructure of cement composite with GNP reinforcements.

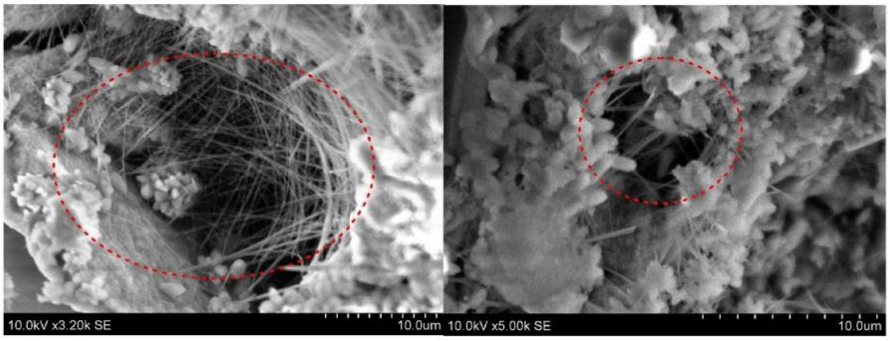

Fig. 10. Pore filling effects of GNP.

4.4.1. Scanning electron microscopy

The SEM image in Fig. 6 shows that GNP particles were almost homogeneously distributed in the cementitious composites. These phenomena suggest the effectiveness of ultrasonication to successfully disperse nanoparticles. SEM image depicted in Fig. 7shows the ITZ of EGA with and without GNP reinforcement. In this SEM image, it is clearly evident that EGA has greater adhesion with cementitious composites. GNP particles can clearly observed in the ITZ of EGA. A separation gap between aerogel and cementitious materials is clearly visible in Fig. 8 a) for the composite without GNP reinforcement. While the GNP reinforced cement composite sample shows comparatively improved ITZ, as shown in Fig. 8 b), c) and d) d). Adhikary et al. [12,23,24] and Gao et al. [46] reported that aerogel has lower adhesion with the cementitious materials, leading to weaker ITZ. The presence of GNP was also observed in the

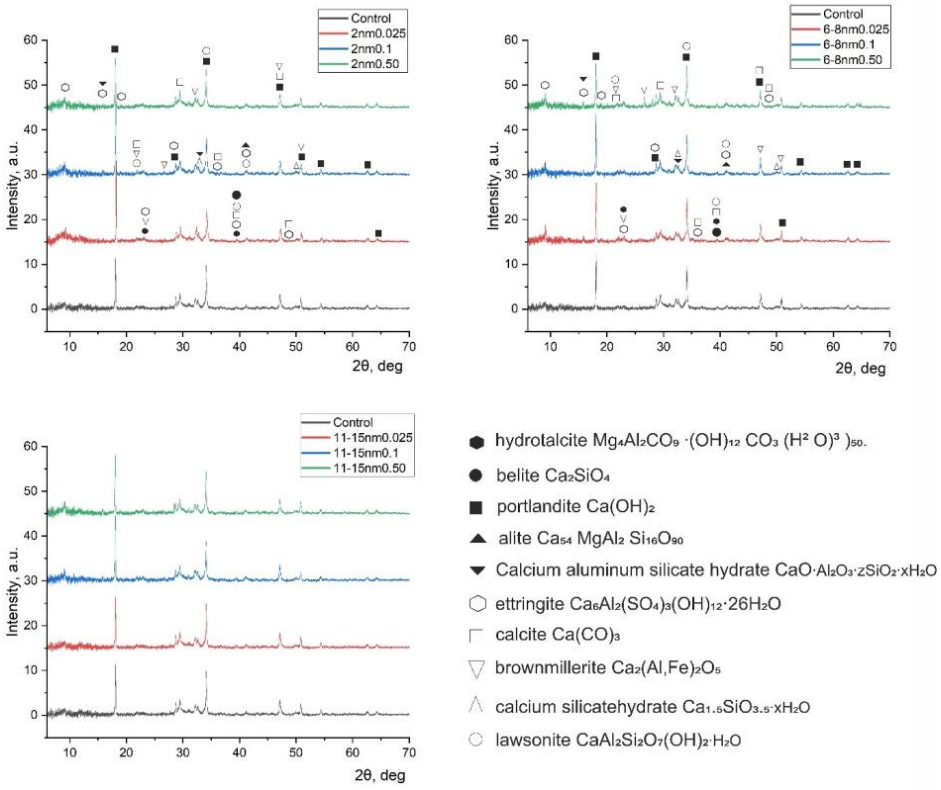

Fig. 11. XRD pattern of GNP reinforced lightweight cement composites.

ITZ of aerogel and EGA, as shown in Fig. 8.Adhikary et al. [47] observed a similar improved ITZ of aerogel incorporating carbon nanotubes. Air and/or water may easily penetrate through the gaps, weakening the cementitious system. The presence of hydration products surrounding the GNP particles, shown in Fig. 9 is evidential of the nucleation effect of GNP. The presence of hydration products can be clearly observed in the GNP reinforced cementitious system. Guo et al. [26] observed similar growth of hydration products surrounding graphene. While the pore filling effects of GNP can be observed in Fig. 10, which may lead to an improvement in the mechanical performance of cementitious composites [48,49].

4.5. XRD analysis

In Fig. 11, the XRD patterns of the GNP reinforced cement composites are presented. XRD analysis of the cement composite revealed that all the composite specimens had similar peaks and didn't have any additional peaks, adding GNP. The intensity of the pecks varied depending upon the concentrations of the GNP. That suggests that almost similar hydration products were grown and the crystalline of the hydration products were impacted by incorporating GNP. A similar observation was reported by Wang and Pang [50]. XRD analysis suggests that calcite, portlandite, ettringite, calcium silicate hydrate, lawsonite, and brownmillerite are the primary hydration products of the cement composites. It was observed that the intensity of ettringite at 8° and 19° was slightly enhanced by the rise in GNP concentrations. All the peaks of portlandite near 18° and 34° were noticed for all the cementitious composites. However, the intensity of portlandite varied depending upon the concentration of GNP. The peak of portlandite near 18° contained 0.025% and 0.1% GNP. While the composite sample containing 0.5% GNP had a higher intensity of portlandite near 34°. The higher peaks of the portlandite of the GNP reinforcement cementitious system might be due to the acceleration in pozzolanic activity. Due to the acceleration in pozzolanic activity, the intensity of ettringite and calcium aluminate silicate hydrate was also increased. This phenomenon suggests that probably at higher GNP concentrations, pozzolanic activity increased and the aerogel partially dissolved and reacted with cement.

5. Conclusions

In this experimental study, various concentrations of different thickness of GNP were incorporated into a lightweight cementitious composite. GNP and its thickness were studied for their effects on fresh, mechanical, water absorption, and microstructural properties. The ultrasonic dispersion of GNP in polycarboxylate superplasticiser was observed to be effective in dispersing the GNP uniformly. The flowability of the GNP reinforced cement composite was significantly impacted by the thickness of the GNP. The workability of the GNP reinforced cement composite was reduced compared to the control sample. C_S and F_S of the lightweight cement composite were increased up to a certain concentration of GNP and subsequently decreased by the rise in GNP concentrations. At optimum concentrations, an almost similar rate of enhancement in compressive strength was observed incorporating different thickness of GNP, while at low concentrations of GNP, a significant difference in C_S was observed. The impact of the thickness of GNP on the rate of improvement in F_S was more significant than that of C_S. The water absorption properties of the GNP reinforced cement composite were significantly improved, and 2 nm GNP was observed to be more effective at lowering the water absorption. GNP was observed to promote the growth of hydration products such as C–S–H and portlandite. Incorporation of GNP improves the microstructure by filling the voids/pores.

CRediT authorship contribution statement

Conceptualization, S.K.A. and Z.R.; Methodology, S.K.A. and Z.R.; Investigation, S.K.A; Supervision, S.K.A. and Z.R.; SEM and XRD, S.T.; Writing – Original draft, Review & Editing, S.K.A.; Resources, Z.R. and S.T.

Declaration of competing interest

The authors declare that they have no known competing financial interests or personal relationships that could have appeared to influence the work reported in this paper.

References

[1] S. Stankovich, D.A. Dikin, G.H.B. Dommett, K.M. Kohlhaas, E.J. Zimney, E.A. Stach, R.D. Piner, S.B.T. Nguyen, R.S. Ruoff, Graphene-based composite materials, Nature 442 (2006) 282–286, https://doi.org/10.1038/nature04969.

[2] B. Han, S. Sun, S. Ding, L. Zhang, X. Yu, J. Ou, Review of nanocarbon-engineered multifunctional cementitious composites, Compos. Part A Appl. Sci. Manuf. 70 (2015) 69–81, https://doi.org/10.1016/j.compositesa.2014.12.002.

[3] H. Du, S.D. Pang, Enhancement of barrier properties of cement mortar with graphene nanoplatelet, Cement Concr. Res. 76 (2015) 10–19, https://doi.org/10.1016/j.cemconres.2015.05.007.

[4] A. Peyvandi, P. Soroushian, A.M. Balachandra, K. Sobolev, Enhancement of the durability characteristics of concrete nanocomposite pipes with modified graphite nanoplatelets, Construct. Build. Mater. 47 (2013) 111–117, https://doi.org/10.1016/j.conbuildmat.2013.05.002.

[5] J.L. Le, H. Du, S.D. Pang, Use of 2-D Graphene Nanoplatelets (GNP) in cement composites for structural health evaluation, Compos. B Eng. 67 (2014) 555–563, https://doi.org/10.1016/j.compositesb.2014.08.005.

[6] X. Cui, S. Sun, B. Han, X. Yu, J. Ouyang, S. Zeng, J. Ou, Mechanical, thermal and electromagnetic properties of nanographite platelets modified cementitious composites, Compos. Part A Appl. Sci. Manuf. 93 (2017) 49–58, https://doi.org/10.1016/j.compositesa.2016.11.017.

[7] H. Du, H.J. Gao, S.D. Pang, Improvement in concrete resistance against water and chloride ingress by adding graphene nanoplatelet, Cement Concr. Res. 83 (2016) 114–123, https://doi.org/10.1016/j.cemconres.2016.02.005.

[8] B. Wang, R. Jiang, Z. Wu, Investigation of the mechanical properties and microstructure of graphene nanoplatelet-cement composite, Nanomaterials 6 (2016), https://doi.org/10.3390/nano6110200.

[9] N. Ranjbar, M. Mehrali, M. Mehrali, U.J. Alengaram, M.Z. Jumaat, Graphene nanoplatelet-fly ash based geopolymer composites, Cement Concr. Res. 76 (2015) 222–231, https://doi.org/10.1016/j.cemconres.2015.06.003.

[10] A. Peyvandi, P. Soroushian, N. Abdol, A.M. Balachandra, Surface-modified graphite nanomaterials for improved reinforcement efficiency in cementitious paste, Carbon N. Y. 63 (2013) 175–186, https://doi.org/10.1016/j.carbon.2013.06.069.

[11] Z. Jiang, D.K. Harris, Graphene nanoplatelets-based self-sensing cementitious composites, in: Proc. ASME 2016 Conf. Smart Mater. Adapt. Struct. Intell. Syst, 2016.

[12] S.K. Adhikary, D.K. Ashish, Ž. Rudžionis, Aerogel Based Thermal Insulating Cementitious Composites: A Review, Energy Build, 2021, https://doi.org/10.1016/j.enbuild.2021.111058.

[13] G. Ma, R. A, P. Xie, Z. Pan, L. Wang, J.C. Hower, 3D-printable aerogel-incorporated concrete: anisotropy influence on physical, mechanical, and thermal insulation properties, Construct. Build. Mater. 323 (2022), 126551, https://doi.org/10.1016/j.conbuildmat.2022.126551.

[14] K. Ghazi Wakili, C. Dworatzyk, M. Sanner, A. Sengespeick, M. Paronen, T. Stahl, Energy efficient retrofit of a prefabricated concrete panel building (Plattenbau) in Berlin by applying an aerogel based rendering to its façades, Energy Build. 165 (2018) 293–300, https://doi.org/10.1016/j.enbuild.2018.01.050.

[15] M. Ibrahim, E. Wurtz, P.H. Biwole, P. Achard, H. Sallee, Hygrothermal performance of exterior walls covered with aerogel-based insulating rendering, Energy Build. 84 (2014), https://doi.org/10.1016/j.enbuild.2014.07.039.

[16] T. Stahl, K. Ghazi Wakili, S. Hartmeier, E. Franov, W. Niederberger, M. Zimmermann, Temperature and moisture evolution beneath an aerogel based rendering applied to a historic building, J. Build. Eng. 12 (2017), https://doi.org/10.1016/j.jobe.2017.05.016.

[17] M. Ibrahim, L. Bianco, O. Ibrahim, E. Wurtz, Low-emissivity coating coupled with aerogel-based plaster for walls' internal surface application in buildings: energy saving potential based on thermal comfort assessment, J. Build. Eng. 18 (2018), https://doi.org/10.1016/j.jobe.2018.04.008.

[18] C. Buratti, E. Moretti, E. Belloni, F. Agosti, Development of innovative aerogel based plasters: preliminary thermal and acoustic performance evaluation, Sustain. Times 6 (2014), https://doi.org/10.3390/su6095839.

[19] H. Zhang, J. Yang, H. Wu, P. Fu, Y. Liu, W. Yang, Dynamic thermal performance of ultra-light and thermal-insulative aerogel foamed concrete for building energy efficiency, Sol. Energy 204 (2020) 569–576, https://doi.org/10.1016/j.solener.2020.04.092.

[20] P. Liu, W. Wu, B. Du, G. hua Tian, Y. feng Gong, Study on the heat and moisture transfer characteristics of aerogel-enhanced foam concrete precast wall panels and the influence of building energy consumption, Energy Build. 256 (2022), 111707, https://doi.org/10.1016/j.enbuild.2021.111707.

[21] P. Zhu, S. Brunner, S. Zhao, M. Griffa, A. Leemann, N. Toropovs, A. Malekos, M.M. Koebel, P. Lura, Study of physical properties and microstructure of aerogel-cement mortars for improving the fire safety of high-performance concrete linings in tunnels, Cem. Concr. Compos. 104 (2019), https://doi.org/10.1016/j.cemconcomp.2019.103414.

[22] P. Zhu, X. Xu, H. Liu, S. Liu, C. Chen, Z. Jia, Tunnel fire resistance of self-compacting concrete coated with SiO2 aerogel cement paste under 2.5 h HC fire loading, Construct. Build. Mater. 239 (2020), https://doi.org/10.1016/j.conbuildmat.2019.117857.

[23] S.K. Adhikary, Ž. Rudžionis, D. Vaičiukynienė, Development of flowable ultra-lightweight concrete using expanded glass aggregate, silica aerogel, and prefabricated plastic bubbles, J. Build. Eng. 31 (2020), 101399, https://doi.org/10.1016/j.jobe.2020.101399.
[24] S.K. Adhikary, Ž. Rudžionis, S. Tučkutė, Characterization of novel lightweight self-compacting cement composites with incorporated expanded glass, aerogel, zeolite and fly ash, Case Stud. Constr. Mater. 16 (2022), e00879, https://doi.org/10.1016/j.cscm.2022.e00879.
[25] D. Torres, S. Pérez-Rodríguez, D. Sebastián, J.L. Pinilla, M.J. Lázaro, I. Suelves, Graphene oxide nanofibers: a nanocarbon material with tuneable electrochemical properties, Appl. Surf. Sci. 509 (2020), 144774, https://doi.org/10.1016/j.apsusc.2019.144774.
[26] L. Guo, J. Wu, H. Wang, Mechanical and perceptual characterization of ultra-high-performance cement-based composites with silane-treated graphene nano-platelets, Construct. Build. Mater. 240 (2020), 117926, https://doi.org/10.1016/j.conbuildmat.2019.117926.
[27] S.K. Adhikary, D.K. Ashish, Ž. Rudžionis, Expanded glass as light-weight aggregate in concrete – a review, J. Clean. Prod. 313 (2021), https://doi.org/10.1016/j.jclepro.2021.127848.
[28] R. Vijayalakshmi, S. Ramanagopal, Structural concrete using expanded clay aggregate: a review, Indian J. Sci. Technol. 11 (2018) 1–12, https://doi.org/10.17485/ijst/2018/v11i16/121888.
[29] F. Ahmad, M.I. Qureshi, Z. Ahmad, Influence of nano graphite platelets on the behavior of concrete with E-waste plastic coarse aggregates, Construct. Build. Mater. 316 (2022), 125980, https://doi.org/10.1016/j.conbuildmat.2021.125980.
[30] M.X. Wang, Z.H. Huang, W. Lv, Q.H. Yang, F. Kang, K. Liang, Water vapor adsorption on low-temperature exfoliated graphene nanosheets, J. Phys. Chem. Solid. 73 (2012) 1440–1443, https://doi.org/10.1016/j.jpcs.2011.10.048.
[31] S. Chuah, Z. Pan, J.G. Sanjayan, C.M. Wang, W.H. Duan, Nano reinforced cement and concrete composites and new perspective from graphene oxide, Construct. Build. Mater. 73 (2014) 113–124, https://doi.org/10.1016/j.conbuildmat.2014.09.040.
[32] F. Ahmad, A. Jamal, M. Iqbal, M. Alqurashi, M. Almoshaogeh, H.M. Al-Ahmadi, E.E. Hussein, Performance evaluation of cementitious composites incorporating nano graphite platelets as additive carbon, Mater. Mater. (Basel) 15 (2022), https://doi.org/10.3390/ma15010290.
[33] M. Schönlein, J. Plank, A TEM study on the very early crystallization of C-S-H in the presence of polycarboxylate superplasticizers: transformation from initial C-S-H globules to nanofoils, Cement Concr. Res. 106 (2018) 33–39, https://doi.org/10.1016/j.cemconres.2018.01.017.
[34] X. Zhu, X. Kang, J. Deng, K. Yang, L. Yu, C. Yang, A comparative study on shrinkage characteristics of graphene oxide (GO) and graphene nanoplatelets (GNPs) modified alkali-activated slag cement composites, Mater. Struct. Constr. 54 (2021) 1–15, https://doi.org/10.1617/s11527-021-01695-w.
[35] S.K. Adhikary, Ž. Rudžionis, R. Ghosh, Influence of CNT, graphene nanoplate and CNT-graphene nanoplate hybrid on the properties of lightweight concrete, Mater Today: Proc 44 (1) (2021) 1979–1982, https://doi.org/10.1016/j.matpr.2020.12.115.
[36] M. li Cao, H. xia Zhang, C. Zhang, Effect of graphene on mechanical properties of cement mortars, J. Cent. South Univ. 23 (2016) 919–925, https://doi.org/10.1007/s11771-016-3139-4.
[37] S. Arslan, N. Öksüzer, H.S. Gökçe, Improvement of mechanical and transport properties of reactive powder concrete using graphene nanoplatelet and waste glass aggregate, Construct. Build. Mater. 318 (2022), https://doi.org/10.1016/j.conbuildmat.2021.126199.
[38] F. Matalkah, P. Soroushian, Graphene nanoplatelet for enhancement the mechanical properties and durability characteristics of alkali activated binder, Construct. Build. Mater. 249 (2020), 118773, https://doi.org/10.1016/j.conbuildmat.2020.118773.
[39] G. Chen, M. Yang, L. Xu, Y. Zhang, Y. Wang, Graphene nanoplatelets impact on concrete in improving freeze-thaw resistance, Appl. Sci. 9 (2019), https://doi.org/10.3390/app9173582.
[40] A. Nazari, S. Riahi, The effects of zinc dioxide nanoparticles on flexural strength of self-compacting concrete, Compos. B Eng. 42 (2011) 167–175, https://doi.org/10.1016/j.compositesb.2010.09.001.
[41] A.S. Barnard, I.K. Snook, Thermal stability of graphene edge structure and graphene nanoflakes, J. Chem. Phys. 128 (2008), https://doi.org/10.1063/1.2841366.
[42] Z. Jiang, O. Sevim, O.E. Ozbulut, Mechanical properties of graphene nanoplatelets-reinforced concrete prepared with different dispersion techniques, Construct. Build. Mater. 303 (2021), 124472, https://doi.org/10.1016/j.conbuildmat.2021.124472.
[43] F. Seddighi, G. Pachideh, S.B. Salimbahrami, A study of mechanical and microstructures properties of autoclaved aerated concrete containing nano-graphene, J. Build. Eng. 43 (2021), 103106, https://doi.org/10.1016/j.jobe.2021.103106.
[44] S.C. Devi, R.A. Khan, Effect of graphene oxide on mechanical and durability performance of concrete, J. Build. Eng. 27 (2020), 101007, https://doi.org/10.1016/j.jobe.2019.101007.
[45] F. Gao, W. Tian, Z. Wang, F. Wang, Effect of diameter of multi-walled carbon nanotubes on mechanical properties and microstructure of the cement-based materials, Construct. Build. Mater. 260 (2020), 120452, https://doi.org/10.1016/j.conbuildmat.2020.120452.
[46] T. Gao, B.P. Jelle, A. Gustavsen, S. Jacobsen, Aerogel-incorporated concrete: an experimental study, Construct. Build. Mater. 52 (2014) 130–136, https://doi.org/10.1016/j.conbuildmat.2013.10.100.
[47] S.K. Adhikary, Ž. Rudžionis, S. Tučkutė, D.K. Ashish, Effects of carbon nanotubes on expanded glass and silica aerogel based lightweight concrete, Sci. Rep. 11 (2021), https://doi.org/10.1038/s41598-021-81665-y.
[48] H. Du, S.D. Pang, Dispersion and stability of graphene nanoplatelet in water and its influence on cement composites, Construct. Build. Mater. 167 (2018) 403–413, https://doi.org/10.1016/j.conbuildmat.2018.02.046.
[49] J. Tao, J. Wang, Q. Zeng, A comparative study on the influences of CNT and GNP on the piezoresistivity of cement composites, Mater. Lett. 259 (2020), 126858, https://doi.org/10.1016/j.matlet.2019.126858.
[50] B. Wang, B. Pang, Mechanical property and toughening mechanism of water reducing agents modified graphene nanoplatelets reinforced cement composites, Construct. Build. Mater. 226 (2019) 699–711, https://doi.org/10.1016/j.conbuildmat.2019.07.229.

ACKNOWLEDGMENTS

Prof. Dr. Žymantas Rudžionis (Faculty of Civil Engineering and Architecture, Kaunas University of Technology) is sincerely thanked for the supervision of my doctoral research, consultations, valuable advice and great support.

Most importantly, the author wants to thank his mother and father who set him up for a career as a scientist from his very first appearance on Earth.

UDK 666.973+666.972.125+691.32](043.3)
SL 344. 2023-xx-xx, xx leidyb. apsk. l. Tiražas 14 egz. Užsakymas xxx.
Išleido Kauno technologijos universitetas, K. Donelaičio g. 73, 44249 Kaunas
Spausdino leidyklos „Technologija“ spaustuvė, Studentų g. 54, 51424 Kaunas